Part VI Reference Technical Data for Part III

Chapter 1 Basic Items for Earthquake Resistance Design

1 Details of Seismic Coefficients for Verification

1.1 Classification of the Methods for Calculating Seismic Coefficients for Verification

The methods for calculating the seismic coefficients to be used for verifying facilities subjected to technical standards are classified into the following four groups depending on the structural types of the facilities to be verified.

Group 1: A group of facilities for which an equation considering the reduction rates with respect to the duration of earthquake ground motions is used for calculating the seismic coefficients for verification.

Group 2: A group of facilities for which an equation not considering the reduction rates with respect to the duration of earthquake ground motions is used for calculating the seismic coefficients for verification.

Group 3: A group of facilities for which acceleration response spectra are used for calculating the seismic coefficients for verification.

Group 4: A group of facilities for which the maximum ground acceleration is used for calculating the seismic coefficients for verification.

Table 1.1.1 shows into which groups the respective structural types of facilities subjected to technical standards are categorized in the calculation of the seismic coefficients for verification. The seismic coefficients for verification of respective structural types in the column of "Structural type to which the method for calculating the seismic coefficients for verification is applied" shall be calculated through the methods corresponding to the categories of "Typical structural type" into which respective structural types are categorized.

For the structural types of gravity-type quaywalls, sheet pile quaywalls with vertical anchor piles, and sheet pile quaywalls with coupled anchor piles in Group 1, the appropriateness of the equation for calculating the seismic coefficients for verification has been confirmed through the disaster damage verification method using the data on the damage to the existing facilities and facilities that once existed due to actual earthquake ground motions.[1)] For the evaluation result of the appropriateness of the equation for calculating the seismic coefficients for verification and the results of the disaster damage verification by allowable deformation amount D_a obtained through the disaster damage verification method, reference can be made to the literature 1). When using nonstandard values for the allowable deformation amounts, it is preferable to use them after giving due consideration to the disaster damage verification result.

Table 1.1.1 Structural Types Corresponding to the Classification of the Methods for Calculating the Seismic Coefficients for Verification

Group	Method for calculating seismic coefficient for verification	Typical structural type	Structural type to which the method for calculating the seismic coefficients for verification is applied
1	Equation for seismic coefficient for verification (with reduction rate)	Gravity-type quaywall	Quaywall with relieving platform
			Grounding cellular-bulkhead quaywall
			Upright wave-absorbing–type wharf
			Open-type wharf on vertical piles (earth retaining section)
			Shallow draft wharf
			Revetment (gravity type)
		Sheet pile quaywall	Sheet pile quaywall with batter anchor piles
			Open-type quaywall with sheet pile wall anchored by forward batter piles (sheet pile section)
			Mooring pile
			Revetment (sheet pile type)
		Cantilevered sheet pile quaywall	–
		Double sheet pile quaywall	–
		Embedded cellular-bulkhead quaywall	–

Group	Method for calculating seismic coefficient for verification	Typical structural type	Structural type to which the method for calculating the seismic coefficients for verification is applied
2	Equation for seismic coefficient for verification (without reduction rate)	Gravity-type breakwater (composite breakwater)	Gravity-type breakwater (upright breakwater)
			Gravity-type breakwater (sloping breakwater)
			Breakwater covered with wave-dissipating blocks
			Gravity-type breakwater (upright wave–absorbing block breakwater)
			Gravity-type breakwater (wave-absorbing caisson breakwater)
			Gravity-type breakwater (caisson type sloping breakwater)
			Sediment control groin
			Training jetty
3	Method using acceleration response spectrum	Open-type wharf on vertical piles (main structural work)	Open-type quaywall with sheet pile wall anchored by forward batter piles (piled pier section)
			Open-type wharf on coupled piles
			Panel point strut type piled pier
			Jacket pier
			Dolphin
			Detached pier
			Shallow draft wharf
			Pile type breakwater
		Breast wall	–
4	Method using the maximum ground acceleration	Breakwater sitting on soft ground	–

* "–" means no corresponding structural type.

1.2 Procedure for Calculating Seismic Coefficients for Verification

This section describes the procedure for calculating the seismic coefficients for verification in detail for Groups 1 and 2 in which the seismic coefficients for verification are calculated with filters.

1.2.1 Procedure for Calculating Seismic Coefficients for Verification in Group 1

The procedure for calculating the seismic coefficients for verification[2)] used for verifying the failures of gravity-type quaywalls (with water depths greater than 7.5 m) due to the sliding and overturning of wall bodies, as well as insufficient bearing capacity of the foundation ground under variable situations with respect to Level 1 earthquake motions is described as follows.

(1) For the performance verification of the failures due to the sliding and overturning of wall bodies, as well as insufficient bearing capacity of foundation ground under the variable situation with respect to Level 1 earthquake motions, it is possible to use detailed methods such as nonlinear effective stress analyses that directly evaluate deformation amounts; however, simplified methods such as the seismic coefficient method can also be used. When using the simplified methods in the performance verification, it is necessary to use appropriate seismic coefficients for verification determined in accordance with the deformation amounts of object facilities considering the influences of the frequency characteristics and duration of earthquake ground motions. The general procedure for calculating the seismic coefficients for verification is provided in **Fig. 1.2.1**.

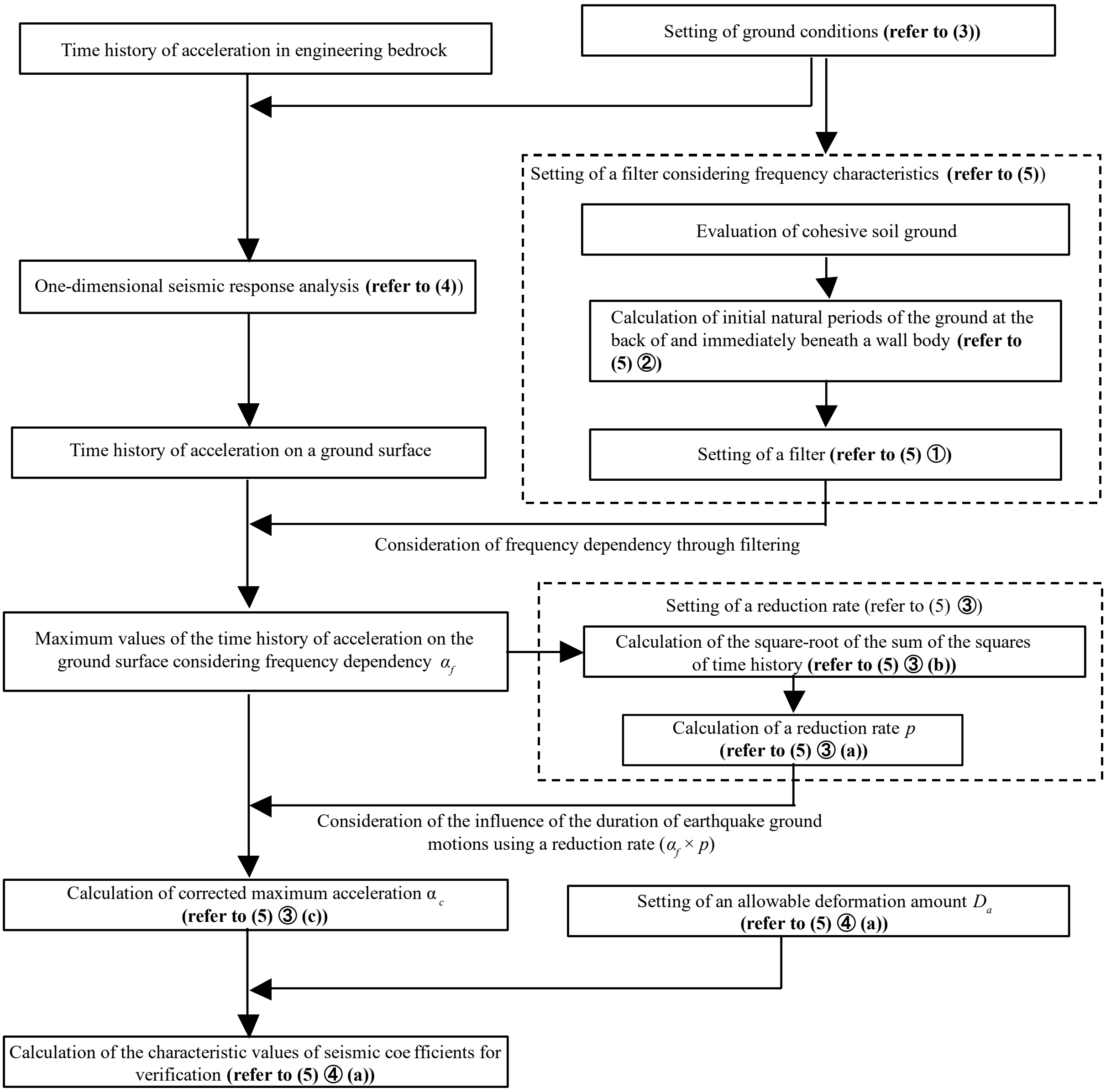

Fig. 1.2.1 Example of the Procedure for Calculating Seismic Coefficients for Verification

(2) The outline of the method for calculating the seismic coefficients for verification is provided in **Fig. 1.2.2**. First, Level 1 earthquake motions in engineering bedrock is set, followed by the calculation of the time history of the acceleration on the ground surface at the back of a gravity-type quaywall through one-dimensional seismic response analysis with Level 1 earthquake motions as input. Next, an acceleration spectrum on the ground surface is obtained through the discrete-time Fourier transformation of the time history of the acceleration and the spectrum is subjected to filtering in consideration of the frequency characteristics in accordance with the deformation of the gravity-type quaywall. The filter used in the filtering is the maximum acceleration on the surface of free ground determined based on the results of the seismic response analyses conducted for plural sine waves with different frequency so that the horizontal displacement of the levee crowns of the gravity-type quaywalls becomes equal to a target value and is also obtained as a result of evaluating the degree of contribution of the waves having respective frequency components constituting earthquake ground motions to the deformation of the quaywalls. Thus, the filtering turns the acceleration spectrum into a uniform deformation spectrum so that the maximum acceleration obtained through the discrete-time Fourier inverse transformation corresponds to a constant deformation amount regardless of the frequency. Then, the maximum acceleration α_f is obtained from the time history of acceleration after the filtering, followed by the calculation of the corrected maximum acceleration α_c on the ground surface with α_f multiplied by the reduction rate p considering the duration of the earthquake ground motions. Last, the characteristic value for the seismic coefficient for verification is calculated using the corrected maximum acceleration α_c and the allowable deformation amount D_a at the levee crown of the quaywall. A different method is

required for calculating the characteristic values for the seismic coefficients for verification when implementing ground improvement through the deep mixing method or the sand compaction pile (SCP) with a replacement rate of 70% or more. In such a case, it is necessary to refer to **Part III, Chapter 2, 5.5 Deep Mixing Method** and **Part III, Chapter 2, 5.10 Sand Compaction Pile Method (for Cohesive Soil Ground)**.

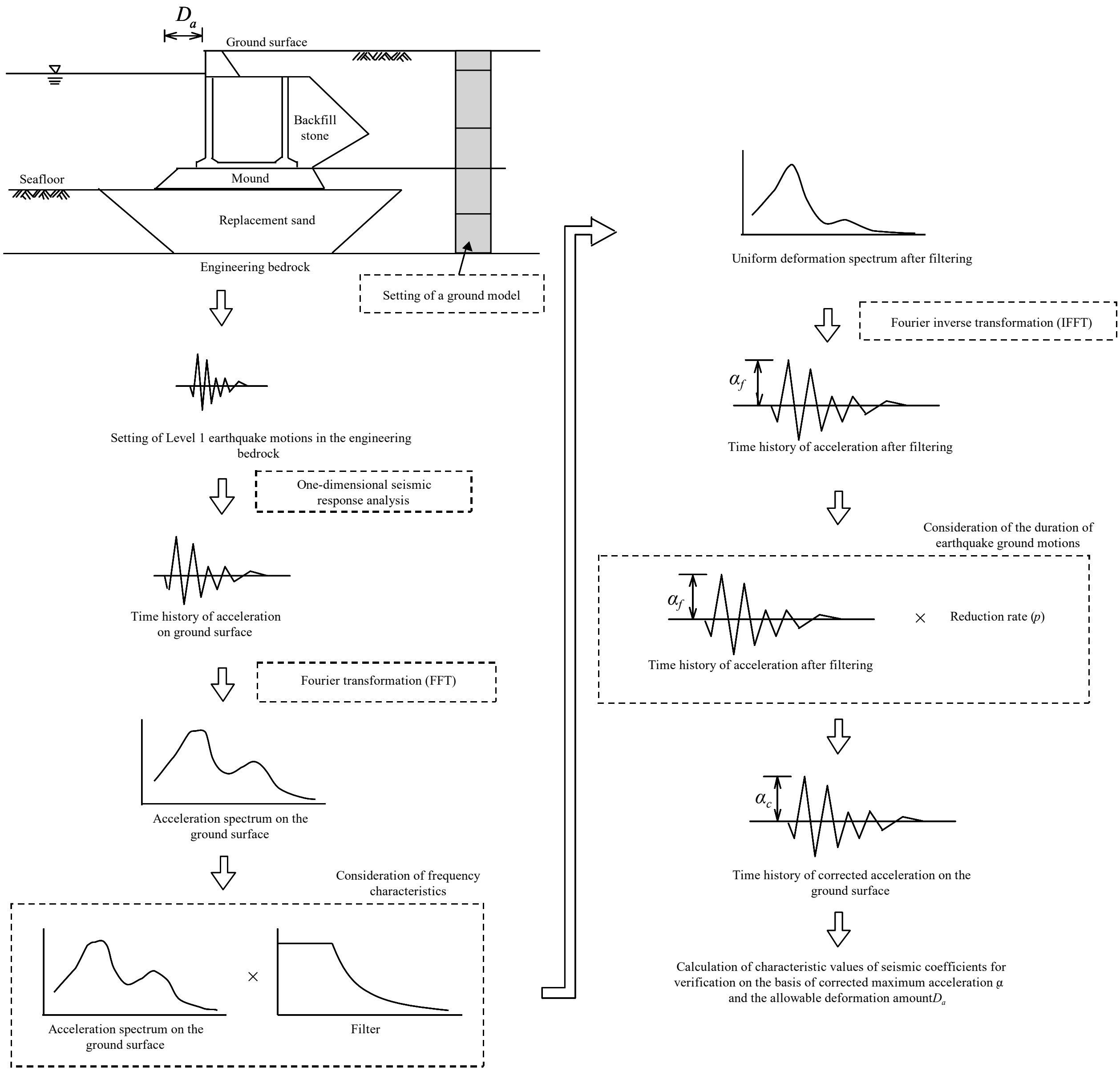

Fig. 1.2.2 Outline of the Method for Calculating Seismic Coefficients for Verification

(3) When calculating seismic coefficients for verification, it is necessary to set ground conditions to appropriately evaluate the ground properties at the location of the quaywall. For the setting of ground conditions, reference can be made to **Part II, Chapter 3 Ground Conditions**, **Part II, Chapter 6, 1.2.3 Seismic Response Calculations of Surface Ground**, and **Reference (Part III), Chapter 1, 2.3.5 Setting of Ground Properties**. As shown in **Fig. 1.2.2**, the ground model used in the one-dimensional seismic response analyses is based on stratified ground without local effects of a mound, backfill stones, and replacement sand.

(4) One-Dimensional Seismic Response Analysis

The time history of the acceleration on the surface of the ground at the back of the quaywall shall be calculated through the one-dimensional seismic response analysis capable of appropriately considering the ground characteristics at the location of the quaywall with Level 1 earthquake motions set in the engineering bedrock as input. The one-dimensional seismic response analysis shall be conducted on the basis of appropriate methods and analysis conditions with reference to **Part II, Chapter 6, 1.2.3 Seismic Response Calculations of Surface Ground** and **Part III, Chapter 5, 2.2.2 Actions (2), (j)**.

(5) Setting of a Filter Considering Frequency Characteristics

① Setting of a filter

The filter obtained through **equation (1.2.1)** can be used as the one that considers the frequency characteristics of the earthquake ground motions for the verification of gravity-type quaywalls. The filter is the maximum acceleration on the surface of free ground determined based on the results of the seismic response analyses conducted for plural sine waves. These analyses are performed using models of quaywalls having different ground conditions and water depths so that the horizontal displacement of the levee crowns of the gravity-type quaywalls becomes equal to a target value and is also obtained as a result of evaluating the contribution degree of the waves having respective frequency components constituting earthquake ground motions to the deformation of the quaywalls. According to the equation, when frequency is high, significantly large earthquake ground motions need to be input to cause a wall body to undergo deformation. In contrast, when frequency is low, earthquake ground motions in a certain frequency range cause a wall body to have equal deformation. That is, because wall bodies are hard to be deformed when frequency is high and easy to be deformed when frequency is low, the filter is composed of a region where a value of *b* is kept constant when frequency is 1.0 Hz or less and a region where a value of *b* drastically decays with the increase in frequency greater than 1.0 Hz, as shown in **Fig. 1.2.3**.

$$a(f) = \begin{cases} b & (0 < f \leq 1.0) \\ \dfrac{b}{1 - \left[0.34(f-1.0)\right]^2 + i6.8\left[0.34(f-1.0)\right]} & (1.0 < f) \end{cases}$$

$$b = 1.05\frac{H}{H_R} - 0.88\frac{T_b}{T_{b_R}} + 0.96\frac{T_u}{T_{u_R}} - 0.23 \qquad \textbf{(1.2.1)}$$

where

a : filter considering the frequency characteristics of earthquake ground motions

f : frequency (Hz)

H : wall height (m)

H_R : reference wall height (= 15.0 m)

T_b : initial natural period of the ground at the back of a wall body (s)

T_{b_R} : reference initial natural period of the ground at the back of a wall body (= 0.8 s)

T_u : initial natural period of the ground beneath a wall body (s)

T_{u_R} : reference initial natural period of the ground beneath a wall body (= 0.4 s)

i : imaginary unit

Here, the value of *b* needs to be set in the range expressed by **equation (1.2.2)** using a height *H* of a wall body provided, however, that the lower limit value of *b* shall be 0.28 in no circumstances regardless of the range defined by **equation (1.2.2)**.

$$0.04H + 0.08 \leq b \leq 0.04H + 0.44$$

$$\text{however,} \quad b \geq 0.28 \qquad \textbf{(1.2.2)}$$

where

H : wall height (m)

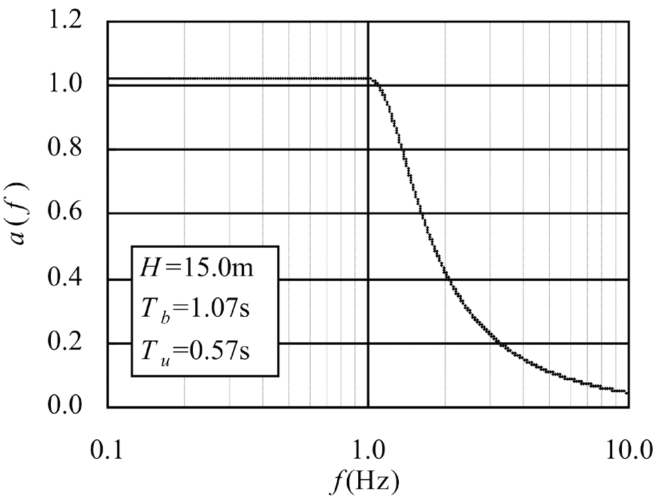

Fig. 1.2.3 Example of a Filter

For other structural types classified as Group 1, the values of b and the filters can be obtained using **equations (1.2.3)** and **(1.2.4)** with the substitution of the coefficients listed in **Table 1.2.1**. The example used for calculating the seismic coefficients for verification in this section is applicable to the gravity-type quaywalls having water depths of −7.5 m or deeper. For the gravity-type quaywalls having water depths less than −7.5 m, the seismic coefficients for verification can be calculated with reference to the coefficients for gravity-type quaywalls (the Fisheries Agency) in **Table 1.2.1**.

$$a(f)=\begin{cases} b & (0<f\le f_c) \\ \dfrac{b}{1-\left[\xi_1\left(f-f_c\right)\right]^2+i\,\xi_2\,\xi_1\left(f-f_c\right)} & (f_c<f) \end{cases} \tag{1.2.3}$$

$$b=\xi_3\frac{H}{H_R}+\xi_4\frac{T_b}{T_{b_R}}+\xi_5\frac{T_u}{T_{u_R}}+\xi_6\frac{k}{k_R}+\xi_7$$

$$\xi_8 H+\xi_9\le b\le \xi_8 H+\xi_{10}$$
$$\text{however,}\qquad b\ge \xi_{11} \tag{1.2.4}$$

where

• Cantilevered sheet pile quaywall

k : lateral resistance constant of ground (C-type ground: kN/m$^{2.5}$, S-type ground: kN/m$^{3.5}$)

k_R : reference value of a lateral resistance constant of ground (C-type ground: kN/m$^{2.5}$, S-type ground: kN/m$^{3.5}$)

• Embedded cellular-bulkhead quaywall

k : coefficient of lateral subgrade reaction (MN/m^3)

k_R : reference value of a coefficient of lateral subgrade reaction (MN/m^3)

Table 1.2.1 List of Coefficients Related to Filter

Item	Gravity-type quaywall	Gravity-type quaywall (Fisheries Agency)	Sheet pile quaywall with vertical anchor piles	Sheet pile quaywall with coupled anchor piles	Cantilevered sheet pile quaywall	Double sheet pile quaywall	Embedded cellular-bulkhead quaywall
Basis material	National Institute for Land and Infrastructure Management No. 310[2]	Reference for the Design of Fishery Port and Ground Facilities[3]	National Institute for Land and Infrastructure Management No. 310[2]		National Institute for Land and Infrastructure Management No. 454[4]		National Institute for Land and Infrastructure Management No. 562[5]
Object water depth (m)	−7.5 m or deeper	Less than −7.5 m	–				
Object wall height (m)	-				4.0 m or more	-	
f_c (Hz)	1.0	1.2	1.0		1.5	1.0	
ξ_1	0.34	0.099	0.34				
ξ_2	6.8	18.5	11.0		4.5	11.0	8.8
ξ_3	1.05	0.43	2.25		2.97	2.4	1.09
ξ_4	−0.88	1.33	−0.88				
ξ_5	0.96	−0.66	0.96				
ξ_6	–				0.32	–	−0.03
ξ_7	−0.23	0.32	−0.96	−0.76	−1.18	−0.97	−0.34
ξ_8	0.04	–	0.12		0.35	0.12	0.04
ξ_9	0.08	–	−0.78		−0.47	−0.66	−0.13
ξ_{10}	0.44	–	−0.24	−0.04	0.59	−0.17	0.39
ξ_{11}	0.28		0.41		–	0.41	0.30
H_R (m)	15.0				8.0	15.0	
T_{bR} (s)	0.8						
T_{uR} (s)	0.4						
k_R	–				C-type ground: 1000 (kN/m$^{2.5}$); S-type ground: 550 (kN/m$^{3.5}$)	–	12.65 (MN/m^3)

* "–" means no corresponding item.

② **Calculation of the natural periods of the ground at the back and immediately beneath a wall body**

The natural period used in **equation (1.2.1)** can be calculated by **equation (1.2.5)** using the thicknesses of respective layers on the engineering bedrock set for the one-dimensional seismic response analysis and shear wave velocities. Also, the natural period of ground can be the primary natural period of the frequency response function obtained by using the linear multiple reflection theory. When the shear wave velocities are not available, they can be estimated from *N*-values of ground with reference to **Part II, Chapter 3, 2.4 Dynamic Analyses**. Provided, however, that the initial natural period of the ground at the back of the wall body T_b and immediately beneath the wall body T_u shall be calculated not by using the physical properties of backfill stones and rubble immediately beneath the wall body as they are but by replacing them with those of the original ground. Also, in the case of partially improving the ground in a manner that replaces the normal consolidated cohesive soil layer just beneath the wall body of a gravity-type quaywall with replacement sand, the values of T_b and T_u shall be calculated with the ground in the state before the improvement. That is, it is necessary to calculate T_b and T_u of the locations shown in **Fig. 1.2.4**. In addition, the natural period of the ground below the seafloor cannot be used, because such ground has different effective surcharge loads from the portions of the ground indicated in **Fig. 1.2.4** used for calculating T_b and T_u.

$$T = 4\sum_i \frac{H_i}{V_{s_i}} \qquad \textbf{(1.2.5)}$$

where

T : natural period of ground (s)

H_i : thickness of layer i (m)

V_{S_i} : shear wave velocity of layer i (m/s)

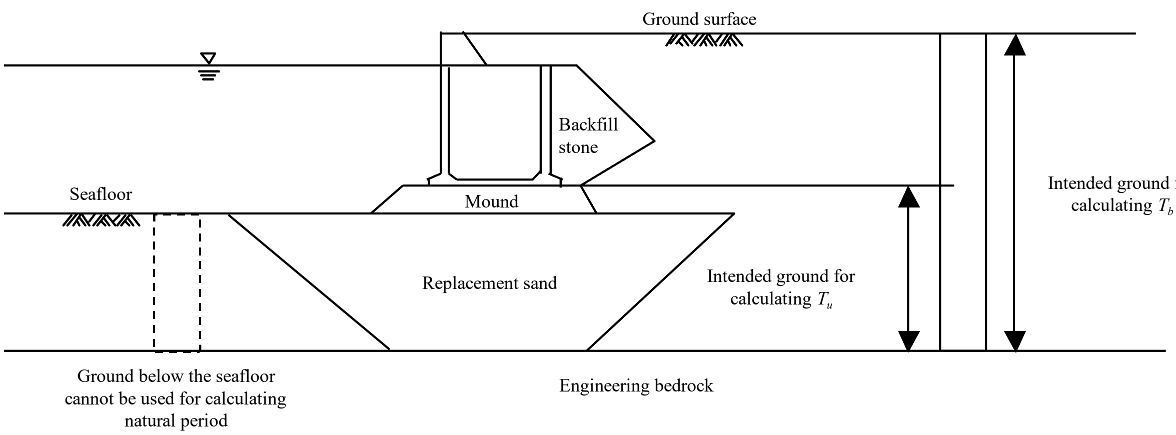

Fig. 1.2.4 Intended Ground for Calculating Natural Period

③ Setting of a reduction rate

(a) Calculation of a reduction rate

Even earthquake ground motions having identical maximum acceleration can cause different damage to facilities depending on their duration. The reduction rate *p* considering the influence of the duration of earthquake ground motions can be calculated by **equation (1.2.6)** using the square-root of the sum of the squares of time history *S* of the acceleration on the ground surface after filtering and maximum acceleration α_f. This equation is statistically obtained on the basis of the abovementioned numerical analysis results. It shall be noted that the reduction rate is capped at 1.0.

$$p = 0.36 \ln\left(\frac{S}{\alpha_f}\right) - 0.29 \tag{1.2.6}$$

where

p : reduction rate ($p < 1.0$)

S : square root of the sum of the squares of time history of the acceleration after filtering (cm/s^2)

α_f : maximum acceleration after filtering (cm/s^2)

The reduction rates of other structural types classified as Group 1 can be calculated by **Equation (1.2.7)** using the coefficients listed in **Table 1.2.2**. For the gravity-type quaywalls having water depths less than −7.5 m, the same reduction rate as gravity-type quaywalls having water depths of −7.5 m or deeper can be used as shown in the column of gravity-type quaywall (Fisheries Agency) of **Table 1.2.2**.

$$p = \eta_1 \ln\left(\frac{S}{\alpha_f}\right) + \eta_2 \tag{1.2.7}$$

Table 1.2.2 List of Coefficients for Calculating Reduction Rates

Item	Gravity-type quaywall	Gravity-type quaywall (Fisheries Agency)	Sheet pile quaywall with vertical anchor piles	Sheet pile quaywall with coupled anchor piles	Cantilevered sheet pile quaywall	Double sheet pile quaywall	Embedded cellular-bulkhead quaywall
Basis material	National Institute for Land and Infrastructure Management No. 310[2]	Reference for the Design of Fishery Port and Ground Facilities[3]	National Institute for Land and Infrastructure Management No. 310[2]		National Institute for Land and Infrastructure Management No. 454[4]		National Institute for Land and Infrastructure Management No. 562[5]
Object water depth (m)	−7.5 m or deeper	Less than −7.5 m	-				
Object wall height (m)	-				4.0 m or more	-	
η_1	0.36			0.31	0.39	0.35	0.31
η_2	−0.29		−0.20	−0.10	−0.42	−0.20	−0.08

* "—" means no corresponding item.

(b) Calculation of the square-root of the sum of the squares of time history

The square-root of the sum of the squares of time history S of acceleration used for calculating the reduction rate can be obtained by **equation (1.2.8)** using the time history of acceleration on ground surface after filtering. It shall be noted that the square-root of the sum of the squares of time history needs to be calculated on the basis of the total duration of earthquake ground motions with a sampling frequency of 100 Hz.

$$S = \sqrt{\sum acc^2} \tag{1.2.8}$$

where

S : square-root of the sum of the squares of the time history of acceleration (cm/s^2)

acc : acceleration after filtering at respective times (cm/s^2)

(c) Calculation of corrected maximum acceleration

The corrected maximum acceleration α_c can be calculated by **equation (1.2.9)** using the maximum acceleration α_f considering the frequency characteristics of earthquake ground motions on the ground surface after filtering and the reduction rate p considering the influence of duration.

$$\alpha_c = p\alpha_f \tag{1.2.9}$$

where

α_c : corrected maximum acceleration (cm/s^2)

α_f : maximum acceleration after filtering (cm/s^2)

p : a reduction rate

④ **Calculation of the characteristic values of seismic coefficients for verification**

(a) Characteristic values of seismic coefficients for verification

The characteristic values k_{h_k} of the seismic coefficients for verification used for the performance verification of gravity-type quaywalls can be calculated by **equation (1.2.10)** using the corrected maximum acceleration α_c described in ③ (c) and the allowable deformation amount D_a at the levee crowns of quaywalls. It shall be noted that the seismic coefficients for verification need to be rounded to the nearest hundredths of a unit. When calculating the seismic coefficients for verification for the ground improvement through the deep mixing method or the sand compaction pile (SCP) with a replacement rate of 70% or more, reference can be made, respectively, to **Part III, Chapter 2, 5.5.3 Conditions for**

Actions on Stabilized Bodies (6) and **Part III, Chapter 2, 5.10.5 Characteristic Values of Seismic Coefficient for Verification of Gravity-Type Quaywalls with Ground Improvement (1)**.

$$k_{h_k} = 1.78 \left(\frac{D_a}{D_r} \right)^{-0.55} \frac{\alpha_c}{g} + 0.04 \tag{1.2.10}$$

where

k_{hk} : characteristic value of the seismic coefficient for verification

α_c : corrected maximum acceleration (cm/s^2)

g : gravitational acceleration (= 980 cm/s^2)

D_a : allowable deformation at the levee crown of a quaywall (= 10 cm)

D_r : reference deformation (= 10 cm)

The seismic coefficients for verification of other structural types classified as Group 1 can be calculated by **equation (1.2.11)** using the coefficients listed in **Table 1.2.3**. For the gravity-type quaywalls having water depths less than −7.5 m, the same seismic coefficients for verification as gravity-type quaywalls having water depths of −7.5 m or deeper can be used as shown in the column of gravity-type quaywall (Fisheries Agency) of **Table 1.2.3**.

$$k_{h_k} = \zeta_1 \left(\frac{D_a}{D_r} \right)^{\zeta_2} \frac{\alpha_c}{g} + \zeta_3 \tag{1.2.11}$$

Table 1.2.3 List of Coefficients for Calculating Seismic Coefficients for Verification

Item	Gravity-type quaywall	Gravity-type quaywall (Fisheries Agency)	Sheet pile quaywall with vertical anchor piles	Sheet pile quaywall with coupled anchor piles	Cantilevered sheet pile quaywall	Double sheet pile quaywall	Embedded cellular-bulkhead quaywall
Basis material	National Institute for Land and Infrastructure Management No. 310[2]	Reference for the Design of Fishery Port and Ground Facilities[3]	National Institute for Land and Infrastructure Management No. 310[2]		National Institute for Land and Infrastructure Management No. 454[4]		National Institute for Land and Infrastructure Management No. 562[5]
Object water depth (m)	− 7.5 m or deeper	Less than −7.5 m	-				
Object wall height (m)	-				4.0 m or more	-	
Reference value of D_a (cm)	10		15		20	15	10
Dr (cm)	10						
ζ_1	1.78		1.91	1.32	1.40	1.91	1.62
ζ_2	–0.55		–0.69	–0.74	–0.86	–0.69	–0.58
ζ_3	0.04		0.03	0.05	0.06	0.03	0.04

* "–" means no corresponding item.

1.2.2 Procedure for Calculating Seismic Coefficients for Verification in Group 2

The following are the descriptions of the procedure for calculating the seismic coefficients for verification[6] used for verifying the failures of gravity-type breakwaters (composite breakwaters) due to the sliding and overturning of upright sections, as well as the insufficient bearing capacity of the foundation ground with respect to Level 1 earthquake motions.

(1) General

For the performance verification of the failures due to the sliding and overturning of upright sections, as well as the insufficient bearing capacity of the foundation ground under the variable situation with respect to Level 1 earthquake motions, it is possible to use detailed methods such as the dynamic analysis method, which directly evaluate deformation amounts; however, simplified methods such as the seismic coefficient method can also be used. When using the simplified methods in the performance verification, it is necessary to use appropriate seismic coefficients for verification determined in accordance with the deformation amounts of object facilities considering the frequency characteristics of earthquake ground motions. The seismic coefficients for verification are generally smaller than the acting seismic coefficients (α_{max}/g), which are the ratios of the maximum values of the time history of acceleration α_{max} on the bottom faces of caissons obtained through the one-dimensional seismic response analyses with Level 1 earthquake motions in engineering bedrock as input to the gravitational acceleration g.

Fig. 1.2.5 presents the outline of the procedure for calculating the seismic coefficients for verification. First, Level 1 earthquake motions in engineering bedrock are set, followed by the calculation of the time history of the acceleration on the bottom face of a caisson through one-dimensional seismic response analysis with Level 1 earthquake motions as input. Next, the time history of acceleration after filtering on the bottom face of a caisson is calculated in a manner that multiplies the time history of acceleration subjected to the discrete-time Fourier transformation by a filter considering the frequency characteristics of earthquake ground motions. Then, the characteristic values of seismic coefficients for verification can be calculated using the maximum value of the time history of acceleration after filtering.

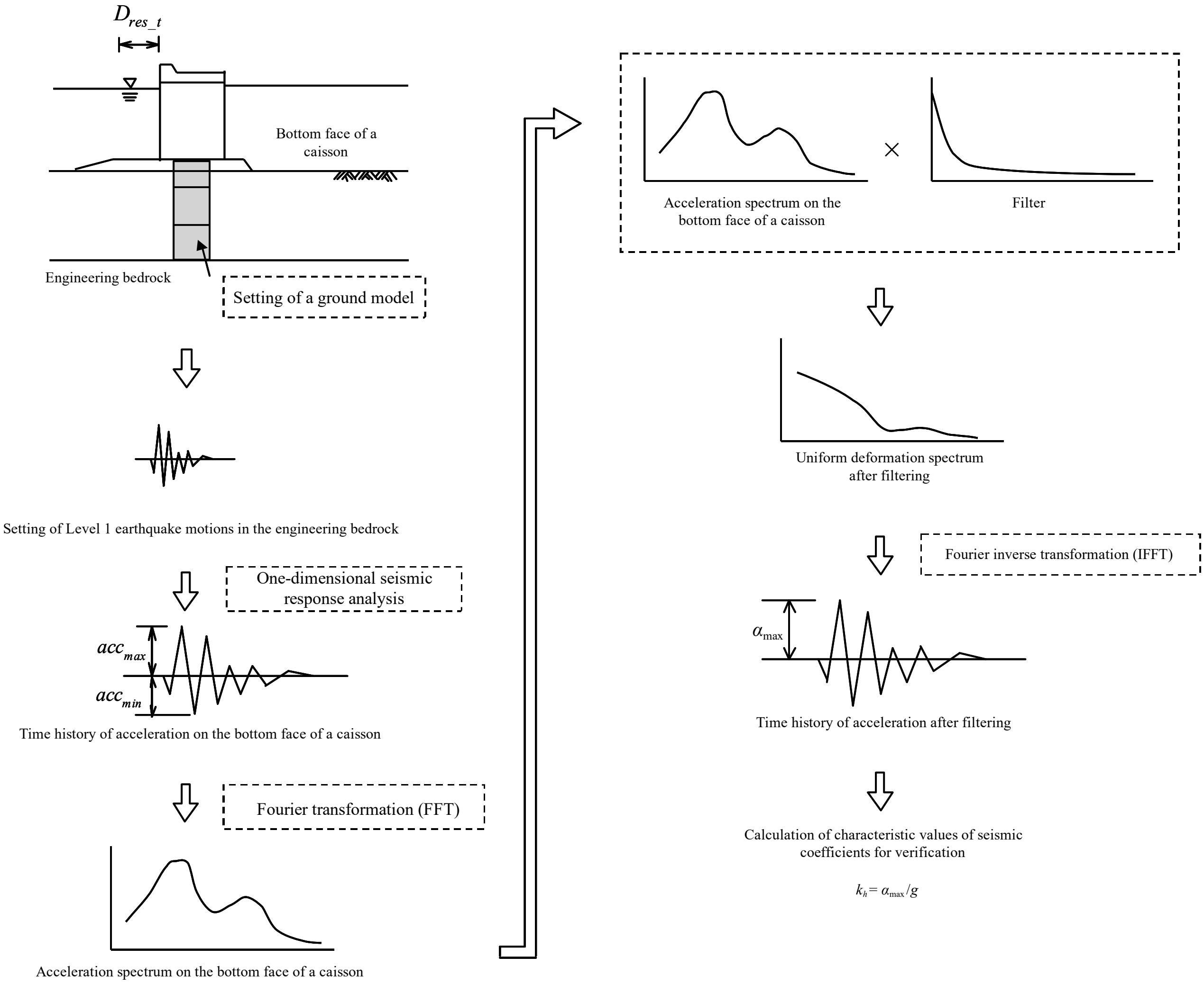

Fig. 1.2.5 Outline of the Method for Calculating Seismic Coefficients for Verification

(2) Setting of Ground Conditions

When calculating the seismic coefficients for verification, it is necessary to set ground conditions to appropriately evaluate the ground properties at the location of a breakwater. For the setting of ground conditions, reference can be made to **Part II, Chapter 3 Ground Conditions**, **Part II, Chapter 6, 1.2.3 Seismic Response Calculations of Surface Ground**, and **Reference (Part III), Chapter 2, 2.3.5 Setting of Ground Properties**.

(3) One-Dimensional Seismic Response Analysis

The time history of acceleration on the bottom face of a caisson can be calculated through the one-dimensional seismic response analysis capable of appropriately considering the ground properties at the location of a breakwater with Level 1 earthquake motions in the engineering bedrock as input. The one-dimensional seismic response analysis shall be conducted on the basis of appropriate methods and analysis conditions with reference to **Part II, Chapter 6, 1.2.3 Seismic Response Calculations of Surface Ground**.

(4) Setting of Filter Considering Frequency Characteristics and Deformation

① Setting of maximum deformation

Because of the frequency characteristics of earthquake ground motions and the influence of cyclic actions unique to breakwaters, they have different deformation accumulation processes from quaywalls. Therefore, the residual deformation of breakwaters cannot be directly evaluated in the calculation of the seismic coefficients for verification. Therefore, by defining the maximum deformation as the largest deformation caused by one of seismic waves of earthquake ground motions, a filter can be calculated to obtain the constant maximum deformation at any frequency. Here, depending on the presence or absence of friction enhancement mats, the relationship between the maximum deformation D_{max} and the target values of residual deformation D_{res_t} can be expressed by **equation (1.2.12)**. According to the equation, the maximum deformation can be calculated once the residual deformation is known. Also, a value of 30 cm can be set for the allowable value of standard deformation D_{res_t} of breakwaters with respect to Level 1 earthquake motions and the shape of the filter in such a case can be as shown in **Fig. 1.2.6**.

$$D_{max} = \begin{cases} \dfrac{D_{res\_t}}{0.87\,R_{acc} + 0.52} & \text{(with a friction enhancement mat)} \\ \dfrac{D_{res\_t}}{0.87\,R_{acc} + 0.44} & \text{(without a friction enhancement mat)} \end{cases} \qquad \textbf{(1.2.12)}$$

$$R_{acc} = \frac{\left| acc_{max} + acc_{min} \right|}{\max\left\{ acc_{max}, \left| acc_{min} \right| \right\}}$$

where

D_{max} : maximum deformation (cm)

D_{res_t} : target value of residual deformation (= 30 cm)

acc_{max}, acc_{min} : maximum and minimum values of the time history of acceleration on the bottom face of a caisson (cm/s^2)

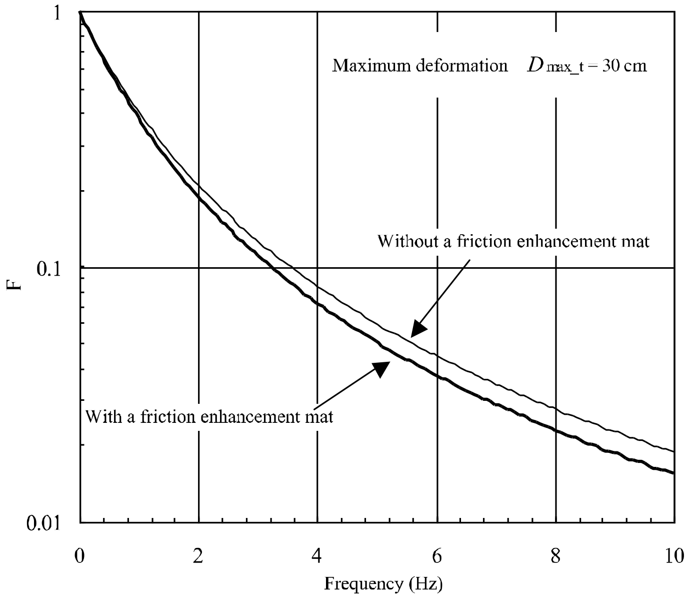

Fig. 1.2.6 Filter for Calculating the Seismic Coefficients for Verification

② **Setting of a filter**

The filter considering the frequency characteristics of the earthquake ground motions and deformation to be used in the performance verification of breakwaters can be calculated using the maximum deformation obtained in ① and substituting the coefficients listed in **Table 1.2.4** into **equation (1.2.13)**. The filter is the relationship between the maximum deformation of object breakwater caissons and the maximum input acceleration on the bottom faces of the caissons obtained through the seismic response analyses of a single-degree-of-freedom system using models of quaywalls having different ground conditions and water depths subjected to plural sine waves. Also, the filter is obtained as a result of evaluating the degree of contribution of the waves having respective frequency components constituting earthquake ground motions to the deformation of the breakwaters. **Fig. 1.2.6** shows the shape of a filter in the case of D_{res_t} = 30 cm.

$$F = \frac{1}{a f^2 + b f + 1}$$

$$\begin{cases} a = \xi_1 D_{max} + \xi_2 \\ b = \xi_3 D_{max} + \xi_4 \end{cases} \qquad \textbf{(1.2.13)}$$

where

F : filter for calculating a seismic coefficient for verification

f : frequency (Hz)

a, b : coefficients

D_{max} : maximum deformation (cm)

Table 1.2.4 List of Coefficients Related to Filter

Item	Friction enhancement mat	
	Presence	Absence
ξ_1	0.0145	0.0178
ξ_2	−0.022	−0.0035
ξ_3	0.0074	0.0095
ξ_4	0.8542	0.8174

③ **Calculation of characteristic values of seismic coefficients for verification**

The seismic coefficients for verification used in the performance verification of breakwaters can be calculated by **equation (1.2.14)**.

$$k_h = \frac{\alpha_{max}}{g} \tag{1.2.14}$$

where

α_{max} : maximum value of the acceleration on the bottom face of a caisson after filtering (cm/s^2)

g : gravitational acceleration (cm/s^2)

1.2.3 Procedure for Calculating Seismic Coefficients for Verification in Group 3

For the procedure for calculating the seismic coefficients for verification used in the performance verification of open-type wharves on vertical piles and breast walls with respect to Level 1 earthquake ground motions, reference can be made to **Part III, Chapter 5, 5.2.3 Actions ⑭** and **Part III, Chapter 4, 17.5.1 Performance Verification (2)**, respectively.

1.2.4 Procedure for Calculating Seismic Coefficient for Verification in Group 4

For the procedure for calculating the seismic coefficients for verification used in the performance verification of breakwaters sitting on soft ground with respect to Level 1 earthquake ground motions, reference can be made to **Part III, Chapter 4, 3.9.2**.

[References]

1) Fukunaga, Y., Miyata, M., Takenobu, M., Nozu, A., Kohama, E.: Evaluation of the applicability of equation for seismic coefficient for verification by verifying damaged gravity-type and sheet pile quaywalls, National Institute for Land and Infrastructure Management document No. 920, 2016.

2) Nagao, T., Iwata, N., Fujimura, K., Morishita, N., Sato, H., Ozaki, R.: Setting method of seismic coefficients for performance verification of earthquake-resistance of gravity-type and sheet pile quaywalls against level 1 earthquake ground motions, National Institute for Land and Infrastructure Management document No. 310, 2006.

3) Fisheries Agency: Reference Book for Designing Fishing Ports and Fishing Ground Facilities, 2015.

4) Tsukiji, K., Tagawa, S., Nagao, T.: Setting method of seismic coefficients for performance verification of earthquake-resistance of cantilevered and double sheet pile quaywalls against level 1 earthquake ground motions, National Institute for Land and Infrastructure Management document No.454, 2008.

5) Shibata, D., Nagao, T.: Setting method of seismic coefficients for performance verification of earthquake-resistance of embedded cellular-bulkhead quaywalls against level 1 earthquake ground motions, National Institute for Land and Infrastructure Management document No.562, 2010.

6) Nagao, T., Ozaki, R.: Study on earthquake-resistance performance design of caisson type breakwater, Proceedings of structural engineering Vol.50A, pp.217-228, 2004.

2 Basic Points of Seismic Response Analyses

2.1 General

This material describes the general concepts and technical details of the verification of deformation through seismic response analyses. There are several types of seismic response analyses, such as the equivalent linear analysis, which is generally used for the calculation of equivalent acceleration for the prediction and determination of liquefaction, and the one-dimensional total stress truly nonlinear analysis, which is generally used for the calculation of seismic intensity in the performance verification of earthquake-resistance through the seismic coefficient method. This material also describes seismic response analyses that use a formulation based on the effective stresses of soil, the finite element method, and the step-by-step integration method, as well as examples of analyses and designs using a program called "FLIP" (Finite Element Analysis Program of Liquefaction Process).

The FLIP is a two-dimensional seismic response analysis program based on the effective stress method developed by the Port Research Institute of the Ministry of Transport in 1988.[1), 2)] The FLIP is capable of deformation analyses while taking into consideration the liquefaction phenomenon of the ground as a factor that causes earthquake damage to port structures, and the dynamic interactions between fluids such as seawater, structural members such as sheet piles and pipe piles, and between the ground and structural members. In 1997, the first FLIP (Ver. 3.3) was published as a program for predicting structural damage due to liquefaction by the Coastal Development Technology Center.[3)] Since then, the FLIP has been improved through development of the three-dimensional analysis method and constitutive laws, and there have been examinations of the applicability of the FLIP to earthquake damage analyses.

2.2 Outline of the Verification of Deformation and Its Use in Design

2.2.1 Purposes and Methods of the Verification of Deformation

Generally, whether or not port facilities that are to be design objects maintain the required performance when subjected to Level 2 earthquake ground motions can be determined by appropriately implementing the performance verification of earthquake-resistance. Then, in the performance verification of the earthquake-resistance of port structures subjected to Level 2 earthquake ground motions, the deformation of the facilities is verified through the appropriate seismic response analyses or shake table tests. Even for those structures for which not only deformation but also stresses and strains in members pose problems, it is necessary to understand the degree of ground deformation because the behavior of port structures during an earthquake is largely affected by the deformation of the foundation ground (including structures when the structures consist of ground).

The methods for performance verification with respect to the deformation of facilities are largely twofold: the seismic response analysis (numerical calculations using computers) and model experiments using shaking tables. Generally, technical skills are required for accurate implementation of the model experiments. In addition, because the model experiments require high costs and a large amount of time in many cases, it is difficult to implement the model experiments many times for a large number of cross sections. Thus, seismic response analyses have been frequently used for verifying the deformation of facilities.

However, it is necessary to examine the applicability of the seismic response analyses before using them. In cases where there is a concern about the applicability of the seismic response analyses to new types of structures, it is necessary to select the appropriate analysis methods after examining the applicability of the seismic response analyses in a manner that implements model experiments and compares the results of the seismic response analyses with those of the model experiments and past earthquake damage cases.

The seismic response analyses can be classified into several types depending on the modeling concepts. For example, for the prediction and determination of liquefaction and the prediction of the deformation behavior of the soil, the seismic response analyses are classified into those based on the effective stress method and those based on the total stress method.

There are many cases where the prediction of the deformation of port structures during an earthquake requires the examination of the reduction in the effective stress of the soil due to the generation of excess pore water pressure in the ground (the state of the soil when its effective stress is extremely reduced is called liquefaction). This is because the changes in the stress states of the soil, including the reduction in the effective stress, affect the response characteristics of the ground in the forms of changes in the restoring force and damping of the soil, and the deformation characteristics of the ground in the forms of changes in the stress-strain relationships of the soil.

The seismic response analyses based on the effective stress method can directly calculate the excess pore water pressure to be generated in the ground. In contrast, the seismic response analyses based on the total stress method cannot calculate the changes in excess pore water pressure. Thus, when predicting the seismic responses of the ground with a certain degree of excess pore water pressure (approximately 0.5 or more, although the value fluctuates depending on the conditions), the seismic response analyses based on the total stress method have a high possibility of producing calculation results that are widely different from the actual seismic responses of the ground. Easy-to-use seismic response analyses based on the total stress method can be used for simple seismic response calculations for practical purposes, but the seismic response analyses based on the effective stress method are basically used for the verification of the deformation of port structures, which have a high possibility of undergoing liquefaction.

Depending on the object regions to be examined, the seismic response analyses can also be classified into one-dimensional, two-dimensional and three-dimensional types. The one-dimensional seismic response analyses are often used when examining ground that has stratified structures with extensive planar deposit of soil. However, seismic response analyses with higher dimensions are required for examining those facilities that have two- or three-dimensional structures, which are generally the objects of the verification of deformation. The two-dimensional seismic response analyses are generally used for the verification of deformation of structure-ground systems, such as quaywalls, which can be considered to have uniform structures in the depth directions. Even in the case of regions that include structures like piles, although they are supposed to be examined as three-dimensional structures, they are often approximated as two-dimensional structures using special elements such as pile-ground interaction springs.[4)] Although there are cases of using the three-dimensional seismic analyses for important structures and research purposes, they have not been practical methods for the verification of deformation because of constraints related to complex modeling and long calculation times.

The modeling of the material nonlinear behaviors of the soil that make up the ground is important when evaluating the deformation amounts of the ground. Here, the systems that regulate the behavioral characteristics of the soil, such as the stress-strain relationship, are called constitutive laws. Soil shows a linear stress-strain relationship while the shear strain remains at a relatively low level during an earthquake, but shows a remarkably nonlinear relationship when the shear strain exceeds a moderate level or is at a high level. Thus, the verification of the soil deformation requires constitutive laws that can deal with the nonlinearity of the stress-strain relationship.

In terms of the applicability to the material nonlinearity of the ground, the seismic response analyses can be classified into the linear seismic response analysis method, which does not consider the material nonlinearity of the ground, the equivalent linear seismic response analysis method, which applies linear analyses to the ground using material constants corresponding to the strain levels of the ground, and the nonlinear seismic response analysis method, which considers nonlinear stress-strain relationships up to a high shear strain level. However, considering that the purpose of the verification of deformation is to examine the residual deformation of the ground, the verification of deformation needs to be examined, not through the linear and the equivalent linear seismic response analysis methods, but through the nonlinear seismic response analysis method, which is capable of dealing with the nonlinear constitutive model of the ground.

The analysis results of the nonlinear seismic response analysis method require technical reviews and evaluations from skilled engineers to determine their appropriateness, even when these results are obtained through an analysis method that uses advanced constitutive laws with the deformation amounts of the ground and the changes in member stresses along with the deformation of the ground estimated in the analyses. Generally, it is quite possible to roughly estimate the ground deformation when the seismic response analysis method and model are appropriately selected, and a numerical analysis is stably executed. However, the seismic response analyses cannot ensure prediction accuracy for detailed amounts in the analysis results. Thus, there is no engineering significance in pursuing economic cross sections with the amounts of deformation close to the amounts allowable through repeatedly calculating the amounts of deformation by changing the cross-sectional shapes, ground improvement areas and member strength in detail. That is, the verification of deformation for Level 2 earthquake ground motions is preferably considered as a process of applying an advanced engineering evaluation to the determination of the appropriateness of the structural design on the assumption that the allowable ground deformation amounts and calculated prediction amounts fluctuate to some extent.

Basically, the soil parameters can be set by selecting the most reliable values from the data obtained through soil tests. In general, there is no necessity for repeated analyses to find the most severe conditions for the object facilities by changing the soil parameters within reasonably applicable ranges because such conditions cause the design of the facilities to be excessively on the safe side for Level 2 earthquake ground motions.

2.2.2 Selection Method Concept for the Verification of Deformation

The "Bases for design of structures—Seismic actions for designing geotechnical works (ISO 23469)" requires that the earthquake-resistant performance of the geotechnical works be evaluated through the most appropriate analysis method selected in terms of the following aspects:[5)]

(1) available data;

(2) the degree of importance and performance targets;

(3) the performance verification parameters; and

(4) the degrees of complexity and nonlinearity.

Similarly, in the verification of the deformation of port structures, the analysis methods need to be selected in terms of the performance criteria for the verification of deformation such as the quality and quantities of data, including the progress of the ground surveys, the degree of importance and allowable deformation of the structures, the horizontal displacement and subsidence of the quaywall levee crowns and the inclinations of the quaywalls; the degree of complexity; and the possibility of liquefaction.

In ISO 23469, the seismic response analyses are classified into: (1) the equivalent static method and (2) the dynamic method, depending on whether or not dynamic responses are directly calculated; and (A) the simplified method and (B) the detailed method, depending on whether or not the interaction of a ground-structure system is incorporated in the model.[5)] Thus, according to ISO 23469, all the analysis methods are fourfold: (1-A) the simplified equivalent static analysis method; (1-B) the detailed equivalent static analysis method; (2-A) the simplified dynamic analysis method; and (2-B) the detailed dynamic analysis method. Several methods have been proposed for the verification of deformation of port structures, but applying the classification method used in ISO 23469 can facilitate the determination of the appropriateness and selection of the methods.

2.2.3 Interpretation of the Results of the Verification of Deformation

In the verification of deformation, a careful engineering determination is required not only for the appropriateness of implementing numerical analyses, but also for the interpretation of the analysis results. Particularly, it is necessary to determine whether or not the analysis object structures have the required earthquake-resistant performance by taking the following points into consideration.

(1) Concept of allowable deformation values

The types of values to be output as numerical analysis results include acceleration, velocity, displacement, stress and strain. Generally, in a design based on the results of the finite element method, the analysis results are evaluated with a focus on displacement.[6)] However, it shall be noted that the reliability and accuracy of the analysis results vary depending on the types of values to be output.

For example, the items for examining the serviceability of gravity-type quaywalls include the level differences behind the quaywalls and the meandering (convex and concave amounts) of the face lines of the quaywalls.[7)] However, when predicting the level differences behind quaywalls, the accuracy of the prediction results is considered to be reduced because the prediction of the behavior of the ground close to surfaces and structural members is more difficult than the prediction of, for example, the seaward displacement and subsidence of the quaywalls. In addition, evaluations of the meandering of the face lines of quaywalls in two-dimensional seismic response analyses are practically difficult because such evaluations are equivalent to evaluations of the variation of analysis results in the depth directions of the analysis cross sections. Thus, focusing on the fact that the seaward displacement amounts of the quaywall levee crowns is one of the damage cases for which the seismic response analyses have high reproducibility, it is acceptable to employ a method which uses the seismic response analyses as a means to output the seaward displacement amounts of the levee crowns and indirectly estimates the indexes specifying the performance of the facilities, such as serviceability, from the seaward displacement of the levee crowns based on past damage cases. For example, it is preferable to evaluate indexes specifying the performance of the facilities using the correlation between the maximum seaward displacements of face lines and the degrees of meandering of face lines which have been under examination[7)].

In this way, when verifying the deformation based on the seismic response analysis results, it is necessary not to verify simply by the amounts from the calculation results but to comprehensively verify while taking into consideration the characteristics of the output values of the calculation results, for example, through the analyses of the deformation modes.

(2) Variation in the deformation of actual damage and analysis accuracy

The applicability of the FLIP to the verification of the deformation of gravity-type quaywalls has been confirmed through reproductive analyses of damage due to the 1995 Hyogo-ken Nambu Earthquake.[for example 8), 9)] As an example, this section focuses on the case of damage to Quaywall No. RF3 (with a water depth of -8.5 m and design seismic coefficient of 0.15, and foundation improvements through excavation and replacement) on Rokko Island, Kobe Port. **Fig. 2.2.1** and **Table 2.2.1** show the typical cross section and dimensions of the examination object quaywall, respectively. In addition, **Figs. 2.2.2** and **2.2.3** show the layout of the damage situations summarized in the **Reference 10)** and A-A cross section indicated in the layout, respectively. Furthermore, **Fig. 2.2.4** shows the seaward displacement and subsidence of the superstructure levee crowns on Caissons Nos. 7 to 21 shown in the layout of the damage situations, as well as the inclination angles of these caissons, and **Table 2.2.1** summarizes the damage situations of the quaywall.

As can be seen in **Fig. 2.2.4**, each caisson had slightly different deformation amounts. The typical damage to the caissons due to the Hyogo-ken Nambu Earthquake was uniform seaward displacement. Although the seaward displacement was uniform along the face line of the quaywall compared to past damage cases, there was a wide difference in the displacement between the corner sections and the central section of the berth. In addition, there was also a slight difference in displacement among the caissons located at the central section of the berth, where the displacement was maximized. Thus, when determining the applicability of the analysis methods to actual damage situations, it is necessary to pay attention to whether the values obtained through the analysis methods are the average or the maximum values of deformation.

Furthermore, the existence of the variations in observed deformation means that the analyzed deformation is expected to have large variations when the analyzed deformation actually occurs. Thus, the results of the verification of deformation need to be interpreted from the viewpoint that the analysis results should include errors caused by the variation. This is one of the reasons for mentioning in **Part III, Chapter 1, 2.2.1 Purposes and Methods of the Verification of Deformation** that currently there is no engineering significance in pursuing the economic cross sections with the amounts of deformation close to the allowable amounts through repeatedly calculating the amounts of deformation by changing the cross-sectional shapes, ground improvement areas and member strength in detail.

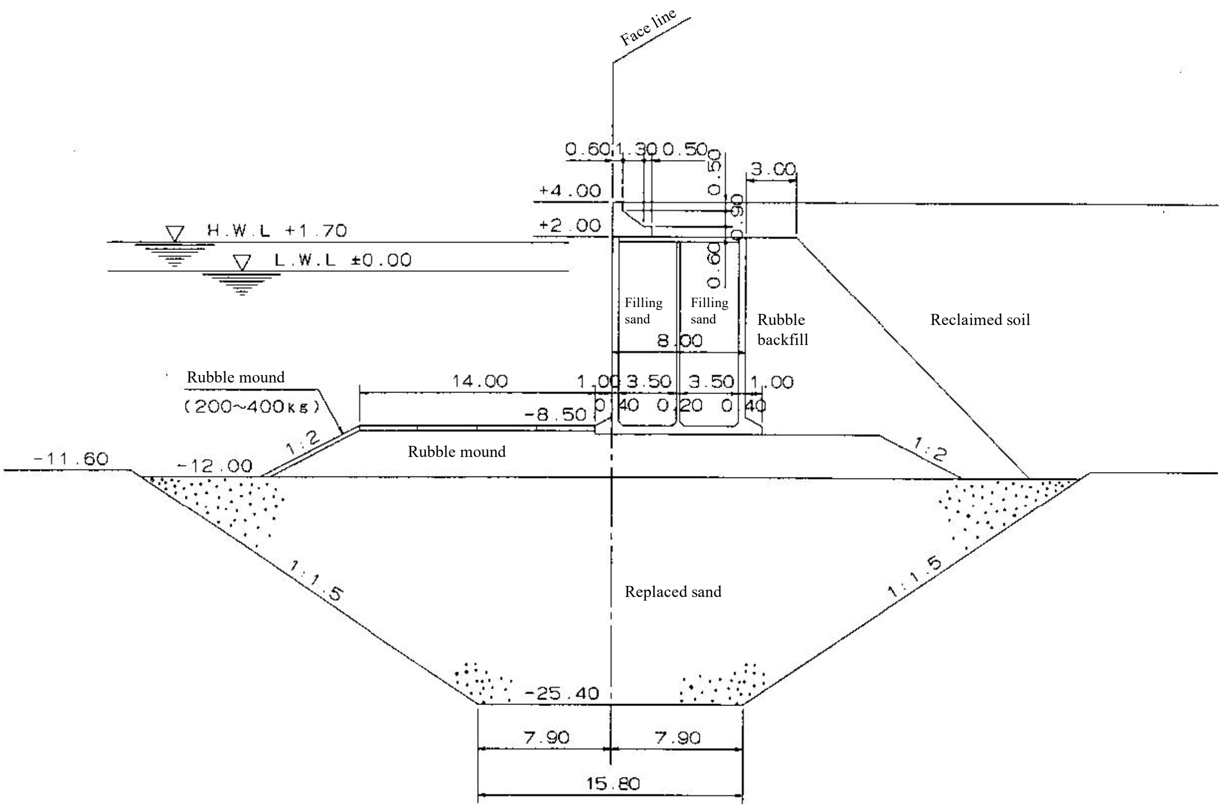

Fig. 2.2.1 Typical Cross Section of Quaywall No. RF3 on Rokko Island, Kobe[10)]

Table 2.2.1 Dimensions of Caisson Type Quaywall (Damaged) and Damage Situations (after **Reference 10)**)

Depth	Design seismic coefficient	Caisson width	Caisson height	Thickness of replaced sand layer	Seaward displacement	Subsidence of levee crown	Inclination angle of caisson	Ratio of deformation due to damage	Face line direction
(m)		(m)	(m)	(m)	(cm)	(cm)	(degree)	(%)	
-8.5	0.15	8.0	11.5	13.4	464/370	198/158	6.4/3.1	34	East-west direction

(1) Ratio of deformation due to damage: The maximum seaward displacement / (caisson height + 2 m) × 100%
(2) The maximum and average values of Caissons Nos. 7 to 21 in **Fig. 2.2.2** are shown for the seaward displacement and inclination angle

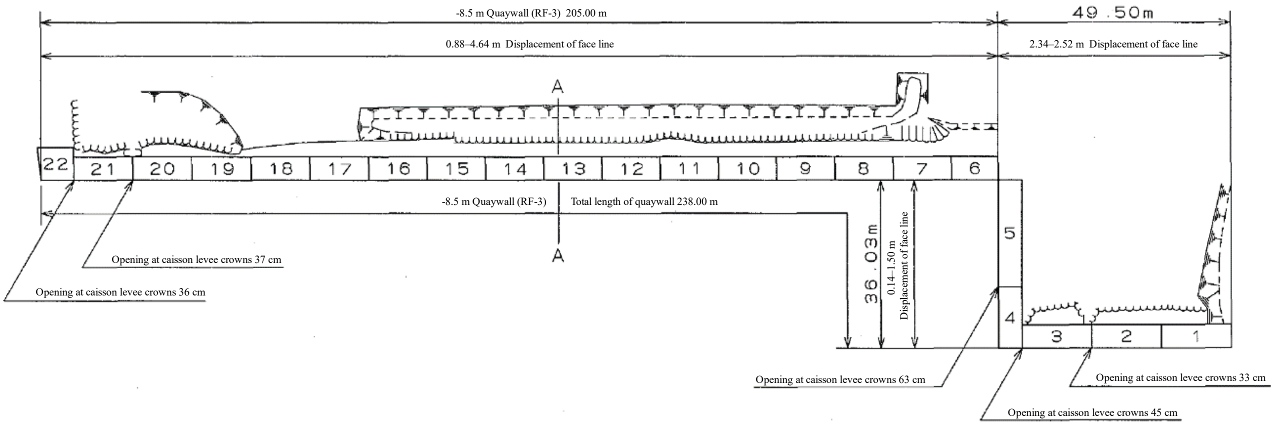

Fig. 2.2.2 Layout of Damage Situations of Quaywall No. RF3 on Rokko Island, Kobe10)

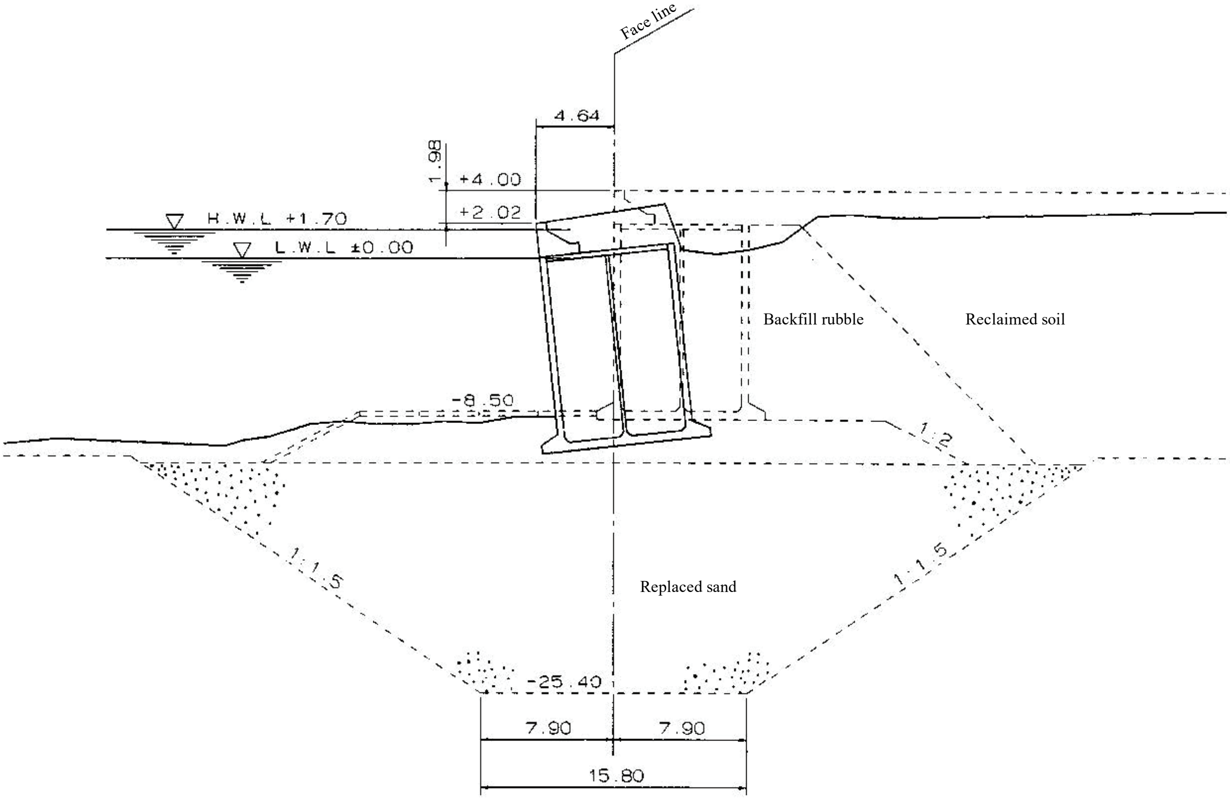

Fig. 2.2.3 Cross Section of Damage Situations of Quaywall No. RF3 on Rokko Island, Kobe10)

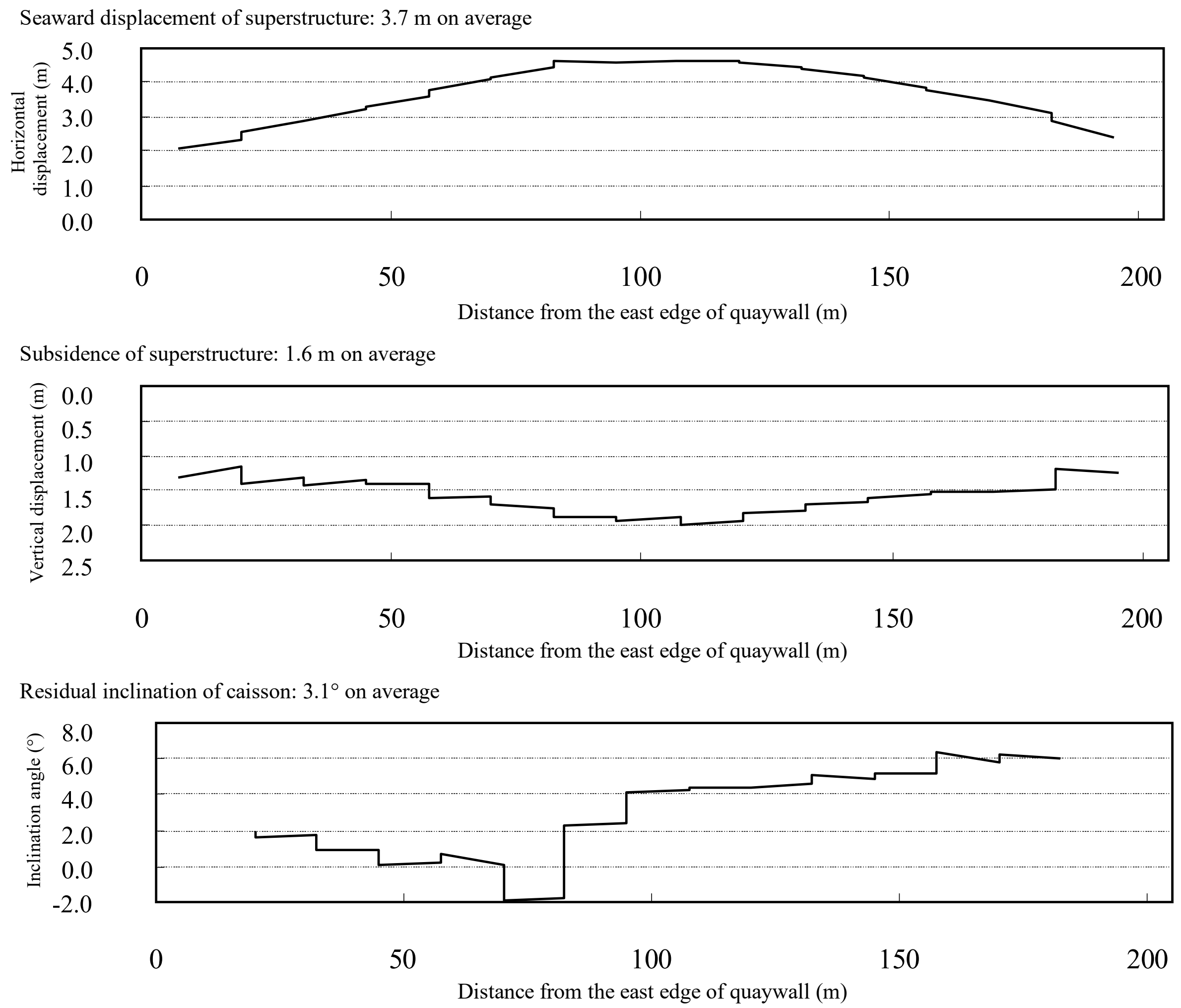

Fig. 2.2.4 Distribution of Seaward Displacement, Subsidence of Superstructures (from the Original Design Crown Height) and Residual Inclination Angles (Positive Figure for Seaward Inclination) of Caissons Nos. 7 to 21 in **Fig. 2.2.2** from the Top (after **Reference 10)**)

2.3 Points of Caution for Ensuring Accuracy for the Verification of Deformation

2.3.1 Procedure for Verification of Deformation

Fig. 2.3.1 shows the overall procedure of the verification of deformation including cases using a dynamic analysis method and a shake table test. The procedure starts with the selection of the verification method and setting of the conditions for the external earthquake force. As previously mentioned, dynamic analysis methods are generally used for the verification of deformation. However, in cases where the applicability of the analysis methods has not been confirmed, the verification of deformation needs to be performed by examining the dynamic and deformation characteristics of the analysis object structures through shake table tests in a 1 g field [for example 11)] or in a centrifugal field. For dynamic analyses, there are many cases of using the finite element method, for which a theoretical system has already been established, but other methods [for example 12)] have been planned to be used, such as a finite difference method and a distinct element method, or a combination of these methods with the finite element method. [for example 13)] Because the finite element method has generally been used in practical design work, the following descriptions of dynamic analyses are based on that method.

When a dynamic analysis is selected for the verification of deformation, the analysis conditions need to be set, followed by the input ground conditions. The analysis conditions include analysis regions, boundary conditions and the selection of the type of time integration method. When a shake table test is selected for the verification of deformation, the experiment conditions need to be set followed by the ground conditions. The experiment conditions include the selection of a 1 g or centrifugal field, selection of the type of similitude law, and the boundary conditions.

After setting the conditions, the deformation is evaluated by executing either a dynamic analysis or a shake table test. When the deformation is within an allowable range in light of the performance criteria of the structure, the verification of deformation is completed. If not, countermeasures such as the modification of a design cross section are required. In the case of modifying the design cross section of a structure, it is necessary to reexamine the analysis or experiment conditions while taking into consideration the contents of the modification. However, considering that liquefaction has often been the main reason for the deformation of port structures, it is reasonable, in many cases, to control the deformation within an allowable range by taking liquefaction countermeasure works or modifying the areas subjected to these works. In such cases, a dynamic analysis or shake table test needs to be repeated by revising the ground conditions only.

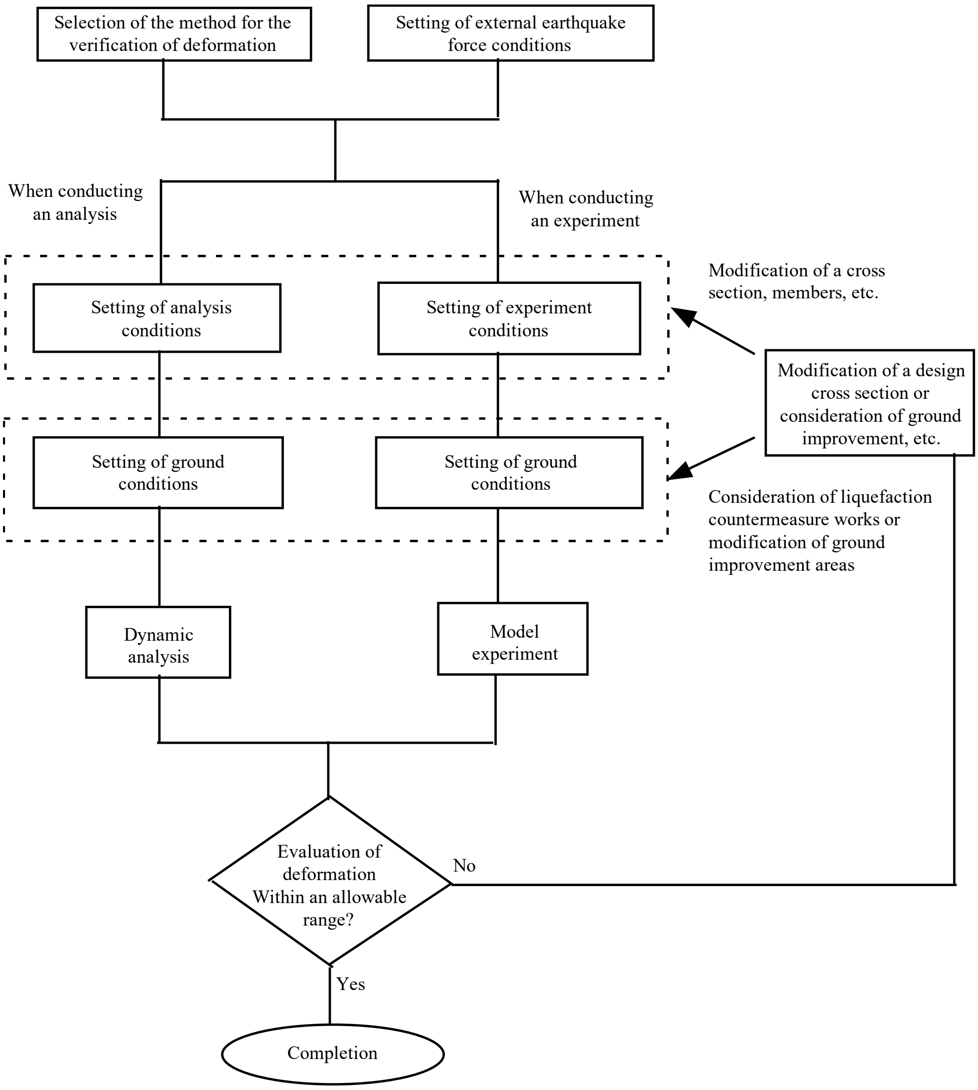

Fig. 2.3.1 Procedure for the Verification of Deformation

2.3.2 Confirmation of Program Applicability

The applicability of the analysis programs needs to be verified using past damage cases (or shake table test results). However, analysis programs have been continuously updated, and even programs with identical names may produce completely different analysis results depending on the operation of the switches for setting the analysis conditions. Thus, it is necessary to use programs under conditions identical to those used when these programs were verified.

For example, in the case of the FLIP, the applicability of the FLIP Ver. 3.3 published in November 1997 was verified with damage cases of gravity-type quaywalls at Kobe Port. [for example 8), 9)] However, because of insufficient accuracy when analyzing the deformation of the sheet pile quaywalls, FLIP Ver. 3.3 has been revised in the light of the constitutive laws.[14)] Furthermore, after every revision, the program was subjected to verification to confirm whether or not the revised program could reproduce the previous damage cases with equal accuracy.[15)] As above, when selecting an analysis program, it is necessary to carefully examine not only the names but also the states of the candidate analysis programs.

Tables 2.3.1 to **2.3.4** show examples of the points of caution when applying the FLIP to different types of structures in terms of the selection of the FLIP versions and the setting of the analysis methods. In addition to the applicability of the FLIP to gravity-type and sheet pile wharves to be described later, the applicability of the FLIP to open-type wharves on vertical piles[16] and composite breakwaters[17] has also been examined, and there have been proposals of versions and settings of analysis methods for these cases. It shall be noted that the settings of the programs need to be determined for individual structural types even when identical programs are used. Because there are many more setting items than those listed in the tables, it is necessary to appropriately select a version and set the analysis conditions with reference to the manuals. It is also necessary to constantly pay attention to the latest technical trends of the programs because the versions and settings are subject to change due to future improvements.

For seawalls, the verification of the deformation of gravity and sheet pile type seawalls can be analyzed with reference to the analysis methods applicable to gravity and sheet pile type quaywalls. For sloping seawalls, applicability of the FLIP has been studied based on the damage mechanisms identified through shake table tests.[18] In the case of embankment type seawalls, which are generally called sea and river embankments, applicability of the FLIP was verified with a river embankment at Shiribeshi-Toshibetsu River, which was damaged by the 1993 Hokkaido-Nansei-oki Earthquake.[19]

When implementing analyses, it is preferable to record the analysis results in combination with detailed descriptions of the analysis conditions on data sheets prepared for the different types of programs and to keep the data sheets. This is a measure to prevent setting erroneous analysis conditions, but it is also preferable that the descriptions of the data sheets include not only the analysis conditions but also the grounds for the engineering decisions. **Fig. 2.3.2** shows an example of entering the analysis conditions for the FLIP in a data sheet.

When implementing analyses, it is also preferable to keep the input data and the programs used for the analyses in addition to the analysis results, because these data and programs enable the damage situations of the structural members on the occurrence of an earthquake to be estimated in a manner that analyzes the deformation with the observed earthquake ground motions, thereby creating reference materials useful when determining the usability of the facilities.

2.3.3 Setting an Analysis Range

It is necessary to set a sufficiently large analysis range and divide the range into mesh cells with cell sizes suitable for the analysis purposes when using the finite element method. For example, an analysis range in the vertical direction is generally extended to the engineering bedrock face with a viscous boundary set on the bottom face of the analysis range. An analysis range in the lateral direction needs to be wide enough to ensure that the influence of the object facility can be barely felt at the lateral ends of the range, with the result of the preliminary analysis of the free ground section (a one-dimensional analysis assuming horizontally layered ground) generally applied to the lateral viscous boundaries of the analysis range. An analysis range in the lateral direction needs to normally be 3 to 5 times the width of the analysis object facility. In the case of the 1995 Hyogo-ken Nambu Earthquake, the influences of the lateral flow of the ground were felt about 100 m behind the face line of the quaywall.[20] Thus, it is preferable to set a lateral viscous boundary at a position 100 m or more away from the face line of the quaywall.

The analysis range is divided into finite element meshes with appropriate mesh sizes. The upper limit of the sizes of the meshes is generally considered to be 1/5 of the wavelength of the object seismic wave. In this case, if there is a risk of liquefaction, it is necessary to consider the wavelength after the ground undergoes liquefaction, and the same applies to an analysis using the FLIP. Practically, the wavelength after liquefaction is calculated based on the assumption that the shear stiffness G of liquefied ground is about 1/50 of the shear stiffness G_0 of the original ground. Furthermore, it is preferable to set small mesh sizes if there is a risk of stress concentration around the object facility or if a detailed examination is required in a manner, for example, that examines the stress distribution obtained through an analysis to identify the locations where the stress is concentrated or the stress distribution is discontinuous, sets smaller mesh cells in those locations and performs another analysis. It is also preferable to minimize meshes that have triangular shapes because they may induce micro-vibrations, which affect the analysis results. Similarly, it is necessary to avoid the use of meshes that have extreme aspect ratios because they reduce analysis accuracy.

Table 2.3.1 Selection of FLIP Versions and Setting of Analysis Methods Suitable for Gravity-Type Quaywalls

Recommended FLIP version	FLIP Ver. 6.0.6 or later FLIP Ver. 3.3 is still applicable when using the conventional method
Method for evaluating the contribution of shear work to negative dilatancy in a stress space beyond the phase transformation line	It is preferable to use the tmp7 method (a model where the contribution of plastic shear work to the negative dilatancy in a stress space beyond the second phase transformation line becomes 0 with the second phase transformation line drawn in a manner that sets the second phase transformation angle between the phase transformation angle and failure angle).
Method for nonlinear iterative calculation of the stress-strain relationship	It is preferable to use the improved nonlinear iterative calculation method (a method which follows the variations of a state variable S in each time step).
Element integral method (a method for avoiding a locking phenomenon)	SRI method (an element integral method with the order of the Gaussian integral with respect to an average component reduced).
Time integral method	Wilson-θ method ($\theta = 1.4$)
Method for evaluating the initial stress state	It is acceptable to use a simple one-stage analysis with a gravity force applied to the entire analysis model in the initial analysis stage.
Criterion for the Rayleigh damping stiffness proportionality coefficient β of the entire system	It is preferable to use the critical value of β, the largest value of the Rayleigh damping stiffness proportionality coefficient, which does not cause the distribution of the maximum response displacement to be changed in the one-dimensional nonlinear non-liquefaction analysis.
Joint element stiffness proportionality coefficient β (elimination of damping control over the sliding behavior of joint elements)	The value of 0 is used for β so that the Rayleigh damping does not control the sliding behavior of the joint elements when the sliding of the caisson is considered to be the main failure mode (Rayleigh damping by element).
Consideration of the three-dimensional effect in pile-ground interactions	
Method for setting the material constant of rubble mound (backfill rubble)	It is appropriate to use a new rubble constant (c = 20 kPa, ϕ_f = 35 degrees, no bearing of negative pressure, pore water volume stiffness 1/100 or less of the volume stiffness in an undrained state)
Modeling of steel products	
Time step interval Δt	0.01 seconds or less. It is preferable to reduce Δt (for example 0.001 seconds) to a level that can ensure the convergence of the joint elements when the joint element stiffness proportionality coefficient β is set at 0).
Remarks	The analysis function (conventional method) of FLIP Ver. 3.3 can be used if a failure pattern is similar to the caisson type quaywall at Kobe Port, which was damaged by the 1995 Hyogo-ken Nambu Earthquake, because the analysis function of FLIP Ver. 3.3 is proven to be able to reproduce the damage situations of the quaywall. When using the improved nonlinear iterative calculation method and tmp7 methods, and sliding is not the main failure mode of the caisson, the conventional rubble constant which makes the caisson more likely to slide than the new rubble constant can be used, because this type of method is proven to be able to analyze the displacement of a caisson consistent with the actual displacement, in place of controlling the sliding behavior of the joint elements by applying the Rayleigh damping stiffness proportionality coefficient β of the entire system to the joint elements. The advantage of the method is the availability of setting Δt at 0.01 seconds. When using the method, it is preferable to compare the analysis results of the method with that of a case using β of the joint elements set at 0 and a new rubble constant for a final confirmation.

Table 2.3.2 Selection of FLIP Versions and Setting of Analysis Methods Suitable for Sheet Pile Quaywalls

Recommended FLIP version	FLIP Ver. 6.0.6 or later
Method for evaluating the contribution of shear work to negative dilatancy in a stress space beyond the phase transformation line	It is preferable to use the tmp7 method (a model where the contribution of plastic shear work to the negative dilatancy in a stress space beyond the second phase transformation line becomes 0 with the second phase transformation line drawn in a manner that sets the second phase transformation angle between the phase transformation angle and failure angle).
Method for nonlinear iterative calculation of the stress-strain relationship	It is preferable to use the improved nonlinear iterative calculation method (a method which follows the variations of a state variable S in each time step).
Element integral method (a method for avoiding a locking phenomenon)	SRI method (an element integral method with the order of the Gaussian integral with respect to an average component reduced).
Time integral method	Wilson-θ method (θ = 1.4)
Method for evaluating the initial stress state	A multistage analysis simulating the construction process
Criterion for the Rayleigh damping stiffness proportionality coefficient β of the entire system	It is preferable to use the critical value of β, the largest value of the Rayleigh damping stiffness proportionality coefficient, which does not cause the distribution of the maximum response displacement to be changed in the one-dimensional nonlinear non-liquefaction analysis.
Joint element stiffness proportionality coefficient β (elimination of damping control over the sliding behavior of joint elements)	The stiffness proportionality coefficient β of the entire system may be applied to the joint elements arranged on the passive side of the front sheet pile. However, there may be cases where the displacement of a sheet pile is significantly reduced when arranging the joint elements on the active side and controlling its sliding behavior. In this type of case, β for the joint elements needs to be set at 0 (Rayleigh damping by element). It is also acceptable to arrange no joint elements on the active side and to allow the sheet pile to have a friction-free slide with only the horizontal freedom of the sheet pile and soil subjected to MPC (multi-point constraints).
Consideration of the three-dimensional effect in pile-ground interactions	It is preferable to use a pile-ground interactive spring element for an anchor pile. However, in the case of a multi-step analysis, the analysis model which simulates an anchor pile as a sheet pile (wall structure) that has a stiffness equivalent to the pile has been proven to be able to reproduce the actual damage. The same points of caution with respect to the joint elements for the front sheet pile apply to modeling a pile as a sheet pile.
Method for setting the material constant of rubble mound (backfill rubble)	It is preferable to use the conventional constant (c = 0 kPa, ϕ_f = 40 degrees, with the pore water volume stiffness equal to the volume stiffness in an undrained state). However, it has been proven that the new rubble constant also can produce acceptable analysis results.
Modeling of steel products	Nonlinear beam elements need to be used when the steel product is within a nonlinear region.
Time step interval Δt	0.01 seconds or less. It is preferable to reduce Δt (for example, 0.001 seconds) to a level that can ensure the convergence of the joint elements when the joint element stiffness proportionality coefficient β is set at 0.
Remarks	In addition to the above combination of the version and settings, there are other combinations which can reproduce the damage situations. However, it shall be noted that they may underestimate the deformation in some instances.

Table 2.3.3 Selection of FLIP Versions and Setting of Analysis Methods Suitable for Open-Type Wharves on Vertical Piles

Recommended FLIP version	FLIP Ver. 6.0.6 or later
Method for evaluating the contribution of shear work to negative dilatancy in a stress space beyond the phase transformation line	It is preferable to use the tmp7 method (a model where the contribution of plastic shear work to negative dilatancy in a stress space beyond the second phase transformation line becomes 0 with the second phase transformation line drawn in a manner that sets the second phase transformation angle between the phase transformation angle and failure angle).
Method for nonlinear iterative calculation of the stress-strain relationship	It is preferable to use the improved nonlinear iterative calculation method (a method which follows the variations of a state variable S in each time step).
Element integral method (a method for avoiding a locking phenomenon)	SRI method (an element integral method with the order of the Gaussian integral with respect to an average component reduced).
Time integral method	Wilson-θ method (θ = 1.4)
Method for evaluating the initial stress state	It is acceptable to use a simple one-stage analysis with a gravity force applied to the entire analysis model in the initial analysis stage.
Criterion for the Rayleigh damping stiffness proportionality coefficient β of the entire system	It is preferable to use the critical value of β, the largest value of the Rayleigh damping stiffness proportionality coefficient, which does not cause the distribution of the maximum response displacement to be changed in the one-dimensional nonlinear non-liquefaction analysis.
Joint element stiffness proportionality coefficient β (elimination of damping control over the sliding behavior of joint elements)	It is preferable to set the stiffness proportionality coefficient of joint elements β at 0 because it does not cause any analysis problems. It is still acceptable to apply the stiffness proportionality coefficient β of the entire system to the joint elements when it is determined that controlling the sliding behavior of the joint elements arranged around L-type blocks does not affect the behavior of the entire system.
Consideration of the three-dimensional effect in pile-ground interactions	It is preferable to use pile-ground interaction spring elements.
Method for setting the material constant of rubble mound (backfill rubble)	It is preferable to use the conventional constant (c = 0 kPa, ϕ_f = 40 degrees, with the pore water volume stiffness equal to the volume stiffness in an undrained state). However, it has been proven that the new rubble constant can also produce acceptable analysis results.
Modeling of steel products	Nonlinear beam elements need to be used when the steel product is within a nonlinear region.
Time step interval Δt	0.01 seconds or less. It is preferable to reduce Δt (for example, 0.001 seconds) to a level that can ensure the convergence of the joint element when the joint element stiffness proportionality coefficient β is set at 0.
Remarks	The proposed method above is preferably used but it shall be noted that the applicability of the method to undamaged facilities is still under deliberation.

Table 2.3.4 Selection of FLIP Versions and Setting of Analysis Methods Suitable for Composite Breakwaters

Recommended FLIP version	FLIP Ver. 6.0.6 or later FLIP Ver. 3.3 is still applicable when using the conventional method
Method for evaluating the contribution of shear work to negative dilatancy in a stress space beyond the phase transformation line	Conventional model
Method for nonlinear iterative calculation of the stress-strain relationship	It is preferable to use the conventional method but the improved nonlinear iterative calculation method (a method which follows the variations of the state variable S in each time step) can be used if the calculation of the conventional method is unstable with attention to the risk of an underestimation of the displacement amounts.
Element integral method (a method for avoiding a locking phenomenon)	SRI method (an element integral method with the order of the Gaussian integral with respect to an average component reduced).
Time integral method	Wilson-θ method (θ = 1.4)
Method for evaluating the initial stress state	It is acceptable to use a simple one-stage analysis with a gravity force applied to the entire analysis model in the initial analysis stage.
Criterion for the Rayleigh damping stiffness proportionality coefficient β of the entire system	It is preferable to use the critical value of β, the largest value of the Rayleigh damping stiffness proportionality coefficient, which does not cause the distribution of the maximum response displacement to be changed in the one-dimensional nonlinear non-liquefaction analysis.
Joint element stiffness proportionality coefficient β (elimination of damping control over the sliding behavior of joint elements)	The value of 0 is used for β so that the Rayleigh damping does not control the sliding behavior of the joint elements when the sliding of the caisson is considered to be the main failure mode (Rayleigh damping by element).
Consideration of the three-dimensional effect in pile-ground interactions	
Method for setting the material constant of rubble mound (backfill rubble)	It is preferable to use the conventional constant (c = 0 kPa, ϕ_f = 40 degrees, with the pore water volume stiffness equal to the volume stiffness in an undrained state). However, it has been proven that the new rubble constant also can produce acceptable analysis results.
Modeling of steel products	
Time step interval Δt	0.01 seconds or less. It is preferable to reduce Δt (for example, 0.001 seconds) to a level that can ensure the convergence of the joint element when the joint element stiffness proportionality coefficient β is set at 0.
Remarks	In addition to the above combination of the version and settings, there are other combinations which can reproduce the damage situations. However, it shall be noted that they may underestimate the deformation due to damage in some instances.

Analysis name: Performance Verification of Earthquake Resistance for XXX Quaywall at XXX District at XXX Port
(Report title:) Date: (month/day/year) Reported by: ( )

Name of facility to be analyzed: XXX Quaywall at XXX District at XXX Port

- Type of facility:
  Gravity-type quaywall (○) / Sheet pile quaywall ( ) / Piled pier (simultaneous analysis of piles) ( )
  Embankment ( ) / Sloped seawall ( ) / Gravity-type breakwater ( ) / Immersed structure ( )
  Other ( ) Please specify: ( )
- Earthquake motion to be input:
  Seismc wave from ocean trench earthquake (○) / (Object earthquake: Tonankai and Nankai earthquakes
  Seismic wave from inland active fault earthquake ( ) / (Object earthquake:)
  Seismic wave from M6.5 epicentral earthquake ( )
  Other seismic waves ( ) Please specify: ( )
  Sine wave ( )

(Note: Conversion of a 2E wave in the engineering bedrock into a 2E wave at the lower edge of the model through XXX.)

- Time step: 0.01 seconds (○) / Other ( ) Please specify: ( )
- Number of analysis steps: 2,000 steps (Analysis time: 20 seconds)
- Basis for setting the ground properties:
  Simplified parameter based on N values and fine content (conventional method) ( )
  Simplified parameter based on N values and fine content (with tmp7) ( ) / Fitting to liquefaction strength curve (○)
  Other ( ) Please specify: ( )
- Version of FLIP: Ver. 4.3
- Method for evaluating the contribution of shear work in the stress space exceeding the phase transformation line to negative dilatancy:
  Conventional method (○) / tmp3 method ( ) / tmp7 method ( ) / (Note: tmp3 and tmp7 methods are available with FLIP Ver. 5.0 or later)
- Selection of method for nonlinear iterative calculation of stress-strain relationship:
  Conventional method (○) / Improved method (available with FLIP Ver. 5.0 or later) ( )
- Selection of method for evaluating initial stress state:
  Single-stage self-weight analysis method (○) / Multi-stage self-weight analysis method (available with FLIP Ver. 4.2.5 or later) ( )
- Criterion for Rayleigh damping:
  Critical value beyond which the maximum response displace distribution does not change any further (○)
  Value corresponding to certain damping of natural period ( ) (equivalent to %) /
  Setting based on the reproduction of previous disasters ( ) / Setting based on a comparison with the analysis results of SHAKE ( )
  Other ( ) Please specify: ( )
- Update of Rayleigh damping at each time:
  Fixed value (○) / Initial tangential stiffness at each time ( ) / Tangential stiffness at each time ( )
- Rayleigh damping of joint element:
  No Rayleigh damping (available with FLIP Ver. 4.2 or later) ( ) / Value identical to the entire system (○)
  Other ( ) Please specify: ( )
- Modeling of pile-ground interaction:
  Modeling of piles as a wall ( ) / Pile-ground interaction springs (available with FLIP Ver. 5.1.6 or later) ( )
  Other (○) Please specify: (No piles)
- Material constant of rubble:
  c = 0 kPa, ϕf = 40 degrees ( ) /
  c = 20 kPa, ϕf = 35 degrees (no bearing of negative pressure) (available with FLIP Ver. 4.3 or later) (○)
  Other ( ) Please specify: ( )
- Volume stiffness of pore water at rubble section:
  Conventional (2.2 x 10^6 kPa) ( ) / Improved method (about 1/100 of the conventional method) (○)
  Combined use of conventional and improved method depending on areas ( )
  Other ( ) Please specify: ( )
- Setting of bottom boundary:
  Fixed boundary ( ) / Viscous boundary (○) (Vp: 1,600 m/s) (Vs: 313 m/s)
  Other ( ) Please specify: ( )
- Setting of side boundary:
  Combined use of viscous and reaction boundaries (available with FLIP Ver. 4.3 or later) ( )
  Viscous boundary (○) (Vp: 1,445 to 1,575 m/s) (Vs: 53 to 252 m/s)
  Other ( ) Please specify: ( )
- Reference point for displacement output:
  Relative displacement from the input point of the 2E wave ( ) / Relative displacement from the node on the viscous boundary directly beneath (○) /
  Relative displacement from a specific point on the viscous boundary ( ) (Object node:)
  Other ( ) Please specify: ( )
- Setting of sea level:
  L.W.L. (○) / H.W.L ( )
  Other ( ) Please specify: ( )
- Definition of large deformation:
  Conventional method (infinitesimal deformation theory) (○) / Simplified large deformation analysis function (available with FLIP Ver. 4.4 or later) ( )

Material(s) to be attached to analysis report

Analysis cross section (○) / Soil histogram ( ) / List of ground properties (○) / Damping parameter setting grounds (○)
Residual deformation diagram (○) / Maximum excess pore water pressure ratio diagram (○) / Time history of deformation (○)
Other ( ) Please specify: ( )

Types of input data to be attached

Input data (CD-ROM): Static analysis (○) / Free field analysis (○) / Dynamic analysis (○) / Earthquake ground motion ( )
Other ( ) Please specify: ( )

Other items and points of caution for the interpretation of the analysis results

The entries above are provided as examples.

Fig. 2.3.2 Example of Entering the Analysis Condition Data Sheet

2.3.4 Setting of Earthquake Ground Motions and Bottom Boundaries

A waveform (2E wave) that has an amplitude double the incident wave on the engineering bedrock is generally used as the external earthquake force condition for the verification of deformation. Thus, when executing numerical analyses, it is necessary to set an appropriate engineering bedrock and a viscous boundary on the engineering bedrock.

In addition, even if it is the engineering bedrock, its velocity of S wave has a considerable range. Thus, it is necessary to confirm that the S wave velocity in the layer considered as the engineering bedrock when setting the Level 1 earthquake ground motions is consistent with, to some extent, that in the layer considered at the engineering bedrock in the seismic response analysis. In cases where there is a difficulty in including the entire region above the engineering bedrock face in an analysis range for too large a depth of the engineering bedrock or other reasons, a layer which has a certain level of stiffness, though not to the extent of the engineering bedrock, needs to be set as an alternative foundation face for analysis purposes, and the 2E wave incident on the engineering bedrock needs to be converted to an alternative 2E wave incident on the alternative foundation face for analysis purposes through the seismic response calculation method.

Many of the programs for two-dimensional analyses used in designing work allow the vertical and horizontal components of earthquake ground motions to be input. However, because the influence of the vertical components of earthquake ground motions on the displacement of port facilities is not considered to be significant, it is acceptable to input only the horizontal components,[8] except for cases where detailed analyses are required or structures are susceptible to vertical ground motions. In the case of inputting earthquake ground motions that have two horizontal components, these two components are normally subjected to a coordinate conversion to obtain the earthquake ground motions in the direction perpendicular to the face line of the quaywall as input earthquake ground motions.

As above, a viscous boundary is normally used in the analyses. However, because the viscous boundary may characteristically have an accumulation of displacement, it is necessary to evaluate the displacement of the entire system by deducting the accumulated displacement on the boundary (specifically, by obtaining the relative displacement between the analysis object point and the upper face of the viscous boundary).

2.3.5 Setting the Ground Properties

The appropriateness of the numerical analysis results depends on the characteristics of the constitutive laws used in the analyses and the appropriateness of the parameters set for the constitutive laws. The parameters related to ground properties shall be basically determined based on the data obtained through detailed in-situ soil tests. The types of ground surveys necessary to be executed for setting the ground conditions and the types of parameters to be set as a result of these surveys are summarized below.

Here, it is necessary to carefully refer to the specific parameter setting procedures in accordance with the constitutive laws used in the programs. For example, in the case of the parameter setting procedures for the FLIP, refer to **Reference 21)**. When no soil test data are available, there may be a possibility to obtain such data by following simplified parameter setting procedures, as with the FLIP, in which a simplified procedure to obtain the parameters from the *N*-values (equivalent *N*-values corrected in terms of confining pressure) and fine contents are proposed.[21] However, it shall be noted that parameters obtained through simplified procedures reduce the reliability of the analysis results. Attention is also required when setting parameters through simplified procedures not to set the wrong parameters, which may be incompatible with the setting conditions because the setting conditions of different analysis methods or constitutive laws in the FLIP require different parameters to be set.

(1) PS logging (velocity logging)

PS logging is used to measure the propagation velocity of S waves V_s, which can be used to determine the shear modulus of ground G_0. Because the shear modulus is generally a parameter subject to confining pressure, the shear modulus G_{ma}, under the reference confining pressure σ_{ma} (the confining pressure during measurement), is used in the case of the FLIP.

In addition, the rebound modulus K_{ma} (also as a value under reference confining pressure σ_{ma}) of the soil particle structure can be set with a Poisson's ratio (generally set at about 0.33 through laboratory tests). Because these physical property parameters are extremely important in seismic response analyses, the execution of PS logging is of particular significance. Although there are a variety of PS logging methods, the methods using suspension type equipment are preferable for the purpose of ensuring measuring accuracy.

In the case of the FLIP, the basic input parameters are a shear modulus G_{ma}, a rebound modulus K_{ma} and a Poisson's ratio. However, the Poisson's ratio is not used for automatic calculation of the rebound modulus K_{ma}, and, therefore, does not affect the analysis results. Because the FLIP is based on the two-dimensional analysis, the Poisson's ratio is used for calculating stresses in the depth direction of the cross sections only as reference values. However, it shall be noted that different analysis programs have different condition settings for these parameters.

Furthermore, it is necessary to pay attention to the fact that because the actual ground has a coefficient of earth pressure at rest of about 0.5, some programs calculate initial stresses through an elastic initial gravity analysis using the shear modulus and rebound modulus based on a Poisson's ratio of 0.33, while the FLIP requires the formulation of elements[22)] and adjustments of the shear modulus, rebound modulus and material strength according to the constitutive laws[23)] in order to obtain the coefficient of earth pressure at rest (a ratio of a horizontal component to a vertical component of a direct stress in a horizontally layered ground) of 0.5 as a result of the initial gravity analysis.

(2) Sampling

The liquefaction resistance of the ground can be known through sampling and liquefaction tests. Thus, it is extremely important to obtain undisturbed soil specimens in-situ for the cyclic triaxial compression test to be described later. For the details of sampling for the liquefaction test, refer to **Reference 24).**

Because frozen sampling, which is considered to be the best method for obtaining undisturbed soil specimens, is very expensive, a static press-in sampling is frequently used as an alternative. For example, a fixed piston sampler (hydraulic type) is one of the devices used for static press-in sampling, and the appropriate equipment is preferably used according to the ground conditions (refer to **Reference (Part II) Chapter 1, 3.6 Sampling**).

(3) Liquefaction test (cyclic triaxial compression test) or hollow cylindrical torsional shear test

The liquefaction strength is calculated from the results of the cyclic triaxial compression test (JGS 0541) or other tests using undisturbed soil specimens. Regarding the cyclic triaxial compression test, in addition to the liquefaction strength curves as described in detail in the reference 24), it is necessary to closely examine the states of the specimens when the excess pore water pressure is on the rise and the states of strain accumulation in the specimens (rapid or gradual accumulation). This is because the parameters (particularly those related to liquefaction) used in analysis programs like the FLIP are normally determined through parameter fitting so as to accurately reproduce the test results. In addition, the characteristics related to the rise in excess pore water pressure and strain accumulation states are important items to be incorporated in the parameter fitting. Because the strain to be generated in the soil specimens is largely affected by confining pressure, it is necessary to pay attention to using the same values of the confining pressure in the numerical calculations for setting the parameters and in the cyclic triaxial compression test.

The "Method for torsional shear test on hollow cylindrical specimens of soils (JGS 0551)" can be used as the liquefaction test. The torsional shear test on hollow cylindrical specimens is particularly suitable for the verification of deformation that allows soil to have a certain degree of deformation because the test can measure the deformation of specimens in large strain regions. However, the torsional shear test has a risk of producing different test results depending on the skills of the test engineers in terms of the preparation of the specimens. Thus, it is practically recommended to conduct both the torsional shear test and the cyclic triaxial compression test.

(4) Standard penetration test

Although the standard penetration test is not required if accurate PS logging and liquefaction tests are available, it is preferable to conduct a standard penetration test because the N-values may be used for obtaining parameters, such as the shear resistance angles, when they cannot be accurately calculated from the stress paths obtained through the triaxial compression test, and the shear modulus of ground G_0 of layers close to the ground surfaces and thin layers for which accurate PS logging cannot be expected. In addition, the standard penetration test is one of the major ground surveys frequently conducted for confirming changes in the properties of the entire ground around a structure.

Although there are methods for simply obtaining physical values from the N-values and fine contents in the FLIP, they are simplified methods prepared for preliminary examinations. Even with some budgetary restrictions, it is recommended to conduct detailed ground surveys, in addition to the standard penetration test, because the costs for ground surveys such as the PS logging are small compared to the main construction costs, and accurate as well as detailed analyses can contribute to the reduction in the main construction costs.

(5) Confirmation of grain size distribution

It is necessary to confirm the grain size distribution when determining the possibility of soil liquefaction. The presence or absence of fine fractions (and the plasticity index) creates a particularly large influence on the liquefaction strength.

(6) Uniaxial compression test (or triaxial compression test)

The parameters of the cohesive soil are often determined based on the results of the uniaxial and triaxial compression tests. For example, the details of the parameter setting methods in the FLIP are described in the reference 21). Specifically, the shear modulus and shear resistance angle of the cohesive soil can be determined from the test results and existing research outcomes. In addition, the strength of the cohesive soil can be determined based on either the shear resistance angle, cohesion or a combination of the two. In many cases, the strength of the cohesive soil is determined based on the shear resistance angle for the purpose of expressing the strength changes in the depth direction and avoiding unstable numerical analyses due to extreme strength changes. However, considering that the shear resistance angle becomes significantly large when expressing the strength of over-consolidated clay, it is necessary to determine the strength of the cohesive soil based on its cohesion. When determining whether the analyses are based on normal consolidated or over-consolidated clay, it is necessary to pay attention to the possibility that the over-consolidated clay layer at the time of sampling, with reclaimed soil in preparation for facility construction placed on top, may transformation to a normal consolidated clay layer when the facility construction is completed.

For the shear resistance angle of normal consolidated clay, following an existing research outcome reporting that the shear resistance angle of the normal consolidated clay is almost 30 degrees across Japan,[25)] a value of 30 degrees is used for analyses in many cases. Here, it shall be noted that some analysis programs use calculation equations different from those for effective confining pressure even for horizontally layered ground under an identical K_0 stress condition. For example, the calculation equation of the effective confining pressure is as shown in **equation (2.3.1)**, while the equation used in the FLIP is as shown in **equation (2.3.2)**.

$$\sigma_m' = \frac{\sigma_x' + \sigma_y' + \sigma_z'}{3} \tag{2.3.1}$$

$$\sigma_m' = \frac{\sigma_x' + \sigma_y'}{2} \tag{2.3.2}$$

Thus, there may be cases where the increase rates of strength in normal consolidation differ between the actual situations and analyses, but in many cases, the influence of such differences on the structural design is considered to be small.

The strength obtained with a shear resistance angle of 30 degrees for normal consolidated clay as mentioned above corresponds to the strength parameter that is based on the effective stress and represents the strength under drained conditions. In contrast, the strength obtained with q_u values for over-consolidated clay corresponds to the strength parameter that is based on the total stress and represents the strength under undrained conditions. The strength of cohesive soil normally used in analyses is the strength after the completion of consolidation. When evaluating the strength according to the increment of confining pressure associated with reclamation, the strength parameter based on the effective stress is used as the strength of the normal consolidated clay.

(7) Cyclic shear test

The cyclic shear test is used to apply staged loading to specimens and obtain the shear modulus and damping constant from the relationships between the shear stress and shear strain obtained at the respective loading stages. The methods which can test the deformation properties in a wide strain range include the “Method for cyclic triaxial test to determine deformation properties of geomaterials (JGS 0542)” and the “Method for cyclic torsional shear test on hollow cylindrical specimens to determine deformation properties of soils (JGS 0543).” As is the case with the liquefaction test, the torsional shear test on hollow cylindrical specimens is suitable for the verification of deformation by allowing soil to have a certain degree of deformation because the test can measure the deformation of specimens in large strain regions. However, the torsional shear test has a risk of producing different test results depending on the skills of the test engineers in terms of the preparation of the specimens. Thus, it is practically recommended to conduct both the torsional shear test and the cyclic triaxial compression test.

Depending on the analysis programs (and constitutive laws), the parameters can be set regardless of the dynamic deformation test results. For example, in the case of the FLIP, because it uses a hyperbolic stress-strain relationship, the dependence of the equivalent shear stiffness on the strain levels (except for the strain due to the changes in the effective stress) is fixed, and, therefore, the dynamic deformation test results do not directly affect the parameter setting except for the test results of damping constants in large strain regions, which are referred to when setting data. However, the dynamic deformation test results can indirectly contribute to improving the accuracy of the parameter setting in a manner that, for example, confirms the consistency of the FLIP's analysis results based on the parameters set regardless of the dynamic deformation test with the strain dependency curve, the G/G_0-γ curve, of the equivalent shear stiffness.

2.3.6 Setting the Analysis Conditions

(1) Time steps and duration

The time steps need to be appropriately set according to the characteristics of the program to be used for the analyses. Generally, input earthquake ground motions are set as digital data of the seismic observation recorded at intervals of 0.01 seconds. In cases where there is a necessity to make calculations with shorter intervals depending on the characteristics of the analysis program, it is necessary to appropriately interpolate the digital data.

Basically, the duration of the earthquake ground motions needs to be sufficiently long to allow the deformation to be analyzed until the convergence of the earthquake ground motions. From the viewpoint of the calculation time, however, it is practical to select only the main part of the earthquake ground motions that has a large influence on deformation in the parametric studies. Still, out of these parametric studies, at least one analysis case is preferably conducted for the full duration. In addition, there may be cases where unstable numerical analyses cause the object ground to show deformation behavior even without earthquake ground motions. This is attributed to the initial gravity analyses failing to reproduce the initial state of the object ground correctly before applying the earthquake ground motions. Thus, it is preferable to simulate a case with an analysis step without input acceleration for several tens of seconds when the earthquake ground motions are first input to confirm analysis stability at the beginning of the dynamic analyses.

(2) Damping constant

Generally, nonlinear seismic response analyses use Rayleigh damping to enhance the stability of the numerical dynamic analyses. The FLIP also uses minute Rayleigh damping of about 1% in the natural period of the ground as a substitute for several types of damping, which cannot be solved by the internal damping of materials, to ensure the practical stability of the numerical analyses. Because the use of Rayleigh damping is just for expediency and has a risk of underestimating the deformation, it is preferable to stabilize the numerical analyses with the lowest possible Rayleigh damping coefficient. Actually, the deformation predicted in the verification of deformation through numerical analyses relies largely on the Rayleigh damping coefficient.[26] Thus, it is necessary to carefully set the Rayleigh damping coefficient and clarify the grounds for setting the coefficient in the verification of deformation results.

Although there are some methods for setting Rayleigh damping, none of them is conclusive. Thus, it is necessary to set a reasonable value with reference to the ones used when reproducing damage cases. For example, the Rayleigh damping coefficient generally used in the FLIP is the maximum value in a range with no change in the distribution of ground displacement obtained by conducting several cases of numerical analyses with different Rayleigh damping coefficients under non-liquefaction conditions with respect to the free ground section (a section which can be assumed as lateral horizontally layered ground).[27] This is because of the necessity to select values capable of obtaining the maximum stability in the numerical analyses within a range that can prevent a reduction in the predicted values of deformation and to confirm that the values determined in this way can reproduce the damage cases and experimental results.

Because Rayleigh damping is generally obtained by calculating damping matrixes based on the matrixes of the initial tangent stiffness (or mass in some cases) of the respective elements, large damping is likely to be set when a large initial stiffness is set for the joint elements. In such cases, there is a high possibility of setting excessive damping, thereby underestimating the relative displacement, even when the joint elements undergo sliding or detachment. Thus, it is necessary to set Rayleigh damping for the respective joint elements so as to invalidate or reduce Rayleigh damping. Some programs allow damping constants β to be finely set for the respective elements, and for damping to be set in proportion to the stiffness matrixes, which vary from hour to hour.

(3) Numerical integration methods

There are several ways of dealing with the numerical integration methods based on the element integration and sequential integration methods. It is difficult to simply describe which conditions are right or wrong, and, therefore, the conditions shall be appropriately set in accordance with the characteristics of the analysis programs and object structures in view of the reproducibility of past damage cases and analysis stability.

(4) Boundary conditions

In addition to irregular regions with analysis object structures and surrounding ground separated from semi-infinite ground, lateral boundaries need to be set so as to prevent the reflection of disturbance generated on the analysis regions and bottom boundaries on which seismic waves are incident. However, there are no perfect boundary conditions, and it is basically necessary to set sufficiently large irregular regions so as to reduce the influence of the boundary conditions on the behavior of the analysis object structures.

The lateral boundaries are set so as to prevent the disturbance generated in irregular regions from being reflected on the boundary positions and returning to the irregular regions. Basically, the lateral boundaries comprise viscous boundaries, reaction boundaries and free field sections. The free field sections represent horizontally layered ground that is not subjected to the behavior of the analysis regions. The lateral boundaries receive force in accordance with the differences in velocities between the irregular regions and free field sections.

The bottom boundaries need to be appropriately set depending on the types of input earthquake ground motions used for analyses. When using 2E waves on engineering bedrock, the viscous boundaries are set on the bottom faces of the models. In contrast, when applying earthquake data recorded underground using a vertical array to the bottom faces of the models as input earthquake ground motions, because compound waves the sum of the incident wave and reflected wave (E+F waves) are to be input, viscous boundaries are not set on the bottom faces of the models.

2.3.7 Checking Analysis Reliability

(1) Checking input data

The recent development of pre-post-processors (pre-processors: software to create input data necessary for analysis programs; post-processors: software to display the results output by the analysis programs) has simplified the operation to create input data and output results, thereby enabling analysts to work on analyses without understanding the operation contents of the analysis programs. With default values for the setting of several types of analysis methods that are input preliminarily, the pre-processors enable analysts to conduct analyses without inputting the setting values or making errors. However, because the nonlinear seismic response analyses require detailed settings of the analysis methods in accordance with the object structures as described below, there may be a risk of errors caused by using default values by mistake in place of the detailed settings. Thus, it is necessary to check the echo files or log files of the input data to be output from the analysis programs to confirm whether or not the settings of the analysis methods have been made as planned. In addition, organizing the analysis conditions using the data sheet shown in **Fig. 2.3.2** is considered to help improve the possibility of finding mistakes in the input data. When checking the input data, it is preferable to have persons different from those who prepared the input data conduct the check.

(2) Checking by visualizing the analysis results

The method generally used for the first confirmation of whether or not the analysis results are correct is to output a large number of the calculation results and confirm whether or not the deformation modes are natural. For example, when numerical calculations are destabilized, the output of the acceleration waveforms may show a series of spike-like acceleration responses, which suggests a possible progress of deformation due to the accumulation of numerical analysis errors.

The progress of deformation due to the accumulation of numerical analysis errors is a common phenomenon in analyses, and there are extreme cases where structures collapse in several tens of seconds of analysis time in a state before being subjected to earthquake ground motions. Similarly, in the case of effective stress analyses, it is important to confirm the analysis results by outputting time history waveforms of deformation and excess pore water pressure to check for possible occurrences of liquefaction with the excess pore water pressure of the ground increased. In addition, there have been numerous reports on the analysis results of continuing deformation after the conversion of earthquake ground motions. In such cases, it is necessary to carefully examine whether the continued deformation is obtained as a result of analytical problems or the correct evaluations of actual phenomena because there have been reported examples of flow phenomena with continued deformation even after the conversion of earthquake ground motions. In the case of unsymmetrical structures, there is a possibility of deformation in the form of the movement of entire analysis regions with strain accumulated on viscous boundaries due to an asymmetrical force from the lateral boundaries. It is also necessary to examine the relative displacement with respect to the nodes at the sides of the analysis regions on viscous boundaries when evaluating deformation.

Simultaneously displaying animated images of the deformation progress and the increase in excess pore water pressure using post-processors is an effective method for understanding the phenomena and finding analytical errors. However, because there are many ways of displaying the results of post-processors, it is necessary to determine whether the results of the analysis programs can be displayed directly or after properly processing them. Examples of the latter case include displaying the results when the post-processors interpolate and smooth the output of stresses from the analysis programs and excess pore water pressure at the element integration points obtained by the analysis programs with respect to the values at the element nodes. In this case, it is necessary to pay attention to the possibility that post-processors may display elements that do not generate excess pore water pressure, as if they have an increase in excess pore water pressure, or they may underestimate the stress values of the surrounding elements when the stress values are relatively small.

Although deformation diagrams and colored contour figures of the stresses output by post-processors have been frequently used in the evaluation of analysis results, it is necessary to use the data directly output by the analysis programs to determine whether or not destabilized numerical calculations cause spike-like acceleration responses, and whether or not the displacement of the object facilities or the excess pore water pressure of the ground is increased in response to the waveforms of the input earthquake ground motions.

2.3.8 Points of Caution for Interpretations of the Analysis Results

As numerical analyses become more advanced, the number of items that require analyzers to make determinations for setting parameters and modeling structural members increases, and there is an increasing concern over the risk that the analysis results are dependent on the skills of analysts. Thus, it is preferable to check the reliability and accuracy of the numerical analysis results by appropriately comparing them with past damage cases or shake table test results.

The methods for checking the accuracy of numerical analyses in actual performance verifications include the following.

(1) Standard cross sections representing the structural types of the object structures subjected to verification of deformation shall be created and analyzed, focusing on the adherence to the ground properties and ground conditions of the object structures.

(2) The results of the above analyses shall be compared with past damage cases. In the case of large discrepancies between the past earthquake damages and the analysis results with input earthquake ground motions similar to previous disasters, the numerical analyses are considered to have some analytical problems and low reliability. In the case of minor discrepancies between past damage cases and analysis results, such discrepancies are considered to be due to fundamental differences in the ground conditions, and, therefore, the analysis accuracy of the numerical analyses can be examined through variations in the results of the analysis cases with different ground properties. For some types of structures, such as gravity-type quaywalls, the results of parametric studies using the FLIP under several standard conditions have been compiled,[28] and, therefore, the accuracy of the numerical analyses can be examined by using these study results as substitutes of past damage cases. However, some analysis results show the relationships between the maximum acceleration of input earthquake ground motions and the deformation of the quaywalls. In such cases, because the deformation of the quaywalls is largely affected not only by the maximum acceleration but also by the waveforms of the input earthquake ground motions, it is necessary to consider that the relationships between the maximum acceleration and the deformation of the quaywalls may not be effectively used for evaluating accuracy when the quaywalls differ between those used in parametric studies and numerical analyses.

    The levels of deformation vary depending on the settings of the parameters for Rayleigh damping. Thus, it is necessary to set the analysis conditions in a manner that examines the appropriateness of the settings of basic analysis conditions through the above process and adjusts the parameters within a theoretically reasonable range as needed.

(3) Series of analyses shall be implemented by shifting the analysis object cross sections from the standard cross sections to actual ones while modifying the meshes. Because this process causes the analysis results to vary every time the structural members and ground improvement areas are modified, the accuracy of the numerical analyses can be evaluated by checking whether or not such variations are consistent with the predicted results in design. This process enables the influences from introducing new construction methods or new materials on the stability of the analyses and analysis results to be understood, thereby securing the reliability of the numerical analyses.

2.4 Examples of Examining the Applicability of the Analysis Methods

2.4.1 Selection of Analysis Methods

It is necessary that the applicability of the analysis methods to be used for the actual verification of deformation through seismic response analyses be confirmed in view of the reproducibility of the damage cases. The FLIP is one of the methods confirmed to be applicable to port structures such as gravity-type quaywalls. In addition to the FLIP, other analysis methods confirmed to be applicable can be selected as optimal methods depending on their characteristics at the designers' discretion. In the case of newly developed structures for which there have not been enough past damage cases to confirm the applicability of the analysis methods, their applicability can be confirmed by checking the reproducibility of the analysis methods with respect to the results of appropriately conducted shake table tests The following sections introduce examples of an analysis method, whose applicability has been confirmed with past damage cases, and an analysis method subjected to re-examination because it could not reproduce past damage cases.

2.4.2 Example of the Analysis Method for Gravity-Type Quaywalls

This section describes an outline of an examination of the applicability of an analysis method under several analysis conditions based on the reproducibility of the damage case of Quaywall No. RF3 on Rokko Island in Kobe Port.[29)]

The input earthquake ground motion used in the examination was from the observation record of the 1995 Hyogoken-Nambu Earthquake obtained through the vertical array seismic observation network installed at Rokko Island in Kobe Port by the Development Bureau of Kobe City. In the vertical array seismic observation network, three-component accelerometers have been installed at depths of GL±0 m, -16 m, -32 m and -83 m. The acceleration waveforms used in the examination were NS and UD components recorded with the accelerometer at a depth of GL -32 m at the time of the 1995 Hyogoken-Nambu Earthquake. In actuality, for the NS component, the recorded signs of the component were inverted (-NS component) while taking into consideration the direction of the examination object quaywall.

An accelerometer at the depth of GL -32 m has been installed on the upper section of the first diluvial gravel layer (equivalent to the Tenma gravel layer). The propagation velocity of S waves V_s and the average N-value in the upper section of the gravel layer (GL -27 m–33 m) were 245 m/s and 13.5 (4.2 to 38), respectively. In the foundation ground of the examination object quaywall, a sandy layer with an N-value of 10 to 30 exists at a depth of GL -26.4 m. Considering that this sandy layer corresponds to the abovementioned first diluvial gravel layer, the bottom face of the analysis model was set at a depth with fixed boundary conditions and the observation record of the 1995 Hyogoken-Nambu Earthquake as input earthquake ground motions applied to the bottom face.

Fig. 2.4.1 shows the waveforms of the acceleration (for 20 seconds) observed at a depth of GL -32 m. As shown in the figure, the duration used in the seismic response analyses was 20 seconds.

Figs. 2.4.2 and **2.4.3** show the classification of soil layers in the analysis object cross section and the finite element mesh of the main section, respectively. In addition, **Tables 2.4.1** and **2.4.2** show the analysis ground properties of each layer. In the examination, modeling was conducted in a manner that applied the multiple shear mechanism model (multiple spring model + excess pore water pressure model) to the reclaimed soil, setting soil and replaced sand, and applied only the multiple shear spring model without the excess pore water pressure model to the reclaimed soil (above the groundwater level), cohesive soil, rubble mound and rubble backfill.

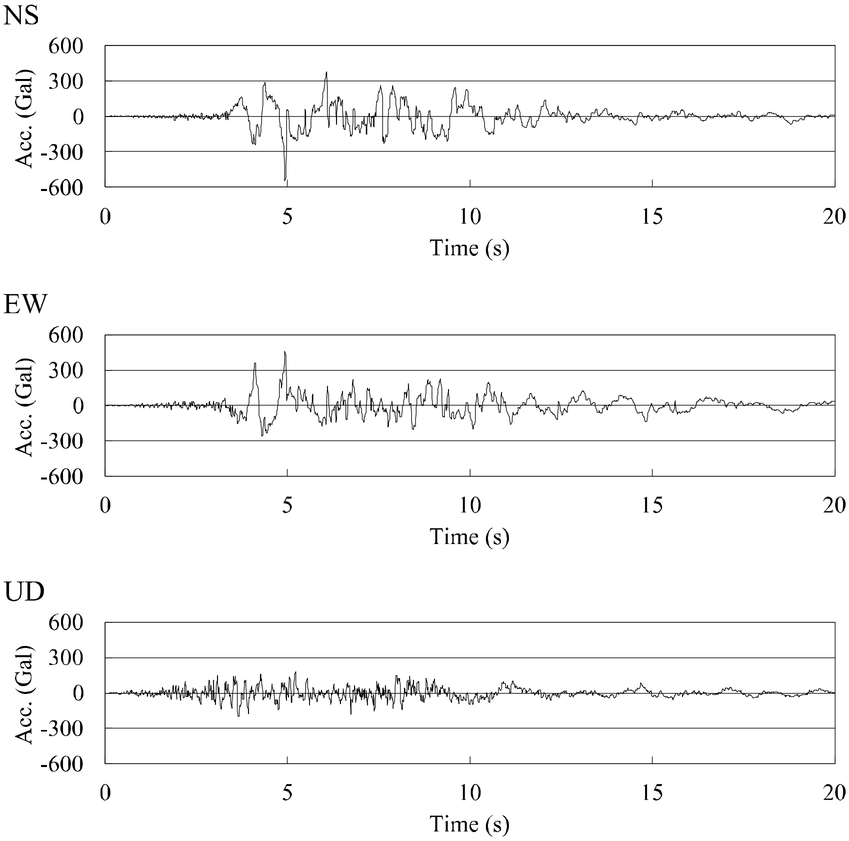

Fig. 2.4.1 Observation Record of the 1995 Hyogo-ken Nambu Earthquake with the Port Island Vertical Array Seismic Observation Network Accelerometer at GL -32 m

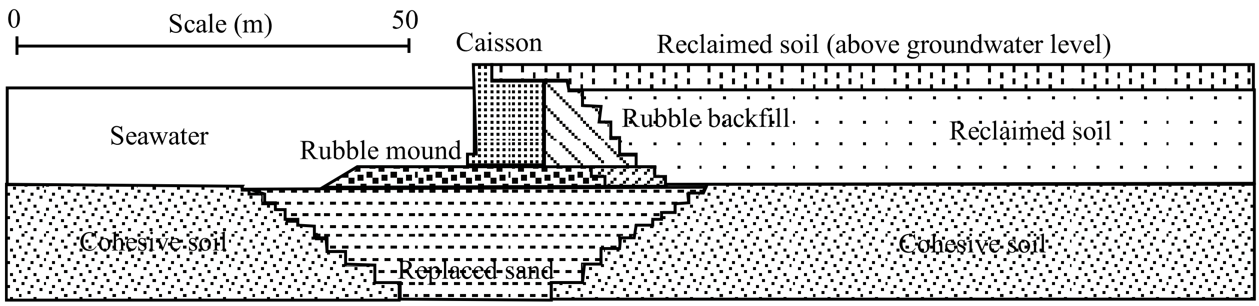

Fig. 2.4.2 Classification of Soil Layers in Object Cross Section

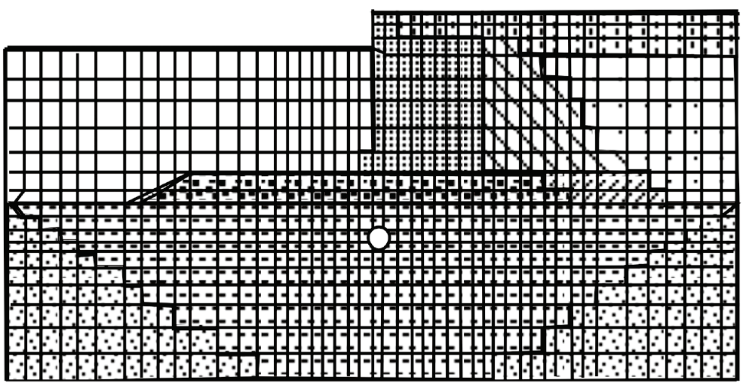

Fig. 2.4.3 Finite Element Mesh of Main Section

Table 2.4.1 Parameters for the Multiple Shear Spring Model and Others

Name of layer	Wet density	Porosity	Deformation characteristics							
			Initial shear modulus	Rebound modulus	Reference confining pressure	Poisson's ratio	Confining pressure dependency coefficient	Internal friction angle	Cohesion	Upper bound for hysteretic damping factor
	ρ_t (t/m^3)	n	G_{ma} (kPa)	K_{ma} (kPa)	σ_{ma}' (kPa)	ν	m	ϕ_f (degree)	c (kPa)	h_{max}
Reclaimed soil (above groundwater level)	1.8	0.45	79,380	207,000	63	0.33	0.5	36	0	0.30
Reclaimed soil	1.8	0.45	79,380	207,000	63	0.33	0.5	36	0	0.30
Replaced sand	1.8	0.45	58,320	152,000	44	0.33	0.5	37	0	0.30
Cohesive soil	1.7	0.45	74,970	195,500	143	0.33	0.5	30	0	0.30
Rubble mound and rubble backfill (old rubble constant)	2.0	0.45	180,000	469,000	98	0.33	0.5	40	0	0.30
Rubble mound and rubble backfill (new rubble constant)	2.0	0.45	180,000	469,000	98	0.33	0.5	35	20	0.30

*1: $m_G = m_K = m$

*2: Cases with old and new rubble constants were tested for rubble mound and rubble backfill.

*3: The values for the porosity, Poisson's ratio, confining pressure dependency coefficient and upper bound for hysteretic damping factor are estimated.

*4: The rebound modulus was set so that the coefficient of earth pressure at rest K_0 became almost 0.5.

Table 2.4.2 Parameters for the Excess Pore Water Pressure Model (Common to All Cases)

Name of layer	Liquefaction characteristics					
	Phase transformation angle	Liquefaction parameter				
	ϕ_p (degree)	w_1	p_1	p_2	c_1	S_1
Reclaimed soil	31.0	7.5	0.45	0.85	2.2	0.005
Replaced sand	30.0	9.0	0.6	0.9	1.8	0.005

At Rokko Island in Kobe Port, several surveys, including frozen sampling and PS logging, were implemented after the earthquake.[10] The physical properties of each layer were calculated from the survey results through the following procedure.

(1) Wet density

The wet density of the reclaimed soil and replaced sand was set at 1.8 t/m^3 based on the results of the density logging implemented on Rokko Island of Kobe Port. It shall be noted that the initial gravity analyses to obtain the stress states before the earthquake ground motions use the underwater weight while taking into consideration **buoyancy.**

(2) Initial shear modulus

The initial shear modulus of reclaimed soil, replaced sand and cohesive soil was calculated based on the PS logging results. The shear modulus of each layer was calculated based on the assumption that the shear modulus is proportional to the average effective confining pressure to the power of 0.5. Although the initial shear modulus of cohesive soil is generally considered to be proportional to the mean effective confining pressure to the power of 1, it was determined that inputting values obtained by using in-situ confining pressure as the reference confining pressure could solve the problem, assuming that it was proportional to the mean effective confining pressure to the power of 0.5, as was the case with sandy soil.

(3) Shear strength of reclaimed soil and replaced sand

The internal friction angles of reclaimed soil and replaced sand were estimated in a manner that obtained the relative density from the *N*-value using the equation proposed by Meyerhof[30] and applied the relative density to the relationship between the relative density and shear resistance angle of decomposed granite sand.[31] In addition, the cohesion *c* was considered to be 0.

(4) Shear strength of cohesive soil

The shear strength of cohesive soil *c* was set at c = 0 kPa and ϕ_f = 30° with reference to the relationship between the plasticity indexes and internal friction angles (drained conditions) of normal consolidated clay.[25]

An undrained cyclic shear test was conducted using test pieces of replaced sand and reclaimed soil obtained through frozen sampling at a -10 m quaywall on Rokko Island in Kobe Port.[10] **Fig. 2.4.4** shows the test results on the liquefaction resistance curves (the filled circles in the figure). Based on these liquefaction resistance curves, the liquefaction parameters were set as shown in **Table 2.4.2**. In the element simulations conducted for setting these parameters, the element was first subjected to isotropic consolidation at an effective confining pressure identical to the test and then the undrained cyclic shear stress. The application of cyclic shear to the element was conducted by dividing 1 cycle into 200 loading steps. In addition, the second phase transformation angle was set at just the intermediate between the phase transformation angle and failure angles using the improved nonlinear interactive calculation method. As a result of the element simulation based on the above conditions and the liquefaction parameters shown in **Table 2.4.2**, the liquefaction resistance curves were obtained as shown by the solid lines (Cases B and D) in **Fig. 2.4.4**.

It was thought that the liquefaction resistance curves vary depending on the analysis conditions even when using identical parameters. Thus, an additional element simulation was conducted through the conventional nonlinear interactive calculation method using identical parameters for cases where the failure angle coincided with the second phase transformation angle (conventional model). The simulation results are shown as the broken lines (Case A) in **Fig. 2.4.4**. Furthermore, another additional element simulation was conducted through the improved nonlinear interactive calculation method for cases where the phase transformation angle coincided with the second phase transformation angle. Here, the simulation results are shown as the solid lines (Case C) in the same figure. For the differences between the conventional and improved interactive calculation methods, the old and new rubble constants, and the definition of the second phase transformation angle, refer to the reference.[15]

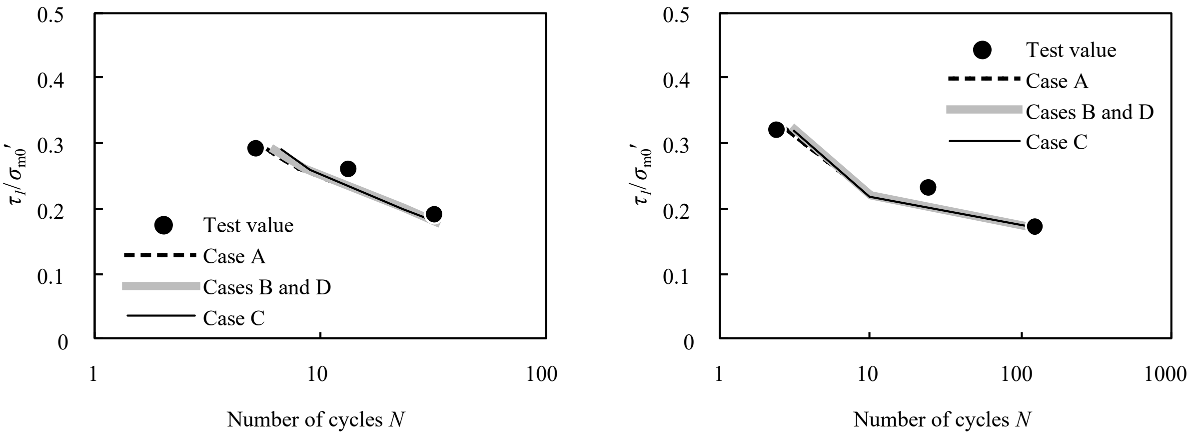

(a) Replaced sand (σ_{m0}'= 225.4 kPa) (b) Reclaimed soil (σ_{m0}'= 117.6 kPa)

*1: The test values were based on the liquefaction strength test results with test pieces obtained through frozen sampling.[10]

*2: The element simulations were conducted under the conditions of Case A, where the second phase transformation angle coincided with the failure angle (conventional model), and the conventional nonlinear interactive calculation method was used; Cases B and D, where the second phase transformation angle was just in the intermediary between the phase transformation and failure angles, and the improved nonlinear interactive calculation method was used; and Case C, where the second phase transformation angle coincided with the phase transformation angle, and the improved nonlinear interactive calculation method was used.

Fig. 2.4.4 Comparison of Liquefaction Resistance Curves between Test Results and Element Simulations (Liquefaction Assessment based on Double Amplitude Axial Strains of 5%)

Because the liquefaction test was conducted for types of soil that have a low shear stress ratio, there was no significant influences from the differences in the conditions for the element simulations on the liquefaction resistance curves.

The modeling of the structure was conducted while taking into consideration the presence of the footing of the caisson. Regarding the footing in front of the caisson, the width was equal to the actual width, and the thickness was adjusted to that of the fluid elements in front of the footing. In addition, the mass of the footing was set at 0. The existence of the footing at the back of the caisson was expressed by setting the stiffness of the rubble backfill on the footing equal to that of the caisson. That is, in the modeling, the caisson had a structure where its rear face was extended 1.0 m horizontally in a direction toward the inner harbor side, and the extended portion had a density equal to that of the rubble backfill.

In addition, in the modeling, the contact face between the caisson's bottom face (including the bottom face of the footing) and the rubble mound was expressed as joint elements, which could be slid and separated. Furthermore, the contact face between the caisson's rear face (after extension) and the rubble backfill was modeled in the same way. Here, the slide friction angles between the caisson's bottom face and the rubble mound and between the caisson's rear face and the backfill stones were 31 and 15 degrees, respectively.

Tables 2.4.3 and **2.4.4** show the analysis constants of the caisson and the joint elements, respectively.

Table 2.4.3 Analysis Constants of the Structures (Expressed by Linear Plane Elements)

Structure	Young's modulus E (kPa)	Poisson's ratio ν	Density ρ (t/m^3)
Caisson	2.23×10^7	0.17	2.1
Superstructure concrete	2.94×10^7	0.17	2.3
Footing	2.94×10^7	0.17	0.0
Extended portion of caisson	2.23×10^7	0.17	2.0

Table 2.4.4 Analysis Constants of Joint Elements around the Caisson

Joint position	Stiffness in the normal direction K_n (kPa/m)	Stiffness in the tangential direction K_s (kPa/m)	Cohesion c_J (kPa)	Friction angle ϕ_J (degree)
Caisson's bottom face	1.0×10^6	1.0×10^6	0	31
Caisson's rear face	1.0×10^6	1.0×10^6	0	15

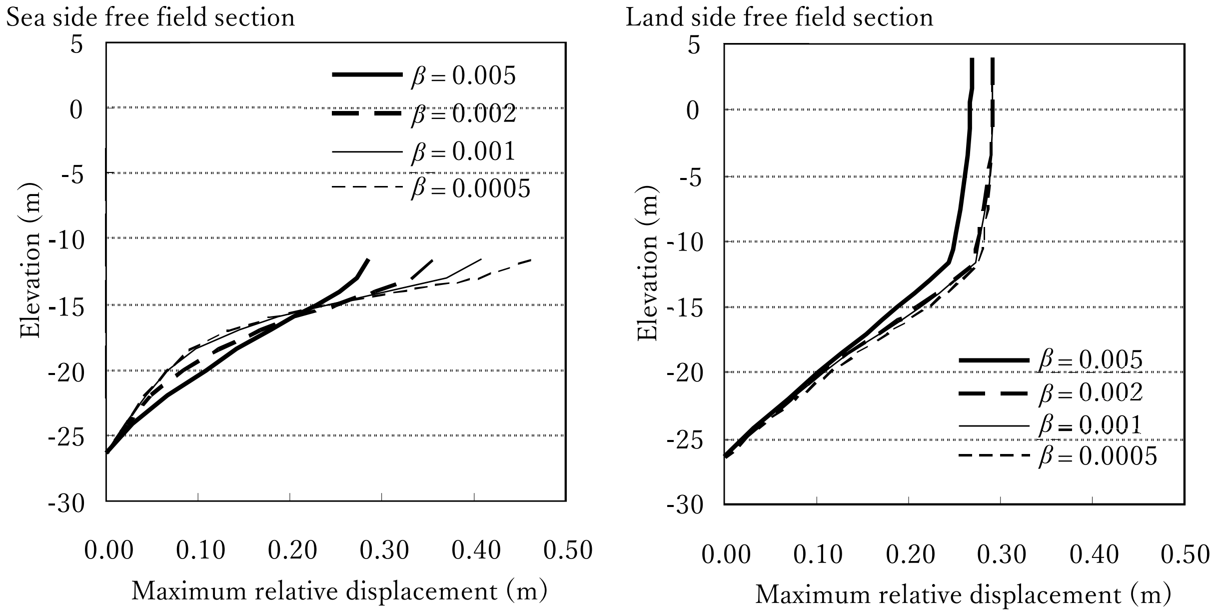

Fig. 2.4.5 Convergence of the Distribution of Maximum Relative Displacement at a Free Field Section in the Depth Direction in the Case of Small Rayleigh Damping Stiffness Proportionality Coefficient β (Non-liquefaction Analysis)

After the modeling, an initial gravity analysis was conducted followed by a seismic response analysis using the results of the initial gravity analysis. In both analyses, the common constitutive laws and analysis ground constants were used.

In the initial gravity analysis, the self-weight (the underwater weight for the portion below the groundwater level) were input as the load under a fully drained condition. In the seismic response analysis, the abovementioned earthquake ground motions were input under an undrained condition. Wilson's θ method was used as the time integration method in the seismic response analysis. When the Rayleigh damping stiffness proportionality coefficient β of the joint elements was 0, time integration interval Δt was 0.001 seconds to improve the convergence situation of the nonlinear iterative calculation, and if this was not the case, the time integration interval Δt was 0.01 seconds.

The initial stiffness proportional type Rayleigh damping matrix was used for stabilizing the calculations. When conducting the seismic response analysis of the free field sections for several cases with different values of the stiffness proportionality coefficient β without considering the increase in excess pore water pressure, a critical stiffness proportionality coefficient β, the maximum value of β beyond which it starts to affect the distribution of maximum horizontal displacement, can be found. In **Fig. 2.4.5**, the critical β is 0.002 in the land side free field section and 0.001 in the sea side free field section. Thus, two types of stiffness proportionality coefficient β, 0.001 and 0.002, were applied to each analysis case.

A total of four cases were analyzed: a case with analysis conditions set in accordance with FLIP Ver. 3.3 (Case A), and three other cases, Cases B, C and D, with different analysis conditions set in accordance with different types of program improvement. Each case was analyzed by switching the values of the stiffness proportionality coefficient β of the initial stiffness proportional type Rayleigh damping matrix between 0.001 and 0.002.

Table 2.4.5 shows the analysis conditions common to all cases, and **Table 2.4.6** shows the analysis conditions unique to each case. The analysis conditions of Case A were based on the conventional dynamic model of sand (the second phase transformation angle = fracture angle) and the conventional nonlinear iterative calculation method. The analysis conditions of Cases B, D and C were based on the modified dynamic model of sand and the improved nonlinear iterative calculation method. In Cases B and D, the second phase transformation angle was set at the intermediary just between the fracture angle (shear resistance angle) and the phase transformation angle. In contrast, in Case C, the second phase transformation angle was set equal to the phase transformation angle. Here, the condition setting in Cases B and D and that in Case C are called tmp7 and tmp3 methods, respectively.

Case A was also analyzed with the initial stiffness proportional type Rayleigh damping applied to the joint elements. That is, the initial stiffness of the joint elements was multiplied by the stiffness proportionality coefficient β of the entire system when creating the Rayleigh damping matrix. In contrast, Cases B, C and D were analyzed with the initial stiffness of the joint element multiplied by the stiffness proportionality coefficient β of 0 when creating the Rayleigh damping matrixes to prevent the Rayleigh damping from curbing the sliding behavior of the joint elements. As a countermeasure to prevent possible unstable behavior of the joint elements due to the above settings, the time integration interval Δt was set at 0.001 seconds, which is 1/10 of the normally used interval of 0.01 seconds.

Table 2.4.5 Analysis Conditions Common to All Cases

Classification	Main factor largely affecting analysis results	Analysis condition setting
① Dynamic model of sand	a. Method for evaluating the contribution of shear work to negative dilatancy in a stress space beyond the phase transformation line	Depends on the case
② Motion equation of a two-phase system and its numerical analysis method	b. Method for nonlinear iterative calculation of the stress-strain relationship	Depends on the case
	d. Concept of damping (method for setting the stiffness proportionality coefficient β of the initial stiffness proportional type Rayleigh damping)	Stiffness proportionality coefficient β at the time of the convergence of displacement response (0.001 and 0.002)
	e. Elimination of damping control over the sliding behavior of the joint elements	Depends on the case
	h. Consideration of large deformation effects	No consideration
③ Boundary conditions, contact conditions and pile-ground interaction	f. Consideration of the three-dimensional effects of the pile-ground interaction	No piles
④ Method for setting the initial state	c. Method for evaluating the initial stress state	Single-stage initial gravirty analysis
⑤ Dynamic models for materials other than sand	g. Dynamic model of rubble stones	Depends on the case

Table 2.4.6 Analysis Conditions Unique to Each Case

Item	Case A	Case B	Case C	Case D
a. Value of the second phase transformation angle (method for evaluating the contribution of shear work to negative dilatancy in a stress space beyond the phase transformation line)	Failure angle: conventional model	Intermediary between failure and phase transformation angles: modified model (tmp7 method)	Phase transformation angle: modified model (tmp3 method)	Intermediary between failure and phase transformation angles: modified model (tmp7 method)
b. Method for nonlinear iterative calculation of the stress-strain relationship	Conventional type	Improved type	Improved type	Improved type
e. Joint element stiffness proportionality coefficient β (elimination of damping control over the sliding behavior of joint elements)	Equal to β of the entire system	0	0	0
g. Dynamic model of rubble stones	Old rubble constant	Old rubble constant	Old rubble constant	New rubble constant

Item	Case A	Case B	Case C	Case D
Remarks	Conventional method	Improvement method I	Improvement method II	Improvement method I + new rubble constant

*1: Each case was analyzed by switching the values of the Rayleigh damping stiffness proportionality coefficient β between 0.001 and 0.002.

*2: The liquefaction parameters shown in **Table 2.4.2** were used (in all cases).

The analysis results are as follows.

Table 2.4.7 shows a list of the analysis results of each case in terms of the evaluation items: the residual horizontal and vertical displacement at the levee crown of the caisson superstructure, the seaward displacement of the bottom section of the caisson, the rotation angles of the caisson, and the level differences on the ground surface at the back of the caisson superstructure. The maximum and average of the actual measurements of each evaluation item are also shown in the table. **Fig. 2.4.6** shows comparison diagrams of the evaluation items (excluding level differences) based on the values in the table.

Figs. 2.4.7 and **2.4.8** show the residual displacement of Cases A to D when the values of β are 0.002 and 0.001, respectively. **Fig. 2.4.9** shows the distribution of duration maximum values of the excess pore water pressure ratios (= 1- σ_m'/σ_{m0}') of Cases A to D (with β of 0.002).

In addition, **Figs. 2.4.10** and **2.4.11** show the time history horizontal displacement and horizontal acceleration at the levee crown of the caisson in Cases A to D (with β of 0.002), respectively, and **Fig. 2.4.12** shows the relationship between the shear stress and shear strain and the relationship between the deviator stress and deviator strain of the output object elements in the replaced sand (elements with ○ in **Fig. 2.4.3**).

Case A (conventional model) with β of 0.002 had reproducible results of the actual measurements of the seaward displacement and subsidence of the levee crown of the caisson. However, Case A with β of 0.001 showed significant increases in the seaward displacement and subsidence of the levee crown of the caisson to a level that exceeded the maximum values of their actual measurements. The result of an additional analysis of Case A with β of 0.0005 showed a further increase in the residual displacement to a level that almost doubled the values of Case A with β of 0.002. Although Cases B to D also showed increases in residual displacement when β was switched from 0.002 to 0.001, the variations were not as large as in Case A. It can be said that the use of the modified model reduced the sensitivity to β. The method used in Case A is likely to become unstable and produce large strain depending on the circumstances, and it is undeniable that the Rayleigh damping matrix curbs the destabilization and the increase in strain.

As mentioned above, Case A with β of 0.002 had reproducible results of the actual measurements of the seaward displacement and subsidence of the levee crown of the caisson. However, it had a smaller caisson inclination angle than the actual measurement and failed to reproduce the level difference at the back of the caisson; Case A with β of 0.001 showed a similar trend. This is because the Rayleigh damping made the joint elements at the back of the caisson difficult to slide, thereby reproducing no level difference on the ground surface at the back of the caisson and curbing its rotation. In addition, as can be seen in the diagrams of residual deformation (**Figs. 2.4.7** and **2.4.8**), Case A had a larger shear deformation of the replaced sand below the caisson and smaller deformation of the rubble mound compared to other cases. In terms of the shear strain (γ_{xy} and γ_d) of the output object elements in the replaced sand layer below the caisson (**Fig. 2.4.12**), Case A had a larger value than Cases B and C. Thus, in Case A, the seaward displacement and subsidence of the levee crown of the caisson were due mainly to the shear deformation and deviator shear deformation of the replaced sand, respectively. Because replaced sand easily produces large strain, deformation is concentrated in the replaced sand with the rubble mound undergoing little deformation, which is a part of the reason why Case A had a large seaward displacement at the bottom section of the caisson and a small caisson inclination angle.

Case B had a smaller seaward displacement and subsidence of the levee crown of the caisson than Case A with the calculation results of the seaward displacement and subsidence corresponding to 70% and 36% of the averages of the actual measurements, respectively. In contrast, with a smaller seaward displacement of the bottom section of the caisson and larger caisson inclination angle, Case B had better reproducible results of the actual measurements than Case A, including the reproduction of the level difference at the back of the caisson. This is because the Rayleigh damping did not curb the behavior of the joint elements at the back of the caisson in Case B, allowing the joint elements to slide. Case B had considerably smaller deformation of the replaced sand than Case A and instead produced clear shear deformation in the rubble mound. In terms of the shear strain (γ_{xy} and γ_d) of the output object elements in the replaced sand layer below the caisson (**Fig. 2.4.12**), the shear strain was curbed in Case B compared to Case A. With the deformation of the replaced sand curbed, the deformation was concentrated in the rubble mound; that is, the seaward displacement of the levee crown of the caisson in Case B was due mainly to the shear deformation of the rubble mound and the rotation of the caisson.

The analysis results of Case C were similar to those of Case B; however, Case C had a smaller seaward displacement and subsidence of the levee crown of the caisson than Case B, with the shear strain of the replaced sand curbed. As a result, Case C produced wider differences between the predicted values and actual measurements than Case B.

Case D was a modification of Case B in terms of the constants of the rubble mound and rubble backfill. As can be seen in **Table 2.4.7** and **Fig. 2.4.6**, Case D had a larger residual horizontal displacement at the levee crown of the caisson than Cases B and C, and the predicted value was about 80% of the average of the actual measurements. Case D also had the seaward displacement at the bottom section of the caisson and the residual inclination angle of the caisson was consistent with the actual measurements. Although Case D had a larger subsidence of the levee crown of the caisson than Cases B and C, the value was still about 40% of the average of the actual measurements.

The actual measurement of the subsidence was based on the design crown height and includes the consolidation settlement before the earthquake; however, the degree of such consolidation settlement remains unknown. Thus, judging from the comparison of the analysis results of each case with the actual measurements, excluding the subsidence, it can be said that Case D, considering the simultaneous application of all the proposed improvement models and updates of the constants of the rubble mounds and rubble backfills based on the latest knowledge, almost explains the degrees of damage to the caisson-type quaywall, Quaywall No. RF3 on Rokko Island in Kobe Port, due to the 1995 Hyogoken-Nambu Earthquake.

Table 2.4.7 Residual Displacement and Rotation Angles of Caissons

	Seaward displacement of caisson superstructure	Subsidence of caisson superstructure	Seaward displacement of caisson bottom section	Residual inclination angle of caisson	Level difference on ground surface at back of caisson superstructure
	(cm)	(cm)	(cm)	(degree)	(cm)
Case A	371/541	149/251	343/462	1.22/3.39	0/0
Case B	240/264	55/58	160/174	3.46/3.84	86/63
Case C	204/241	43/52	122/142	3.54/4.26	67/66
Case D	285/308	63/71	192/212	3.99/4.12	107/69
Actual measurement (maximum)	464	198	238	6.4	200
Actual measurement (average)	370	158	-	3.1	-

*1: The left and right values in each cell correspond to the predicted values with $\beta = 0.002$ and $\beta = 0.001$, respectively.
*2: The positive values in the inclination angle mean the seaward inclination of the head section of the caisson.
*3: The actual measurements are the maximums and averages of Caissons Nos. 7 to 21 in **Fig. 2.2.2**.
*4: The actual measurement of the level difference on the ground surface at the back of the caisson superstructure is based on **Fig. 2.2.3**.

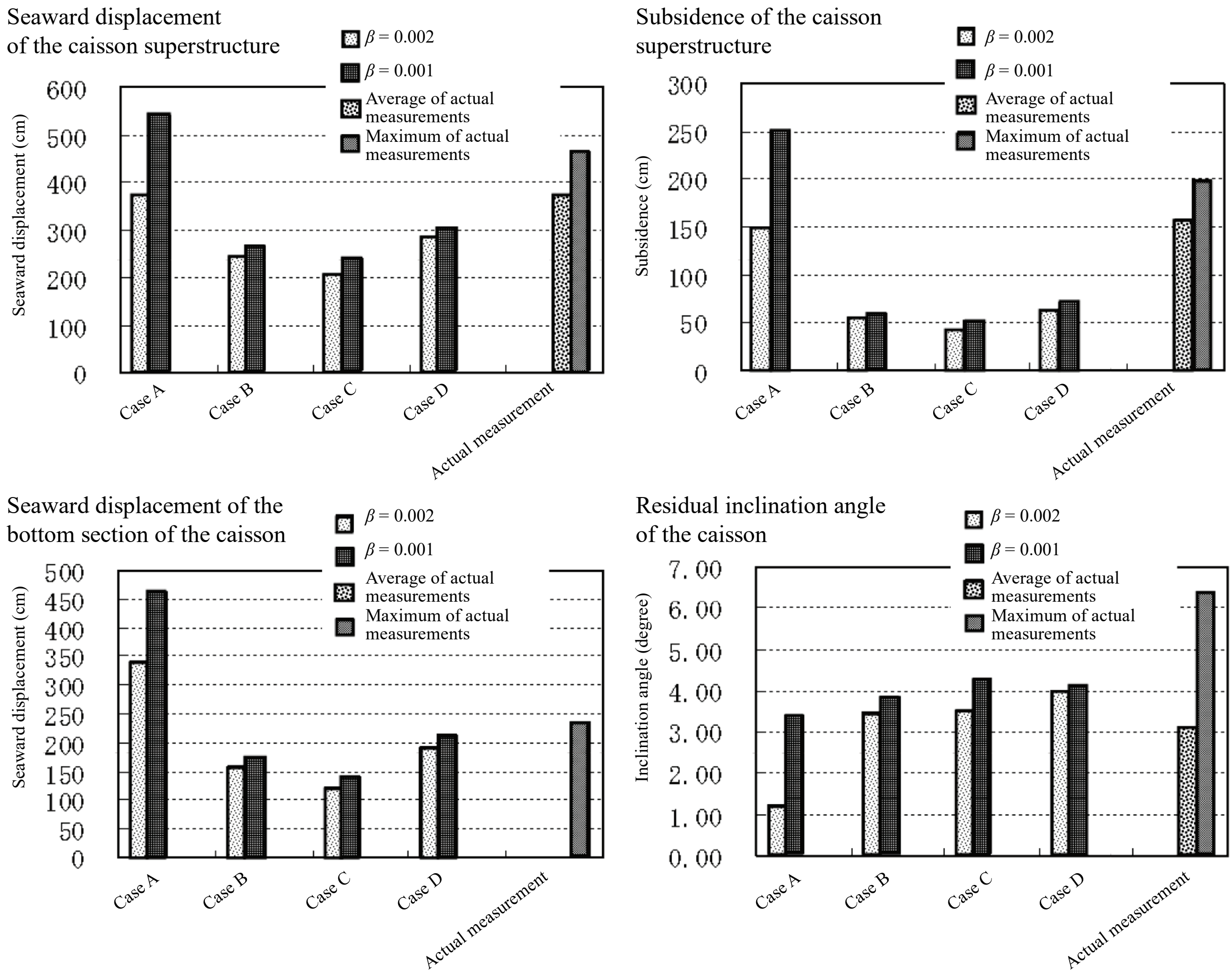

Fig. 2.4.6 Residual Displacement and Inclination Angle of Caissons (Based on **Table 2.4.7**)

In terms of the shear strain (γ_{xy} and γ_d) of the output object elements in the replaced sand layer (**Fig. 2.4.12**), Case D had a larger prediction value than Cases B and C. This is the reason why Case D had a larger seaward displacement and subsidence than Cases B and C. The new rubble constant had a larger effect of increasing the shear strength of rubble in a low confining pressure state than the old rubble constant. It can be said that, with increased hardness of the rubble mound due to the new rubble constant, Case D had a large deformation of the replaced sand.

As above, when analysis programs are improved, it is necessary to examine whether or not the improved programs can show similar applicability as with previous programs. From this viewpoint, the abovementioned example shows that the cases analyzed with the newly proposed improvement methods could reproduce damage cases as well as the conventional methods.

However, as shown in **Fig. 2.4.6**, the cases analyzed using the improvement methods (Cases B to D) showed a tendency to underestimate displacement due to damage compared to the case analyzed under the conventional analysis conditions (Case A). It is reasonable to improve several types of analysis programs for enhancing analysis accuracy in a manner that reduces variations in the analysis results. However, for ensuring continuity from the analysis results obtained using previous programs, it is preferable that the improvement methods be able to predict deformation at a level almost equal to that obtained through conventional methods with respect to past damage cases for which the conventional methods are proven to have reproducibility.

In addition, Cases B to D, analyzed using the improvement methods, required long calculation times because of the short time step (0.001 seconds). Thus, it is preferable in a practical sense that the improvement methods be able to analyze cases with the time step at a level similar to the conventional methods (0.01 seconds).

Thus, in order to find a way to deal with these problems, a parametric study was conducted to compare the analysis results of cases with different combinations of improvement methods. **Table 2.4.8** shows a list of analysis conditions and residual displacement. In the parametric study, some cases (Cases E, J, L and M) were identical to those in the abovementioned example, and are also shown in the table for comparison.

Cases F and G, which were analyzed with the improved nonlinear iterative method, had smaller displacement due to damage than the conventional method (Case E). Then, Cases H, K and N were analyzed so as to find a combination of improvement methods which could achieve displacement at a level equal to the conventional method with a reduced Rayleigh damping stiffness proportionality coefficient β (= 0.0005). As a result, Cases K and N, where the improvement method was applied to the joint sections, produced displacement due to damage almost equal that of the case with the conventional method. Although the displacement was small, Case H, which was analyzed without the improvement methods for joints and rubble properties, showed reproducibility. In contrast, the cases analyzed with the conventional method for joints and shorter calculation times (Cases O, P and Q) had larger caisson inclination angles than the actual measurements, as if the caisson had tipped over.

From a practical viewpoint, it is considered that, even without the improvement methods for both joints and rubble properties, Case H could ensure similar reproducibility to Cases M and N, which were analyzed using the improvement methods for all parameters without losing practical convenience. Therefore, when studying several countermeasure methods, there may be a possibility of using the analysis conditions of the conventional methods or Case H for analyzing multiple cases to understand the tendency of the analysis results, as well as the analysis conditions of Cases M or N, which require long calculation times for making final confirmations.

However, it does not necessarily mean that this approach without the improvement methods for both joints and rubble constants can be applied to all cases. This approach is considered to be available for other cases with similar cross sections because the deformation modes are also similar to each other. Thus, the applicability of this approach needs to be carefully studied when applying it to other cases with different cross sections. For example, when the foundation ground is stiff, it is desirable to analyze strict cases, such as Cases M or N, even if it requires taking long calculation times from the beginning because of the possible sliding failure on the bottom face of the caisson. Furthermore, using the improvement methods for partial parameters, as in Cases O, P and Q, may throw the analyses off balance, thereby reducing reproducibility compared to the conventional methods.

In conclusion, the following points of caution can be extracted from the above.

① It is necessary to examine the applicability of several analysis programs every time they are improved.

② Different combinations of improvement methods produce different tendencies in the analysis results. Therefore, it is necessary to pay attention to the concept of setting the parameters to remain consistent with the existing analysis results.

③ It is difficult to determine the appropriateness of the detailed analysis conditions and parameter settings from damage cases because the actual damage cases have variations in damage.

④ Designing structures using seismic response analyses requires advanced engineering judgment based on a wide variety of discussions on the verification of the applicability of such analyses.

It is also necessary to verify the applicability of the seismic response analyses to not only damage cases but also cases where there is no damage. For gravity-type quaywalls, the verification of the applicability to cases where there is no damage was studied using the cross section of the east side quaywall, which is a caisson-type quaywall (having a water depth of 10.0 m and seismic coefficient of 0.20) at the second wharf in West Kushiro Port, which experienced the 1993 Kushiro Oki Earthquake.[29)]

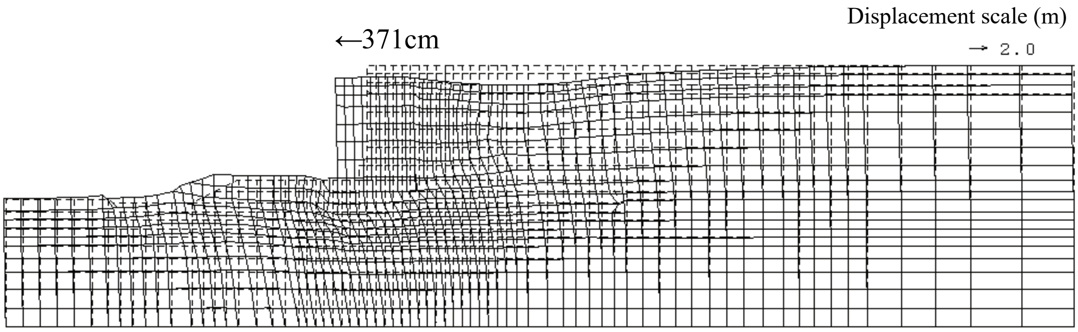

(a) Case A (Conventional Method)

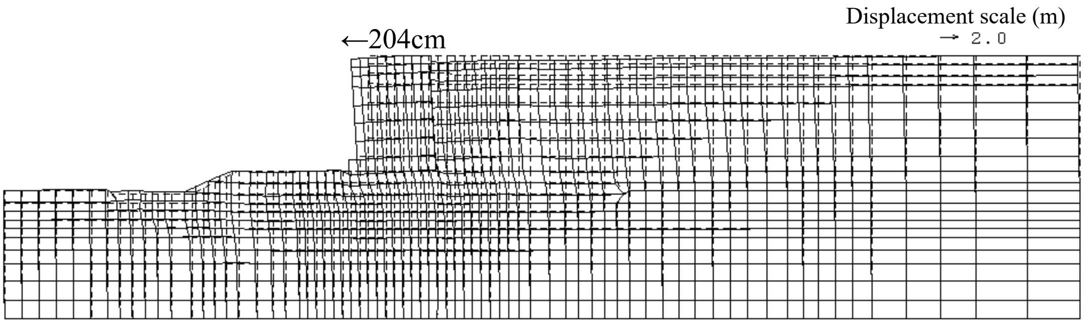

(b) Case B

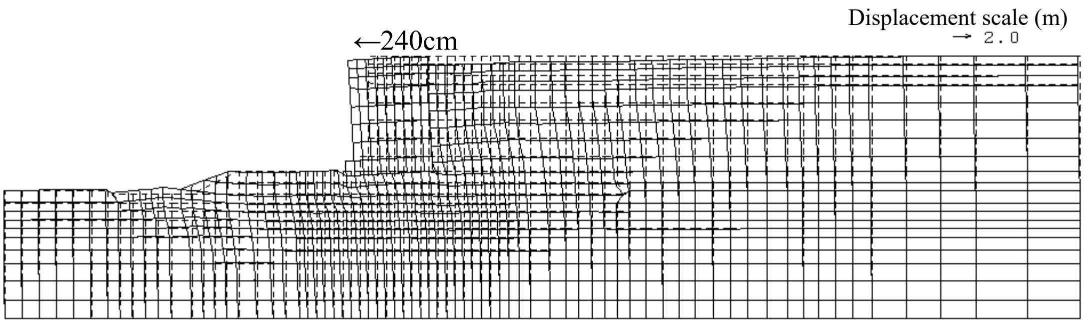

(c) Case C

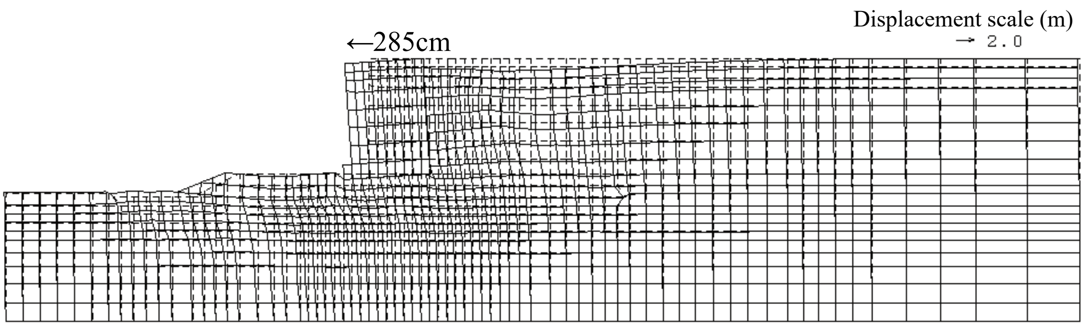

(d) Case D

Fig. 2.4.7 Residual Deformation Diagrams (with β = 0.002 for All Cases)

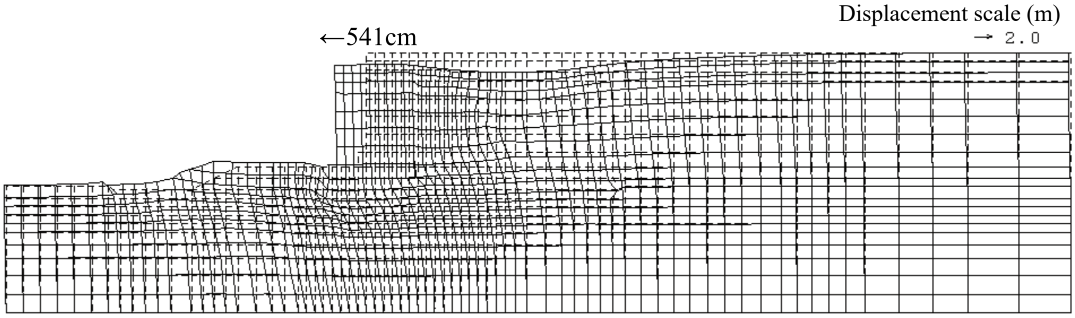

(a) Case A (Conventional Method)

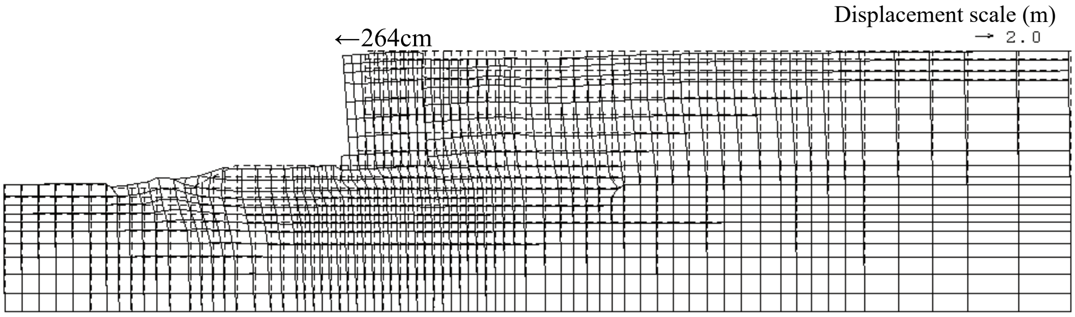

(b) Case B

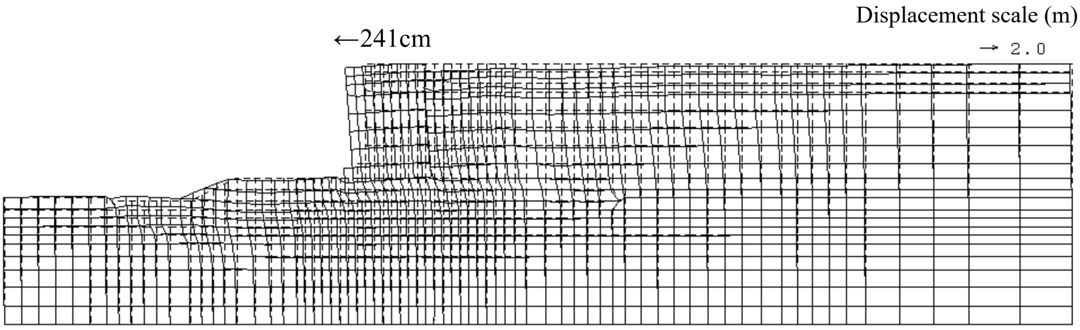

(c) Case C

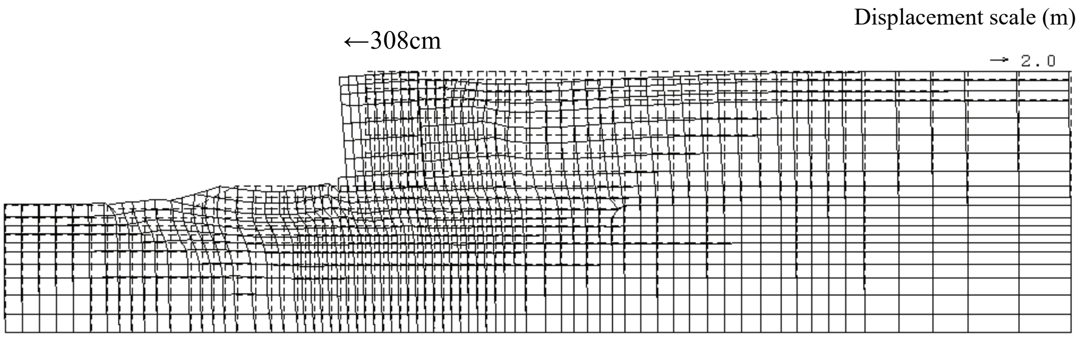

(d) Case D

Fig. 2.4.8 Residual Deformation Diagrams (with β = 0.001 for All Cases)

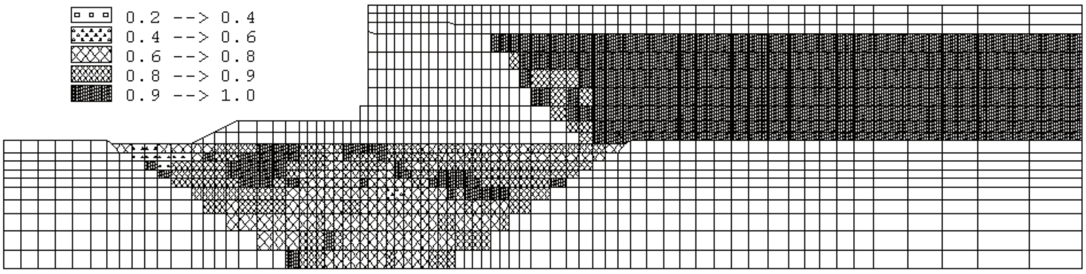

(a) Case A (Conventional Method)

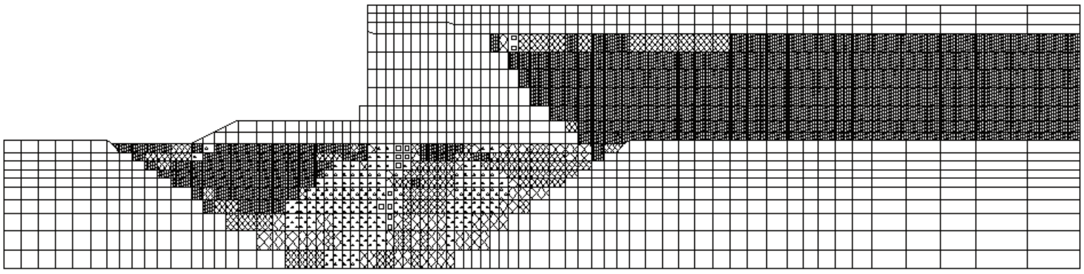

(b) Case B

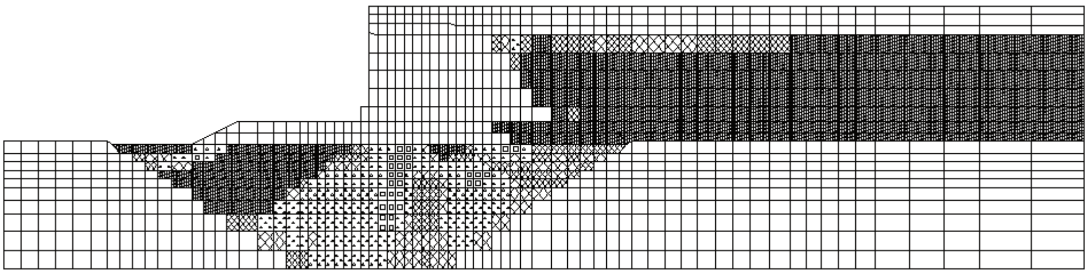

(c) Case C

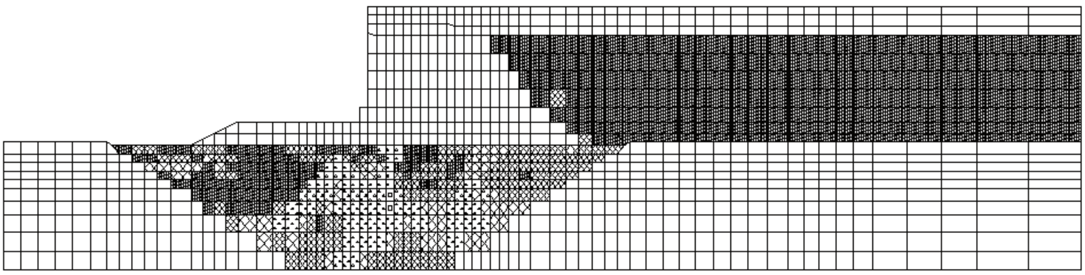

(d) Case D

Fig. 2.4.9 Distribution of Duration Maximum Values of Excess Pore Water Pressure Ratio (= 1- σ_m'/σ_{m0}') (with β = 0.002 for All Cases)

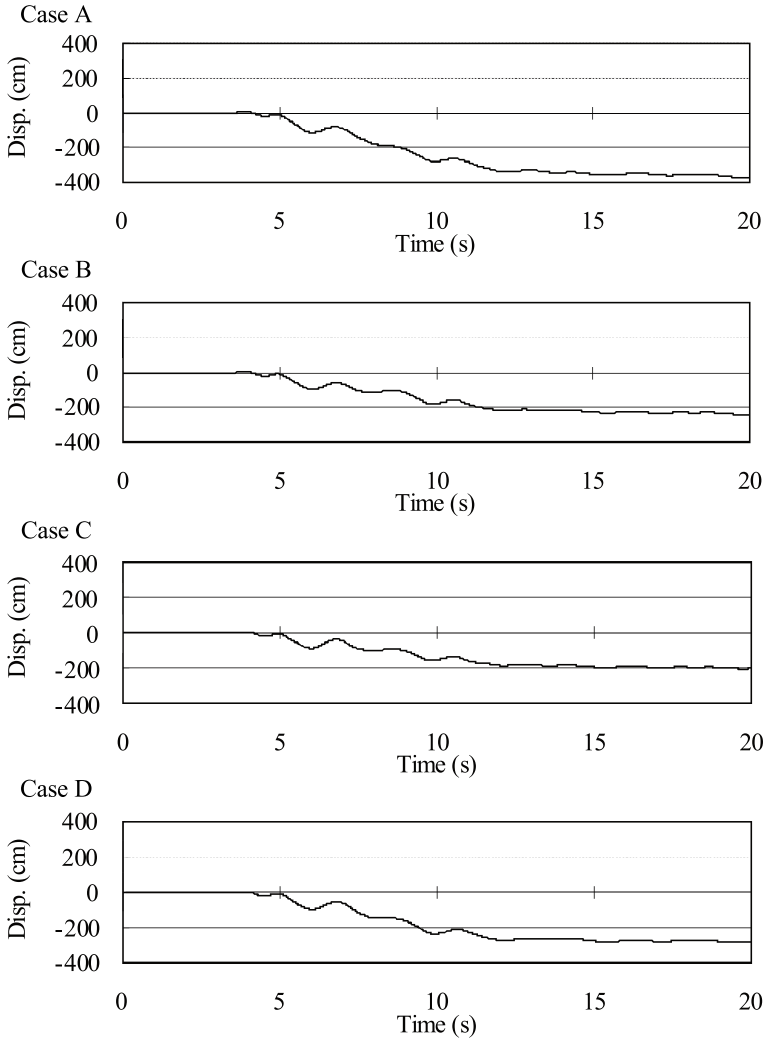

Fig. 2.4.10 Time History of Horizontal Displacement at the Levee Crown of the Caisson Superstructure (with β = 0.002 for All Cases)

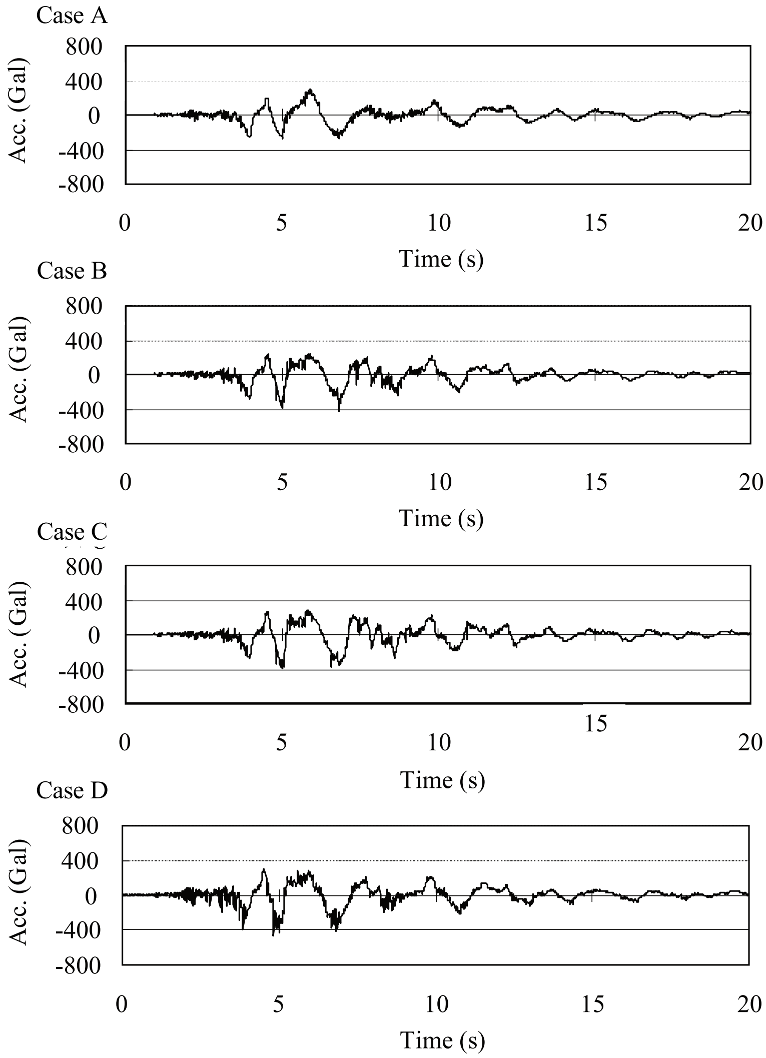

Fig. 2.4.11 Time History of Horizontal Acceleration at the Levee Crown of the Caisson Superstructure (with β = 0.002 for All Cases)

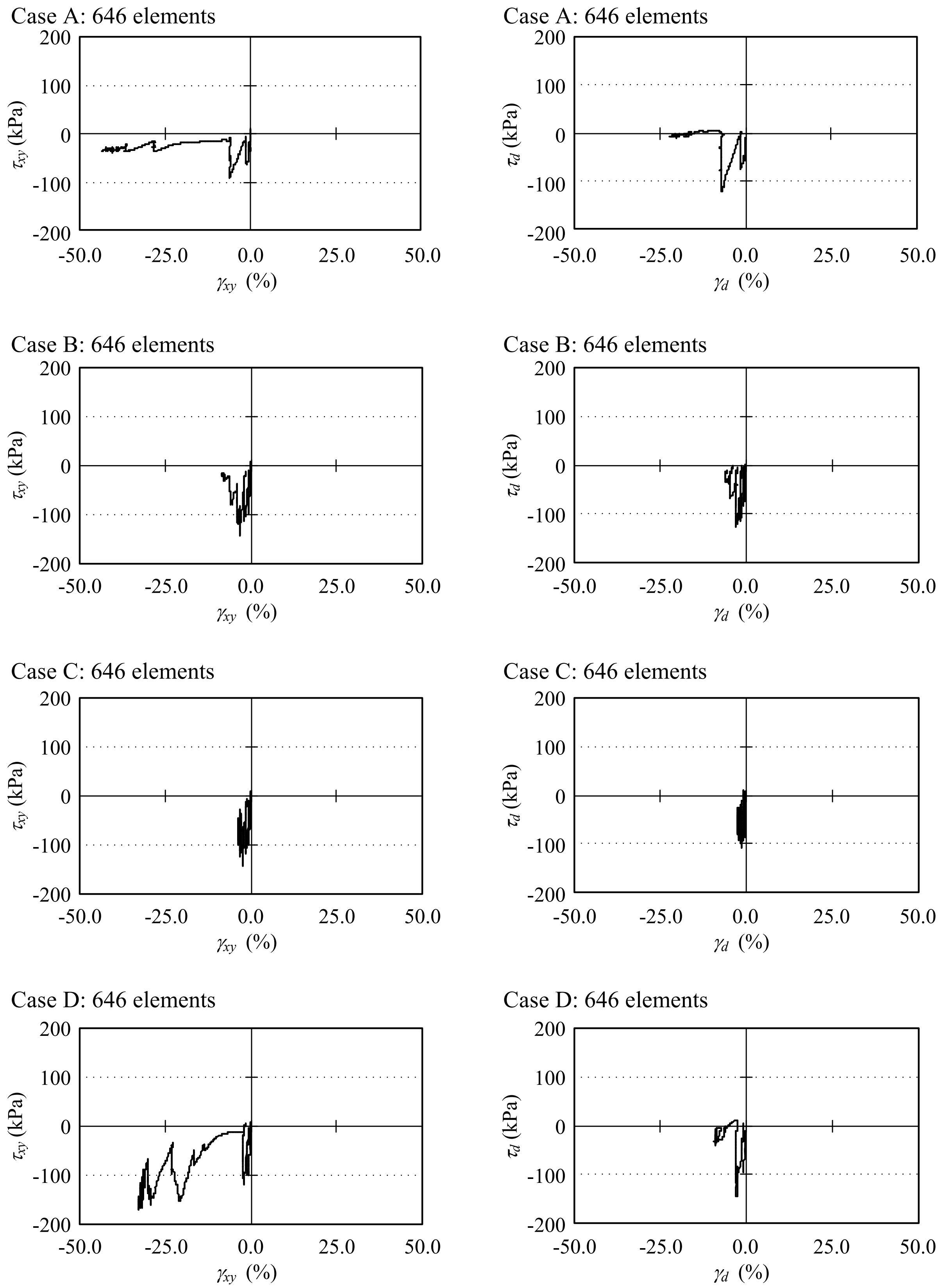

Fig. 2.4.12 $\tau_{xy} - \gamma_{xy}$ Relationship (Left) and τ_d (= $(\sigma_y - \sigma_x) / 2$) - γ_d (= $\varepsilon_y - \varepsilon_x$) Relationship (Right) of Output Object Elements in the Replaced Sand (Elements with ○ in **Fig. 2.4.3**) (with β = 0.002 for All Cases)

Table 2.4.8 Applicability of the Improvement Methods to Quaywall No. RF3 at Kobe Port
(β = 0.002, displacement in the unit of m, time increment in the unit of seconds,
and underlined value means outside the range of the actual measurements)

Case	Iterative method	Shear work	Joint	Time increment	Rubble constant	Horizontal displacement	Vertical displacement	Inclination angle (degree)
Case E	Conventional	Conventional	Conventional	0.01	Conventional	3.71	1.49	1.22
Case F	Improvement	Conventional	Conventional	0.01	Conventional	2.68	0.87	1.52
Case G	Improvement	tmp7	Conventional	0.01	Conventional	2.41	0.59	3.83
Case H	Reduction in Rayleigh damping with respect to Case G (β = 0.0005)					3.00	0.71	4.27
Case I	Improvement	tmp3	Conventional	0.01	Conventional	2.11	0.46	3.37
Case J	Improvement	tmp7	Improvement	0.001	Conventional	2.40	0.55	3.46
Case K	Reduction in Rayleigh damping with respect to Case J (β = 0.0005)					3.12	0.69	4.75
Case L	Improvement	tmp3	Improvement	0.001	Conventional	2.04	0.43	3.54
Case M	Improvement	tmp7	Improvement	0.001	Improvement	2.85	0.63	3.99
Case N	Reduction in Rayleigh damping with respect to Case M (β = 0.0005)					3.29	0.71	4.37
Case O	Improvement	tmp7	Conventional	0.01	Improvement	3.81	1.21	7.44
Case P	Reduction in Rayleigh damping with respect to Case O (β = 0.0005)					4.21	1.12	7.32
Case Q	Improvement	tmp3	Conventional	0.01	Improvement	3.23	0.85	6.19
Damaged situation						2.08 to 4.64	1.14 to 1.98	−2.2 to 6.4

2.4.3 Example of an Analysis Method for Sheet Pile Quaywalls

The following section introduces an example of the verification of the applicability of the FLIP analysis method for sheet pile quaywalls and the examination of the appropriate analysis methods to ensure analysis accuracy.[29)]

At the beginning of the verification of the applicability of the FLIP to sheet pile quaywalls, the FLIP had a problem with producing a large displacement and cross-sectional force even when these sheet pile quaywalls were subjected to acceleration at relatively low levels, thereby leading to evaluation results of very low earthquake resistance capacity for the existing sheet pile quaywalls. However, according to existing reports on earthquake damage, these sheet pile quaywalls did not undergo much deformation, except for cases of sheet pile quaywalls with remarkable liquefaction in the ground behind them. Thus, it was thought that the FLIP might underestimate the earthquake resistance capacity of existing sheet pile quaywalls.

As one of the measures to figure out the reasons for the problem, one-dimensional analyses were first conducted for the sheet pile quaywalls, including the ground behind them. As a result, it was confirmed that the areas of the ground where liquefaction occurred were almost identical to the results of the liquefaction assessment. Then, the FLIP analyses were conducted under non-liquefaction conditions without considering the influence of dilatancy and produced basically appropriate results with significantly small deformation. The deformation of the sheet pile quaywalls that were damaged in past disasters and subjected to the verification this time was due to liquefaction, but the analysis accuracy of the FLIP was considered to be insufficient to evaluate the two-dimensional influences required to determine the liquefaction areas.

Next, FLIP analyses were conducted with the ground condition (N-values) and input acceleration as parameters. As a result, unlike in the cases of the one-dimensional analyses and liquefaction assessment, the liquefaction was reproduced even when the level of acceleration was small in the vicinity of the front sheet piles and anchorage piles. Thus, liquefaction was confirmed to be the reason for the increases in the deformation and cross-sectional force of the sheet piles. The same analysis was conducted with another liquefaction program called LIQCA[for example, 32)] for comparison, and it was confirmed that LIQCA did not reproduce particularly severe liquefaction in the vicinity of the front sheet piles and anchorage piles. That is, the reproduction of severe liquefaction in the vicinity of the front sheet piles and anchorage piles is considered to be a problem unique to the FLIP.

The ground in the vicinity of the front sheet piles and anchorage piles was close to active or passive failure states, with soil elements subjected to large shear force from the initial state. In the FLIP, application of additional shear force to the ground in the above condition with its stress state close to the failure line caused the ground to undergo liquefaction along with an abrupt increase in strain. Thus, the analysis conditions of the FLIP were reviewed in terms of the liquefaction parameters and modeling of the sheet piles and anchorage piles (consideration of wall friction).

As a result, two improvement methods were finally proposed, and their application has been recommended when using the FLIP for analyzing sheet pile quaywalls.

One of the recommended improvement methods is the application of models[14)] (tmp3 and tmp7 methods) which modify the method for evaluating the contribution of shear work to dilatancy in the vicinity of the failure line. In the improvement method, the constitutive model of the analysis program was modified and the analysis programs after Ver. 5.0 enable the conventional and modified models to be used by setting data switches. For the details of the improvement method, refer to the reference 14).

Another recommended improvement method is the application of a high-accuracy evaluation method for the initial stress state of the ground. The method was finally verified as an applicable method that enables adequate analysis results to be obtained by using a three-staged initial gravity analysis to simulate the construction process of a sheet pile quaywall for the purpose of improving the initial stress state of the soil elements. This method is also called the four-staged method and can be referred to when conducting the verification of deformation of sheet pile quaywalls using other analysis methods.[33)]

The conventional FLIP uses a two-staged analysis: the first stage, also called the initial gravity analysis, in which gravitational acceleration is simultaneously applied to the entire analysis region, and the second stage, in which the acceleration of the earthquake ground motions is applied to the analysis region. In contrast, the four-staged method requires analyses to be conducted in the following way.

(1) The initial gravity analysis is conducted for the ground below the seabed and the front sheet pile. Here, in the four-staged method, the self-weight of the steel members are not considered in each stage. In this stage, the stiffness K_s of the joint elements at the passive side of the sheet pile in the sliding direction is set at 0 (**Fig. 2.4.13 (a)**).

Also in this stage, the original ground is set to a stress state before the construction of the quaywall and the stress in the soil elements, to which the joint elements at the passive side of the sheet pile refers in the next stage, is also set to the initial state.

(2) Next initial gravity analysis is conducted with reclaimed soil and an anchorage pile added to the model. In this stage, the stiffness of the anchorage pile is set at 0 with no resistance to deformation. In addition, the tie rod installation point on the sheet pile is constrained with respect to displacement in x direction, and the stiffness K_s of the joint elements at the passive side of the anchorage pile in the sliding direction is also set at 0 (**Fig. 2.4.13 (b)**).

In this stage, the reclaimed soil is consolidated almost in a state with a coefficient of earth pressure at rest K_0 of 0.5 and the stress in the soil elements, to which the joint elements at the passive side of the anchorage pile refers in the next stage, is also set to the initial state. It is thought that the actual construction of the sheet pile quaywall starts with the filling in the area of anchorage pile. Thus, this stage is thought to be implemented for enabling the stress state of soil around the anchorage pile to be reflected in the analysis. Here, the anchorage pile is incorporated into the analysis from this stage only in the form of the relationship with the joint elements.

(3) In this stage, a tie rod is added to the model with force applied to the installation point of the tie rod so as to cancel the reaction force generated in the second stage, and the stiffness of the anchorage pile is restored. Also in this stage, the anchorage pile and its active side ground are separated from each other to prevent the active side ground from being pulled seaward (**Fig. 2.4.13 (c)**). In this way, friction is generated between the soil and the steel member on the sheet pile as well as the anchorage pile with confining pressure appropriately applied to the passive side soil elements of the sheet pile and anchorage pile. The separation of the anchorage pile and its active side ground realizes the automatic generation of two external horizontal forces with identical magnitudes in directions opposite to each other between the anchorage pile and active side reclaimed soil, the stabilization of K_0 of the reclaimed soil at around 0.5, and the application of earth pressure obtained in the second stage to the anchorage pile. Although it is not clear how large or small a value is appropriate for K_0 of the ground at the back of the anchorage pile, at least when the pile is used as the anchorage work, it is estimated that the ground is in a stress state close to horizontally layered ground.

(4) A dynamic analysis is conducted. In this stage, the continuity of the soil is expressed by using the MPC in a manner that equalizes the vertical displacement generated when the soil in front and at the back of the anchorage pile at the same level is subjected to the earthquake ground motions. Then, the two external horizontal forces acting in directions opposite to each other between the anchorage pile and its active side ground are integrated and automatically cancelled through the MPC (**Fig. 2.4.13 (d)**).

Table 2.4.9 summarizes the characteristics of the modeling used in the conventional and four-staged methods. Here, MPC stands for "Multiple Point Constraint," which deals with the degrees of freedom at multiple points as an identical degree of freedom.

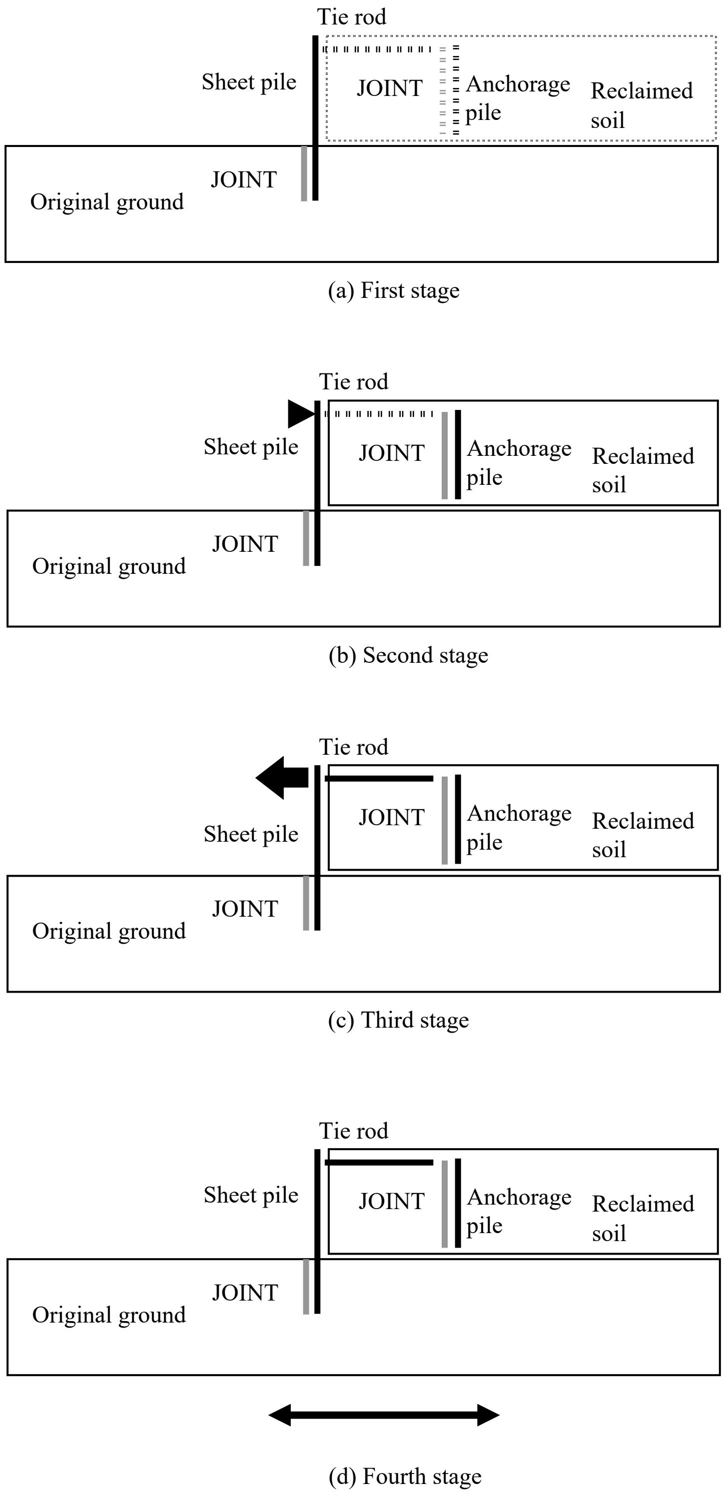

Fig. 2.4.13 Schematic Diagram of the Analysis Process in the Four-Staged Method

Table 2.4.9 Characteristics of Modeling in the Conventional and Four-Staged Methods

Modeling object	Conventional method	Four-staged method
Sheet pile-soil relationship at the passive side of the front sheet pile	No friction MPC in the horizontal direction	Use of joint elements, consideration of friction from the initial gravity analysis stage and a friction angle of 15°
Sheet pile-soil relationship at the active side of the front sheet pile	No friction MPC in the horizontal direction	Same as the conventional method and slidable joints to prevent the generation of negative water pressure
Anchorage pile-soil relationship at the passive side of the anchorage pile	No friction MPC in the horizontal direction	Use of joint element, consideration of friction from the initial gravity analysis stage and friction angle of 15°
Anchorage pile-soil relationship at the active side of the anchorage pile	No friction MPC in the horizontal direction	Same as the conventional method except for the cutting of the MPC in the horizontal direction in the third stage
Continuity of vertical displacement of the soil in front and at the back of the anchorage pile during earthquake ground motions	No continuity	Same displacement in vertical directions
Coefficient of earth pressure at the back of the anchorage pile after initial gravity analysis	Small due to the seaward shifting of the anchorage pile	About 0.5

Table 2.4.10 shows an example of a comparison of analysis results between the conventional and four-staged methods. These analysis results were obtained by commonly using FLIP Ver. 4.2.7 and the improved constitutive model (tmp3 method). In both cases, Ohama No.1 Quaywall which there was no damage and Ohama No. 2 Quaywall which there was damage, suffered the 1983 Nihonkai Chubu Earthquake. Comparing the residual deformation after the dynamic analyses, the four-staged method clearly expresses the differences between the two cases and is considered to be able to reproduce actual damage situations better than the conventional method.

Comparing the displacement and bending moment after the initial gravity analyses, there were no clear differences between the conventional and four-staged methods. However, as can be seen in **Fig. 2.4.14**, the calculated differences in the values of the principal stresses between the conventional and four-stage methods after the initial gravity analyses showed that the two methods had differences in the stresses in the passive side ground near the front sheet pile and the ground around the anchorage pile. It is thought that these differences in the initial stress state caused large differences in the dynamic analysis results.

The example of the analyses introduced in this section modeled the anchorage pile as a sheet pile for simplification, but an analysis method using pile-ground interaction spring elements[4)] capable of incorporating a three-dimensional phenomenon where soil moves between the piles in the analyses has been proposed.[34)] Even when using the pile-ground interaction spring elements, it is necessary to give consideration to the reproduction of the initial stress state that is dependent on the construction processes by using, for example, the four-staged method.

Table 2.4.10 Comparison of Analysis Results between the Conventional and Four-Staged Methods

			Front sheet pile				Anchorage pile 1	Anchorage pile 2	Tie rod
			Horizontal displacement of levee crown (cm)	Vertical displacement of levee crown (cm)	Maximum horizontal displacement (cm)	Bending moment (kNm/m)	Bending moment (kNm/m)	Bending moment (kNm/m)	Tensile force (kN/m)
Ohama No.1 Quaywall	Conventional method	Initial gravity analysis	3.7	0.9	4.6	190	80	–	142
		Completion of dynamic analysis	60.9	2.8	61.1	1,497	2,061	–	462
	Four-staged method	Completion of the third stage	2.8	0.1	2.8	192	43	–	134
		Completion of dynamic analysis	9.4	1.8	28.7	1,737	824	–	489
Ohama No.2 Quaywall	Conventional method	Initial gravity analysis	5.8	0.3	7.2	238	58	71	159
		Completion of dynamic analysis	134	9.7	134	2,141	1,465	1,691	436
	Four-staged method	Completion of the third stage	4.6	0.0	4.6	282	7	0	147
		Completion of dynamic analysis	99.5	2.6	99.5	2,113	1,140	1,388	362

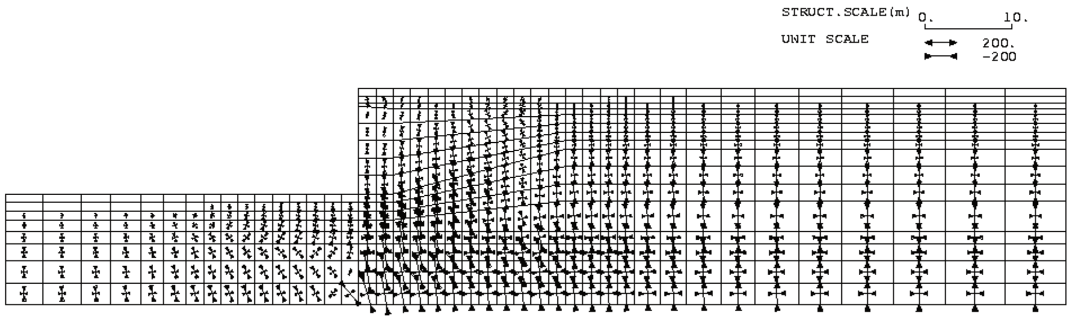

(a) Distribution of Principal Stresses after a Initial Gravity Analysis in the Conventional Method

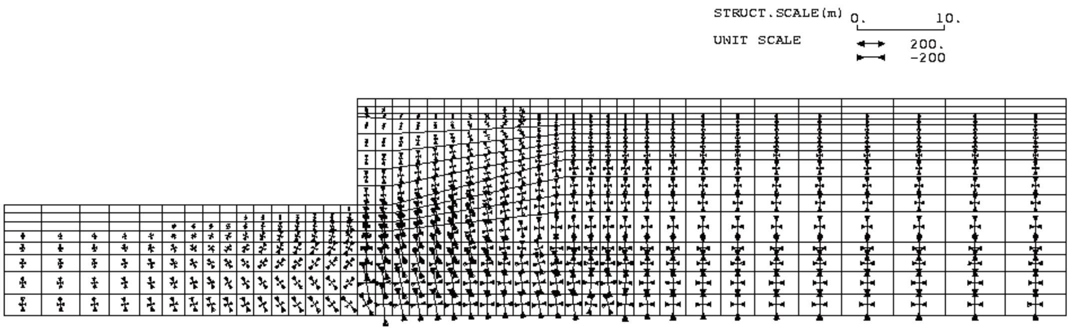

(b) Distribution of Principal Stresses after a Initial Gravity Analysis in the Four-Staged Method

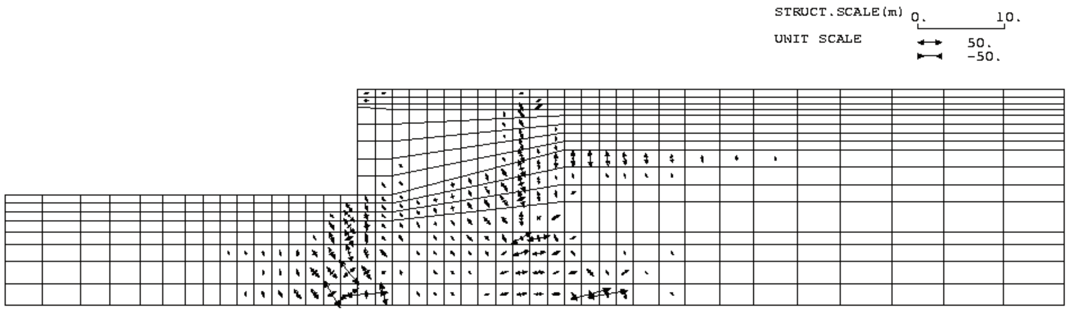

(c) Differences in Principal Stresses after Initial Gravity Analyses between the Conventional and Four-Staged Methods
(Principal Stresses Calculated from the Differences in σ_x, σ_y and τ_{xy} of the Conventional and Four-Staged Methods)

Fig. 2 .4 .14 Changes in Stress States after an Initial Gravity Analysis in the Four-Staged Method

2.5 Points of Caution for Modeling

2.5.1 Modeling of Several Earthquake Resistance Countermeasure Methods

According to the procedure for the verification of deformation shown in **Fig. 2.3.1**, design cross sections need to be modified when the deformation of the design object facility exceeds the allowable values. Then, the verification of deformation needs to be repeated for the cross sections modified with several types of earthquake resistance countermeasure methods, including the ground improvement of liquefiable layers. Thus, it is necessary to appropriately model these earthquake resistance countermeasure methods. Actually, the requirements for modeling vary depending on the types of numerical analysis methods and conditions for model experiments. Therefore, this section introduces the concepts for modeling three types of earthquake resistance countermeasure methods based on using these models in the FLIP.

(1) Ground improvement through SCP (Sand Compaction Pile) method

There are two types of ground improvement through SCP: one for reinforcing soft cohesive soil ground and the other for preventing the liquefaction of sandy soil ground. Generally, the former requires high replacement rates (about 70%) and the latter requires low replacement rates (5 to 20%). In addition, the former type leaves soft cohesive soil layers around the compacted sand piles, while the latter type can improve the sandy soil ground between the piles due to the compaction effect when installing the sand piles. Thus, it is thought that the actual behavior of ground during an earthquake greatly differs depending on the types of ground improvement.

The methods for modeling the ground improvement through SCP used for preventing the liquefaction of sandy soil ground include: ① a method using the ground properties between the sand compaction piles to be on the safe side; ② a method using the ground properties obtained through the weighted average of the ground between the piles and the ground at the pile centers; and ③ a method using two elements which represent the ground between the piles and the ground at the pile centers, and which have a common node combining the two elements as composite ground. It is reported that ① is likely to increase excess pore water pressure compared to ② and ③ but there are no significant differences in the seismic responses as a whole among ① to ③. In contrast, it has been confirmed that when considering the effects of a possible increase in the value of K_0 of the ground due to the installation of sand piles, the variations in seismic responses become significant due to, for example, the increase in the liquefaction strength.[29)]

However, there has been no clear conclusion on whether or not the effect of the increase in K_0 value needs to be considered in the actual design because ① modeling requires complex procedures, ② there may be a risk of double evaluating the countermeasure effects, because the physical properties are set based on the *N*-values measured in a state where the effect of the increased K_0 value was already reflected, and ③ there is uncertainty about the stability of the increased K_0 value throughout the design working life, and so on.

The methods for modeling the sections of cohesive soil ground improved with a high replacement ratio mostly use the ground properties of the sand piles only in defiance of the cohesive soil, and either ① set the density of the ground while taking into consideration the improvement ratios without changing the depth of the model, or ② set the depth of the model in accordance with the improvement ratios. In the case of ②, since not only the stiffness but also the mass of the ground need to be changed in accordance with the depth of the model, the density needs to be set in accordance with the improvement ratio while taking into consideration the presence of the mass of the cohesive soil ground. In addition to the above, modeling requires a decision on whether or not the increase in pore water pressure needs to be considered in the analyses by setting liquefaction parameters for the sand piles.

It is reported that there are no significant differences between ① and ②, and simply selecting the setting method of ② enables past damage cases to be sufficiently reproduced.[29)] Furthermore, the report says that setting the liquefaction parameters is likely to increase deformation, but the analysis accuracy is too insufficient for discussing whether or not the deformation is adequate in comparison with past damage cases.

(2) Drain methods

Drain methods alleviate the severity of liquefaction in a manner that enables drains made of highly permeable materials to reduce the drainage distances at each section of ground, thereby smoothly dissipating the increments in excess pore water pressure. When evaluating the effects of the drain methods in numerical analyses, it is necessary to solve the interactive behavior of the water and soil by modeling not only the soil but also the movement of the water in the ground by taking into consideration the behavior of the pore water based on the pore water pressure in addition to the behavior of soil skeletons based on the effective stress. When evaluating the effect of the drain methods through shake table tests, it is necessary to appropriately set the permeability of the pore water based on the similitude law. To that end, the viscosity of the water needs to be adjusted using methyl cellulose or glycerin solution. However, it is difficult to conduct these shake table tests with sufficient accuracy.

In addition to the analysis method using drainage conditions capable of considering the flow of pore water, there has been a proposal for a method for approximately evaluating the effects of the drain methods using practical and general undrained conditions.[35)] In the method, the liquefaction strength increase effect of gravel drains is evaluated with the ratios of the cumulative damage corresponding to the allowable excess pore water pressure ratio (for example, 0.25) in the design of the gravel drains to the cumulative damage during an earthquake without gravel drains. Then, taking into consideration the effects of the drains, the liquefaction strength is determined in a manner that shifts the target liquefaction strength curve with which the soil properties are determined in analyses in a rightward direction by an amount corresponding to the ratio. Here, it is necessary to additionally consider the effects such as the stiffness of the drain materials. Although it slightly overestimated the pore water pressure, this method could reproduce the acceleration amplitude and displacement amplitude among the results of the 1 g field shake table tests conducted to evaluate the ground improvement effects by installed drains.

(3) Earthquake resistance countermeasures through solidification improvement

There has been an increasing number of cases of implementing earthquake reinforcement countermeasures using solidified improvement soil produced by mixing soil with cement as with CDM and SGM. Since the behavior of ground is considered to vary depending on the properties of the original ground and additive amounts of cement, there are no generalized methods for modeling solidified improvement soil in numerical analyses.

There are many cases of modeling solidified improvement soil as simple linear elastic elements. In these cases, elastic modulus can be the weighted averages of the initial elastic modulus of original ground E_0 and scant elastic modulus of improvement soil E_{50}, or simply the scant elastic modulus of improvement soil E_{50}. There is another case of expressing the behavior of ground using a hyperbolic model (in the FLIP, a multiple spring model using hyperbolic-type springs in the FLIP) with the soil cohesion input as the strength instead of using linear elastic elements. Expressing ground behavior using the hyperbolic model has a risk of overestimating the displacement, while modeling with the linear elastic elements has a risk of obtaining analysis results that are more on the dangerous side because this type of modeling is incapable of expressing the failure and deformation of solidified bodies. Thus, it is necessary to evaluate the analysis results with a focus on the relationship between the strength of the solidified bodies and the maximum as well as minimum values of the internal stress generated during an earthquake.

2.5.2 Methods for Modeling Piles

(1) Methods for analyzing pile-supported structures

In the case of pile-supported structures, it is necessary to analyze the piles and ground three-dimensionally. However, when dealing with soil liquefaction-induced flow, which is typical earthquake damage to port facilities, the finite element method has difficulty expressing the behavior of ground passing through spaces around piles even when using three-dimensional elements. Thus, in many cases, pile-supported structures are analyzed with two-dimensional models using special elements such as pile-ground interaction springs.[4)] Examples of analysis methods for pile-supported structures include a method for integrally analyzing piled piers and ground with a seismic response analysis while taking into consideration the three-dimensional dynamic interaction between the piles and ground, and a response displacement method using frame models of the piled piers into which the ground deformation obtained by the seismic response analysis is input through ground springs.

(2) Bearing strength characteristics of piles that have different diameter-to-thickness ratios

Recently, there has been an increasing number of cases where steel pipe piles with large diameter-to-thickness ratios D/t (diameter (D) / wall thickness (t) = about 100) are used for pile-supported structures in the interest of economic design. As shown in **Fig. 2.5.1**, piles with small diameter-to-thickness ratios are less likely to undergo local buckling and are capable of maintaining bending strength even with the progress of deformation. In contrast, piles with large diameter-to-thickness ratios have a high risk of undergoing a reduction in bearing strength due to local buckling before they are subjected to a fully plastic moment obtained through cross-sectional calculations. Thus, it is necessary to model the steel pipe piles in the nonlinear seismic response analyses with due consideration to the diameter-to-thickness ratios of the piles.

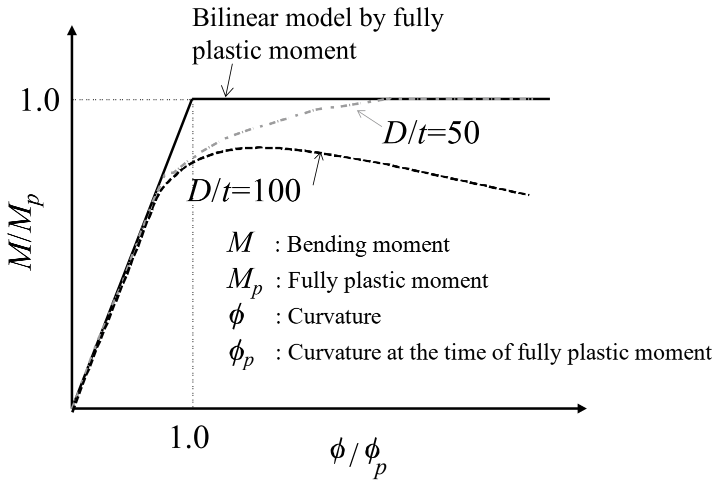

Fig. 2.5.1 Schematic Diagram of the Bending Strength Characteristics of Steel Pipe Piles with Different Diameter-to-thickness Ratios

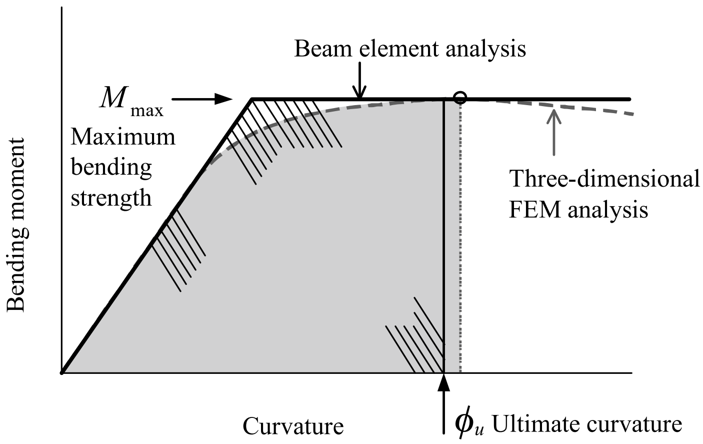

Fig. 2.5.2 Method for Obtaining the Ultimate Curvature of the Beam Element (Bilinear Type)

(3) Method for modeling the steel pipe piles of pile-supported wharves

① Equations for calculating ultimate curvatures

When modeling steel pipe members in seismic response analyses, the relationship between the bending moment obtained through three-dimensional FEM analyses using shell elements and curvatures can be replaced with the relationship of the bilinear type beam elements, as shown in **Fig. 2.5.2**. In the bilinear type (beam element analyses), the ultimate curvatures, which are curvatures at the time of maximum bending strength in the three-dimensional FEM analysis, can be obtained as the curvature ϕ_u, which matches the area below the two straight lines of the bilinear type beam element analyses up to ϕ_u, and the area (of the shaded section) below the curve showing the relationship between the bending moment and curvatures in the three-dimensional FEM analyses up to the curvature corresponding to the maximum bending strength $M_{\max}$. That is, it is necessary to pay attention to the fact that, in the bilinear type relationship between the bending moment and curvatures, the curvature when the bending moment reaches to the maximum bending strength (the break point) is not the ultimate curvature.

When applying the bilinear type relationship to the relationship between the bending moment and curvatures of piles modeled as the beam elements based on the infinitesimal deformation theory, the ultimate curvature can be calculated by the following equations.[36)]

In the case of a compressive axial force ($N \geq 0$)

$$\left.\begin{aligned} \phi_u &= \mu \phi_y' \\ \phi_y' &= \frac{\sigma_y' Z}{EI}\left(1-\frac{N}{N_{yc}'}\right) \end{aligned}\right\} \tag{2.5.1}$$

In the case of a tensile axial force ($N < 0$)

$$\left.\begin{aligned} \phi_u &= \mu \phi_y \\ \phi_y &= \frac{\sigma_y Z}{EI}\left(1+\frac{N}{N_{yt}}\right) \end{aligned}\right\} \tag{2.5.2}$$

where

ϕ_u : the ultimate curvature (1/mm);

ϕ_y : the curvature corresponding to the yield moment (1/mm);

ϕ_y' : the curvature corresponding to the yield moment in consideration of the reduction in yield stress in the direction of the axial compression (1/mm);

EI : the bending rigidity (N·mm^2);

N_{yc}' : the yield axial force in consideration of the reduction in yield stress in the direction of the axial compression (positive value in the unit of N)

N_{yt} : the yield axial force when a steel pipe is subjected to the tensile axial force (negative value in the unit of N);

Z : the section modulus (mm^3);

σ_y : the yield stress (N/mm^2);

σ_y' : the yield stress in the direction of the axial compression (N/mm^2); and

μ : the ductility factor.

$$\left.\begin{aligned} \mu &= \gamma\left[\left(-1.24\,l/r+209\right)t/D-0.0119\,l/r+1.46\right] \text{ (with a retained circular shape)} \\ \mu &= \gamma\left[\left(-4.72\,l/r+440\right)t/D+0.0413\,l/r-2.55\right] \text{ (with an unretained circular shape)} \end{aligned}\right\}$$

t : the wall thickness (mm);

D : the diameter (mm);

l : the effective member length (mm);

r : the radius of gyration of the cross section (mm); and

γ : the correction coefficient with respect to the yield stress.

$$\gamma = \sqrt{235/\sigma_y}$$

The correction coefficient with respect to the yield stress is confirmed to be applicable to stress up to 450 N/mm^2.[37] The prime mark (′) means the reduction of the yield stress in the direction of the axial compression according to the diameter-to-thickness ratio using the equation (2.5.3).[38] Here, because the purpose of the equation is to reduce the yield stress according to the diameter-to-thickness ratio, the upper limit of the coefficient shall be 1 and σ_y' shall not be larger than σ_y.

$$\sigma_y' = \sigma_y\left(0.86+5.4\,t/D\right) \tag{2.5.3}$$

② **Equations for calculating the maximum bending strength**

Similar to the ultimate curvatures, when applying a bilinear type relationship to the relationship between the bending moment and curvatures of piles modeled as beam elements based on the infinitesimal deformation theory, the maximum bending strength can be calculated by the following equations.[36)]

In the case of a compressive axial force ($N \geq 0$)

$$M_{\max} = M_{p0}' \left(1 - \left(\frac{N}{N_{yc}'} \right)^{n} \right) \qquad \textbf{(2.5.4)}$$

In the case of a tensile axial force ($N < 0$)

$$M_{\max} = M_{p0}' \left(1 - \left(\frac{N}{N_{yt}} \right)^{1.9} \right) \qquad \textbf{(2.5.5)}$$

where

$M_{\max}$: the maximum bending strength (N·mm);

M_{p0}' : the fully plastic moment with no axial force in consideration of the reduction in yield stress in the direction of the axial compression (N·mm);

$$M_{p0}' = Z_p \sigma_y'$$

Z_p : the plastic section modulus (mm^3); and

n : the exponent (dependency on the axial force)

$$\left.\begin{array}{l} n = \gamma\left(20t/D - 0.0095l/r + 1.41\right) \text{ (with a retained circular shape)} \\ n = \gamma\left(10t/D - 0.0094l/r + 1.45\right) \text{ (with an unretained circular shape)} \end{array}\right\}$$

These equations are based on the behavior model applicable up to the maximum bending strength and ultimate curvatures and, therefore, do not consider the degree of reduction in bending moment after reaching the maximum bending strength.

③ **Setting the conditions for the circular shape retained conditions and effective member lengths**

The above equations are formulated based on the two boundary conditions shown in **Fig. 2.5.3**. These boundary conditions are a boundary condition with a retained circular shape in the case of steel pipe piles that can maintain a circular cross-sectional shape until they undergo local buckling, and a boundary condition with an unretained circular shape in the case of steel pipe piles that change their circular cross-sectional shape to an elliptical shape due to insufficient ground strength, thereby accelerating the generation of local buckling. Thus, the appropriate equations shall be selected according to the circular shape retained conditions. In the case of an open-type wharf on vertical piles, equations with a retained circular shape condition can be used for the section of vertical piles from the lower edge of the superstructure to the sea surface (or the corrosion control coating section), and equations with an unretained circular shape condition can be used for the other sections of the vertical piled piers, as shown in **Fig. 2.5.4**.

The ratio of the effective member length to the radius of gyration of the cross section l/r is included in the equations of the ductility factor μ and the exponent n, expressing the dependency on the axial force, in order to incorporate the influence of the additional bending moment in the modeling of the piles. The effective member length l needs to be set according to the distribution of the bending moment.[36)] In the case of an open-type wharf on vertical piled piers, the distance from the lower edge of the superstructure to a virtual fixed point can be set as the effective member length l as shown in **Fig. 2.5.4**. The effective member length l needs to be set for each pile in principle. However, because setting longer effective member lengths causes the ductility factors and maximum bending strength to be underestimated, the longest effective member length l can be applied to all the piles at the open-type wharf.

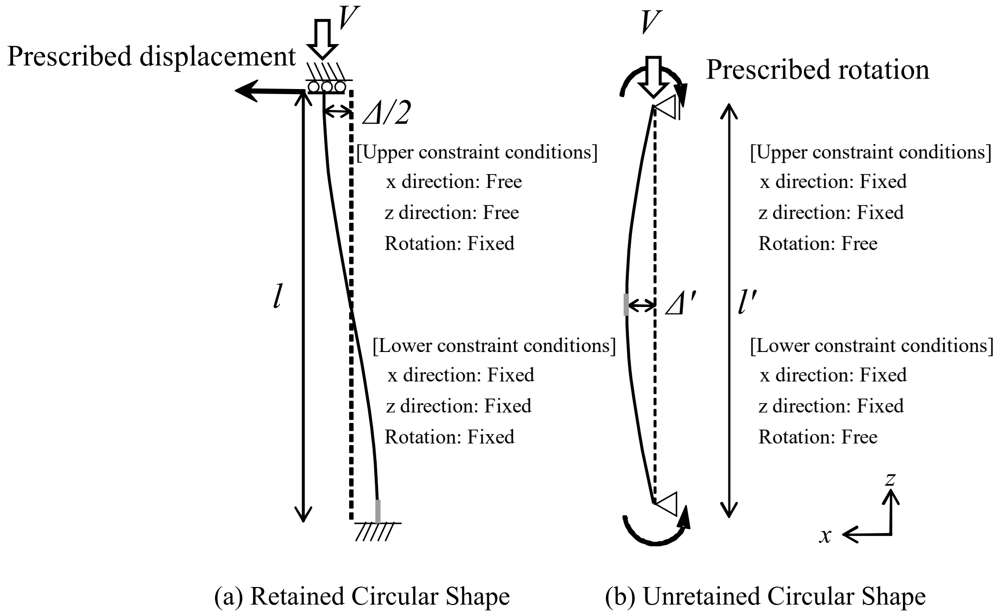

Fig. 2.5.3 Boundary Conditions and Circular Shape Retained Conditions[36)]

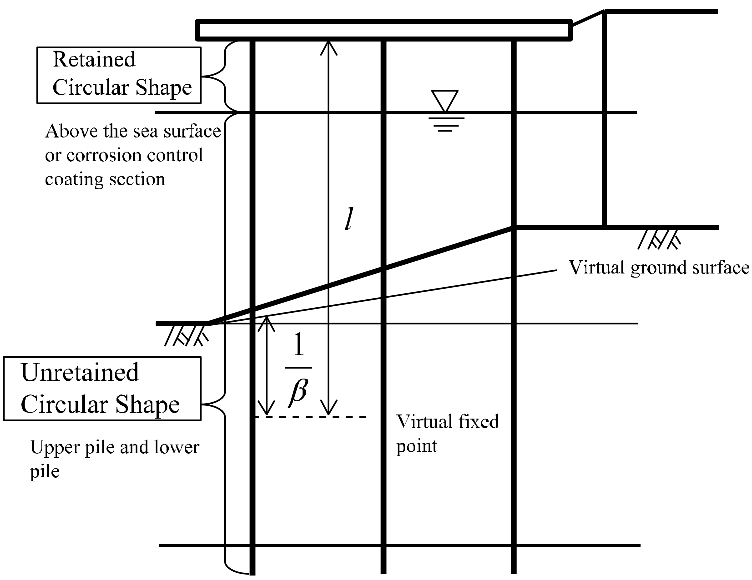

Fig. 2.5.4 Setting the Conditions for Retained or Unretained Circular Shape and Effective Member Lengths in the Case of Open-Type Wharves on Vertical Piled Piers

④ **Influences from the axial force**

Fig. 2.5.5 shows an explanatory diagram of the relationship between the bending moment and axial force (*M-N* curve). The *M-N* curve of the equation for the relationship between the bending moment and axial force is characterized by being located medial to the *M-N* curve (the dotted line in the figure) based on the "AIJ recommendations for the plastic design of steel structures,"[39)] which considers the reduction of the fully plastic moment using a cosine function.

Fig. 2.5.6 shows an explanatory diagram of the relationship between the ultimate curvatures and axial force. The diagram is based on the assumption that ultimate curvatures become larger with an increase in tensile axial force because the cross section at the side of the steel pile subjected to the tensile stress does not undergo local buckling. In contrast, the equivalent curvature of the fully plastic moment (the dotted line in the figure) gets smaller with the increase in axial force in both the compressive and tensile directions.

⑤ **Points of caution for the equations**

The equations above are formulated for steel pipe piles that have standard dimensions frequently used in the design of pile-supported structures. Thus, caution is required when dealing with cases where the steel pipe piles have diameter-to-thickness ratios largely exceeding 100 due to corrosion because the equations cannot be applied to such cases. For example, when the parameters obtained with the equations cause the *M-N* curve to be shifted closer to the origin than the yield curve, the yield moment can be used as the maximum bending strength and a value of 1.0 can be used as the lower limit value of the ductility factor.

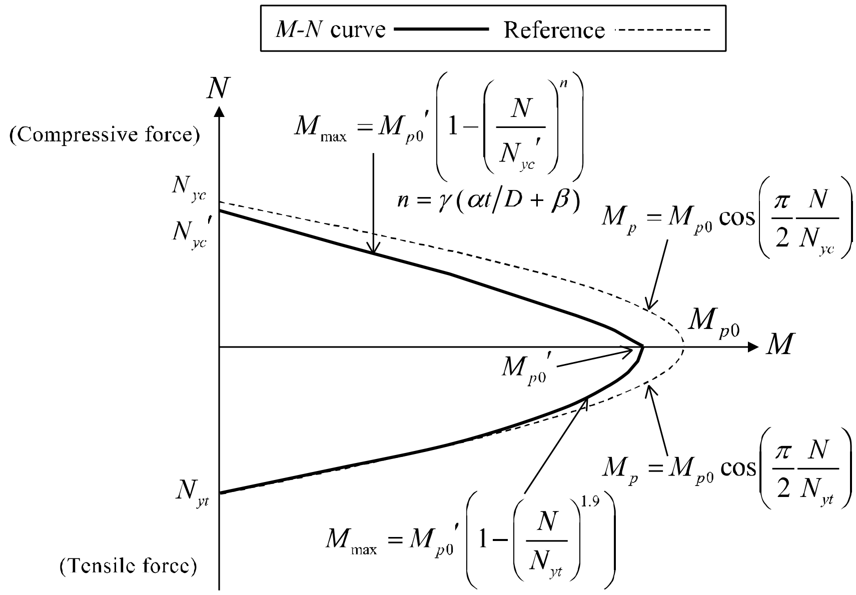

Fig. 2.5.5 Explanatory Diagram of the *M-N* Curve (Modified from the Reference 36))
(Positive axial force (*N*) = compressive force and negative axial force (*N*) = tensile force)

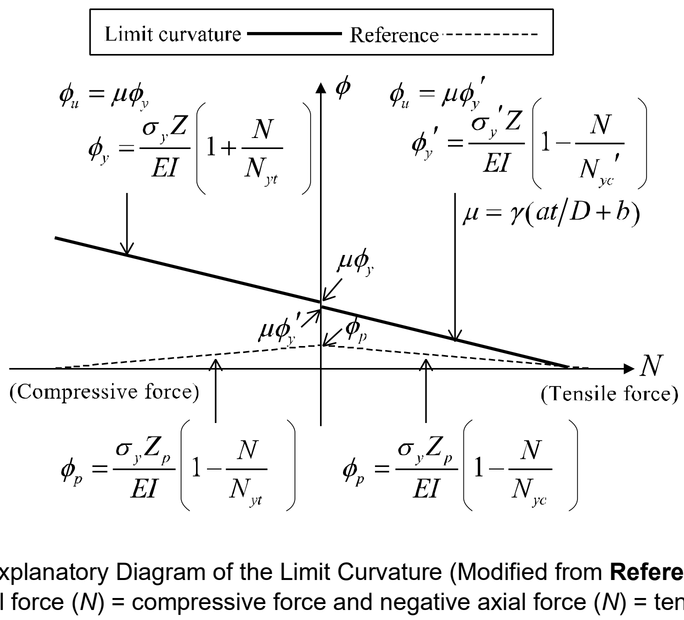

Fig. 2.5.6 Explanatory Diagram of the Limit Curvature (Modified from **Reference 36)**)
(Positive axial force (*N*) = compressive force and negative axial force (*N*) = tensile force)

Furthermore, these equations are formulated through the calculation of curvatures and the correction of bending moment, assuming the beam elements with mesh sizes of 1 m.

(4) Method for modeling steel pipe members on other pile-supported structures

For the purpose of applying the method for modeling steel pipe members while taking into consideration the diameter-to-thickness ratios to other pile-supported structures, equations for calculating the ultimate curvatures and maximum bending strength were formulated according to the loads and boundary conditions of the steel pipe members.[40] The formulated equations for each pile-supported structure are shown in **Tables 2.5.1** and **2.5.2**, together with the parameters used in the equations for the abovementioned open-type wharf on vertical piled piers. Because the axial force is not considered in the case of steel pipe sheet piles and steel sheet piles with vertical anchorage piles, it is not necessary to set exponents n related to the fluctuations in the axial force.

For the structural steel members on jacket piled piers, the equations for piled piers (① and ② in **Table 2.5.1**) can be used by setting the conditions for retained or unretained circular shape and effective member lengths shown in **Fig. 2.5.7**.

Table 2.5.1 Setting the Equations and Effective Member Lengths for Each Facility

	① Piled pier (vertical and inclined piles) (section near superstructure)	② Piled pier (vertical and inclined piles) (other section than that near the superstructure)	③ Steel pipe sheet pile and steel sheet pile with vertical anchorage pile	④ Sheet pile with coupled anchorage piles and foundation pile for cargo handling equipment
Axial force	Considered	Considered	Not considered	Considered
Rotational constraint at edge	Considered	Considered	Not considered	Not considered
Conditions for retained or unretained circular shape	Retained circular shape	Unretained circular shape	Unretained circular shape	Unretained circular shape
Exponent n	$n = \gamma\ (\alpha t/D + \beta)$ Coefficient: Refer to **Table 2.5.2**	$n = \gamma\ (\alpha t/D + \beta)$ Coefficient: Refer to **Table 2.5.2**	–	$n = \gamma\ (\alpha t/D + \beta)$ Coefficient: Refer to **Table 2.5.2**
Ductility factor μ	$\mu = \gamma\ (a t/D + b)$ Coefficient: Refer to **Table 2.5.2**	$\mu = \gamma\ (a t/D + b)$ Coefficient: Refer to **Table 2.5.2**	$\mu = \gamma\ (280\ t/D - 1.2)$	$\mu = \gamma\ (a t/D + b)$ Coefficient: Refer to **Table 2.5.2**
Effective member length l	Lower edge of superstructure to $1/\beta$ below virtual ground surface	Lower edge of superstructure to $1/\beta$ below virtual ground surface	–	π/β

Table 2.5.2 List of Equation Parameters

Piled structure	Parameter		Equation
Piled pier (vertical and inclined piles) (section near superstructure)	Exponent n	α	20
		β	$-0.0095\ l/r + 1.41$
	Ductility factor μ	a	$-1.24\ l/r + 209$
		b	$-0.0119\ l/r + 1.46$
Piled pier (vertical and inclined piles) (other section than that near the superstructure)	Exponent n	α	10
		β	$-0.0094\ l/r + 1.45$
	Ductility factor μ	a	$-4.72\ l/r + 440$
		b	$0.0413\ l/r - 2.55$
Sheet pile with coupled anchorage piles and foundation pile for cargo handling equipment	Exponent n	α	10
		β	$-0.0115\ l/r + 1.45$
	Ductility factor μ	a	$-5.78\ l/r + 440$
		b	$0.0506\ l/r - 2.55$

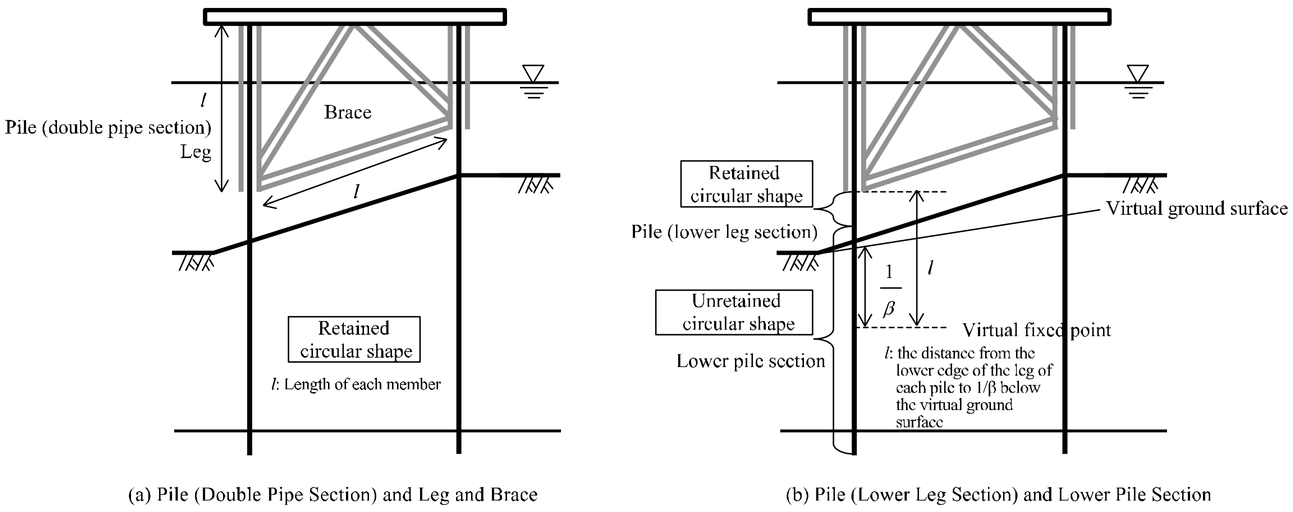

Fig. 2.5.7 Setting the Conditions for Circular or Noncircular Cross Sections and Effective Member Length in the Case of Jacket Type Piers

2.5.3 Evaluation of the influence of water

The finite element method enables seawater to be incorporated in the analyses as a fluid element. In the seismic response analyses, it is also necessary to consider seawater as a part of the analysis models. Generally, the influence of dynamic water pressure in front of the caissons can be incorporated into the analyses by modeling seawater as a fluid element so that it can be analyzed as an incompressible fluid.

In the case of earth structures, analyses are conducted in consideration of the ground water levels obtained through seepage analyses. In contrast, the influences of seepage flows are not generally considered in the seismic response analyses of port structures because they do not have large differences between the water levels in front of the port structures and the residual water levels behind the structures in many cases.

2.5.4 Evaluation of the Ground Subsidence Due to the Dissipation of Excess Pore Water Pressure

In the verification of the deformation of mooring facilities, the analysis methods usually used are those based on undrained conditions which do not consider the inflow and outflow of pore water through soil skeleton. Then, these analysis methods cannot evaluate the volume strain generated by the dissipation of excess pore water pressure in the ground which undergoes liquefaction. Therefore, when it is necessary to evaluate the ground subsidence due to the dissipation of excess pore water pressure, the ground subsidence is evaluated using simplified methods, which sum the volume strain of each layer estimated from the seismic response analysis results. For the evaluation of volume strain, refer to, for example, the chart in the reference 41).

In addition, even in identical sand layers that undergo liquefaction, there are local areas with increased volume strain around the underground structures which have different vibration characteristics from the ground. For the purpose of evaluating the local ground subsidence due to the locally increased volume strain, methods have been proposed that evaluate the volume strain based on the accumulated shear strain.[for example, 42)]

[References]

1) Iai, S., Matsunaga, Y. and Kameoka, T.: Strain Space Plasticity Model for Cyclic Mobility, Report of the Port and Harbour Research Institute, Vol.29, No.4, pp.27 -56, 1990.

2) Iai, S., Matsunaga, Y. and Kameoka, T.: Strain Space Plasticity model for Cyclic Mobility, Soils and Foundations, Vol.32, No.2, pp.1 -15, 1992.

3) Coastal Development Institute of Technology (CDIT): Instruction manual for FLIP, ver.3.3, 1997. (in Japanese)

4) Ozutsumi, O., Tamari, Y., Oka, Y., Iai, S. and Umeki, Y.: Modeling of Soil-Pile Interaction Subjected to Soil Liquefaction in Plane Strain Analysis, Proceedings of the 58th Annual Conference of JSCE, Vol.3, pp.569-570, 2003. (in Japanese)

5) ISO 23469: Bases for design of structures — Seismic actions for designing geotechnical works, 2005.

6) Ichii, K.: An Overview of FEM Application in Practical Design Process, Tsuchi-to-Kiso, JGS, Vol.53, No.8, pp.10-12, 2005. (in Japanese)

7) Ichii, K., Takahashi, H., Nakamoto, T. and Akakura, Y.: Evaluation of Acceptable Deformation of Gravity type Quay Walls, Proceedings of the Japan Earthquake Engineering Symposium, Vol.3, pp.3241-3244, 1998. (in Japanese)

8) Ichii, K., Iai, S. and Morita, T.: Effective stress analyses on the performance of caisson type quay walls during 1995 Hyogoken-nanbu earthquake, Report of the Port and Harbour Research Institute, Vol.36, No.2, pp.41-86, 1997. (in Japanese)

9) Iai, S., Ichii, K., Liu, H. and Morita, T.: Effective stress analyses of port structures, Soils and Foundations, Special Issue on Geotechnical Aspects of the January 17, 1995 Hyogoken-Nambu Earthquake, No.2, pp.97 -114, 1998.

10) Inatomi, T., Zen, K., Toyama, S., Uwabe, T., Iai, S., Sugano, T., Terauchi, K., Yokota, H., Fujimoto, K., Tanaka, S., Yamazaki, H., Koizumi, T., Nagao, T., Nozu, A., Miyata, M., Ichii, K., Morita, T., Minami, K., Oikawa, K., Matsunaga, Y., Ishii, M., Sugiyama, M., Takasaki, N., Kobayashi, N. and Okashita, K.: Damage to Port and Port-related Facilities by the 1995 Hyogoken-nanbu Earthquake, Technical Note of the Port and Harbour Research Institute, No.857, 1762pp, 1997. (in Japanese)

11) Sugano, T., Nozue, Y., Shiozaki, Y. and Kohama, E.: Seismic performance improvement and restoration of damaged quay wall after an earthquake, Technical Note of the Port and Airport Research Institute, No.1145, 142pp., 2006. (in Japanese)

12) Dickenson, S.E., and Yang, D.S.: Seismically-induced deformations of caisson retaining walls in improved soils, Geotechnical Earthquake Engineering and Soil Dynamics III, Geotechnical Special Publication, Vol.2, No.75, ASCE, pp.1071 -1082, 1998.

13) Kanatani, M., Tochigi, H., Kawai: Study on Seismic Stability of Seawall in Man-made Island (Part4) - Deformation Analysis of Seawall during Earthquake by DEM-FEM Coupled Analysis Method(SEAWALL-2D)-, Abiko Research Laboratory Report No.U98025, Central Research Institute of Electric Power Industry, 24pp., 1999. (in Japanese)

14) Ozutsumi, O., Iai, S., Shimazu, T., Miwa, S., Nakayama, H., Tamari, Y., Sawada, S., Takeshima, Y., Mori, H.: Contributions of Shear Work Done in the Stress Space beyond the Transformation line to the Negative Dilatancy, Proceedings of the 46th Symposium on Geotechnical Engineering, pp.83-88, 2001. (in Japanese)

15) Ozutsumi, O., Shiozaki, Y., Ichii, K., Iai, S. and Mori, G.: Study of the improvement of accuracy for the 2-dimensional effective stress analysis method, Journal of Civil Engineering in the Ocean, JSCE, Vol.20, pp.443-448, 2004. (in Japanese)

16) Shiozaki, Y., Nagao, T., Ozutsumi, O. and Miyashita, K.: A numerical simulation on the damaged example of open-type wharves on vertical piles by the 2-dimensional effective stress analysis, Journal of Earthquake Engineering, JSCE, Vol.30, pp.881-891, 2009. (in Japanese)

17) Ohya, Y., Takenobu, M., Sugano, T. and Kohama, E.: A shake table test in 1g gravitational field and an effective stress analysis for dynamic deformation characteristics of the foundation of breakwater, Technical Note of Port and Airport Research Institute, No.1227, 24pp., 2011. (in Japanese)

18) Mizutani, T., Emura, T., Tabata, T., Takenobu, M. and Sugano, T.: Study on residual displacement of rubble mound revetment induced by earthquake, Journal of JSCE, Ser.C, Vol.65, No.4, pp.884-896, 2009. (in Japanese)

19) Japan Institute of Construction and Engineering (JICE): Analytical methods to predict seismically induced dike deformation, JICE Report No.102001, 2002. (in Japanese)

20) Ishihara, K., Yasuda, S. and Nagase, H.: Soil characteristics and ground damage, Special issue on geotechnical aspects of the January 17 1995 Hyogoken-nambu earthquake, Soils and Foundations, pp.109 -118, 1996.

21) Morita, T., Iai, S., Liu, H., Ichii, K. and Sato, Y.: Simplified Method to Determine Parameter of FLIP, Technical Note of the Port and Harbour Research Institute, 36pp., 1997. (in Japanese)

22) Yoshida, N. and Ohya, Y.: Some notes on formulation of two-dimensional analysis of ground, Proceedings of the 46th Japan National Conference on Geotechnical Engineering, pp.1661-1662, 2011. (in Japanese)

23) FLIP research committee: Instruction manual for FLIP, ver.7.0.3, 2005. (in Japanese)

24) Coastal Development Institute of Technology (CDIT): Handbook of liquefaction countermeasure works for reclaimed land, Revised edition, 1997. (in Japanese)

25) Tsuchida, T.: Study on Determination of Undrained Strength of Clayey Ground by Mean of Triaxial Tests, Technical Note of the Port and Harbour Research Institute, No.688, 199pp., 1990. (in Japanese)

26) Iai, S., Ozutsumi, O. and Oka, Y.: Sensitivity analysis of parameters in two-dimensional effective stress analysis (Part 2), Proceedings of the 25th JSCE Earthquake Engineering Symposium, pp.345-348, 1999. (in Japanese)

27) Ozutsumi, O., Iai, S., Oka, Y.: Sensitivity analysis of parameters in one-dimensional effective stress analysis, Proceedings of the 25th JSCE Earthquake Engineering Symposium, pp.337-340, 1999. (in Japanese)

28) Ichii, K., Iai, S., Sato, Y. and Liu, H.: Seismic performance evaluation charts for gravity type quay walls, Structural Eng. / Earthquake Eng., JSCE, Vol.19, No.1, pp. 21s-31s, 2002.

29) Working group to summarize the research results of the FLIP research committee for 14 years: 14years of research results by FLIP research committee - case study, 2011, http://www.flip.or.jp/file/jirei.pdf accessed 2017.7.4. (in Japanese)

30) Meyerhof, G. G.: Discussion, Proc. 4th International Conference on Soil Mechanics and Foundation Engineering (ICSMFE), Vol.3, p.110, 1957.

31) Zen, K., Yamazaki, H. and Sato, Y.: Strength and Deformation Characteristics of Cement Treated Sands Used for Premixing Method, Report of the Port and Harbour Research Institute, Vol.29, No.2, pp.85-118, 1990. (in Japanese)

32) Oka, F., Yashima, A., Shibata, T., Kato, M. and Uzuoka, R.: FEM-FDM coupled liquefaction analysis of a porous soil using an elasto-plastic model, Applied Scientific Research, 52, pp.209-245, 1994.

33) Iai, S, Tatsuta, M., Ozutsumi, O., Tamari, Y. and Yamamoto, Y.: Analytical study of the effect of initial ground stress conditions on seismic behavior of sheet pile quaywalls, Proceedings of the 26th JSCE Earthquake Engineering Symposium, pp.809-812, 2001. (in Japanese)

34) Shiozaki, Y., Sugano, T. and Kohama, E.: Experiment and analysis of earthquake performance of sheet pile quay walls, Journal of Civil Engineering in the Ocean, JSCE, Vol.20, pp.131-136, 2004. (in Japanese)

35) Takeshima, Y., Sawada, S., Iai, S., Ichii, K., Ozutsumi, O., Adachi, M., Yoshida, A., Ikeda, T., Ootsuka, N., and Umeki, Y.: Modeling of drainage behavior for dynamic effective stress analysis by undrained condition, Proc. of 13th World Conference on Earthquake Engineering, Paper No.3146, 12pp., 2004.

36) Ohya, Y., Shiozaki, Y., Kohama, E. and Kawabata, Y.: Proposal of Modeling of Circular Steel Tube for Seismic Performance Evaluation, Report of the Port and Airport Research Institute, Vol.55, No.2, pp.3-33, 2017 (in Japanese)

37) Shiozaki, Y., Ohya, Y. and Kohama, E.: M-ϕ characteristics of high-strength steel pipe piles considering local buckling, Proceedings of the 37th JSCE Earthquake Engineering Symposium, paper ID:12-1242, 8pp., 2017 (in Japanese)

38) Kishida, H. and Takano, A.: The buckling of steel pipe piles and the method to strengthen the end of steel pipe piles, Transactions of the Architectural Institute of Japan, Vol.213, pp.29-38, 1973 (in Japanese)

39) Architectural Institute of Japan (AIJ): AIJ Recommendations for Plastic Design of Steel Structures, 212pp., 2011. (in Japanese)

40) Ohya, Y. and Shiozaki, Y., Kohama, E. and Kawabata, Y.: Application of Modeling of Circular Steel Tube Considering Diameter-to-Thickness Ratio to Various Port Facilities, Technical Note of the Port and Airport Research Institute, No. 1338, 36pp., 2017. (in Japanese)

41) Ishihara, K. and Yoshimine, M.: Evaluation of settlements in sand deposits following liquefaction during earthquakes, Soils and Foundations, Vol.32, pp.173 -188, 1992.

42) Ohya, Y. and Kohama, E.: Evaluation of volumetric strain in liquefied ground around underground structure by using shear strain histories, Journal of Japan Society of Civil Engineers, Ser.A1 (Structural Engineering & Earthquake Engineering (SE/EE)), Vol.73, No.4, pp.I_251-I_257, 2017. (in Japanese).

Chapter 2 Specialized Wharf

1 Container Wharf

1.1 Basic Policy of Design

[Basic point]

Given that a container wharf is a facility that plays a pivotal role in marine container transportation, it shall be developed with consideration to the trend of container transportation (future cargo volume, construction trend of container ships, intention of shipping companies, etc.), the relationship to the hinterland and connecting transportation facilities, the area of the securable lot, etc. Moreover, a wharf shall have facilities for smooth and efficient delivery, sorting, and storage of container cargos and containers, together with container ships and connecting transportation facilities. These facilities shall be arranged in a manner that allows them to function efficiently; accordingly, the wharf shall have sufficient width.

[Commentary]

(1) The container wharf is a nodal point of marine transportation and land transportation in the marine container transportation system, which is also called an intermodal transportation system. The container wharf shall be developed by considering the container cargo demand in Japan and its hinterlands, the operation of the container route network in liner shipping, the traffic network in the hinterlands, and the conditions of container wharf development in neighboring ports. Furthermore, wharfs shall be arranged in locations where they can be efficiently utilized.

(2) Container wharfs differ in scale and form depending on the port to be developed, shipping companies using the port, container routing, cargos types and items, type of transportation facilities to hinterlands, etc.

Terminals that handle containers are divided into the following: container terminals, which are terminals that handle container cargos only, and logistics terminals, which are terminals that handle container cargos and cargos in other packing styles. This chapter provides a fundamental Commentary of container terminals. It can be used as a reference when designing a facility that also handles container cargos and other style cargos such as a logistics terminal. However, it is required to separately examine the facility according to the situation of cargos.

(3) High earthquake-resistance facilities shall be arranged appropriately because the container terminals in Kobe Port damaged by the Great Hanshin-Awaji Earthquake greatly affected the economy and lives of citizens.

(4) Considering that the container terminals in every port in the Tohoku district were damaged by a tsunami in the Great East Japan Earthquake, protection against tsunamis is required. The damages caused by tsunamis are serious, particularly for the inundated traveling part of cargo handling equipment (e.g., container cranes) and for container terminal facilities, owing to the collision of drifting ships or drifting containers. To reduce such damages, waterproofing the structure of the traveling portion of container cranes and others or increasing the higher attachment position of parts to reduce the possibility of inundation may be considered. Moreover, it is effective to improve the spare parts inventory system so that replacement parts can be obtained easily if original parts are damaged. Furthermore, given that the damage to a container crane by empty drifting containers can also be serious, only the minimum required number of empty containers should be stored in the marshaling area around the apron.

(5) A container wharf performs an advanced flow operation together with container ships and connecting transportation facilities. The container wharf comprises a container terminal that unifies the mooring facilities, container yard, cargo handling equipment and management facilities etc., access roads, and logistics-related facilities located in the hinterland such as warehouses, container freight station (CFS), comprehensive logistics center, storage of empty container/chassis according to its functions for smooth delivery, sorting, and storage of container cargos and containers. The function of the container wharf is fully exerted only when these facilities are operated efficiently.

[Reference]

(1) In a container wharf, the following are performed: stevedoring work of containers; storage and delivery of cargos and containers for smooth cargo handling; and inspection and repair of containers, vehicles, and cargo handling equipment. In addition to these tasks, the collection of cargo, the arrangement planning of container ships, and the operation planning of containers may also be performed.

(2) The container wharf is a nodal point of marine transportation and land transportation, and its locational conditions consider the following:

① Trend of container transportation, expansion of the hinterland, and relation to industry and consumption activities in the hinterland

② Relation to infrastructure that provides access to hinterlands such as roads, coastal transportation, and railroads (i.e., cargo transportation network)

③ Relation to the industry that performs port cargo handling

④ Sufficient size of land and water areas and depth of water area

⑤ Status of development of container wharfs in neighboring ports

⑥ Consistency of container orientation at the times of container ship cargo handling, yard storage and cargo storage and transportation, consistency of flow lines, arrangement of facilities, equipment, etc.

The important items among these are as follows: trend of container transportation and relation to the hinterland area and others, evaluation of accumulation or the possibility of the future accumulation of economic/industrial activities in the hinterland that generate sufficient container cargo volume to justify the development of a container wharf, and an analysis of whether the conditions for shipping companies to call at a port in the container transportation network. When analyzing the accumulation of cargos, it is preferable to take into consideration the business practice in international cargo logistics and trade and maritime transportation. Furthermore, it is necessary to consider the whereabouts of the permission organization to obtain information about the port entrance and leaving, customs clearance, and export and import quarantine of animals and plants.

(3) The key items that must be taken into consideration when determining the scale and facility arrangement of a wharf are as follows:

① Sufficient function for efficiently handling and processing cargos

② Economic efficiency of the whole container transportation system such as land–sea intermodal transportation, particularly efficient cooperation with access to land

③ Flexible support of future expansion and innovation in transportation and cargo handling methods

(4) The key items that should be examined in the master plan of facilities in a container wharf are as follows:

① Planned cargo handling volume

② Cargo characteristics (export–import cover ratio, rate of transit, etc.)

③ Allocation interval and type of container ships

④ Management/administration system of a terminal

⑤ Cargo handling method at the quaywall and yard

⑥ Area and form of available land

⑦ Situation of storage facilities in a direct hinterland area

⑧ Circumstance of transportation to hinterlands, traffic condition of roads, etc.

⑨ Usage condition of the surrounding land and ship navigation condition

⑩ Situation of neighboring container wharfs

(5) For the efficient planning and design of wharfs, the movement of container ships, behavior of container cargos and containers at the terminal, and situation of container movement in the hinterlands shall be adequately analyzed. The key items that should be examined are as follows:

① System characteristics of the container terminal

(a) In-service time of the terminal (annual and daily in-service time of gates and container yard)

(b) Arrival characteristics of container ships (arrival distribution)

(c) Distribution of container ships' loading ratios and number of loading and unloading containers

(d) Types of handling containers (ratio of dry, reefer, and special containers; ratio of 40 foot containers and 20 foot containers, etc.) and mode of cargos (ratio of full container load (FCL) cargo (i.e., cargo occupying a full container that is individually transported by land by a trailer) and less than container load (LCL) cargo [i.e., a small lot cargo that does not occupy a full container). LCL cargo is usually loaded in a container with other cargo, and the container is loaded on a ship, packed in a container, or unpacked from a container at the container freight station (CFS) in the container terminal. It is then transported by land as a small cargo.)

(e) Collection and delivery characteristics of a container (carrying in and out distribution)

(f) Container storage characteristics in the container terminal

(g) Moving situation of empty containers

② Characteristics of container handling work plans such as yard storage plans and stevedoring work plans, available number of cargo handling equipment, and work efficiency

③ Facilities in the wharf and container terminal and the principal items of equipment

④ Development cost of container terminals, cargo handling equipment and related equipment, and total cost required for the administration of terminals

⑤ Congestion in gates

Considering the above factors, the whole scale of container terminals, arrangement of facilities, scale of each facility, and the optimum number of cargo handling equipment shall be examined by considering the characteristics of cargo handling methods from the viewpoint of the evaluation of efficiency and safety of terminal use and the cost of cargo handling. In this case, a simulation method that can reflect the cargo handling method, cargo handling equipment, and flow of containers inside and outside of a wharf may be used.

To reduce the waiting time for containers, the transportation cost, and others, it is important to introduce a cargo handling method that contributes to the use efficiency of container wharfs and a wharf operation system that is suitable for the local characteristics.

Moreover, given that container transportation as an intermodal transportation is configured as a system by container ships, container wharfs, trailers, trucks, railroads, coastal marine transportation, and others, each transportation and the scale of transportation facilities are mutually and closely related. Therefore, it is important to evaluate the scale and arrangement of the facilities concerned and to improve the efficiency of the whole transportation system.

Fig. 1.1.1 shows an example of a facility arrangement of foreign trade container terminals.

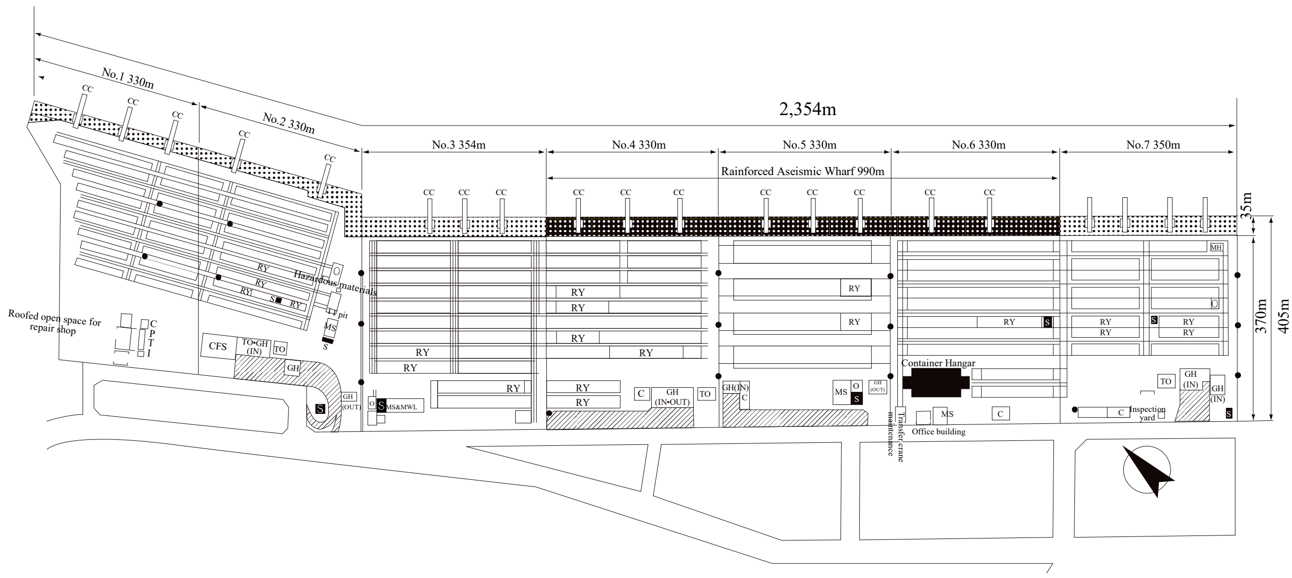

Fig. 1.1.1 Example of a Facility Arrangement of Foreign Trade Container Terminals (Tokyo Port)

1.2 Design of Mooring Facilities

1.2.1 Length and Water Depth of Berths

[Basic point]

The length and water depth of a berth where container ships are moored shall be determined so that the target container ships can use it safely and smoothly.

[Reference]

(1) The ship classes that can carry containers are LO/LO ships, RO/RO ships, semi-container ships, and others. These ship classes have their own features depending on the type of ship. Moreover, even ships of the same class can have different features depending on the type of ship of operating shipping companies. Therefore, when the target type of ship has been identified, the length of a berth and the depth of water shall be determined according to the ship design. However, when the principal dimensions of the design ship cannot be set at the design stage of facilities, the values in **Table 2.1.1** of **Part III, Chapter 5, 2.1.1 Specifications of Quaywall** may be used.

(2) The standard values of the primary specifications of the berth in **Table 2.1.1** of **Part III, Chapter 5, 2.1.1 Specifications of Quaywall** have been determined on the basis of **Part II, Chapter 8, 1 Primary Specifications of Design Ships** conforming to **Part III, Chapter 5, 2.1.1 Specifications of Quaywall (2)**.

(3) Container ships vary significantly in their principal dimensions by operating company, construction date, and navigation channel operation even if they have the same deadweight tonnage (DWT) compared with a general cargo ships. Therefore, even if a facility with a berth length of 350 m and water depth of 15.0 m, a ship with 60,000 DWT or more may be able to dock at it.

1.2.2 Mooring Equipment

[Basic point]

The mooring equipment shall be installed by considering the type of target container ships and by conforming to **Part III, Chapter 5, 9.1 Mooring Post and Mooring Ring**.

[Commentary]

Considering that container ships have higher gross tonnage to DWT ratio than general cargo ships that dock at a quaywall of the same scale in terms of berth length or water depth and given that they load containers on decks, the projected area on the water surface is larger. Therefore, the structure of mooring equipment needs to be defined considering that the heavy pressure area of the wind on the water surface of container ships is generally larger.

1.2.3 Fender Equipment

[Basic point]

The fender equipment shall be installed by considering the type of target container ships and by conforming to **Part III, Chapter 5, 9.2 Fender Equipment**.

[Commentary]

Given that container ships have more displacement tonnage to DWT ratio than general cargo ships with regard to the length or water depth of the same berth, it is necessary to determine the specifications of the fender equipment on the basis of this fact.

Compared with general cargo ships, container ships have different ship types for transporting large quantities of cargos rapidly and smoothly. Therefore, because the contact mode of container ships and fender equipment is considered different from that of general cargo ships, the arrangement of fender equipment needs sufficient consideration.

1.3 Design of Land Facilities

1.3.1 Apron

[Basic point]

The scale and facilities of an apron shall be appropriately determined and designed respectively so that the temporary storage of containers and hatch covers of container ships and the operation of cargo handling vehicles and equipment can be performed safely and smoothly.

[Reference]

(1) For the handling of container cargo in a wharf, the required scale (width) of the apron differs on the basis of the type and quantity of quaywall cranes and the cargo handling method used in the container yard.

(2) The width of an apron is often set to approximately 40 to 70 m in consideration of the rail width of the container crane in a container terminal, vehicle passing width, etc.

(3) The pavement of an apron shall be designed with consideration to the wheel loads of running vehicles and cargo handling equipment. It is common to pave an apron with concrete or asphalt.

Refer to Part III, Chapter 5, 9.18 Apron for pavement.

1.3.2 Container Crane

[Basic point]

A container crane shall have suitable processing capability that is suitable for the type of target container ships, size and type of containers, handling number of containers, quaywall structure, cargo handling method in the yard, type of yard cargo handling facilities and machines, etc.

[Commentary]

(1) Considering that the container crane is a primary cargo handling equipment for loading or unloading cargos from a ship and that its capability becomes a primary element of the handling capability of a wharf, its primary quantity and capability must be defined so that the capability of cranes matches the handling capability of the yard for the docking ships, containers to handle, cargo handling method of the yard, etc.

(2) The container cranes shall be designed according to **Part III, Chapter 7 Sorting Facilities** and this section.

[Reference]

(1) The required number of container cranes differs according to the type of container ships, required cargo handling capability at the quaywall, etc. Two or three container cranes per berth are common in Japan.

(2) When designing a container crane, the items to consider as area conditions are as follows:

① **Type of the target container ship**

Given that the specifications of a container crane are determined by the maximum type of a design ship, the target type of a ship shall be set adequately by considering the water depth and length of the quaywall.

② **Required processing capability**

The processing capability of a container crane shall fully correspond to the frequency of container ships' arrival in a port and the number of loading and unloading containers per container ship. Its processing capability must harmonize with the container processing capability of the yard.

Given that the processing capability of a container crane depends on the speed of main operations (winding up/down and traversing), these speeds shall be determined appropriately.

③ **Rated load of a crane**

The rated load shall be adequately determined on the basis of the expected mass to be handled by the container cranes (e.g., containers, hatch covers of a container ship, and other heavy load carried by container ships).

④ **Earthquake-resistant performance**

Refer to **Part III, Chapter 7 Sorting Facilities** for the earthquake-resistant performance of container cranes.

⑤ **Consideration of aviation restrictions**

According to the Civil Aeronautics Act, an airplane warning light is obliged to be installed for buildings that are 60 m or higher. Moreover, height is restricted so that collision with the level surface and transitional surface near the airport can be avoided. In such a case, a device to fold the derricking boom of a container crane in two steps (folding crane) is needed.

(3) Determination of Specifications of a Container Crane

① **Traversing**

Outreach shall be determined so as to sufficiently support the maximum target type of a ship by considering the molded breadth of a design ship, contact distance between trajectory face lines, height of a fender, inclination of a ship during cargo handling, etc. When setting the distance between trajectory face lines, the following shall be fully considered: contact of the ship to the container crane, size of a mooring post, electric supply cable trench to the crane, structure of the quaywall, and others. The back reach shall be determined by considering the location where containers are temporarily stored and where hatch covers are stored during cargo handling work.

② **Net lifting height**

The net lifting height shall be determined so as to sufficiently support the maximum target type of a ship by considering the draft of design ships, depth of holds, number of container stacks on the deck, inclination during cargo handling, tide level, etc.

③ **Rail span**

The container cargo handling work in an apron usually uses a chassis or a straddle carrier. The rail span width shall be determined so as to perform such cargo handling work smoothly. The number of lanes required for the passage of these vehicles and cargo handling equipment shall be determined by the flow line with consideration to the number of container cranes used for one ship. Therefore, the rail span shall be determined by considering the required number of lanes, required lane width of the type of cargo handling equipment that runs on the lanes, quaywall structure, safety and economic efficiency of a crane, attaching/detaching work of instruments to fix container to be stacked on a deck, etc.

The rail span of a domestic container crane is usually 16 or 30 m. When considering the stability of the crane in case of an earthquake, a larger rail span is better. Container cranes that support 13 rows or more usually have a rail span of 30 m.

④ **Effective space between legs**

The effective space between legs is an inside dimension space of the leg pillar seen from the perpendicular direction of the quaywall face line. This space shall be determined so that the object to be handled with the container crane (e.g., a container hatch cover) can safely pass through between legs.

The effective width between the legs of almost all domestic container cranes is 17.0 m to 18.0 m, including whirling with hanging a container and allowance.

⑤ **Full width**

Considering that two or more container cranes are used for one ship to do neighboring work, a narrower width is preferable as long as it is structurally reasonable.

⑥ **Under beam height**

This shall be high enough for cargo handling equipment such as a chassis or straddle carrier, which runs within the rail span so that it can pass safely.

The under beam height of almost all domestic container cranes is 14 to 15 m because many of them considered the case wherein a straddle carrier passes. The crane shakes less as the under beam height decreases.

⑦ **Critical surfaces on the sea side and on the land side**

To avoid the contact of a container crane with the container ship moored to a quaywall, it is required to examine the critical surface on the sea side of a container crane. This limit size is determined by the quaywall surface height; high tide level; height of a fender; and dimensions of the design ship, particularly the height and width of the navigation bridge wing and draft of the design ship.

The inside of the critical surface on the sea side of the container crane needs to be set so that the crane can move in an inactive condition (condition where the derricking boom is standing) without contacting the ship. Moreover, the width of stairs going up and down from the ship shall be taken into consideration. Examples wherein passenger ships are moored to a container berth resulting from the enlargement of passenger ships in recent years and ships other than container ships shall also be taken into consideration if needed.

Moreover, to avoid the contact of a container crane with cargo handling equipment and others, the critical surfaces on the land side of the container crane is also needed to be examined. The width between legs, under beam height, and marginal surface where cargo handling equipment cannot enter in the back of a container crane shall be determined.

⑧ **Cable reel**

There was an accident wherein the contact of container ships and others with the container crane damaged a cable reel. When installing the cable reel perpendicular to the quaywall face line as a means to avoid this accident, attention should be paid to the following. When introducing a cable reel perpendicular to the quaywall, its weight and others shall be taken into consideration because it should be originally installed on a horizontal brace so that it will not interfere with the cargo handling equipment. Considering that the direction of the cable veered out from the cable reel is required to be changed from the direction perpendicular to the quaywall face line to a direction parallel to the quaywall face line, a flat cable shall be changed to a round cable, and a guide roller shall be installed. The cable trench and cable anchor drum in the cable pit shall be made to support the round cable.

(4) Installation of Monitoring System

It is preferable to have a monitoring system for the efficient operation of cranes and terminals.

In general terms, the monitoring system comprises a failure monitoring function to monitor the control system of cranes, a maintenance function to monitor the condition of portions that need maintenance, and an operation management function to collect track records such as the number of containers, weight, and cycle time.

(5) Installation of Attachment Devices (Fixed Device, Turnover Prevention Apparatus, End Stopper, Jack-Up Plate, Rail Clamp, etc.)

Cranes shall have a crane foundation and a crane anchoring structure so that they stop at the specified position when inactive or during a storm to avoid overrunning or overturning. Moreover, cranes shall be equipped with a rail clamp or others so as not to overrun in unexpected situations, such as during a gust of wind, when cranes are at any position on the rail.

An end stopper shall be equipped at the end edge of the guideway so that the crane does not deviate from a rail. Moreover, a jack-up plate shall be equipped at a predetermined position of the crane foundation so that the crane can be jacked-up when exchanging a running wheel. The predetermined position shall be taken into consideration to avoid contact with arriving or leaving ships.

(6) **Fig. 1.3.1** shows an example of a container crane.

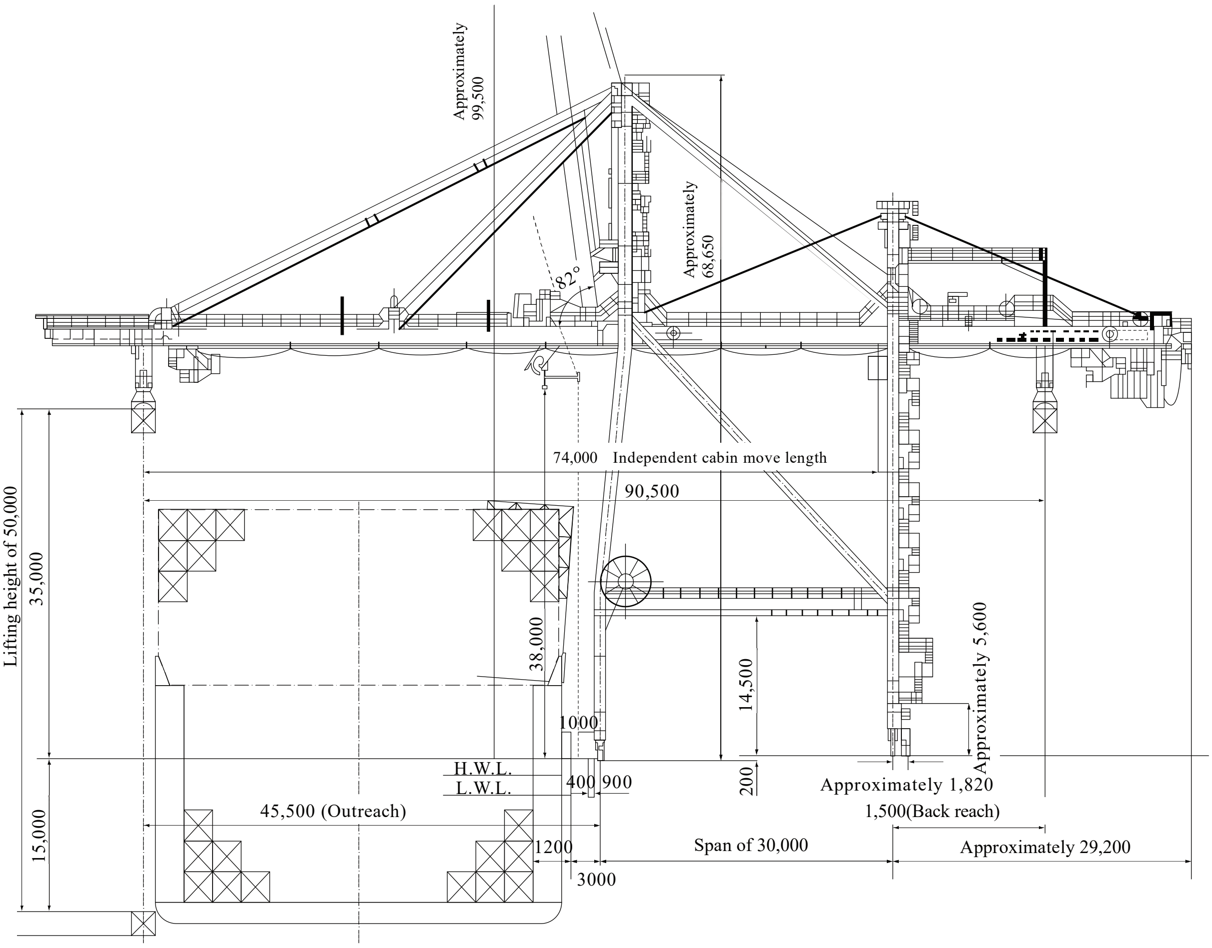

Fig. 1.3.1 Example of a Container Crane

1.3.3 Container Yard

[Basic point]

The cargo handling method, scale, and arrangement of the container yard shall be determined to facilitate the storage and delivery of containers, and facility planning in the yard shall be performed.

[Commentary]

The container yard has a storage function for the efficient cargo handling work of containers unloaded from the ship and containers to be loaded in the ship and has a storage function for empty containers for the efficient handling of empty containers. The scale and arrangement planning of the container yard, facility planning of the yard, and others shall be conducted so that these functions can be performed smoothly.

[Reference]

(1) Fundamentally together with an apron, the container yard loads and unloads containers to/from container ships and visiting chassis, transports, and stores containers. The container yard has a marshaling area wherein cargo handling work such as the transport, cargo handling, or storage of containers is performed and a backyard wherein the gate, administration building, maintenance shop, gas station, parking lot, and others are located. Moreover, empty containers are stored for the use of shipping companies.

(2) The container yard shall be planned by considering two elements: loading and unloading of containers to/from ships and transporting containers to/from the hinterland. The primary items to consider are the ① arrival interval of container ships, ② number of containers to load to and unload from container ships, ③ type and quantity of handled containers such as the classification of loaded or empty containers and classification of dry or reefer, ④ container handling method at the quaywall and in the yard and collection and delivery form of containers, ⑤ storage characteristics of containers in the yard, number of stacks, etc.

(3) The storage form of containers differs by the cargo handling method used in the container yard. Moreover, given that the transport method of containers differs by the cargo handling equipment used, the arrangement and necessary area of a passage differ. Therefore, it is necessary to have a facility plan that corresponds to the cargo handling method in the container yard.

The cargo handling method in the container yard differs according to the number of containers handled. Examples are shown in the following:

① **Terminals where a large number of containers are handled such as international container strategic ports and international base ports**

Many containers in the yard flow in either of the following methods:

(a) Container crane → yard chassis → transfer crane → visiting chassis

(b) Container crane → straddle carrier → visiting chassis

The top lifter, reach stacker, and others are used in the storage yard to process empty containers and the like.

② **Terminals where a small number of containers are handled such as local important ports**

Many containers in the yard flow in either of the following methods:

(a) Container crane → straddle carrier → visiting chassis

(b) Container crane → (yard chassis) → reach stacker → visiting chassis

The top lifter and others may be used in the storage yard to handle empty containers and similar objects.

Equipment in parenthesis may not be used.

Moreover, it is possible to install a multistory container storage facility in a terminal where many containers are handled, but a storage yard has no margin and no room for an extension. This is a facility that has shelves for storing containers in the building and a distribution warehouse with an overhead traveling crane and chassis storage. Given that this enables increased storage capability via the installation of more shelves than the number of stacks in the yard and via the selection of container from the shelf, easing can be expected in terms of the reduction in the cargo handling capability when nearing the limit of the storage capability.

The primary cargo handling methods in the yard are as follows:

1) Transfer crane method

This method uses a yard chassis for container transport in the container yard and uses a transfer crane for loading and unloading containers. This method is classified into a rail type and a tire type according to the type of transfer crane. Considering that containers are placed directly on the ground and can be stacked, the land-use efficiency of the container yard is high.

Moreover, it easily supports the remote control and automation of cargo handling.

However, its early capital investment is larger than other methods.

Considering that the transfer crane is heavy, its guideway shall be equipped with a rail foundation for rail type and shall usually be paved with prestressed concrete or reinforced concrete for tire type. Moreover, although the trailer guideway needs to be heavily paved, if a concrete slab (container mat) is laid in the installation part of the lowest stack container, a low-cost pavement is enough for other portions.

Given that facilities may be installed in the earth for remote control, automatic driving, or others, consideration is required during paving. Furthermore, the space wherein facilities that supply electric power (e.g., a bus bar) are installed is needed when introducing an electric crane.

This method is often adopted in a container yard where a large number of containers are handled.

2) Straddle carrier method

This is a method that uses a straddle carrier with emphasis on carrying. A straddle carrier allows containers to be freely carried anywhere in a container yard.

The advantages of this method include mobility in the transport of containers, capability of stacking, and highly efficient land use of the container yard. Moreover, the initial investment is not that large.

The disadvantage is that when taking out a low-stacked container, its movement is limited only to the lengthwise direction along the row and is restrained more than that in the transfer crane method. Moreover, although the straddle carrier can run freely, it is necessary to focus on the safety of workers in the yard.

The whole guideway needs to be heavily paved because the straddle carrier runs lengthwise and breadthwise. Moreover, the specified guideway in the container storage may be paved with semiflexible material or high standard asphalt to prevent rutting.

This method is often adopted in a container yard wherein a medium number of containers are handled.

3) Reach stacker method

This is a method that uses a reach stacker for cargo handling in a yard. A reach stacker can carry containers freely anywhere in the container yard, similar to the straddle carrier.

The advantage of this method is the mobility in the transport of containers. Although inferior to the straddle carrier method, it is capable of stacking, and the land-use efficiency of the container yard is high to a certain extent. Moreover, the initial investment is not that large.

The disadvantage is that in the makeshift of cargos to take out a low-stacked container, the containers before the row must be moved and restrained more than in the straddle carrier method when taking out a low-stacked container in the second row or after. Moreover, although the reach stacker can run freely, it is necessary to secure the safety of workers in the yard.

The whole yard needs to be heavily paved because the reach stacker can run freely. Moreover, the place where the visiting chassis and reach stacker hand over the containers may be paved with concrete to prevent rutting.

This method is often adopted in a container yard where a small number of containers are handled.

4) Forklift method

A small-scale container yard that is handling a small number of containers may use 1) to 3) and the forklift method. Although this method is simple but inefficient when handling a large number of containers, the operation work area becomes large and the container storage efficiency becomes low.

This method is often used for the storage of empty containers.

There are examples wherein several cargo handling methods are used in separated areas in a yard on the basis of the advantage of each yard cargo handling method.

5) Automated operation method

Some overseas and domestic terminals introduce remote controlled or automated cargo handling equipment to load, unload, and carry containers. The development of unmanned operation in the yard can be achieved by enabling remote control or automatic operations, improving safety in a yard and work environment, and equalizing cargo handling efficiency. **Tables 1.3.1** and **1.3.2** show examples of overseas container yards that are adopting automated operation method.

Table 1.3.1 Examples of Ports Where Automated Stacking Cranes Have Been Introduced in the Storage Yard Crane

Port	Terminal	Operator	Introduced in	Storage direction	Storage yard crane		Container transport vehicle
					Number	Manufacturer	
Rotterdam	Delta	ECT	1993	Vertical	137	Cargotec	AGV
Hamburg	CTA	HHLA	2001	Vertical	52	Kunz	AGV
Virginia	Portsmouth	APMT	2007	Vertical	30	Kone	SC
Antwerp	AGW	DPW	2007	Vertical	14	Gottwald	SC
Hamburg	CTB	HHLA	2008	Vertical	63	Cargotec	SC
Rotterdam	Euromax	ECT	2008	Vertical	58	ZPMC	AGV
Algeciras	Hanjin	TTI	2010	Vertical	32	ZPMC	SC
Khalifa	ADPC	ADPC	2012	Vertical	30	Kone	SC
Pusan New	HPNT	HMM	2012	Vertical	38	ZPMC	SC

Port	Terminal	Operator	Introduced in	Storage direction	Storage yard crane		Container transport vehicle
					Number	Manufacturer	
Port South							
New Jersey	GCT	GCT	2012	Vertical	40	Kone	SC
Barcelona	BEST	HPH	2013	Vertical	36	Kone	SC
London	LGW	DPW	2013	Vertical	40	Cargotec	SC
Sydney	SICTL	HPH	2014	Vertical	6	Kone	SC
Brisbane	DPW Brisbane	DPW	2014	Vertical	14	Cargotec	SC
Los Angeles	MOL	TraPac	2014	Vertical	10	Cargotec	Unmanned SC
Rotterdam	RWG	DPW	2014	Vertical	50	Gottwald	Battery AGV
Rotterdam	MV2	APMT	2015	Vertical	48	Kunz	Battery AGV

Note: ASC: Automated Stacking Crane; AGV: Automated Guided Vehicle; SC: Straddle Carrier

Table 1.3.2 Examples of Ports Where Storage Yard Cranes and Container Transport Vehicles Have Been Remote Controlled or Automated

Port	Terminal	Operator	Introduced in	Storage direction	Storage yard crane			Container transport vehicle
					Method	Number	Manufacturer	
Singapore	PPT	PSA	1998	Horizontal	OHBC	44	MES	Chassis
Brisbane	Patrick	Patrick	2002	Vertical	-	-	-	Unmanned SC (27)
Nagoya	Tobishima South	TCB	2005	Horizontal	RTG	24	MHI	AGV
Pusan New Port North	PNC	DPW	2006	Horizontal	RMG	31	Doosan	Chassis
Pusan New Port North	Hanjin	Hanjin	2006	Horizontal	RMG	42	ZPMC	Chassis
Taipei	Taipei New Port	TPCT	2009	Horizontal	RMG	20	ZPMC	Chassis
Pusan New Port South	Hundai Merchant Marine	HMM	2010	Horizontal	RMG	37	ZPMC	Chassis
Kaohsiung	MYL	YML	2011	Horizontal	RMG	22	ZPMC	Chassis
Sydney	Patrick	Patrick	2015	Vertical	-	-	-	Unmanned SC (44)

Note: OHBC: Overhead Bridge Crane; RTG: Rubber Tired Gantry crane; RMG: Rail Mounted Gantry crane

(4) The arrangement method of the container storage in a container yard differs on the basis of the cargo handling method. The intensity required for the pavement of the yard differ by container storage method, cargo handling equipment, passage, passing method, etc.

Although the yard is completely paved for the storage of containers, running of vehicles and cargo handling equipment, drainage, and others, it is generally paved with asphalt because of the differential settlement of the foundation, maintenance repair, etc. However, in consideration to the severe loading condition, countermeasures against rutting, wear, oil, and others shall be taken. If necessary, semiflexible pavement, reinforced concrete pavement, or prestressed concrete pavement shall be used. Given that the utility form of the container yard is relatively clear, the storage condition of containers, characteristics, run frequency, and others of running vehicles and cargo handling equipment shall be fully examined. Furthermore, the loading conditions shall be set, and the rational design shall be conducted according to the conditions.

Moreover, as stated in (3), the container mat made of prestressed or reinforced concrete slabs are often installed with consideration to the concentration load applied to stacked container corners.

(5) For cargo handling at night, install a lighting facility at a suitable location so that the container yard surface is illuminated at 20 lx (lux) or brighter. In this case, there are methods for centralizing or diverging equipment. When installing a lighting facility, do not dazzle the ship operator entering or leaving a port and the cargo handling equipment operator in the yard at night.

Moreover, consider the illuminance and arrangement required for security and management. A power receptacle and an inspection stand shall be installed if necessary in a reefer container storage. Furthermore, a fence shall be installed as a security facility around the foreign trade container terminal.

1.3.4 Container Freight Station

[Basic point]

A CFS shall be constructed if needed, considering the handling of small lot cargos in the yard. The location shall be determined on the basis of the traffic stream line in the yard. Furthermore, the scale of facilities and the cargo handling equipment to be used shall be determined, and the facilities shall be designed so that the sorting and temporary storage of cargos are performed safely and smoothly.

[Commentary]

Although the CFS is where small lot cargos are loaded to or unloaded from containers, sorted, and stored, the necessity of construction in the yard differs by yard users. Therefore, consider the users' handling method of small lot cargos, and execute constructions if needed.

[Reference]

(1) Given that not only vehicles dedicated to containers but also trucks for general use enter in and out the CFS, its location shall be determined by considering smooth cargo handling activities at a wharf and the flow line of related vehicles.

(2) Although the CFS in a container terminal has a short conveying distance for containers, it is not necessarily located in a container terminal or a wharf but may be constructed in the hinterland. Therefore, consider the handling method used by wharf users for small lot cargos.

(3) The CFS is a building similar to a shed, and the inside and outside of small lot cargos and containers generally face across the freight sorting area. The floor height of the freight sorting area shall be approximately 1.2 to 1.3 m to match the height of the bed of trucks and the floor of the container loaded on a chassis and shall be paved with concrete or asphalt. Moreover, a slip way or lifter shall be installed at a suitable place to facilitate the use of cargo handling equipment, such as a forklift, to the freight sorting area.

The pillar interval shall not obstruct the cargo handling in consideration of containers, vehicles, etc.

(4) The area (length and width) of the CFS shall be set so that the sorting and temporary storage of cargos are performed smoothly on the basis of the arrival interval of container ships, number of containers to be loaded or unloaded, type of containers, ratio of containers going through the CFS, quantity and type of cargos to load and unload from containers, cargo storage characteristics in the CFS, in-service time of the CFS, working time per container, etc.

Moreover, given that the CFS may be used as an inspection station for the import and export of container cargos containing animals and plants, consider setting a scale if necessary.

(5) The width of the space in front of the CFS for the ingress and egress of vehicles shall be approximately 25 m and 15 m if used by a container chassis and trucks, respectively.

1.3.5 Maintenance Shop

[Basic point]

The location and scale of a maintenance shop shall be determined so that the check and repair of containers and the inspection, management, and repair of vehicles and cargo handling equipment are performed smoothly.

[Reference]

(1) The maintenance shop is where the inspection of containers, cleaning before and after use, repair of damages, and maintenance and repair of vehicles and cargo handling equipment used in the container terminal or wharf are performed. It is usually located inside a building.

(2) Although the area of the maintenance shop differs according to the number of containers in a terminal; the type, scale, and inspection frequency of the vehicles and cargo handling equipment used in a terminal; the level of repair performed at the maintenance shop concerned; and others, approximately 800 to 2,000 m^2 per berth is needed in the foreign trade container terminal.

(3) The height of the entrance shall be at least that of vehicles and cargo handling equipment to be accommodated, and an overhead traveling crane is required as an ancillary facility. Furthermore, the power receptacle for reefer containers, compressors, welding machines, chargers, and others shall be installed.

The floor surface is usually paved with concrete.

(4) The width of the space in front of the maintenance shop shall need approximately 10 m if trailers go in and out and approximately 15 m if straddle carriers go in and out.

1.3.6 Administration Building

[Basic point]

The location and scale of an administration building shall be determined so that the administration and operation of the container terminal are performed smoothly.

[Reference]

(1) The administration building is where the administrative operation of container wharfs such as the administration of terminals, processing and management of information concerning cargos, and operation of container ships are performed. Specifically, the storage plan of containers in the terminal, cargo handling plan of container ships, cargo handling work plan and operation plan of cargo handling equipment in the yard, delivery operation of cargos and containers, management of cargo handling equipment, management of empty containers, and others are performed.

A container terminal for international trade generally has a scale of 1,000 to 5,000 m^2 and is usually two to four stories.

(2) A control tower from which it possible to oversee the entire container yard shall be erected so as to allow persons in charge to issue instructions to operators of cargo handling equipment and effectively manage cargo handling works. The control tower shall be established on the highest floor of the administration building.

1.3.7 Gate

[Basic point]

The location and scale of a gate shall be determined so that the three-point check of drivers who go in and out the container terminal, the inspection of containers, the weight measurement, and the transfer of documents are performed smoothly.

[Reference]

(1) The gate is where drivers, containers, and cargos that go in and out the container terminal are confirmed, where the container seal number is confirmed, where containers are inspected, where container weight is measured, where the required documents are transferred, and where the storage location of containers is directed. The foreign trade terminal shall have a gate house, an elevated passage for inspection, and usually one or two approximately 50-ton truck scales if necessary.

Moreover, a common gate jointly used by several terminals may be installed. This is considered to be effective in saving the gate area, improving the work efficiency, and others because the gate operation is aggregated in one location.

(2) The number of gates needs to be determined by considering the quantity of containers handled in the container terminal, the in-service time of a gate, the distribution of carried in and out containers, and the processing time of containers at the gate. The gate is often installed by dividing carrying in and out containers or loaded containers, empty containers, and general trucks.

The confirmation work at the gate may be performed before passing the gate as a prior check gate. This is considered effective to mitigate the traffic congestion resulting from a temporary increase in the number of vehicles passing the gate.

It is also necessary to select the location with consideration to the traffic movement in the container terminal and traffic on the secondary roads.

1.3.8 Other Attached Equipment

[Basic point]

Washing facilities, sewage disposal, gas station, substation equipment, parking lot, chassis storage, and others shall be constructed in the container terminal if necessary.

[Commentary]

Although this section is described on the basis of the feature of a container wharf, **Part III, Chapter 5, 9 Attached Equipment and Others of Mooring Facilities** shall be applied for the attached equipment not stated in this section.

[Reference]

(1) The washing facilities are where containers, vehicles, cargo handling equipment, and other equipment are washed, and the floor surface shall be paved with concrete. The sewage disposal is where sewage from washing facilities, maintenance shop, gas station, and others is oil separated and where effluent is treated. The final effluent must conform to a predetermined standard.

(2) The gas station is where vehicles, cargo handling equipment, and others are refilled with gas, and the floor surface shall be paved with concrete.

(3) The substation equipment provides electric power to the container terminal. Its capability determines the capacity of the substation equipment considering that all pieces of the electric apparatus do not often operate simultaneously and the demand factor, which considers the characteristics, quantity, frequency of use, and others of the electric apparatus versus the load equipment capacity.

Since cold storage facilities in summer usually require a constant power supply, sufficient planning is necessary.

Moreover, it is preferable to have an auxiliary circuit in preparation for an unexpected situation because the interruption of electric power supply due to power failure accidents paralyzes the functions of the container terminal.

(4) Securing sufficient waiting spaces (e.g., parking lot) outside of a gate is needed to eliminate the impacts of trailers waiting for gate passage on general traffic or obstacles to the smooth flow of port cargos in other terminals, particularly in ports where a lot of containers are handled. Furthermore, it is preferable to secure chassis storage for the purpose of improving the efficiency of the inland transportation of containers as a countermeasure for congestion in situations wherein chassis are left in a wharf.

Parking lots and chassis storage shall be placed at a suitable location in the container terminal or container wharf.

1.4 Estimation of the Scale of Container Terminal Area

[Basic point]

(1) The container terminal is located in a port as a nodal point of the marine transportation and land transportation of containers. It is an area for stevedoring work in container ships, temporary storage for cargo handling, storage and delivery of cargo and containers, and an area for loading and unloading cargos to/from containers and for cargo handling equipment required for containers and related facilities.

[Reference]

(1) Scale Estimation of Container Terminal Area

Fig. 1.4.1[1)] shows the procedure for the scale estimation of container terminal area.

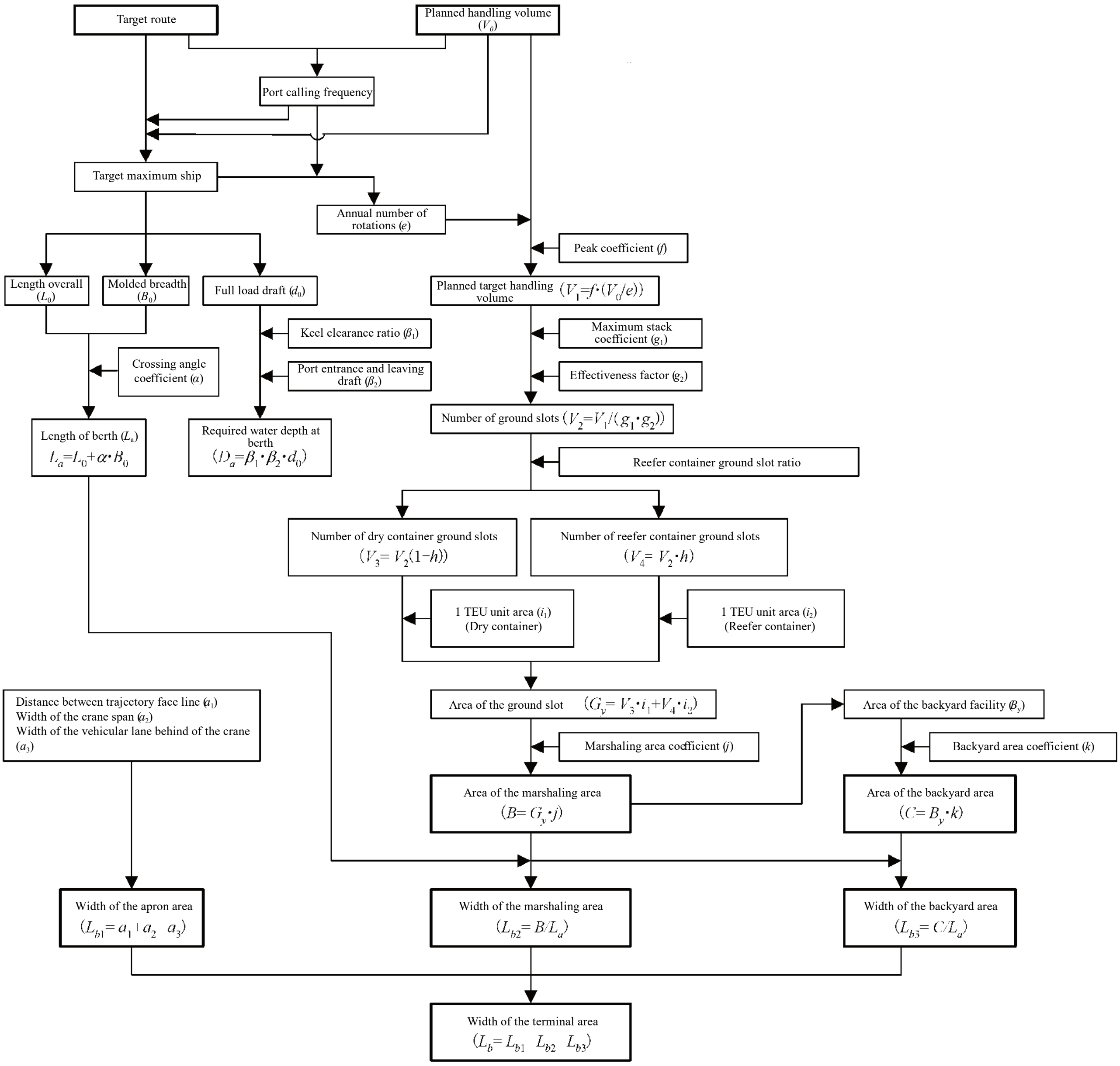

Fig. 1.4.1 Standard Scale Estimation Model of the Container Berth Terminal Area[1)]

(2) Methods (3) to (8), which were reported by Takahashi,[1)] can be used to calculate or set the scale of a container terminal area.

(3) Elements of Container Terminal

The container terminal mainly comprises the berth, apron area, marshaling area, and backyard area. Although two or more berths often share the backyard area, **Fig. 1.4.2**[1)] shows an example of a plan of a container terminal area where all elements are in one terminal.

① **Berth**

A berth is a predetermined place for container ships to berth and anchor to handle cargos in the container terminal, and its scale is set by the berth length L_a and water depth at berth D_a.

② **Apron area**

(a) The apron area is where container cranes and vehicles for cargo handling run, containers, and hatch covers of container ships are temporarily stored. Here L_{b1} in **Fig. 1.4.2**[1)] is the width of the apron area.

(b) The width of the apron area L_{b1} can generally be set from the distance between trajectory face lines, rail span of the container crane, and vehicular lane width.

③ **Marshaling area**

(a) The marshaling area is where the containers to be loaded to or unloaded from container ships are aligned. Here, L_{b2} in **Fig. 1.4.2**[1)] is the width of the marshaling area. The block in which containers are flatly stored according to their size is set in this marshaling area. This is called the ground slot and is set like an intersection on a go board (**Fig. 1.4.2**).[1)] The numbers are given to the blocks and containers are arranged at a predetermined grid according to the loading plan. There are areas for dry containers and for reefer containers that need power supply for freezing in this ground slot.

(b) The width of the marshaling area L_{b2} corresponding to the berth length can generally be set on the basis of the required scale of marshaling area, available land, number of stacks and equipment.

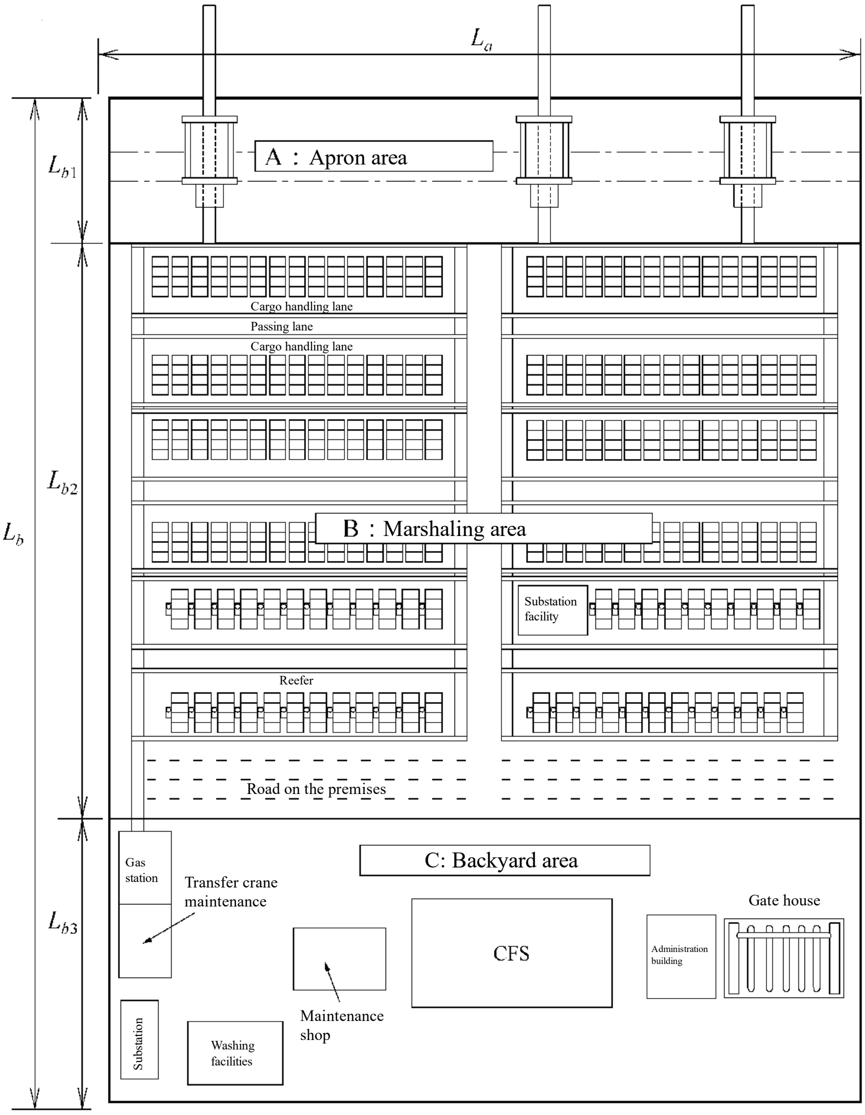

Fig. 1.4.2 Example of a Container Terminal[1)]

④ **Backyard area**

(a) The backyard area is where facilities such as the maintenance shop, administration building, and gate are located. Furthermore, the CFS may be located in this area. Here, L_{b3} in **Fig. 1.4.2**[1)] is the width of the backyard area. The outline of each facility is shown below. The expression “backyard area” is not common but is usually expressed as “container terminal” together with the marshaling area in many cases. However, the backyard area is set here to verify the performance concerning the scale of the container terminal area.

1) Container freight station

This is a building for delivery, temporary storage, loading to and unloading from containers, and other tasks involving small lot cargos. In the case of large-scale terminals, this is not often located in a container terminal but is owned by public carriers near the terminal.

2) Maintenance shop

A building where containers themselves are inspected and where damaged parts are repaired, cleaned before and after use, etc.

3) Administration building

A building where work in the whole yard such as direction, supervision, and others of the work plan in the yard and container arrangement plan are integrated and employed.

4) Gate

A facility where documents for carrying in and out container cargos to/from the container terminal, container number, port security information, damage to containers, and others are checked.

A facility where the yard carrying-in location of containers are indicated, and these data are registered in the terminal management system.

(b) The width of the backyard area L_{b3} corresponding to the berth length can generally be set on the basis of the required scale of the backyard area.

⑤ **Empty container storage**

The empty container storage is where empty containers for lending to or returned from shippers are stored. Although the empty container storage is included in the marshaling or backyard area, its area is not wider than the surplus of each area. If the required number is as many as the loaded containers, an area outside of the terminal shall be assumed.

(4) Berth

① **Length of the berth**

Refer to **Part III, Chapter 5, 2.1 Items Common to Quaywall** for the berth length of the container terminal.

② **Water depth at berth**

Refer to **Part III, Chapter 5, 2.1 Items Common to Quaywall** for the water depth at the berth of the container terminal.

(5) Apron Area

① The width of an apron area L_{b1} can be calculated by **equation (1.4.1)**.

$$L_{b1} = a_1 + a_2 + a_3 \tag{1.4.1}$$

where

a_1 : distance between trajectory face lines

a_2 : width of the rail span

a_3 : width of the vehicular lane behind the crane

② **Distance between trajectory face lines (a_1)**

The distance from the rail on the sea side to the quaywall face line shall be preferably set on the basis of the characteristics of the target container terminal by considering the installation of mooring posts, cable trench for container crane, cable winding equipment, hatchway of a moored container ship, etc. When performing the setting operation, a_1 = 3 to 4 m can be used as a reference value.[4)]

③ **Rail span width (a_2)**

It is preferable that a sufficient width for the same number of lanes as that of cranes used for container cargo handling plus one additional spare lane shall be secured as the rail span. Furthermore, it is preferable to add approximately 5 to 10 m as a pass for pedestrians and miscellaneous-use vehicles. Here, 5.0 m/lane for yard chassis and 5.5 m/lane for straddle carriers can be used as a reference value when setting the required width per lane under the crane.[4)]

When using three cranes per ship and a straddle carrier, the rail span width a_2 can be considered as follows:

a_2 = (3 + 1) lanes × 5.5 m/lane + 8 m (margin width) = 30 m

If the rail span set from the structure aspect of the crane is larger than this required lane width, it is necessary to set that value.

④ **Setting of the vehicular lane width behind the crane (a_3)**

It is preferable to appropriately set the vehicular lane width behind the crane considering specifications, margin width and others of the crane.

For example, in the case of a yard chassis, the vehicular lane behind the crane can be set as the value of the temporary storage of hatch covers (four rows: 11 m; five rows: 13.5 m)[4)] and the minimum lane width of 3.5 m[4)] plus the margin width of 3 m (for example, 20 m in the case of a five-row hatch cover). In the case of a straddle carrier, it may be 37 m (carrier revolution width of 22 m[4)] plus the margin width of 15 m).

⑤ **Standard value for the width of the apron area L_{b1}**

The apron area width L_{b1}, excluding the various conditions concerning the backyard area, can be set by referring to **Fig. 1.4.3**,[3)] which shows the track record value in domestic container terminals. In reference 3), an L_{b1} of 40 to 60 m when the water depth is less than 13 m and 50 to 80 m when the water depth is 13 m or more can be considered the standard value for the width of the apron area.

L_{b1} can be considered as follows when using three cranes per ship and a straddle carrier.

$L_{b1} = a_1 + a_2 + a_3$ = 3 m + 30 m + 37 m = 70 m

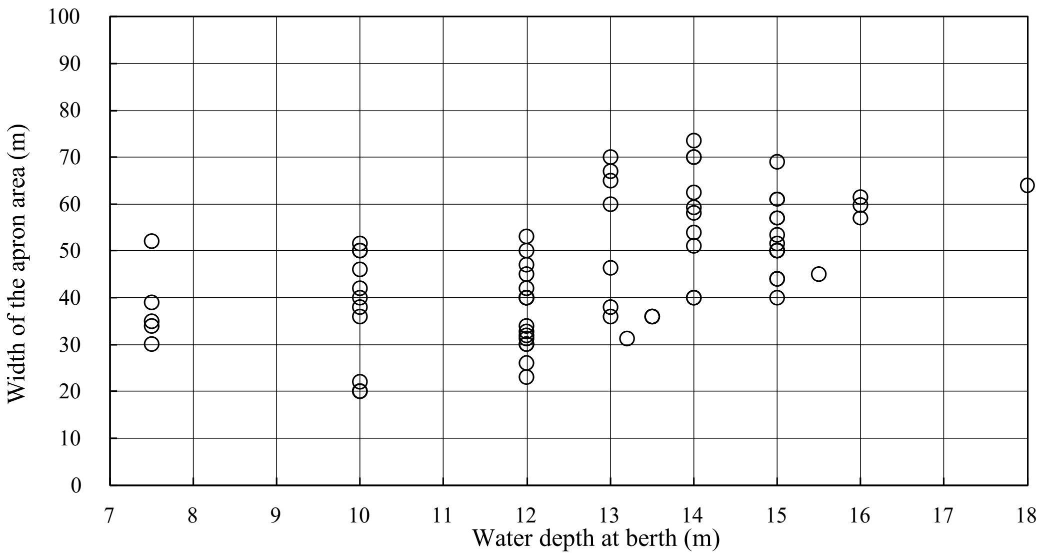

Fig. 1.4.3 Width of the Apron Area (L_{b1})[3)]

(6) Marshaling Area

① The area of the marshaling area can generally be calculated by the procedure shown in **Fig. 1.4.4** on the basis of the planned handling volume: V_0 (TEU).

Calculation of the number of target containers (V_1) to plan the marshaling area: **Equation (1.4.2)**

↓

Calculation of the number of ground slots (V_2): **Equation (1.4.3)**

↓

Calculation of the number of dry container ground slots (V_3): **Equation (1.4.4)**

↓

Calculation of the number of reefer container ground slots (V_4): **Equation (1.4.5)**

↓

Calculation of the area of the ground slot (Gy): **Equation (1.4.6)**

↓

Calculation of the area of the marshaling area (B): **Equation (1.4.7)**

Fig. 1.4.4 Example of the Procedure for Verifying the Performance of Area of the Marshaling Area

The area of the marshaling area can generally be calculated by following **equations (1.4.2)** to **(1.4.7)**.

$$V_1 = fV_0 / e \tag{1.4.2}$$

$$V_2 = V_1 / (g_1 g_2) \tag{1.4.3}$$

$$V_3 = V_2 (1 - h) \tag{1.4.4}$$

$$V_4 = V_2 h \tag{1.4.5}$$

$$G_y = V_3 i_1 + V_4 i_2 \tag{1.4.6}$$

$$B = G_y j \tag{1.4.7}$$

where

V_0 : planned handling volume (TEU)

V_1 : number of target containers to plan the marshaling area (TEU)

e : annual number of rotations (time/year)

$$e = D_y / D_t \tag{1.4.8}$$

where

D_y : annual number of work days (day)

D_t : average storage days in the yard (day)

f : peak coefficient

V_2 : number of ground slots (TEU)

g_1 : maximum stack coefficient

g_2 : effectiveness factor

V_3 : number of dry container ground slots (TEU)

h : reefer container ground slot ratio

V_4 : number of reefer container ground slots (TEU)

G_y : area of the ground slot (m^2)

i_1 : floor area per 1 TEU dry container (m^2)

i_2 : floor area per 1 TEU reefer container (m^2)

B : area of the marshaling area (m^2)

j : marshaling area coefficient

The width of the marshaling area L_{b2} can be calculated by **equation (1.4.9)** from the area of the marshaling area.

$$L_{b2} = B/L_a \tag{1.4.9}$$

where

B : area of the marshaling area (m^2)

L_a : length of the berth (m)

② It is preferable to set specific coefficients on the basis of the characteristics of the target container terminal. Refer to **Figs. 1.4.5**[3)] and **1.4.6**,[3)] which show the track record value in domestic container terminals, when performing the setting operation. References 1) and 4) show the following values for each coefficient:

D_t = 2 to 7 days (export)[3)];

D_t = 3 to 9 days (import)[3)]

f = 1.2 to 1.3[1)];

g_1: transfer crane = four to five stacks[3)];
straddle carrier = three to four stacks[3)];
reach stacker = two to three stacks[3)];
(Applicable to small-scale terminals with few annual handling volume and a water depth at berth of less than 13 m)

g_2: transfer crane 0.6 to 0.8[3)];
straddle carrier and reach stacker 0.65 to 0.8[3)];

h = 0.05 to 0.20[3)];

i_1 = (8 feet × 20 feet =) 14.9 m^2 [1)];

i_2 = 19.5 m^2 (set from the track record of domestic ports)[1)];

j = 2.0 to 4.0[3)].

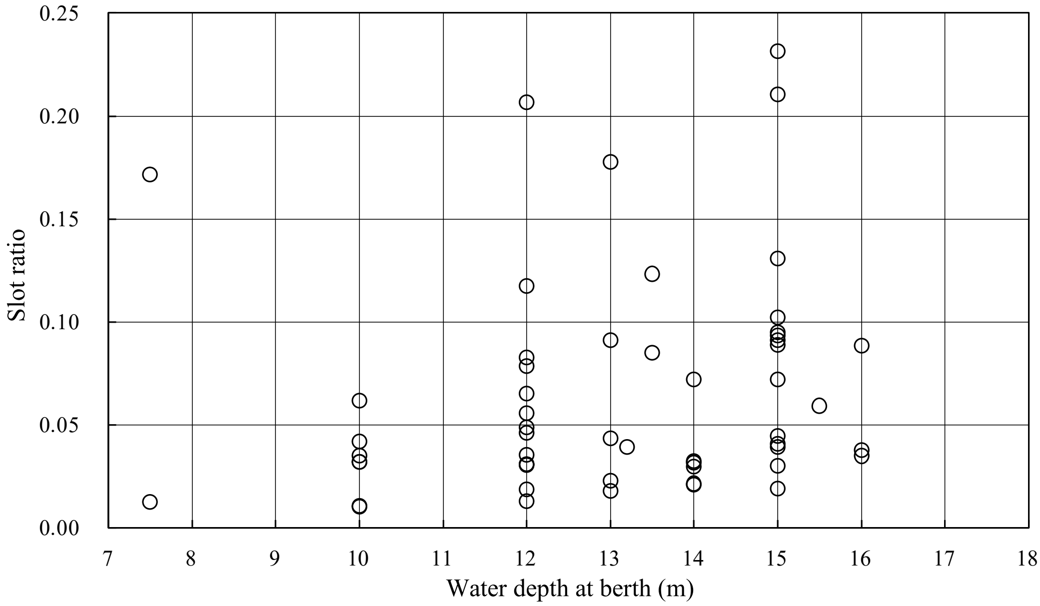

Fig. 1.4.5 Reefer Container Ground Slot Ratio (*h*)[3)]

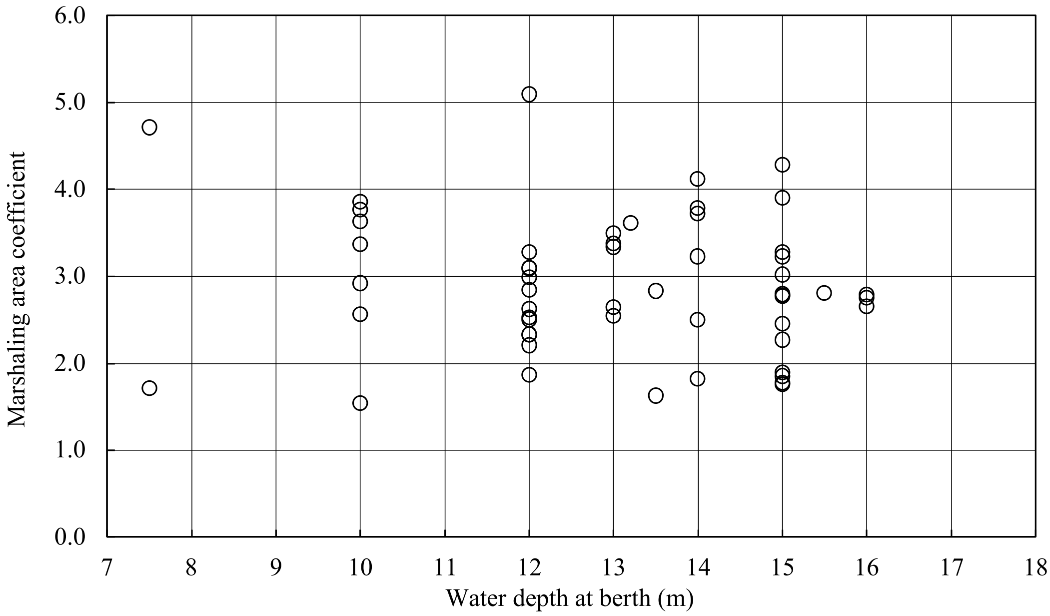

Fig. 1.4.6 Marshaling Area Coefficient (*j*)[3)]

③ **Reference values concerning the coefficient setting**

Given that it is not easy to set e, f, g_1, and g_2 separately, $f/(eg_1g_2)$, which unifies these, can generally be set as one coefficient.

It is preferable to set specific coefficient values on the basis of the characteristics of the target container terminal. Refer to **Fig. 1.4.7**,[3)] which shows the track record value in domestic container terminals, when performing setting operation. Reference 3) shows that $f/(eg_1g_2)$ = 0.005 to 0.020.

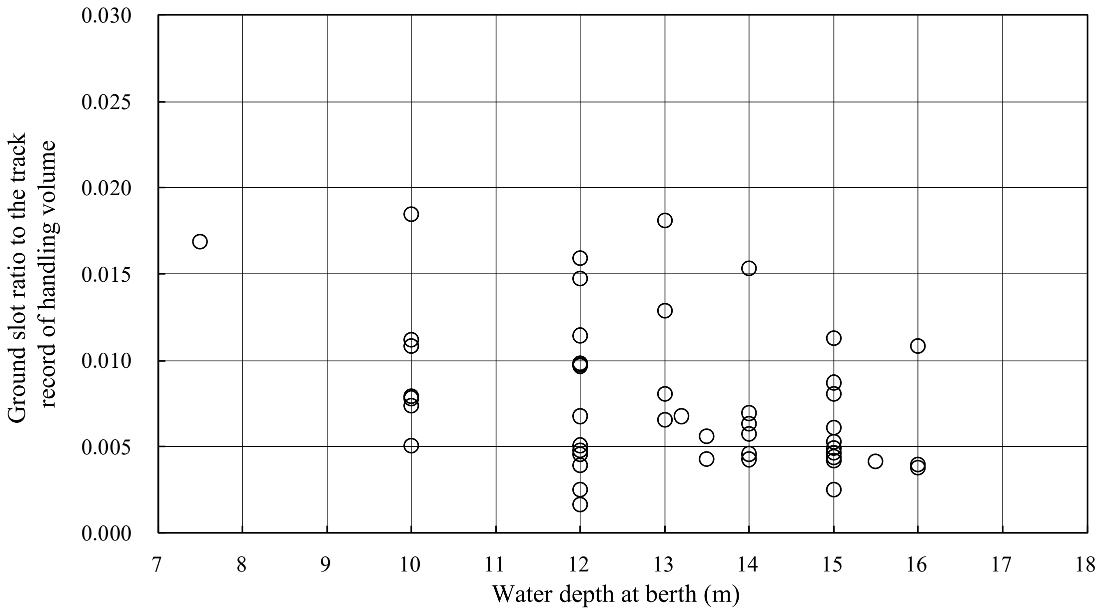

Fig. 1.4.7 Ground Slot Ratio (f/eg_1g_2) to the Track Record of Handling Volume[3)]

④ **Reference value concerning marshaling area**

The values that can be referred to when setting the marshaling area are shown below:

(a) Number of ground slots (V_2)

Fig. 1.4.8,[3)] which shows the track record value in domestic container terminals, may be referred to when setting the number of ground slots (V_2). Reference 3) shows the following values as the number of ground slots:

V_2 = 1,500 to 2,500 TEU (water depth at berth: less than 15 m);

V_2 = 1,500 to 3,000 TEU (water depth at berth: 15 m or more).

The following value can be referred to for a small-scale terminal:

V_2 = 500 to 1,500 TEU (small-scale terminal).

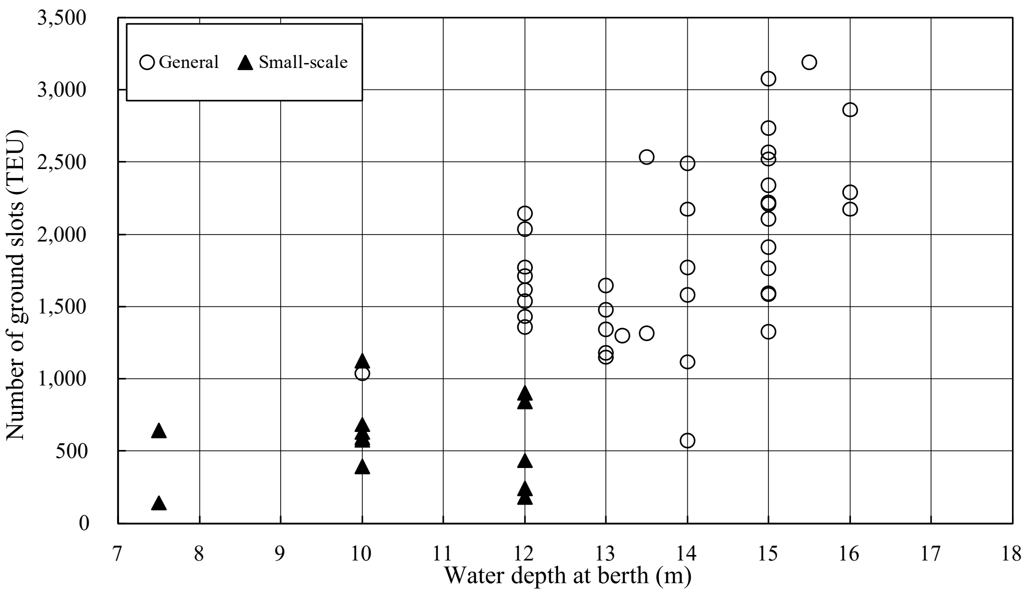

Fig. 1.4.8 Number of Ground Slots (V_2)[3)]

(b) Area of the marshaling area (*B*)

Fig. 1.4.9,[3] which shows the track record value in domestic container terminals, may be referred to when setting the area of the marshaling area *B*. Reference 3) shows the following values as the area of the marshaling area:

B = 40,000 to 100,000 m^2 (water depth at berth: less than 15 m);

B = 70,000 to 120,000 m^2 (water depth at berth: 15 m or more).

The following value can be referred to for a small-scale terminal:

B = 20,000 to 40,000 m^2 (small-scale terminal).

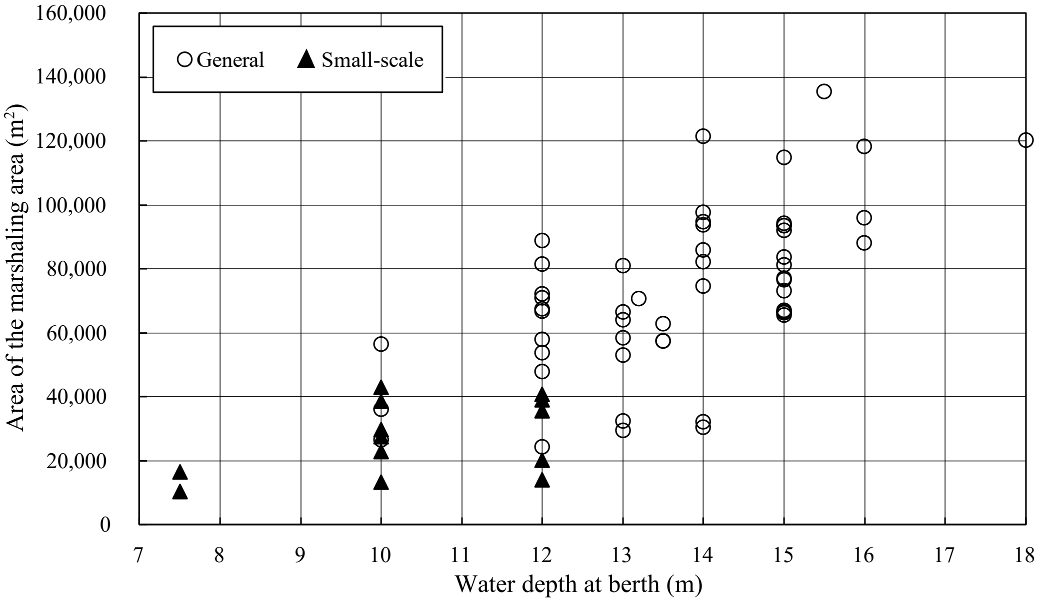

Fig. 1.4.9 Area of the Marshaling Area (*B*)[3]

⑤ Standard value for marshaling area width L_{b2}

The marshaling area width L_{b2}, excluding various conditions concerning the marshaling area, can be set by referring to **Fig. 1.4.10**,[3] which shows the track record value in domestic container terminals. **Reference 3)** shows the following value as the standard value for the width of the marshaling area:

L_{b2} = 150 to 350 m (general terminal).

The following value can be referred to for a small-scale terminal:

L_{b2} = 100 to 200 m (small-scale terminal).

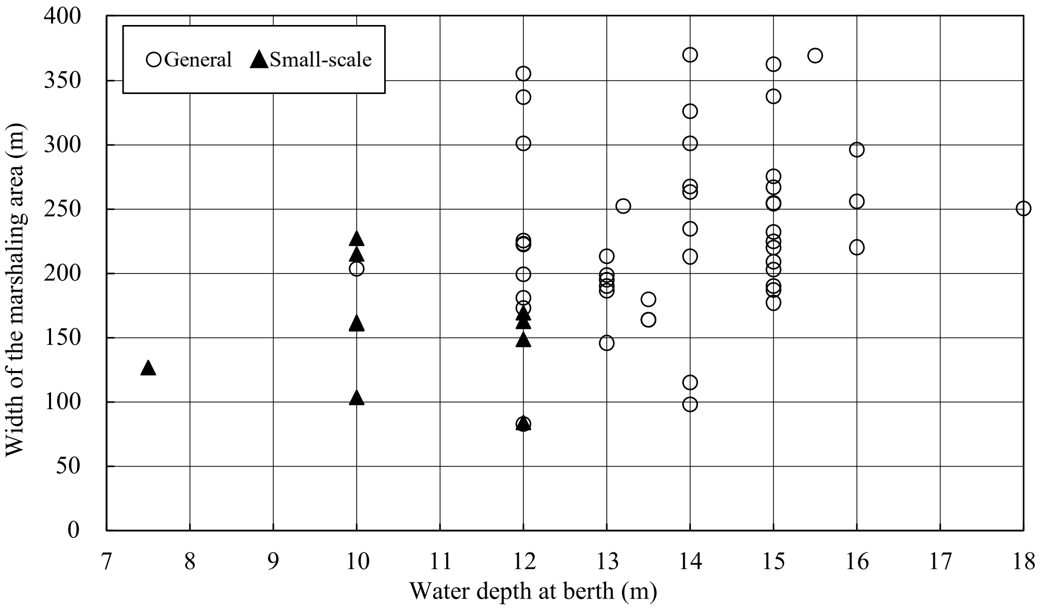

Fig. 1.4.10 Width of the Marshaling Area (L_{b2})[3)]

(7) Backyard Area

① The area of the backyard area can generally be calculated by the following:

$$C = B_y k \tag{1.4.10}$$

where

B_y : area of the backyard area facilities (floor area of CFS, maintenance shop, administration building, gate and others built in the backyard) (m^2)

k : backyard area coefficient

The width of the backyard area L_{b3} can be calculated by **equation (1.4.11)** from the area of the backyard area.

$$L_{b3} = C / L_a \tag{1.4.11}$$

where

C : area of the backyard area (m^2)

L_a : length of the berth

② It is preferable to set specific coefficients on the basis of the characteristics of the target container terminal. Refernces 1) and 2) show the following values for the area of the backyard area facilities B_y.

(a) Area of the backyard area facilities (B_y):

B_y = 7,500 m^2 (area of the marshaling area: less than 90,000 m^2);

B_y = 9,000 m^2 (area of the marshaling area: 90,000 m^2 or more);

B_y = 0.05B + 4,000 m^2 (when area of the marshaling area B is significantly larger than 90,000 m^2).

The following values can be referred to concerning the area of the area in each facility B_y[3) 4)]:

CFS: width (30 to 60 m) × length (100 to 180 m);

Maintenance shop: 800 to 1,000 m^2;

Administration building: 1,000 to 2,000 m^2;

Gate: 300 to 1,500 m^2.

(b) Backyard area coefficient (k):

k = 4.0 to 5.0[1).]

③ **Standard value for the area of the backyard area C**

The area of the backyard area C, excluding various conditions concerning the backyard area, can be set by referring to **Fig. 1.4.11**,[3)] which shows the track record value in domestic container terminals. Literature 3) shows the following values as a standard value for the area of the backyard area:

C = 10,000 to 20,000 m^2 (water depth at berth: less than 13 m);

C = 10,000 to 60,000 m^2 (water depth at berth: 13 m or more).

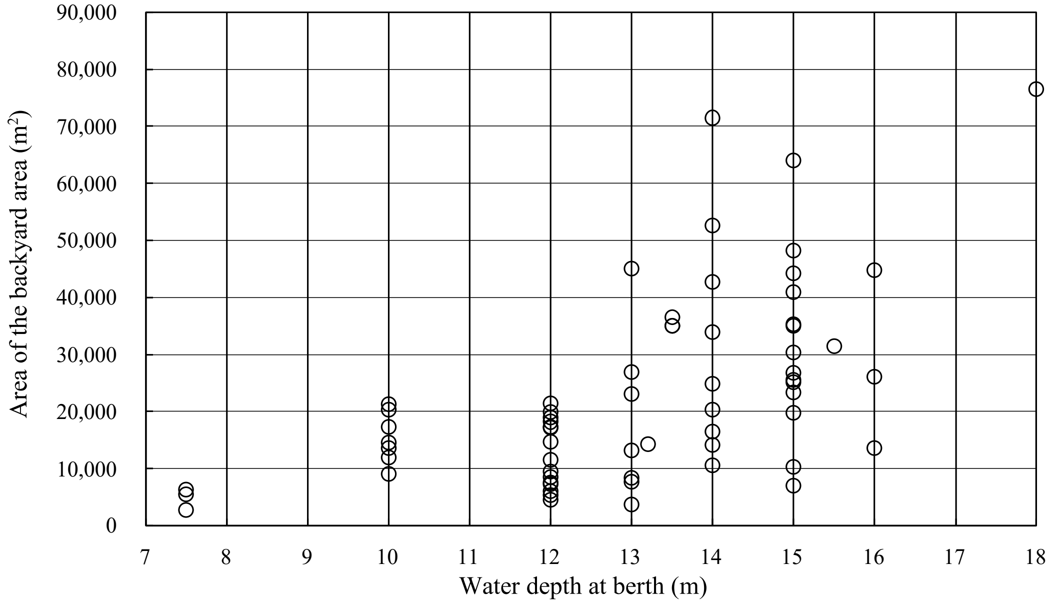

Fig. 1.4.11 Area of the Backyard Area (C)[3)]

④ **Standard value for the width of the backyard area L_{b3}**

The width of the backyard area L_{b3}, excluding various conditions concerning the backyard area, can be set by referring to **Fig. 1.4.12**,[3)] which shows the track record value in domestic container terminals. **Reference 3)** shows L_{b3} = 90 to 150 m as a standard value for the width of the backyard area.

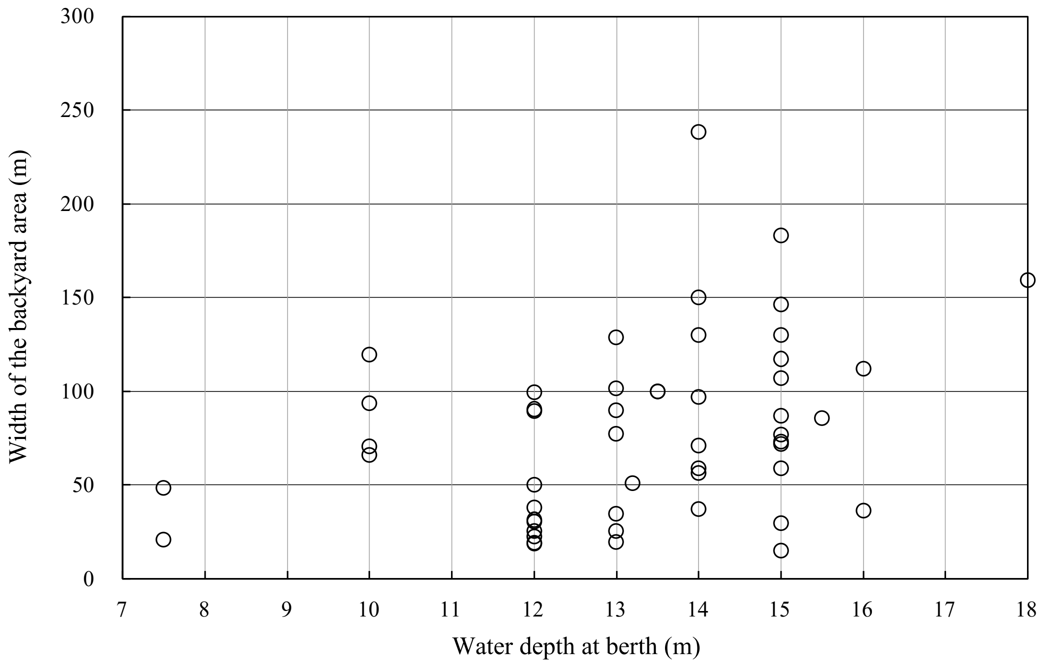

Fig. 1.4.12 Width of the Backyard Area (L_{b3})[3)]

(8) Width of the Container Terminal Area

① The width of the container terminal area L_b can be calculated by the following:

$$L_b = L_{b1} + L_{b2} + L_{b3} \tag{1.4.12}$$

where

L_{b1} : width of the apron area

L_{b2} : width of the marshaling area

L_{b3} : width of the backyard area

② **Standard value for the width of the container terminal area L_b**

The width of the container terminal area L_b, excluding various conditions concerning the container terminal area, can be set by referring to **Fig. 1.4.13**,[3)] which shows the track record value in domestic container terminals. **References 2)** and **3)** show the following values as a standard value for the width of the container terminal area corresponding to the water depth at berth:

L_b = 300 to 600 m (general terminal: water depth at berth: 16 m or less);

L_b = 400 to 700 m (water depth at berth: more than 16 m).

The following value can be referred to for a small-scale terminal:

L_b = 200 to 400 m (small-scale terminal).

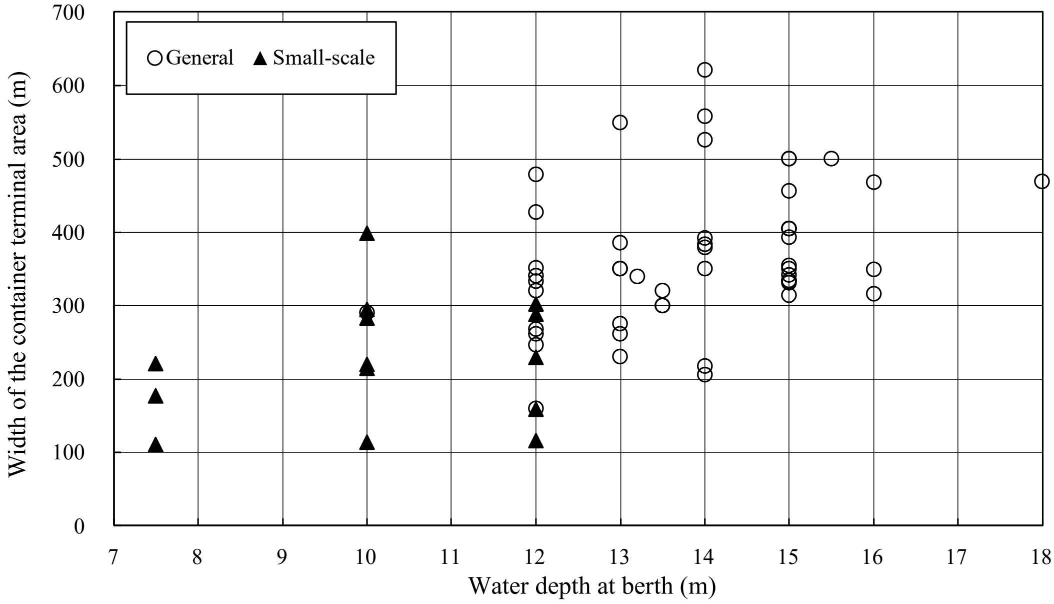

Fig. 1.4.13 Width of the Terminal Area ($L_β$)[3)]

[References]

1) Hironao Takahashi "A Model for estimating Scales of Container Terminal Areas at the Stage of Port and Harbor Planning- A Standard for Designing Principal Sizes in Container Terminals:A Proposal -",Research Report of NILIM No.10 June 2003

2) Yasuhiro Akakura "Dimension of Mega Container Ship and Berth Dimension / Container Terminal Area Compatible", Research Report of NILIM No.45 March 2011

3) Shoichi Emoto, Soichi Yamagata "An Analysis of the Container Terminal Areas",Technical Note of NILIM No.992 October 2017

4) "Report of Container Terminal Equipments Planning", Ports and Harbours Bureau, Ministry of Transport, Japan and OCDI, 1993

2 Cruise Wharves

(English translation of this section from Japanese version is currently being prepared.)

2.1 Purpose, Functions and Definition of Cruise Wharves

(English translation of this section from Japanese version is currently being prepared.)

2.2 Functions and Characteristics of Main Facilities as Constituent Parts of a Cruise Wharf

(English translation of this section from Japanese version is currently being prepared.)

2.3 Basic Concept of Required Performance

(English translation of this section from Japanese version is currently being prepared.)

2.4 Important Points to Consider in Determining the Layout and Sizes of Facilities as Constituent Parts of a Cruise Wharf

(English translation of this section from Japanese version is currently being prepared.)

2.5 Points to Consider for Improving Existing Facilities for Use with Cruise Ships

(English translation of this section from Japanese version is currently being prepared.)

2.5.1 General

(English translation of this section from Japanese version is currently being prepared.)

2.5.2 Points to Consider for Improving Mooring Facilities

(English translation of this section from Japanese version is currently being prepared.)

2.5.3 Other Facilities

(English translation of this section from Japanese version is currently being prepared.)

3 Ferry Wharves

(English translation of this section from Japanese version is currently being prepared.)

3.1 Purpose, Functions and Definition of Ferry Wharves

(English translation of this section from Japanese version is currently being prepared.)

3.2 Functions and Characteristics of Facilities Subject to the Technical Standards and Main Facilities as Constituent Parts of a Ferry Wharf

(English translation of this section from Japanese version is currently being prepared.)

3.3 Basic Concept of Required Performance and Other Requirements

(English translation of this section from Japanese version is currently being prepared.)

3.4 Important Points to Consider in Determining the Layout and Sizes of Facilities as Constituent Parts of a Ferry Wharf

(English translation of this section from Japanese version is currently being prepared.)

4 Marinas

(English translation of this section from Japanese version is currently being prepared.)

4.1 General Information about Marinas

(English translation of this section from Japanese version is currently being prepared.)

4.2 Basic Concept of Required Performance and Other Requirements for Various Facilities of Marinas

(English translation of this section from Japanese version is currently being prepared.)

4.3 Important Points to Consider in Determining the Layout and Sizes of Facilities as Constituent Parts of a Marina

(English translation of this section from Japanese version is currently being prepared.)

4.4 Design, Construction and Maintenance of Marinas and Required Considerations

(English translation of this section from Japanese version is currently being prepared.)

4.5 Countermeasures to be Taken at Marinas against Disasters

(English translation of this section from Japanese version is currently being prepared.)

5 Facilities for Very Large Crude Oil Carriers

(English translation of this section from Japanese version is currently being prepared.)

5.1 General Rules

(English translation of this section from Japanese version is currently being prepared.)

5.1.1 Scope of Application

(English translation of this section from Japanese version is currently being prepared.)

5.1.2 Definition

(English translation of this section from Japanese version is currently being prepared.)

5.2 Selection of Locations and Planning of Facilities

(English translation of this section from Japanese version is currently being prepared.)

5.2.1 Selection of Locations

(English translation of this section from Japanese version is currently being prepared.)

5.2.2 Face Lines of Berths

(English translation of this section from Japanese version is currently being prepared.)

5.2.3 Axes, Widths and Depths of Navigation Channels

(English translation of this section from Japanese version is currently being prepared.)

5.2.4 Areas of Basins

(English translation of this section from Japanese version is currently being prepared.)

5.3 Determination of Sizes

(English translation of this section from Japanese version is currently being prepared.)

5.4 Structural Types

(English translation of this section from Japanese version is currently being prepared.)

5.5 Basic Design Policies

(English translation of this section from Japanese version is currently being prepared.)

5.6 Design of External Forces and Loads

(English translation of this section from Japanese version is currently being prepared.)

5.6.1 Types of External Forces and Loads

(English translation of this section from Japanese version is currently being prepared.)

5.6.2 Berthing Forces of Ships

(English translation of this section from Japanese version is currently being prepared.)

5.6.3 Actions by Moored Ships

(English translation of this section from Japanese version is currently being prepared.)

5.6.4 Wind Pressure

(English translation of this section from Japanese version is currently being prepared.)

5.6.5 Wave Force

(English translation of this section from Japanese version is currently being prepared.)

5.6.6 Current Force

(English translation of this section from Japanese version is currently being prepared.)

5.6.7 Seismic Force

(English translation of this section from Japanese version is currently being prepared.)

5.6.8 Earth Pressure and Water Pressure

(English translation of this section from Japanese version is currently being prepared.)

5.6.9 Self-weight and Load

(English translation of this section from Japanese version is currently being prepared.)

5.7 Design of Stationary Mooring Facilities

(English translation of this section from Japanese version is currently being prepared.)

5.7.1 General

(English translation of this section from Japanese version is currently being prepared.)

5.7.2 Layout and Crown Height of a Dolphin

(English translation of this section from Japanese version is currently being prepared.)

5.7.3 External Force and Load Acting on a Dolphin

(English translation of this section from Japanese version is currently being prepared.)

5.7.4 External Force and Load acting on a Pier-type Mooring Facility

(English translation of this section from Japanese version is currently being prepared.)

5.7.5 Design of Piles

(English translation of this section from Japanese version is currently being prepared.)

5.7.6 Design of Jackets, Steel Sheet Piles and Caissons

(English translation of this section from Japanese version is currently being prepared.)

5.7.7 Fender Equipments

(English translation of this section from Japanese version is currently being prepared.)

5.7.8 Mooring Ship Facilities

(English translation of this section from Japanese version is currently being prepared.)

5.8 Design of Floating Mooring Facilities

(English translation of this section from Japanese version is currently being prepared.)

5.8.1 Design Procedures

(English translation of this section from Japanese version is currently being prepared.)

5.8.2 External Force and Load Acting on Floating Mooring Facilities

(English translation of this section from Japanese version is currently being prepared.)

5.8.3 Buoy Stabilization

(English translation of this section from Japanese version is currently being prepared.)

5.8.4 Design of Mooring Anchors and Sinkers

(English translation of this section from Japanese version is currently being prepared.)

5.8.5 Design of Anchor Chains

(English translation of this section from Japanese version is currently being prepared.)

5.8.6 Fender Equipments

(English translation of this section from Japanese version is currently being prepared.)

5.9 Design of Sorting Facilities

(English translation of this section from Japanese version is currently being prepared.)

5.9.1 Loading Arms

(English translation of this section from Japanese version is currently being prepared.)

5.9.2 Design of Rubber Hoses

(English translation of this section from Japanese version is currently being prepared.)

5.9.3 Oil Pipes

(English translation of this section from Japanese version is currently being prepared.)

5.10 Design of Major Ancillary Facilities

(English translation of this section from Japanese version is currently being prepared.)

5.10.1 Fire Extinguisher Facilities

(English translation of this section from Japanese version is currently being prepared.)

5.10.2 Leaked Oil Treatment Facilities

(English translation of this section from Japanese version is currently being prepared.)

5.10.3 Stagnant Oil Removal and Replacement Equipments

(English translation of this section from Japanese version is currently being prepared.)

6 Submarine Pipelines

(English translation of this section from Japanese version is currently being prepared.)

6.1 General Rules

(English translation of this section from Japanese version is currently being prepared.)

6.1.1 Scope of Application

(English translation of this section from Japanese version is currently being prepared.)

6.1.2 Definition

(English translation of this section from Japanese version is currently being prepared.)

6.2 Selection of Routes

(English translation of this section from Japanese version is currently being prepared.)

6.3 Basic Design Policies

(English translation of this section from Japanese version is currently being prepared.)

6.4 Design External Forces and Loads

(English translation of this section from Japanese version is currently being prepared.)

6.4.1 Types of External Forces and Loads

(English translation of this section from Japanese version is currently being prepared.)

6.4.2 Wind Pressure

(English translation of this section from Japanese version is currently being prepared.)

6.4.3 Wave Force and Current Force

(English translation of this section from Japanese version is currently being prepared.)

6.4.4 Seismic Force

(English translation of this section from Japanese version is currently being prepared.)

6.4.5 Earth Pressure

(English translation of this section from Japanese version is currently being prepared.)

6.4.6 Water Pressure

(English translation of this section from Japanese version is currently being prepared.)

6.4.7 Self-weight and Surcharge

(English translation of this section from Japanese version is currently being prepared.)

6.4.8 Internal Pressure

(English translation of this section from Japanese version is currently being prepared.)

6.4.9 Impact Load Caused by Anchoring

(English translation of this section from Japanese version is currently being prepared.)

6.4.10 Effects of Vibration

(English translation of this section from Japanese version is currently being prepared.)

6.4.11 Effects of Temperature Change

(English translation of this section from Japanese version is currently being prepared.)

6.4.12 Load during Laying Operation

(English translation of this section from Japanese version is currently being prepared.)

6.5 Materials

(English translation of this section from Japanese version is currently being prepared.)

6.6 Design of Pipes

(English translation of this section from Japanese version is currently being prepared.)

6.6.1 Minimum Wall Thicknesses of Pipes

(English translation of this section from Japanese version is currently being prepared.)

6.6.2 Allowable Stress of Pipes

(English translation of this section from Japanese version is currently being prepared.)

6.6.3 Calculation of Intensity of Stress on Pipes

(English translation of this section from Japanese version is currently being prepared.)

6.6.4 Buckling

(English translation of this section from Japanese version is currently being prepared.)

6.6.5 Design of Pipe Joints

(English translation of this section from Japanese version is currently being prepared.)

6.6.6 Design of Bends

(English translation of this section from Japanese version is currently being prepared.)

6.6.7 Design of Valves

(English translation of this section from Japanese version is currently being prepared.)

6.6.8 Design of Risers

(English translation of this section from Japanese version is currently being prepared.)

6.7 Corrosion Control

(English translation of this section from Japanese version is currently being prepared.)

6.7.1 Coating

(English translation of this section from Japanese version is currently being prepared.)

6.7.2 Cathodic Protection

(English translation of this section from Japanese version is currently being prepared.)

6.8 Laying of Pipes

(English translation of this section from Japanese version is currently being prepared.)

6.8.1 General

(English translation of this section from Japanese version is currently being prepared.)

6.8.2 Crossing of Pipes

(English translation of this section from Japanese version is currently being prepared.)

6.8.3 Horizontal Distances to Existing Pipes

(English translation of this section from Japanese version is currently being prepared.)

6.8.4 Laying Depth

(English translation of this section from Japanese version is currently being prepared.)

6.8.5 Measures for Scour Prevention

(English translation of this section from Japanese version is currently being prepared.)

6.8.6 Dredging and Backfilling

(English translation of this section from Japanese version is currently being prepared.)

6.8.7 Prevention of Flotation

(English translation of this section from Japanese version is currently being prepared.)

6.8.8 Unburied Pipes

(English translation of this section from Japanese version is currently being prepared.)

6.9 Tests and Inspections of Pipes

(English translation of this section from Japanese version is currently being prepared.)

6.9.1 Non-destructive Inspection of Welds

(English translation of this section from Japanese version is currently being prepared.)

6.9.2 Pressure Test

(English translation of this section from Japanese version is currently being prepared.)

6.9.3 Evaluation of Integrity of Existing Submarine Pipelines

(English translation of this section from Japanese version is currently being prepared.)

Chapter 3 Techniques for Planning of Port Transportation Facilities

(English translation of this section from Japanese version is currently being prepared.)

1 Setting of the Numbers of Lanes of Port Roads

(English translation of this section from Japanese version is currently being prepared.)

1.1 Methods for Estimating the Trip Generation and Attraction of Port Roads

(English translation of this section from Japanese version is currently being prepared.)

1.2 Method for Converting Traffic Volumes Related to Green Space, Marinas and Ferries into Daily Traffic Volumes

(English translation of this section from Japanese version is currently being prepared.)

1.3 Method for Adding Trip Generation and Attraction for Assumed Peak Months and Peak Days of Week to Traffic Volumes Considered in Urban or Road Planning

(English translation of this section from Japanese version is currently being prepared.)

1.4 Methods for Estimating the K-value for Estimating the Planning Hourly Traffic Volume

(English translation of this section from Japanese version is currently being prepared.)

1.5 Methods for Estimating the K-value for Determining the Numbers of Lanes of Roads

(English translation of this section from Japanese version is currently being prepared.)

Chapter 4 Diagrams for Reference in Design

1 Wave Diffraction Diagrams

(a) S_{max}=10

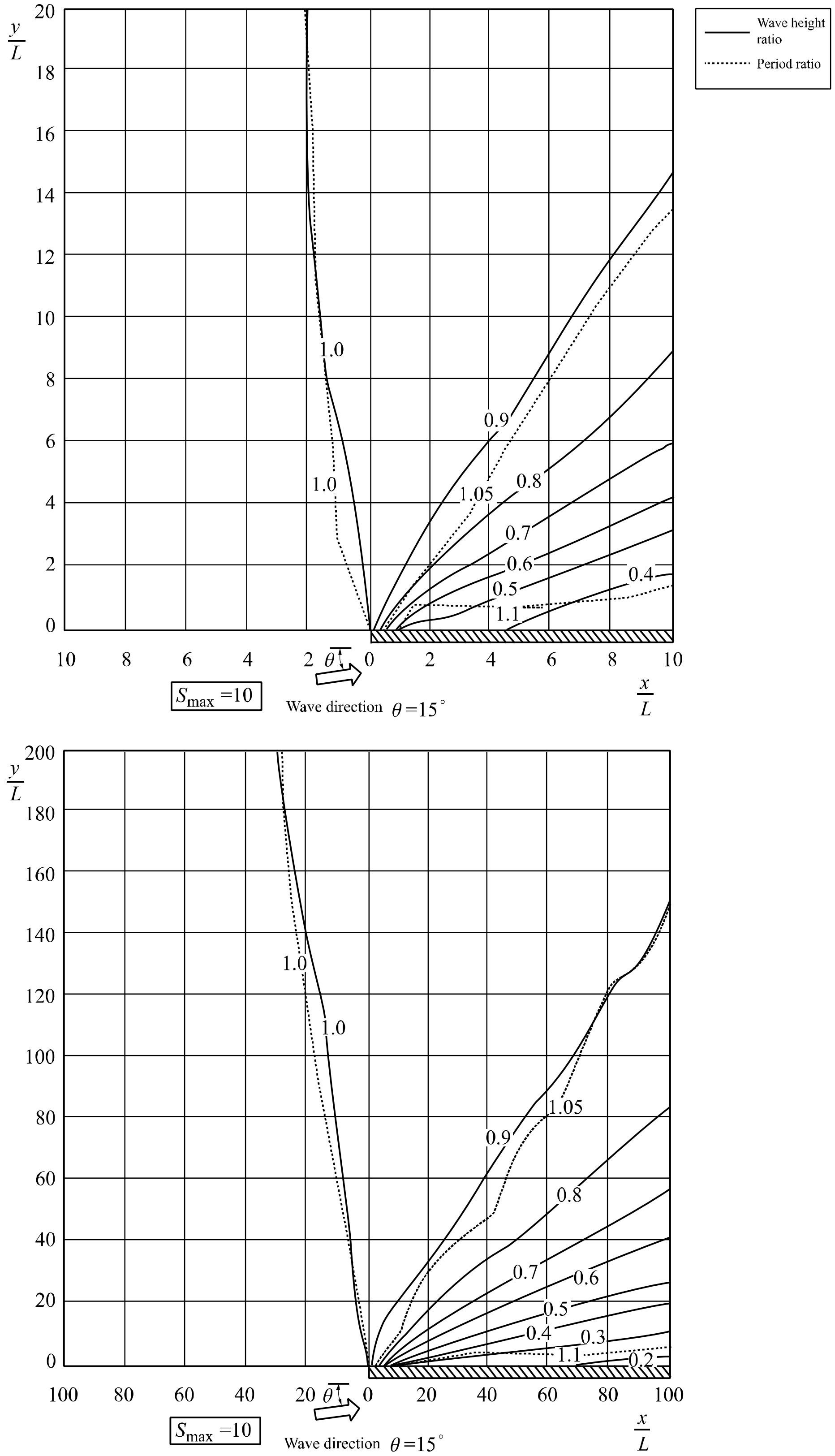

Fig. 1.1.1 (a) Diffraction Diagram for a Semi-Infinite Breakwater (θ = 15°)

(b) S_{max} =25

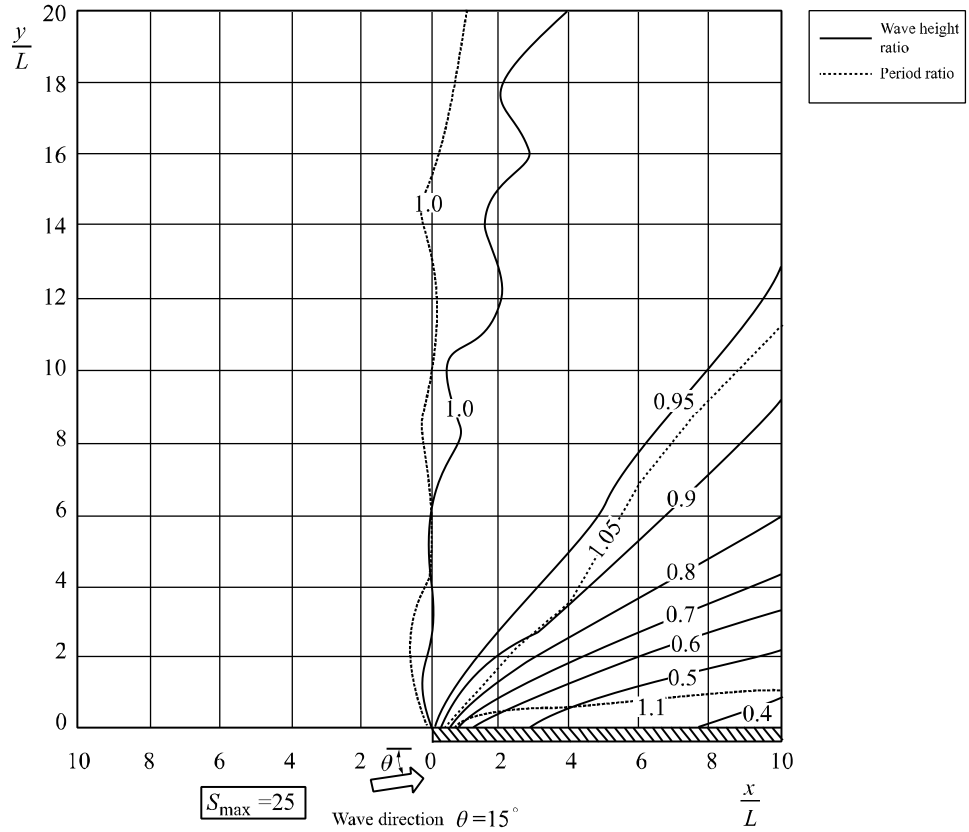

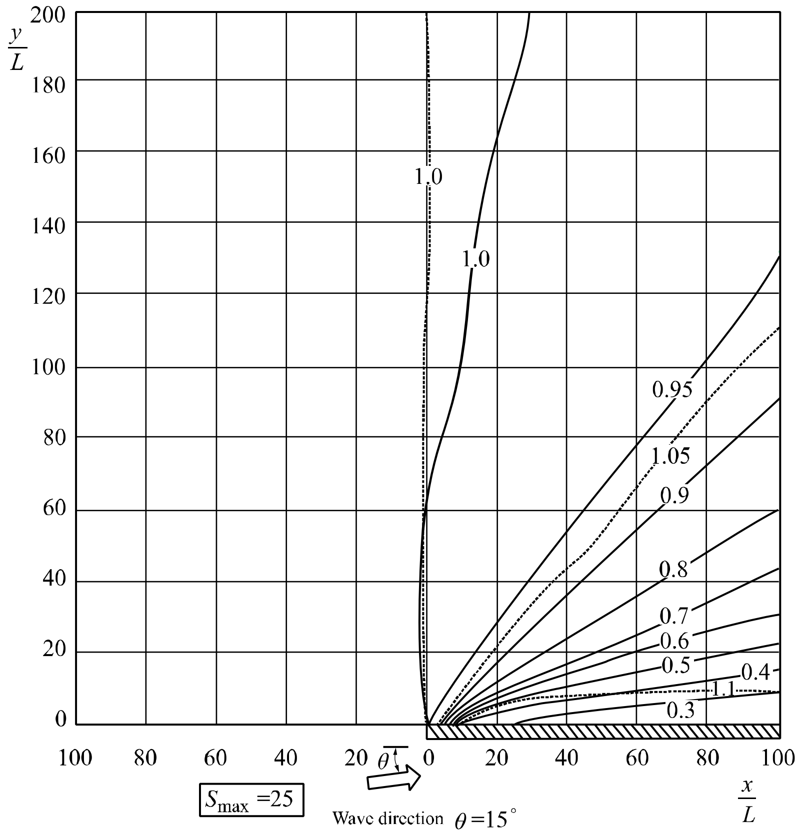

Fig. 1.1.1 (b) Diffraction Diagram for a Semi-Infinite Breakwater (θ = 15°)

(c) S_{max}=75

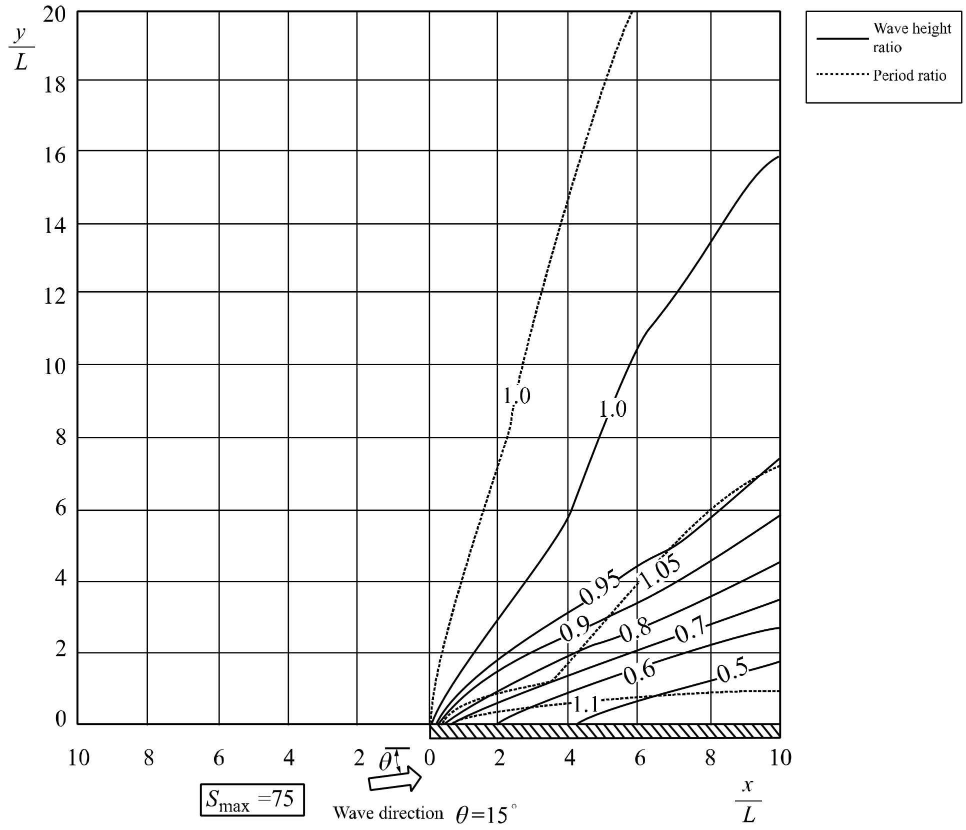

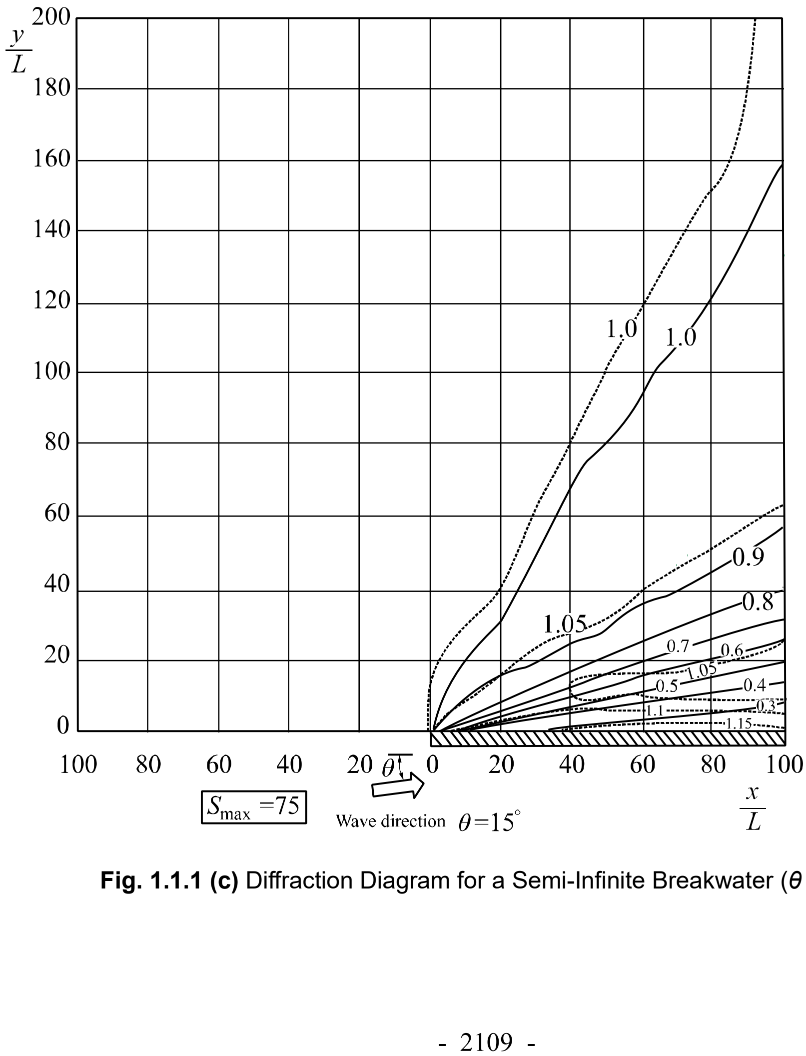

Fig. 1.1.1 (c) Diffraction Diagram for a Semi-Infinite Breakwater (θ = 15°)

(a) S_{max}=10

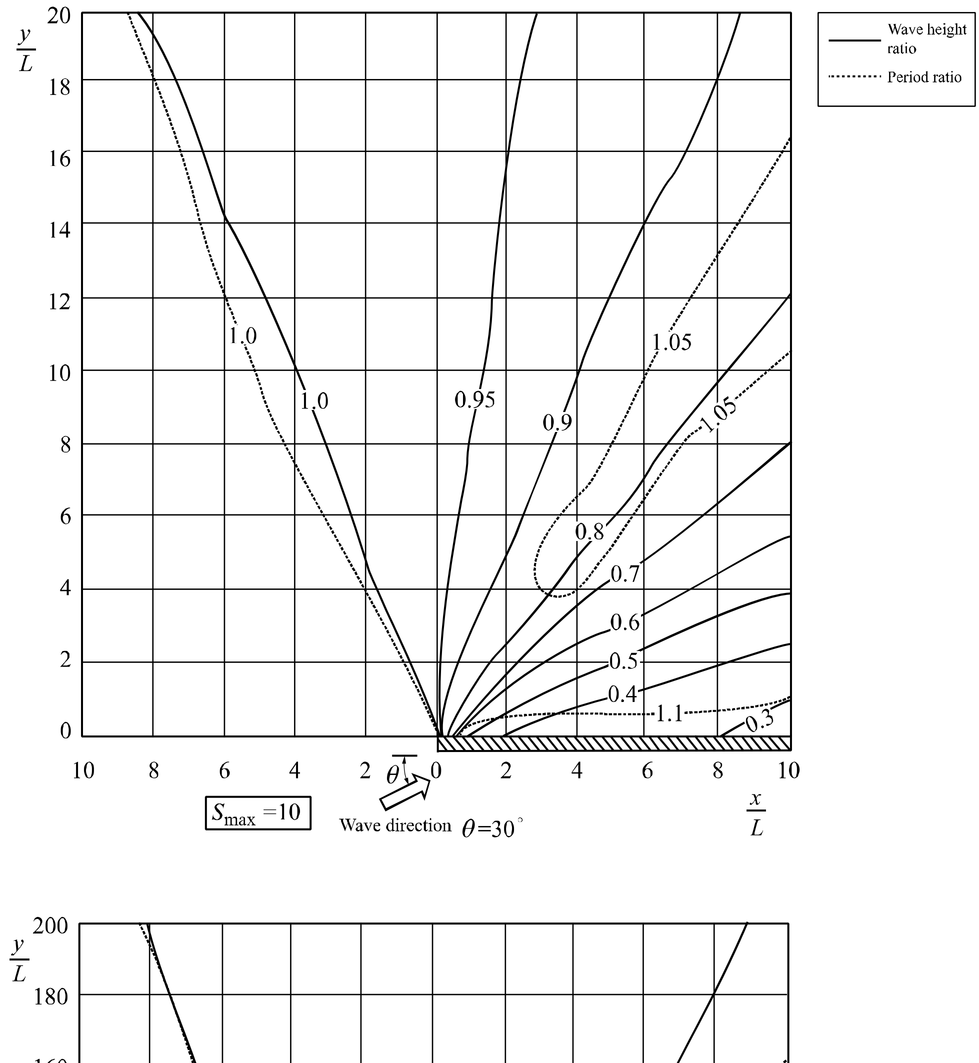

Fig. 1.1.2 (a) Diffraction Diagram for a Semi-Infinite Breakwater (θ = 30°)

(b) S_{max} =25

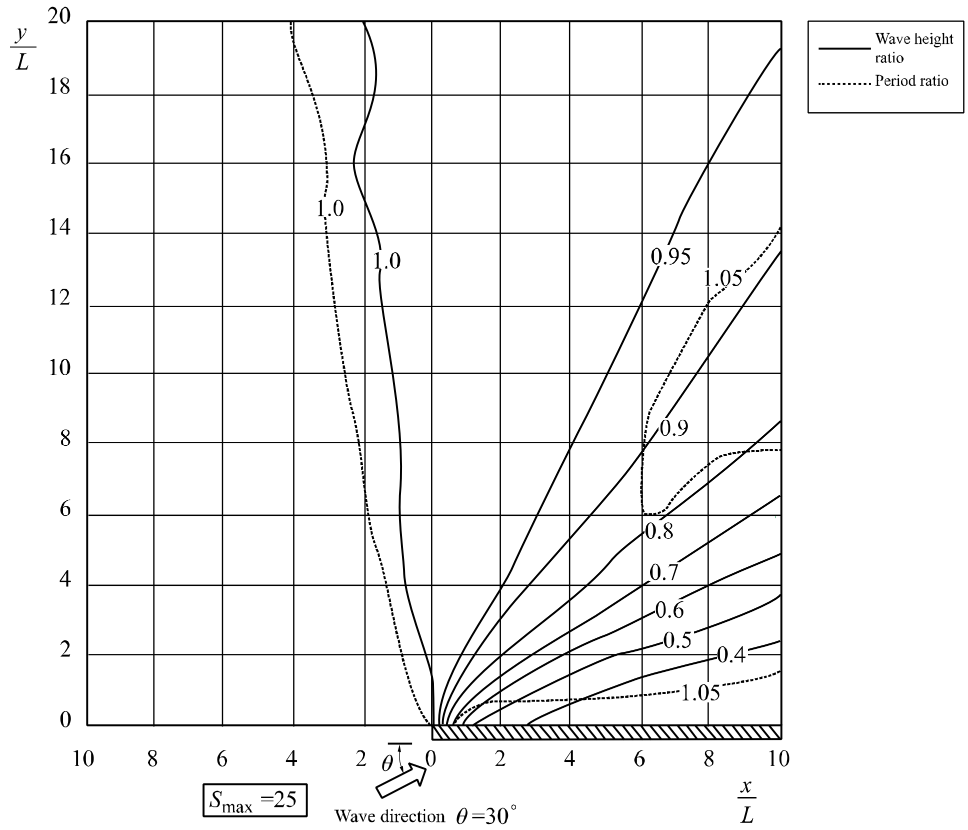

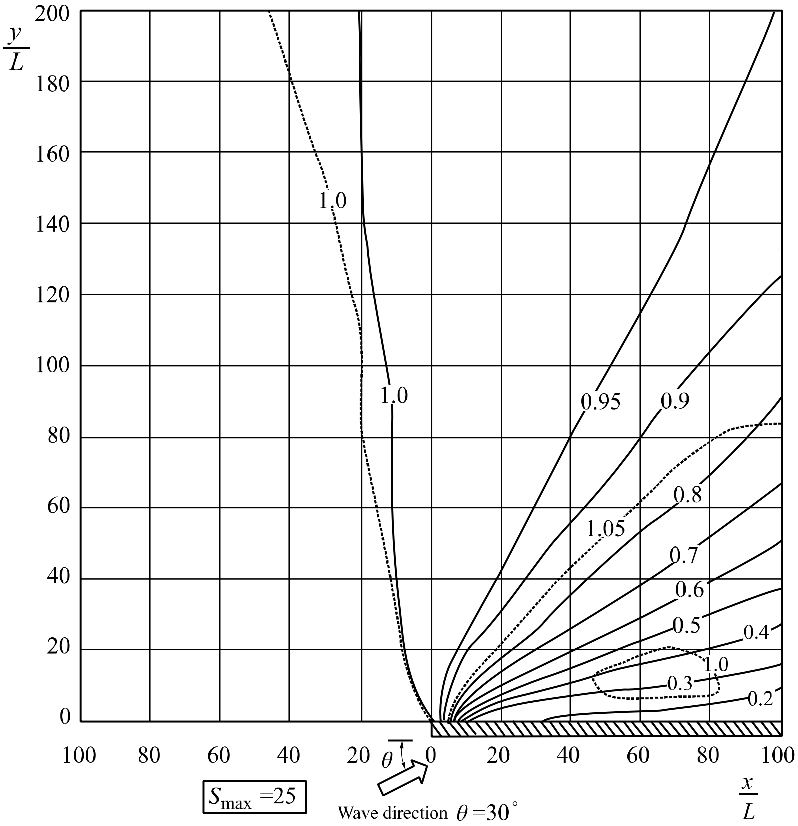

Fig. 1.1.2 (b) Diffraction Diagram for a Semi-Infinite Breakwater (θ = 30°)

(c) S_{max}=75

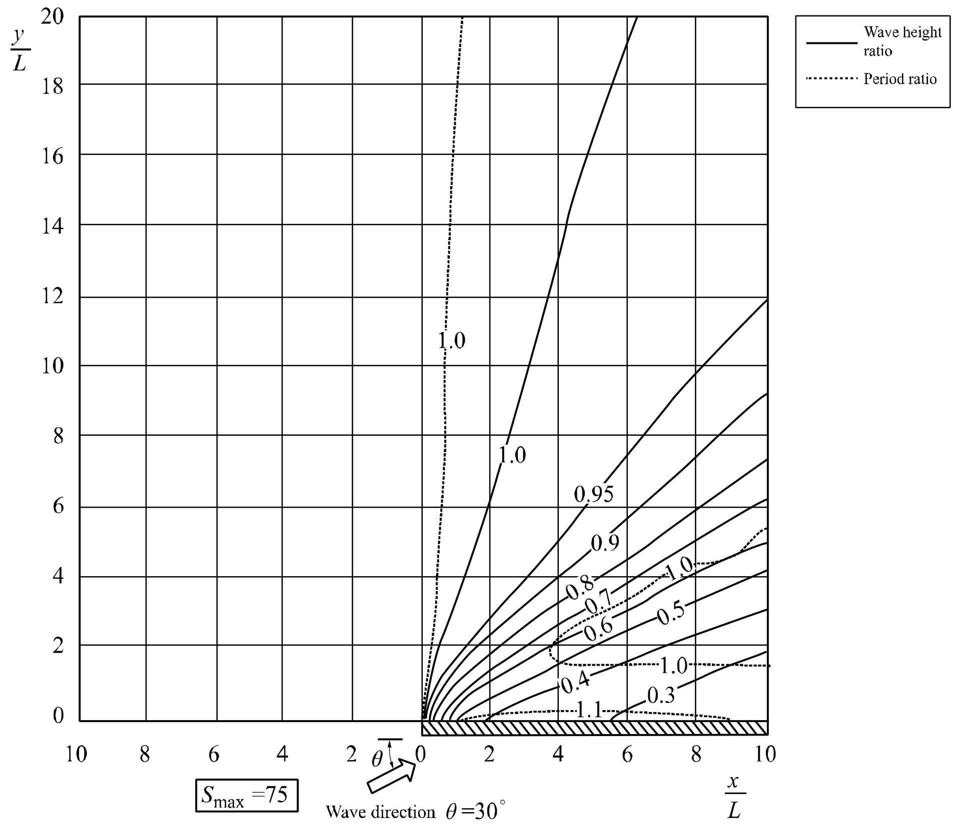

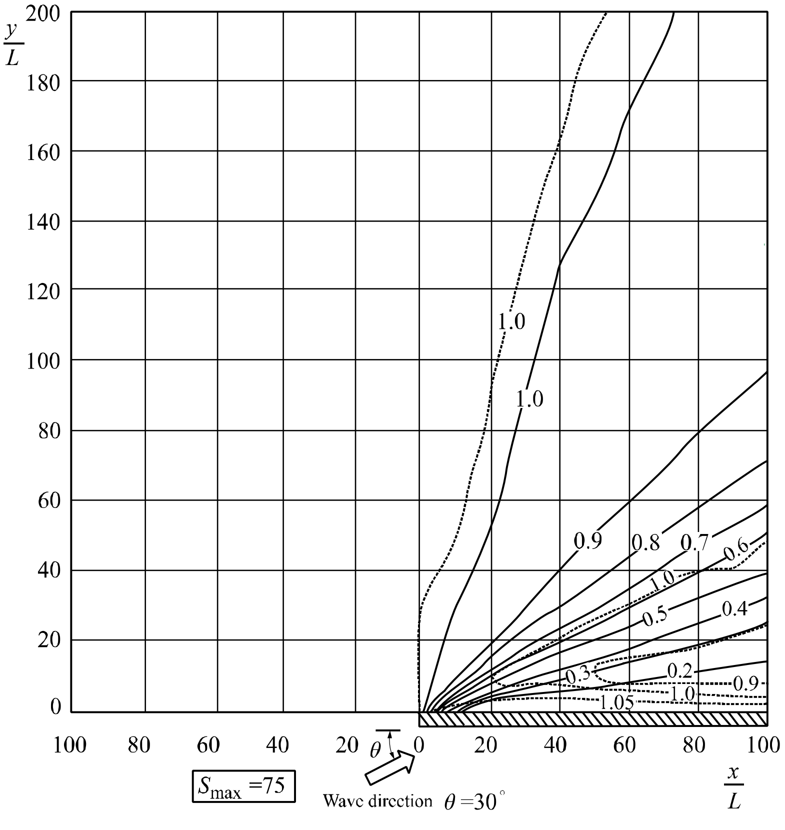

Fig. 1.1.2 (c) Diffraction Diagram for a Semi-Infinite Breakwater (θ = 30°)

(a) S_{max}=10

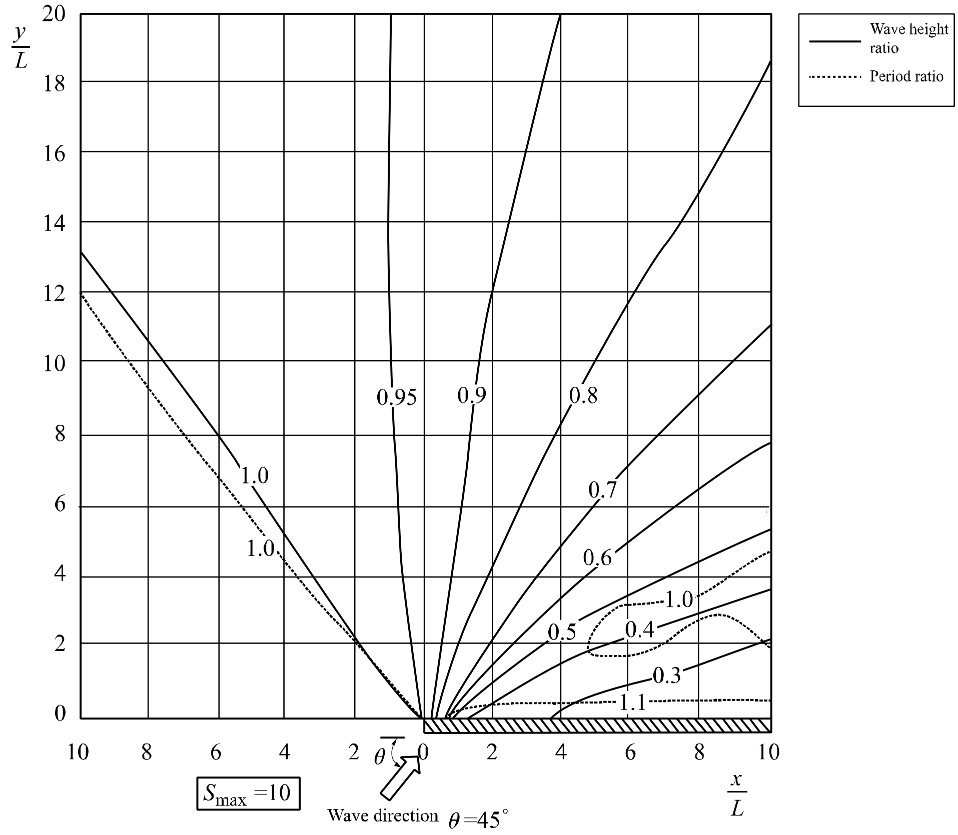

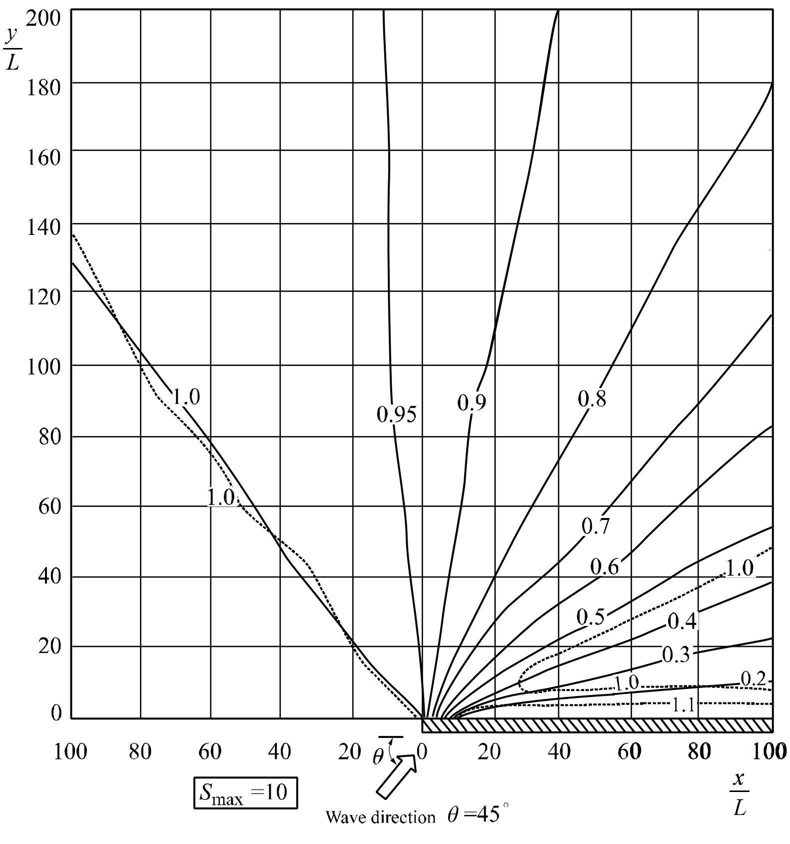

Fig. 1.1.3 (a) Diffraction Diagram for a Semi-Infinite Breakwater (θ = 45°)

(b) S_{max}=25

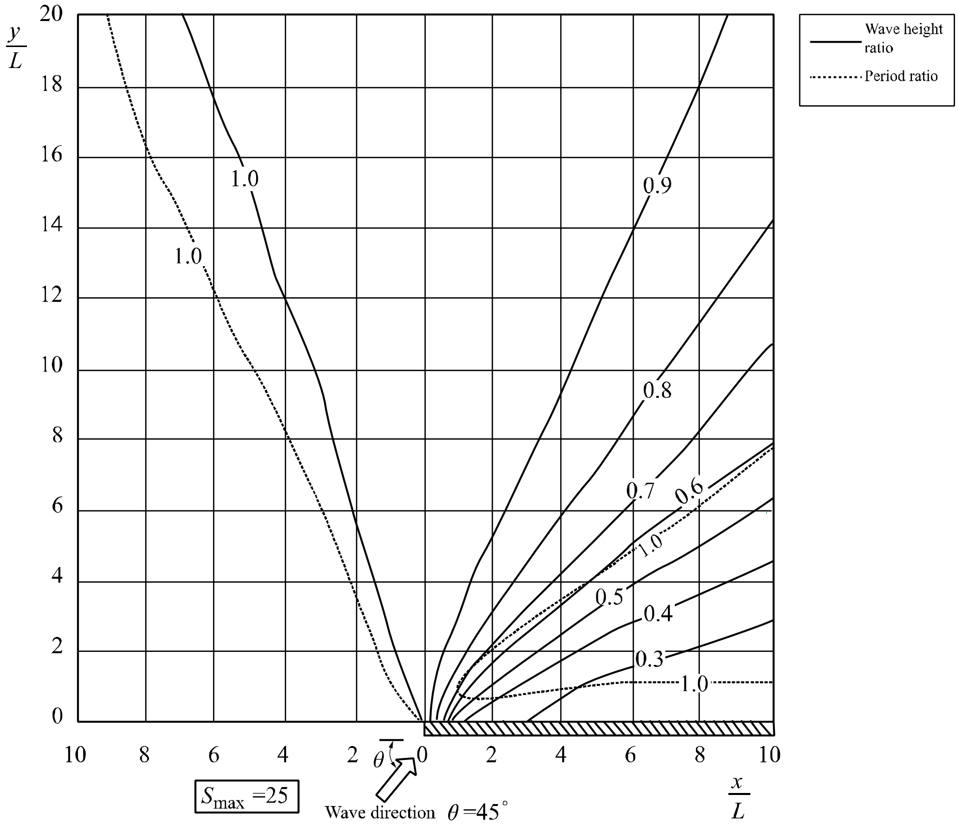

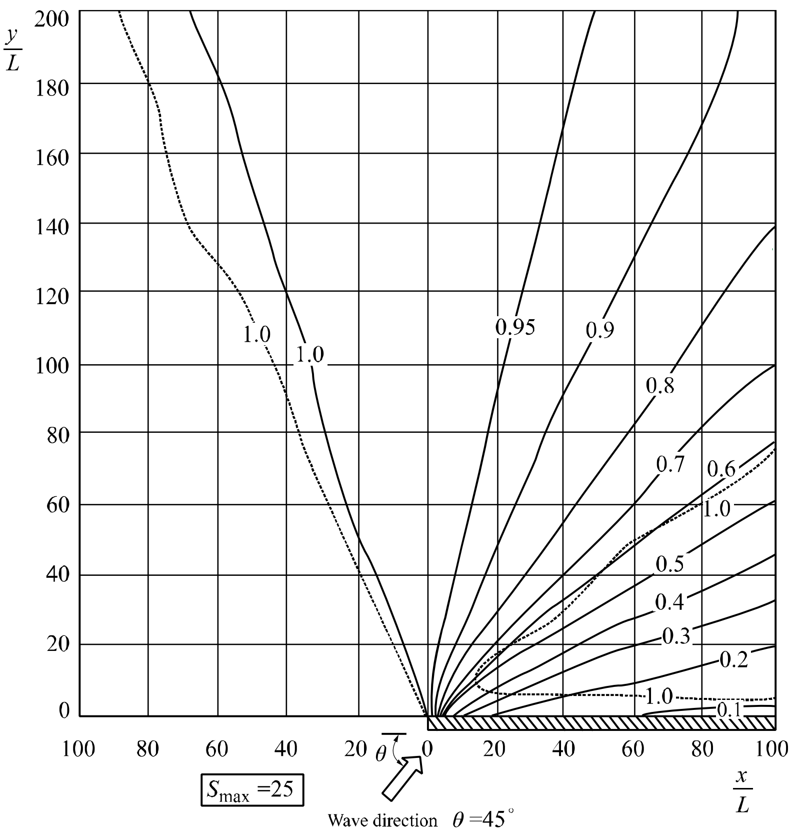

Fig. 1.1.3 (b) Diffraction Diagram for a Semi-Infinite Breakwater (θ = 45°)

(c) S_{max}=75

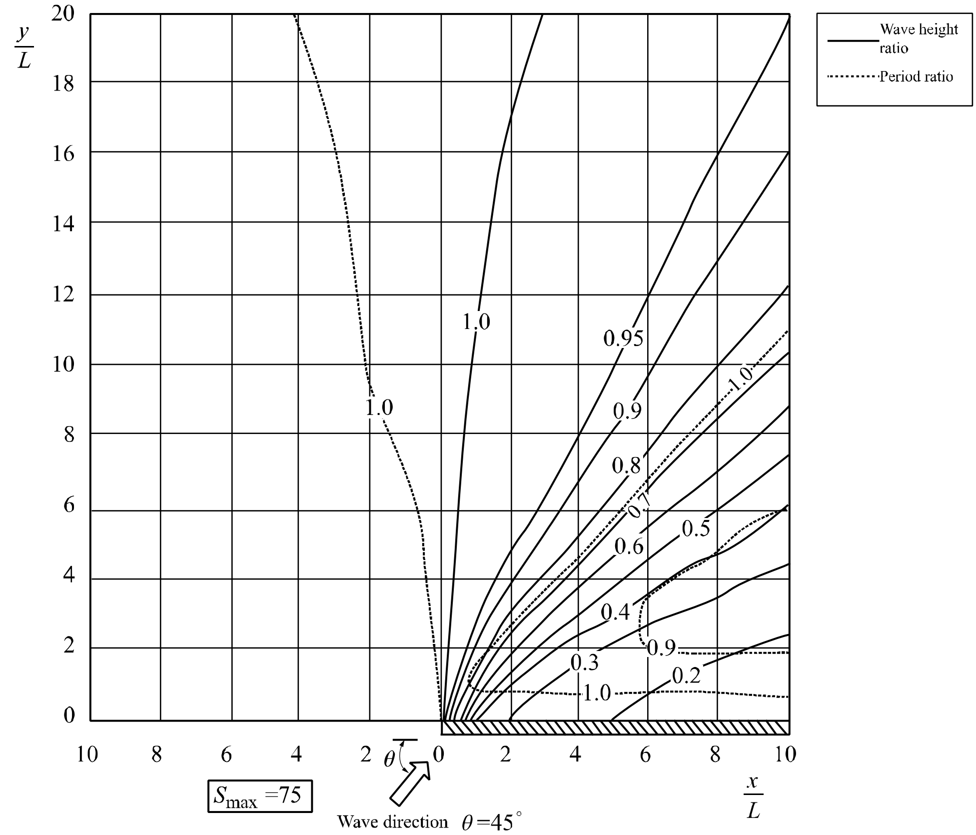

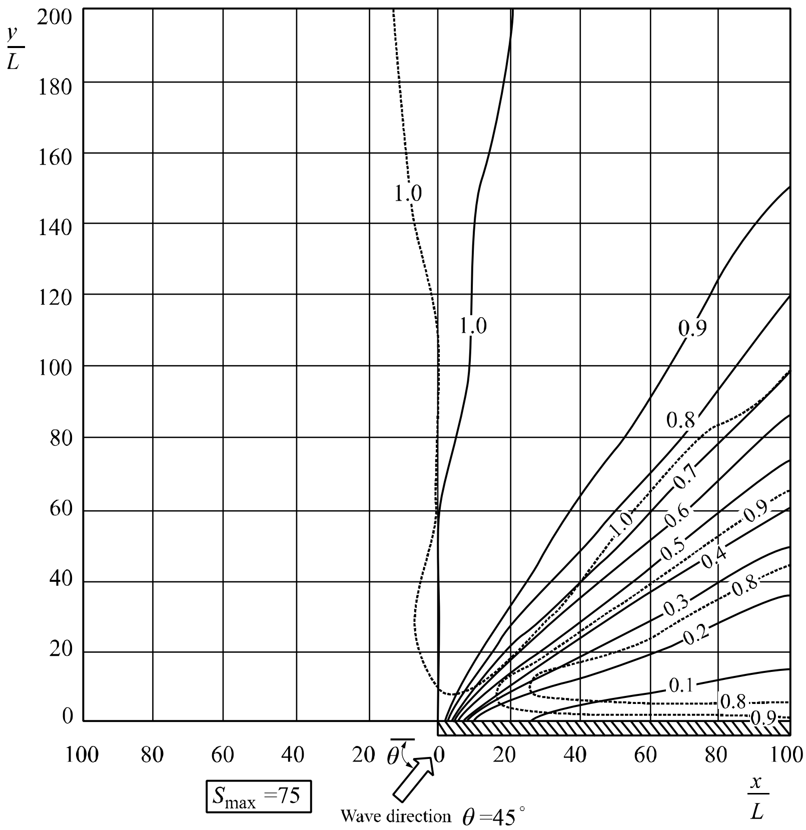

Fig. 1.1.3 (c) Diffraction Diagram for a Semi-Infinite Breakwater (θ = 45°)

(a) S_{max}=10

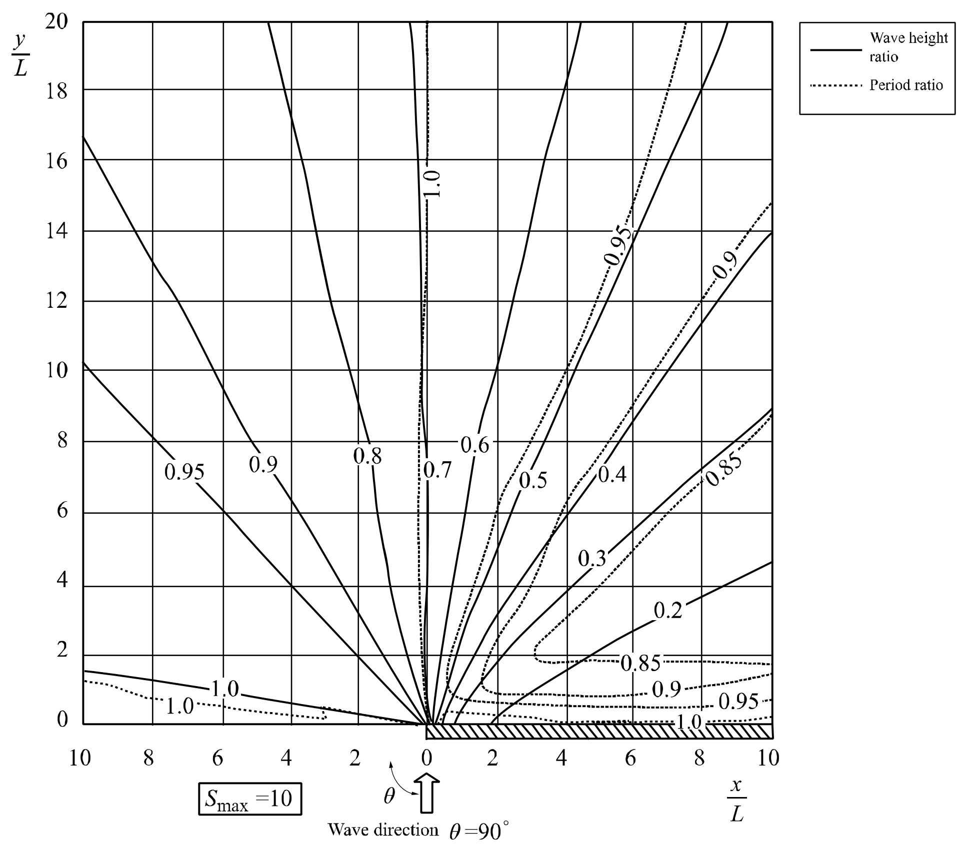

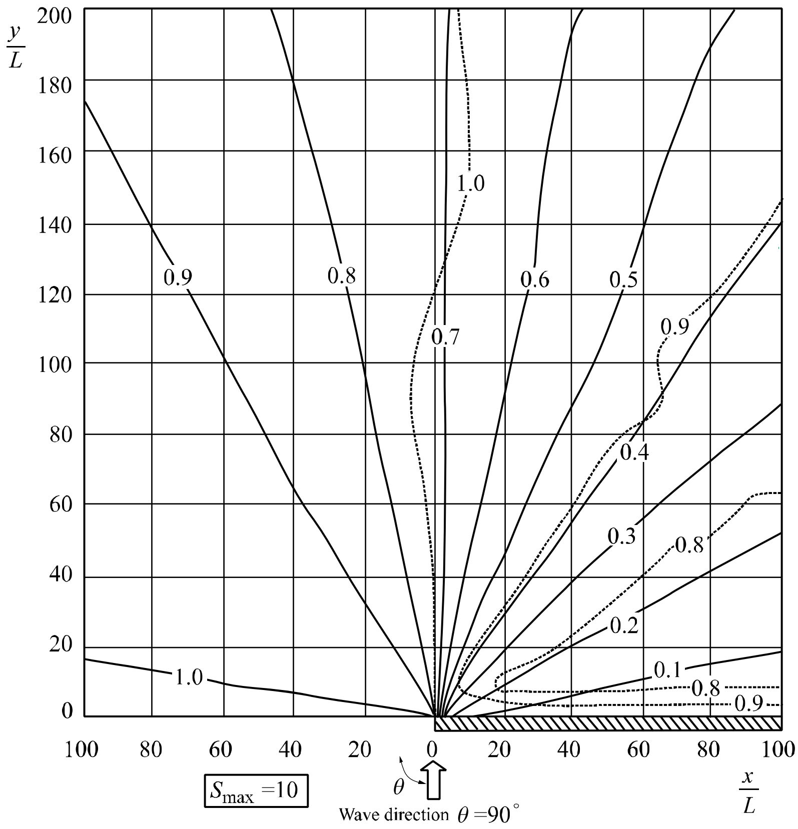

Fig. 1.1.4 (a) Diffraction Diagram for a Semi-Infinite Breakwater (θ = 90°)

(b) S_{max}=25

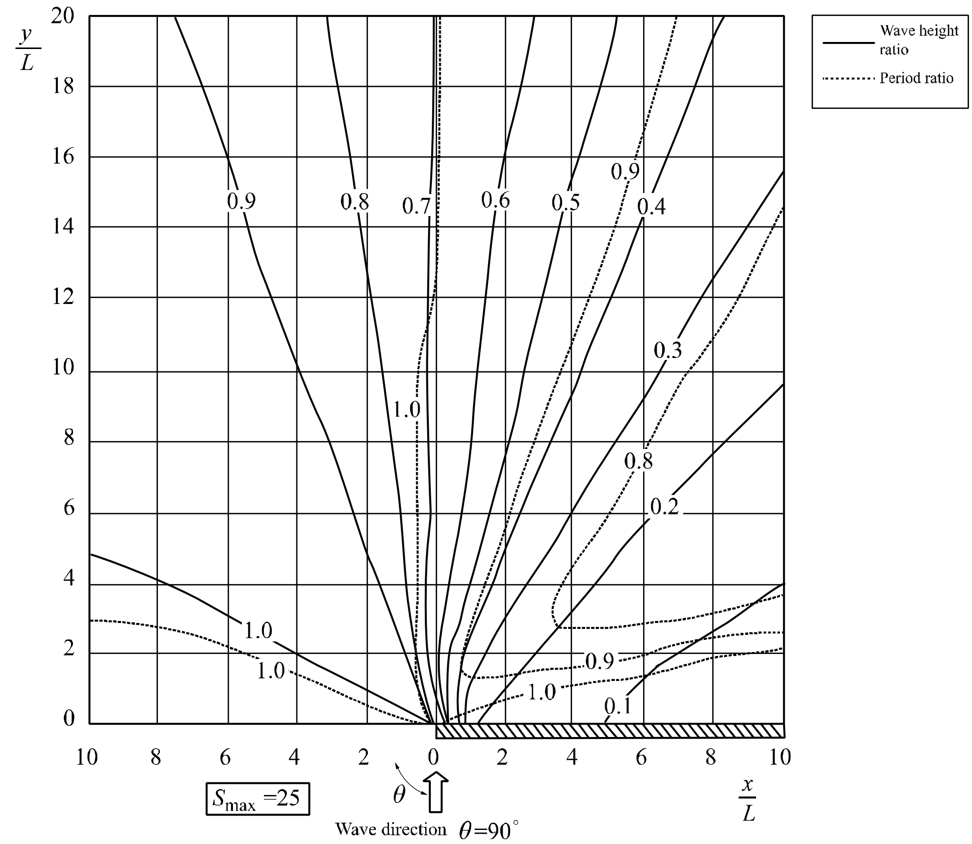

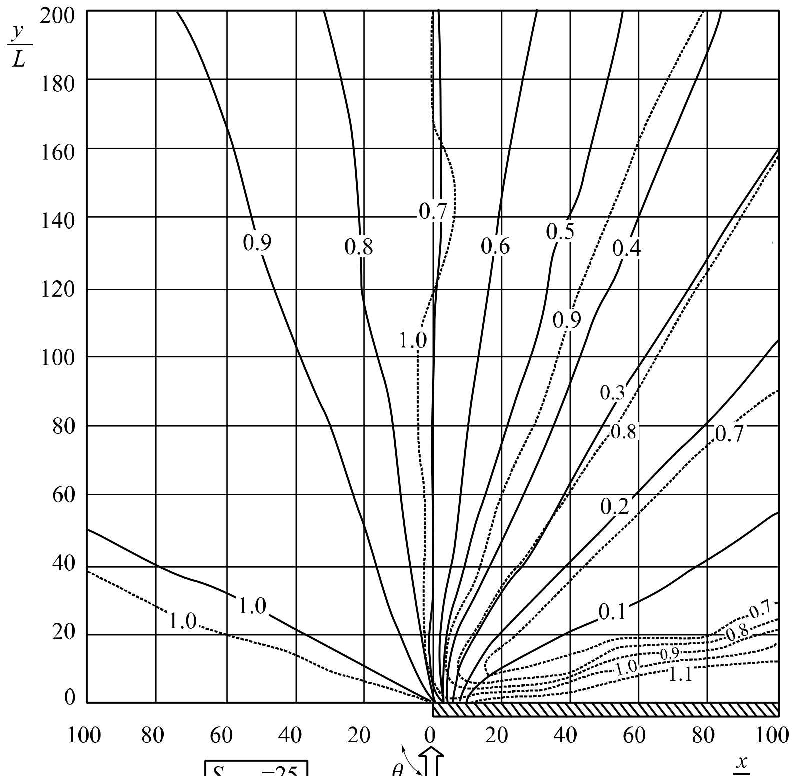

Fig. 1.1.4 (b) Diffraction Diagram for a Semi-Infinite Breakwater (θ = 90°)

(c) S_{max}=75

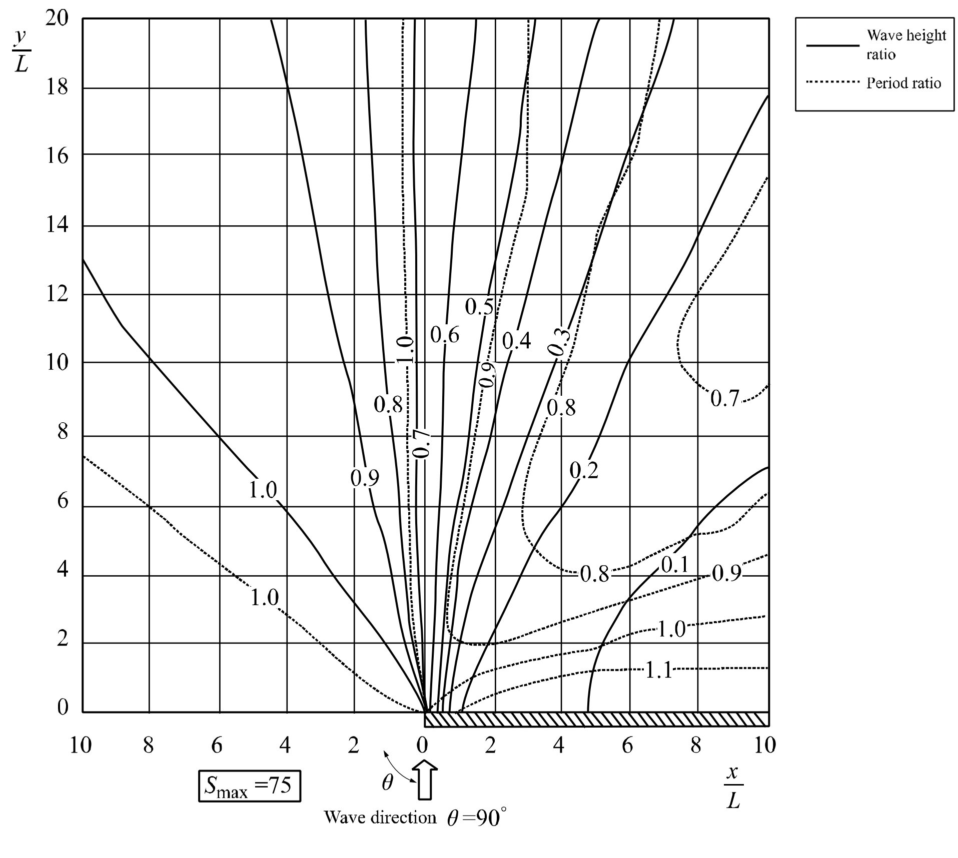

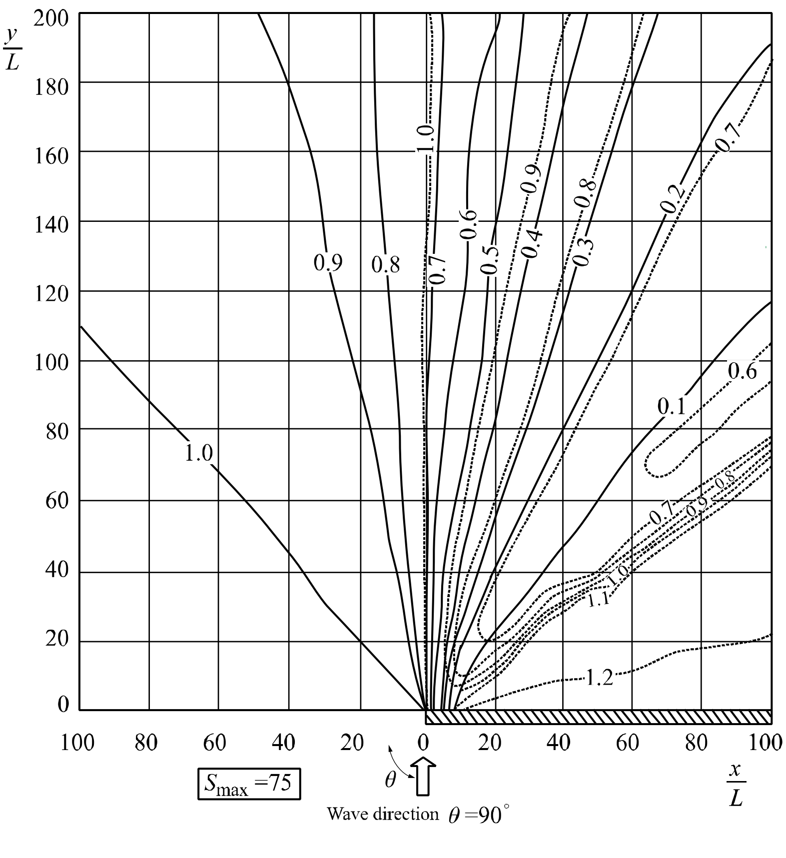

Fig. 1.1.4 (c) Diffraction Diagram for a Semi-Infinite Breakwater (θ = 90°)

(a) S_{max}=10

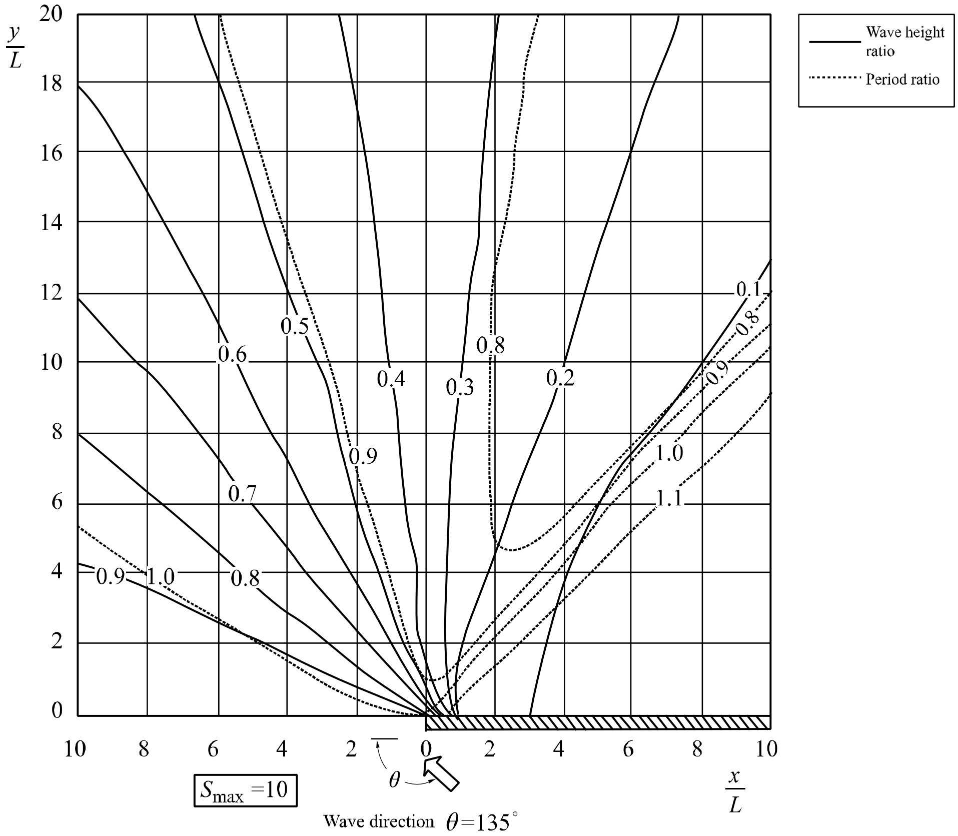

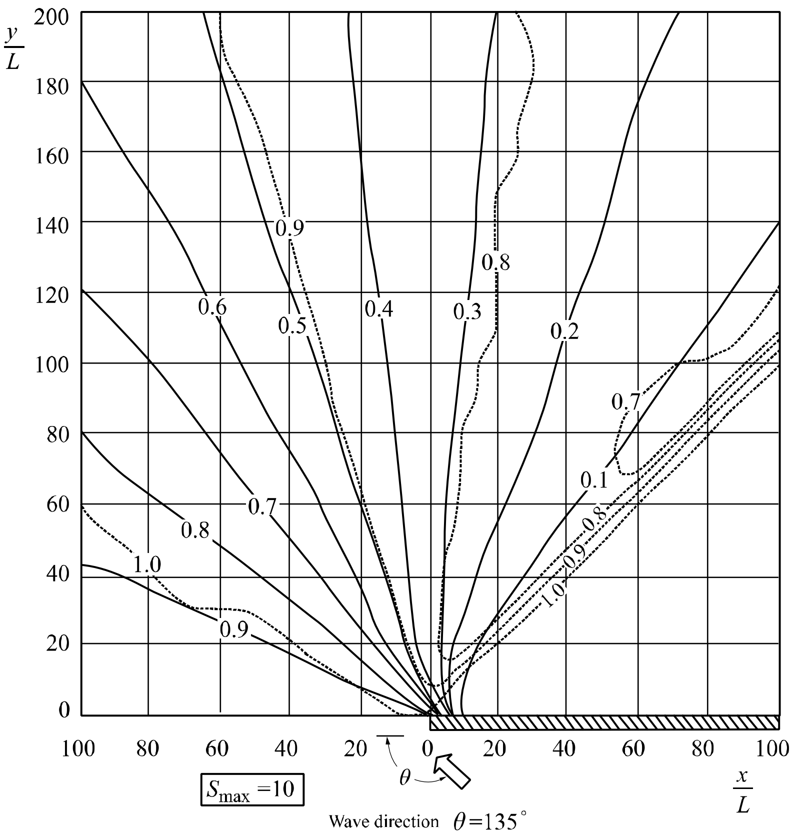

Fig. 1.1.5 (a) Diffraction Diagram for a Semi-Infinite Breakwater (θ = 135°)

(b) S_{max}=25

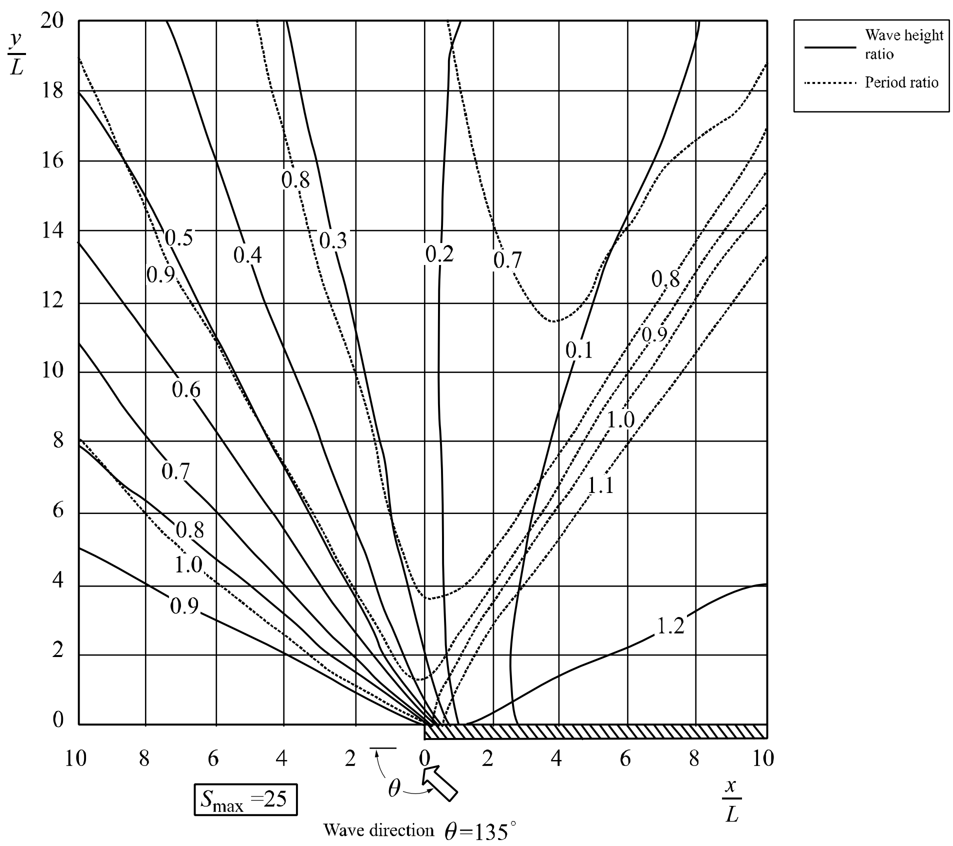

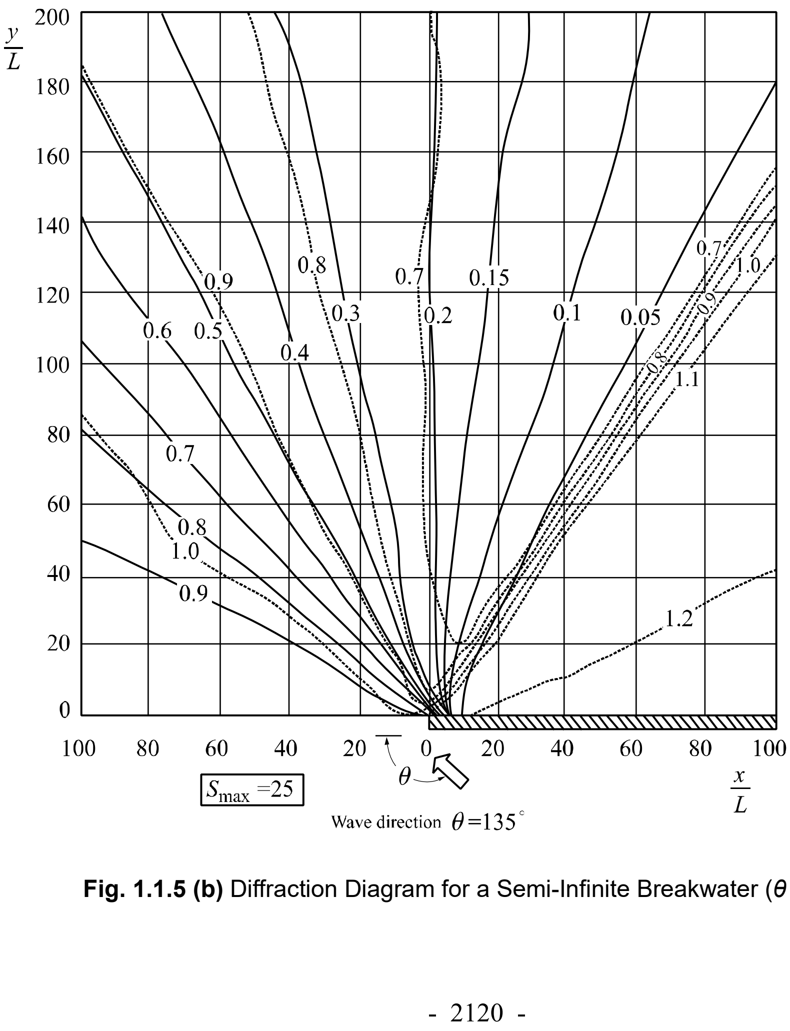

Fig. 1.1.5 (b) Diffraction Diagram for a Semi-Infinite Breakwater (θ = 135°)

(c) S_{max}=75

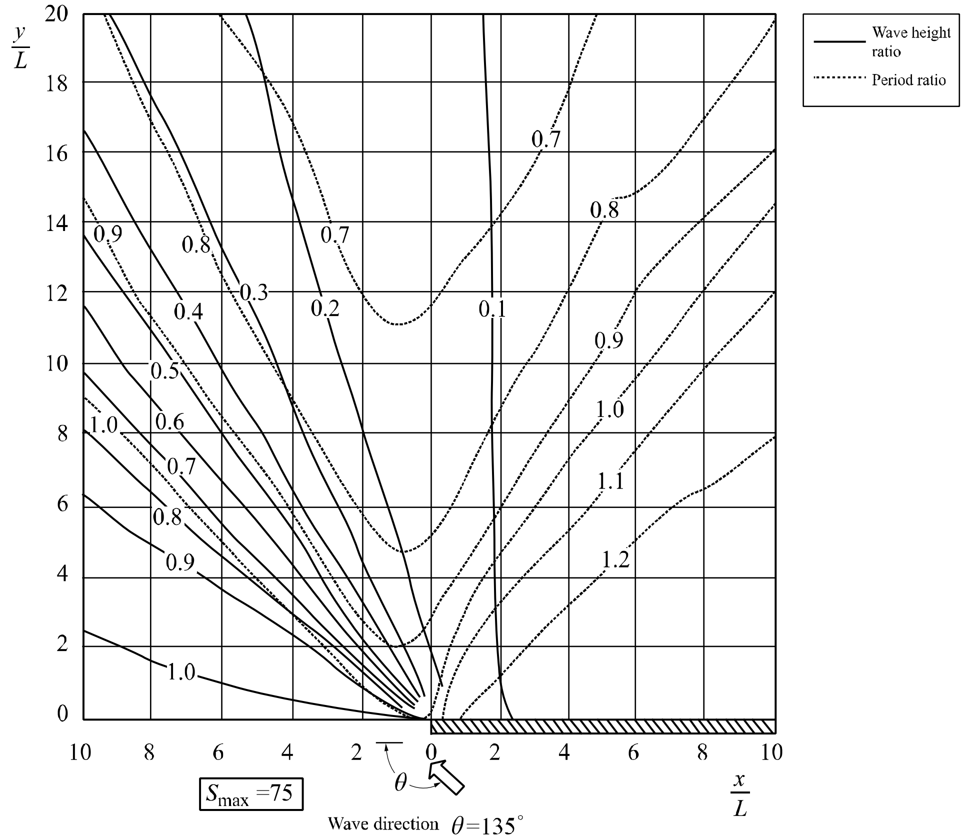

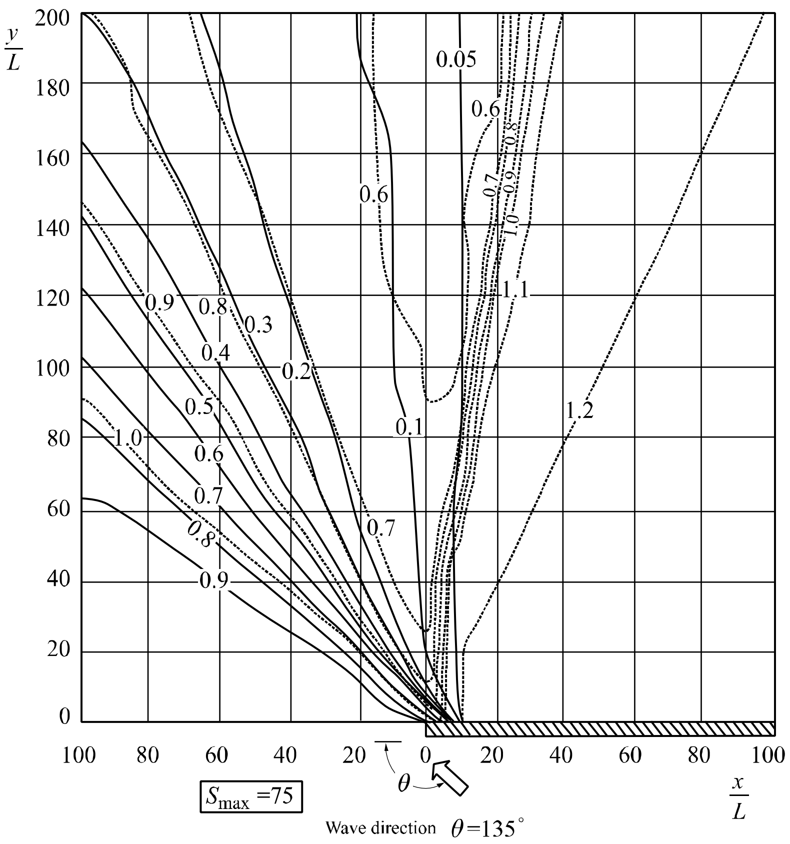

Fig. 1.1.5 (c) Diffraction Diagram for a Semi-Infinite Breakwater (θ = 135°)

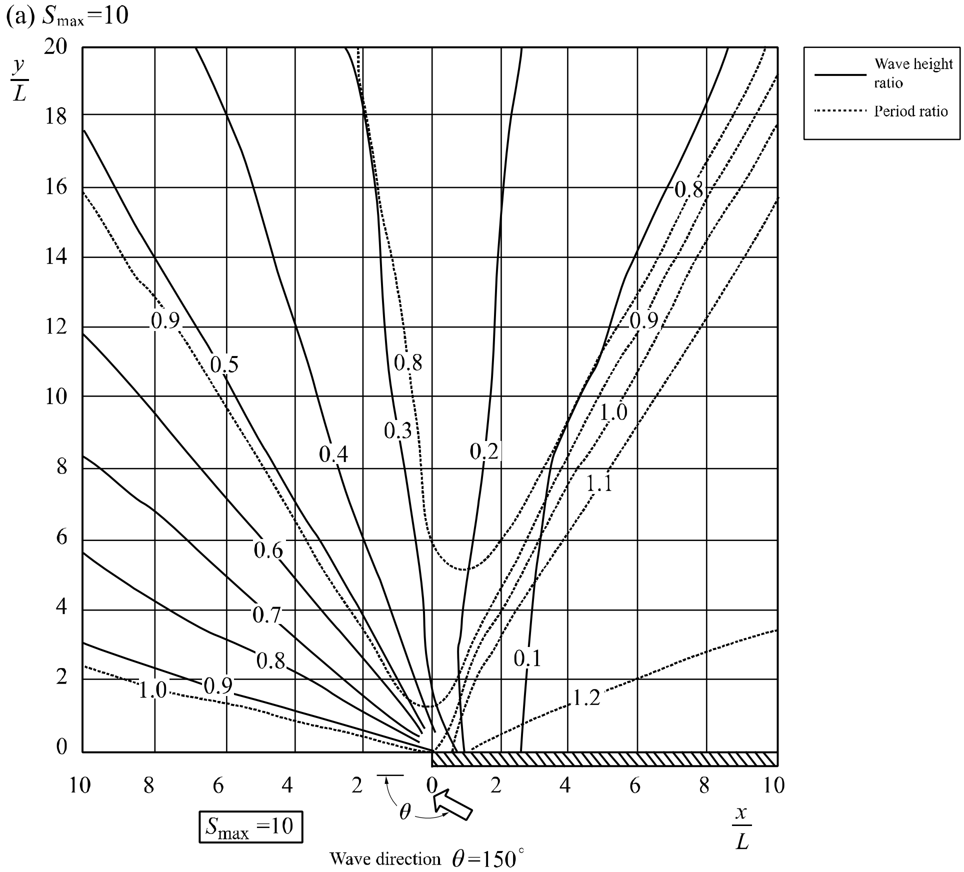

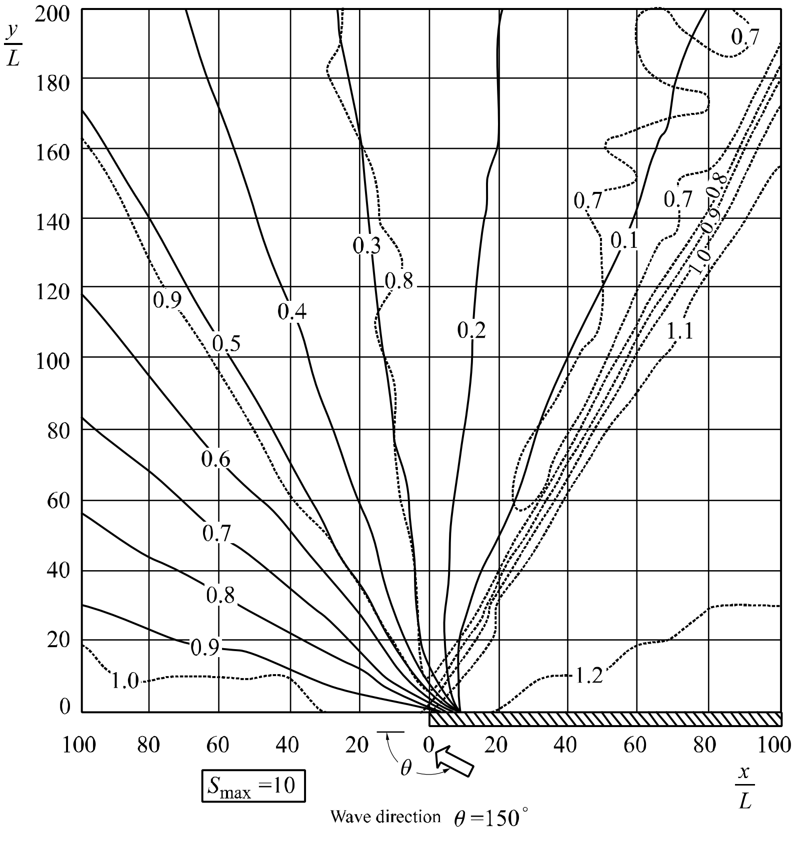

Fig. 1.1.6 (a) Diffraction Diagram for a Semi-Infinite Breakwater (θ = 150°)

(b) S_{max}=25

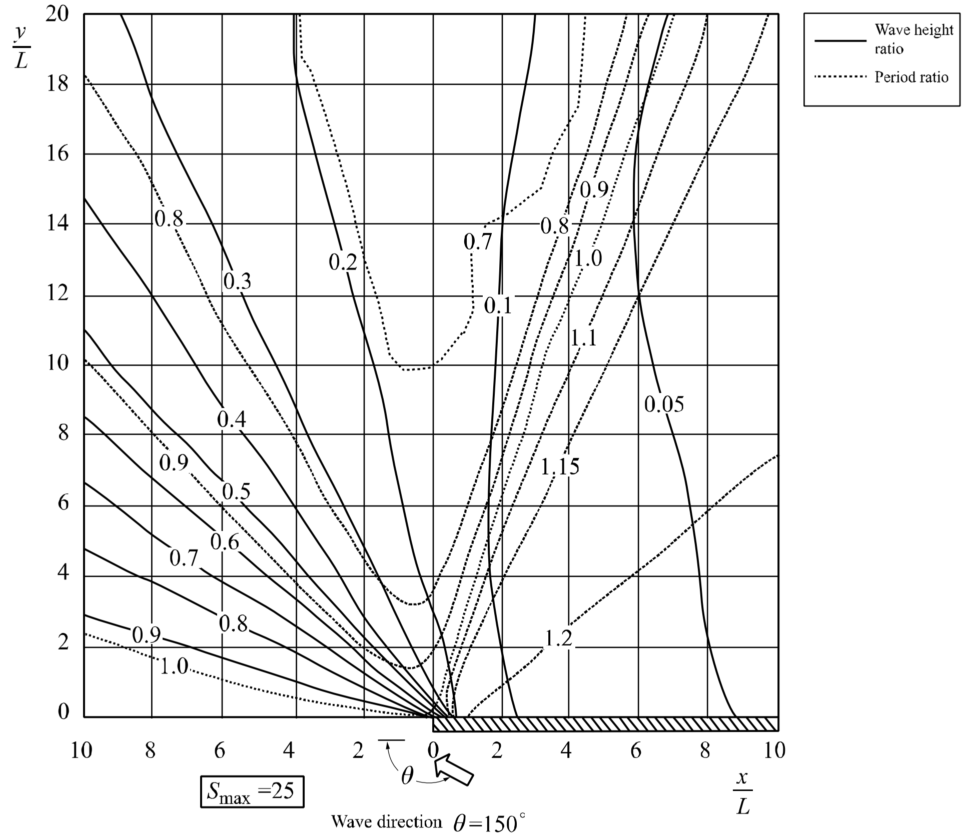

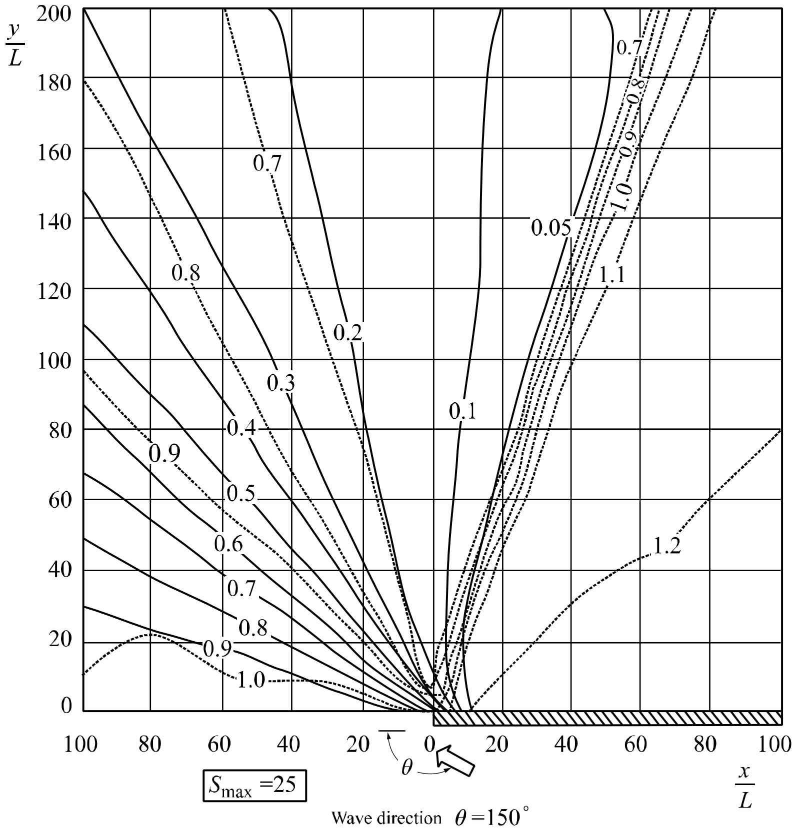

Fig. 1.1.6 (b) Diffraction Diagram for a Semi-Infinite Breakwater (θ = 150°)

(c) S_{max} =75

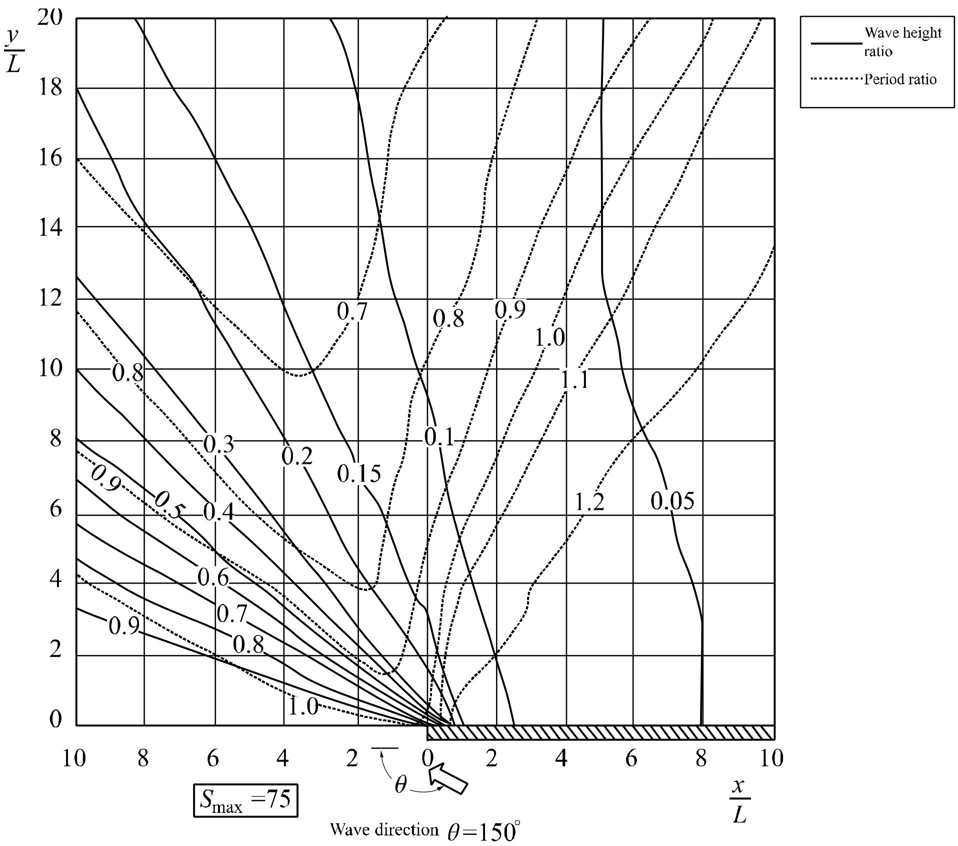

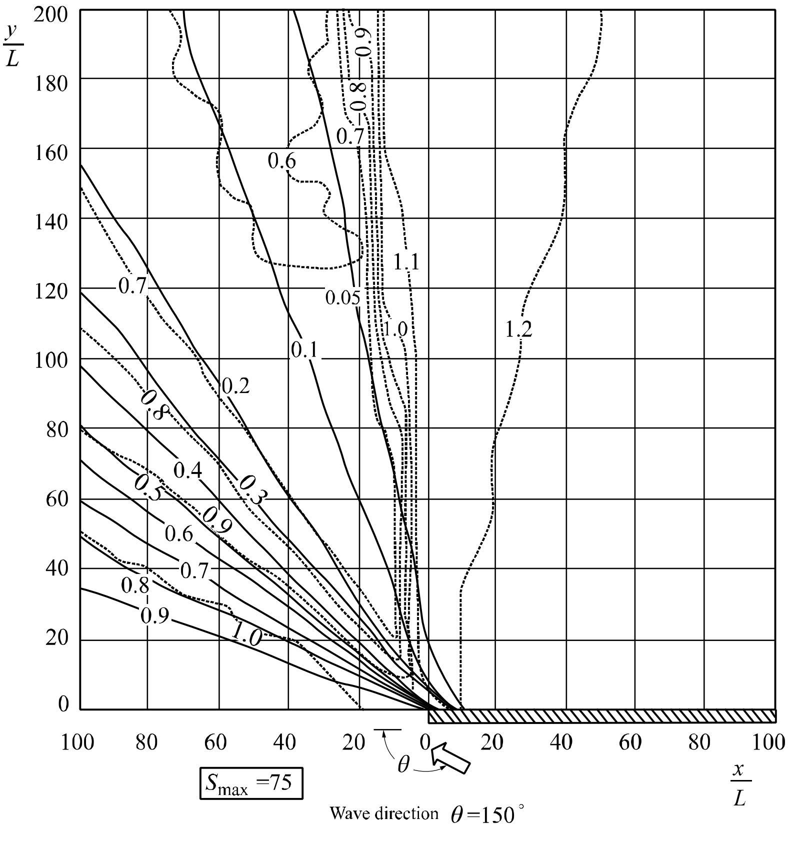

Fig. 1.1.6 (c) Diffraction Diagram for a Semi-Infinite Breakwater (*θ* = 150°)

(a) S_{max}=10

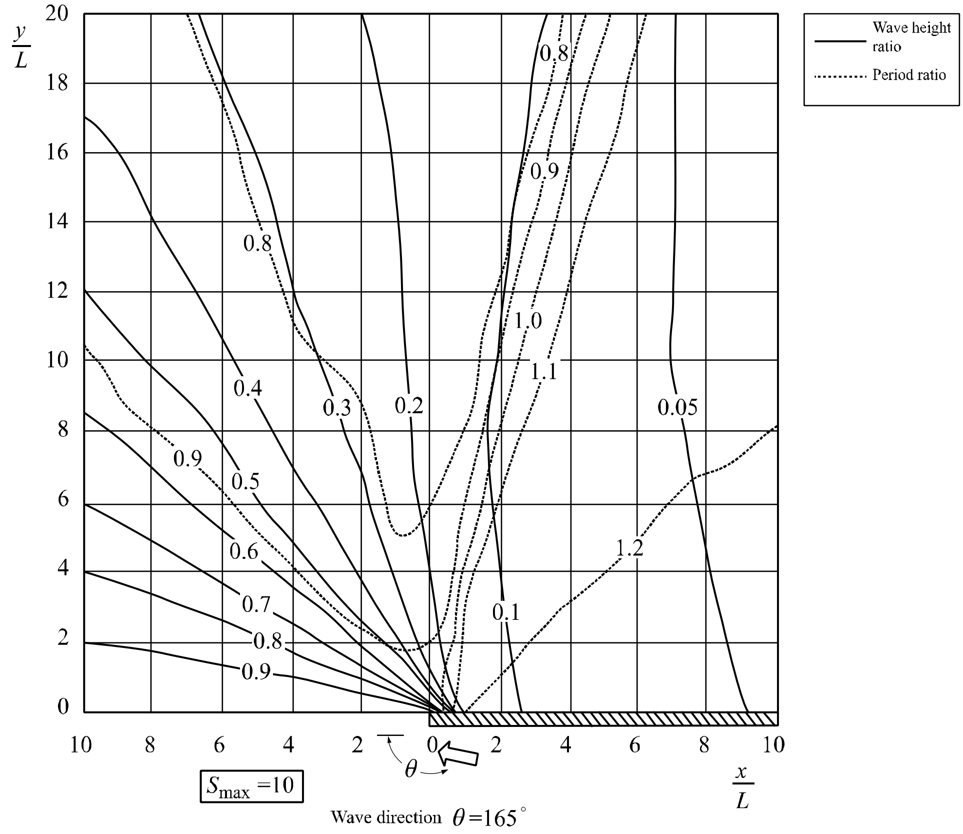

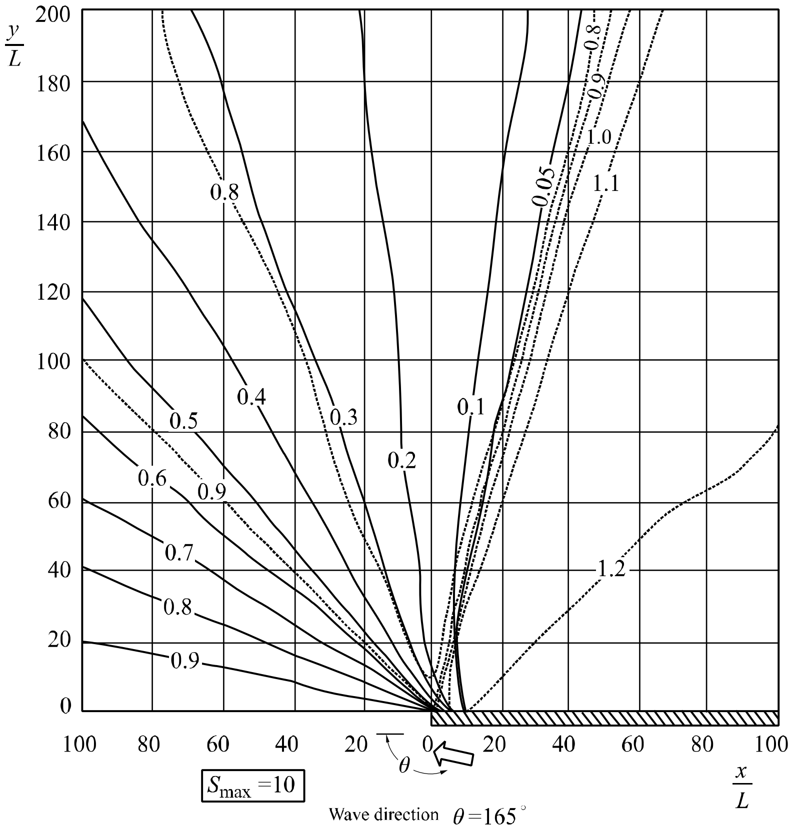

Fig. 1.1.7 (a) Diffraction Diagram for a Semi-Infinite Breakwater (θ = 165°)

(b) S_{max}=25

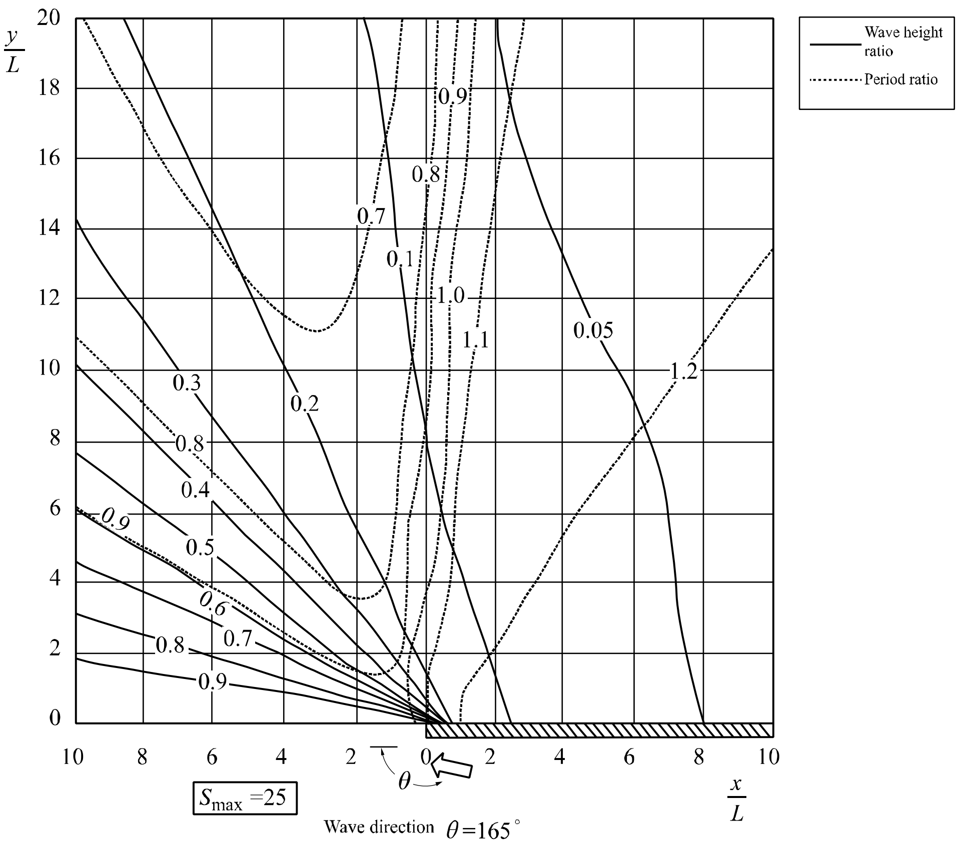

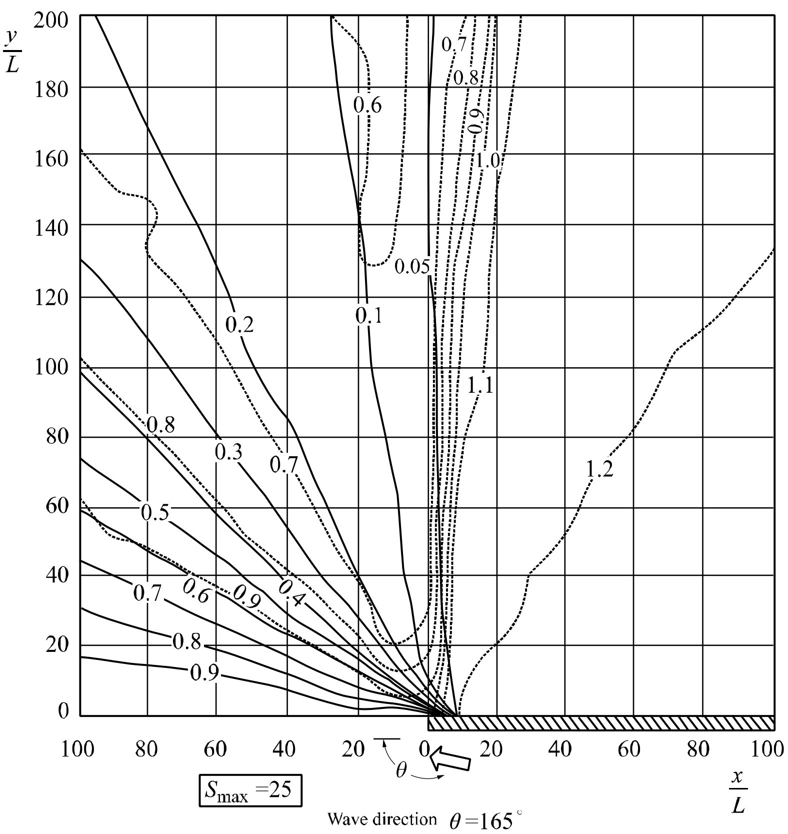

Fig. 1.1.7 (b) Diffraction Diagram for a Semi-Infinite Breakwater (θ = 165°)

(c) S_{max}=75

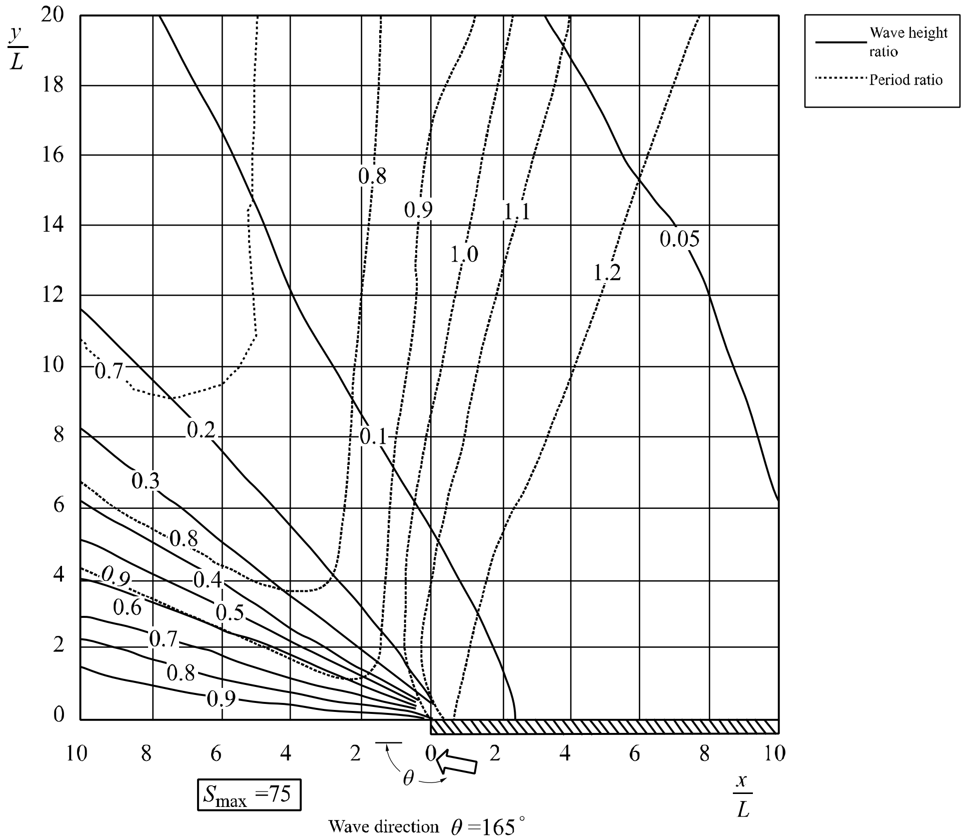

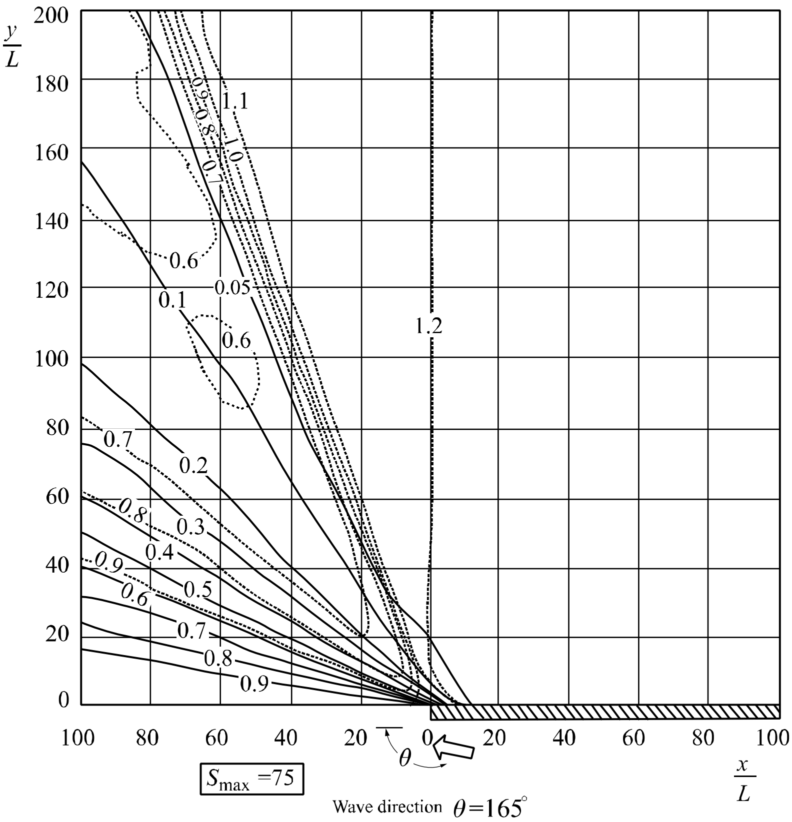

Fig. 1.1.7 (c) Diffraction Diagram for a Semi-Infinite Breakwater (θ = 165°)

(a) S_{max}=10

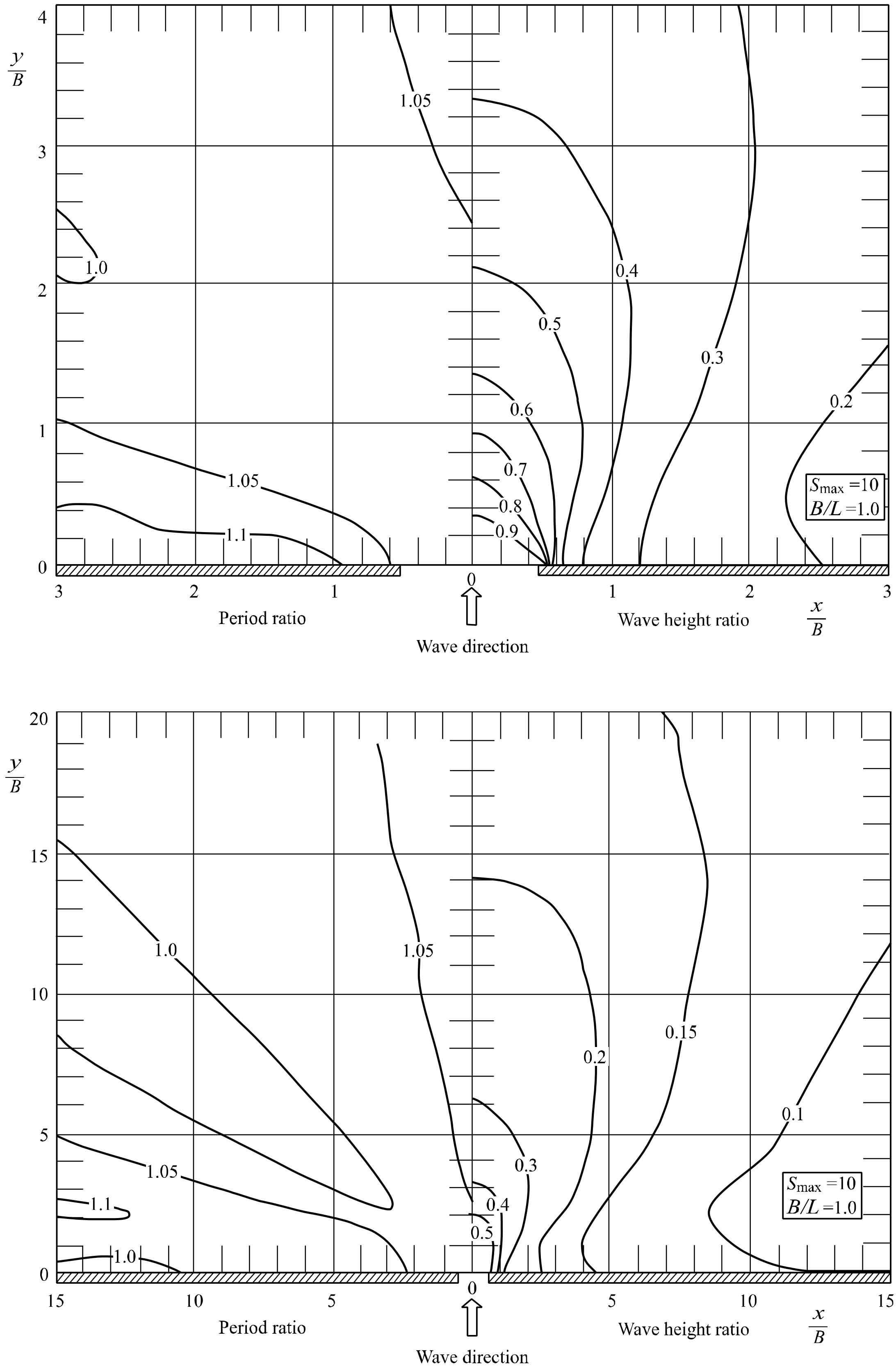

Fig. 1.1.8 (a) Diffraction Diagram for a Breakwater with Opening (B/L = 1.0)

(b) S_{max}=25

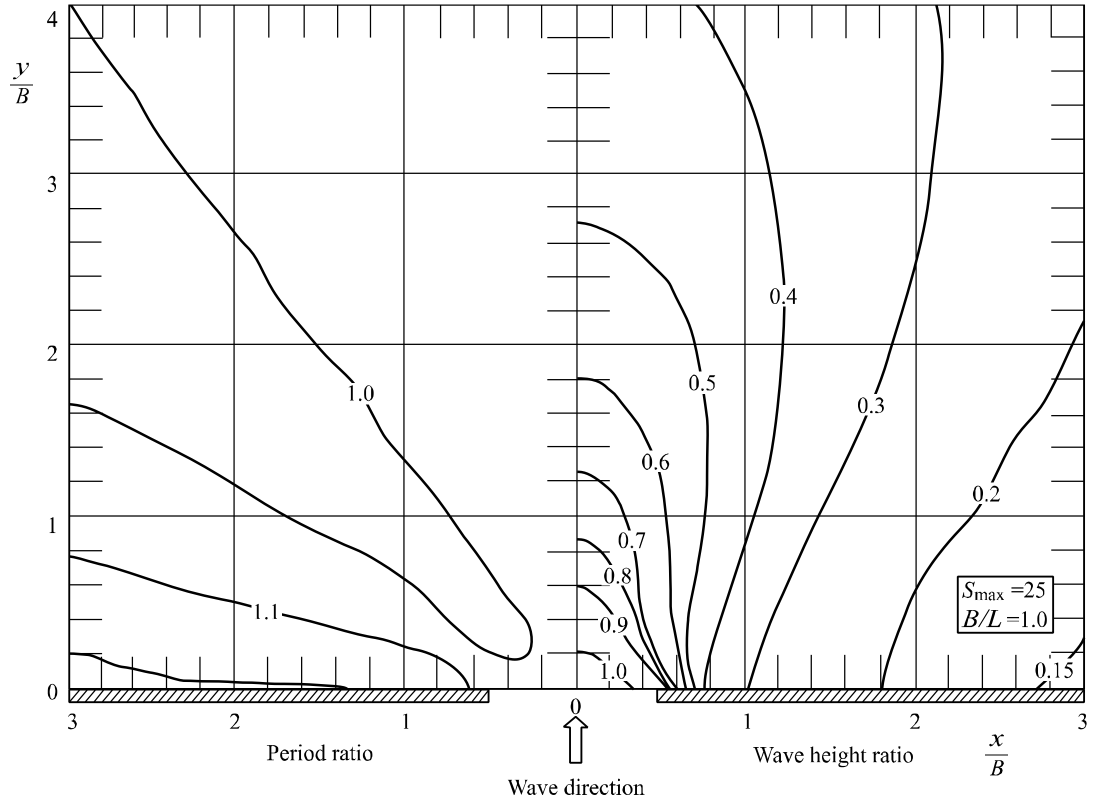

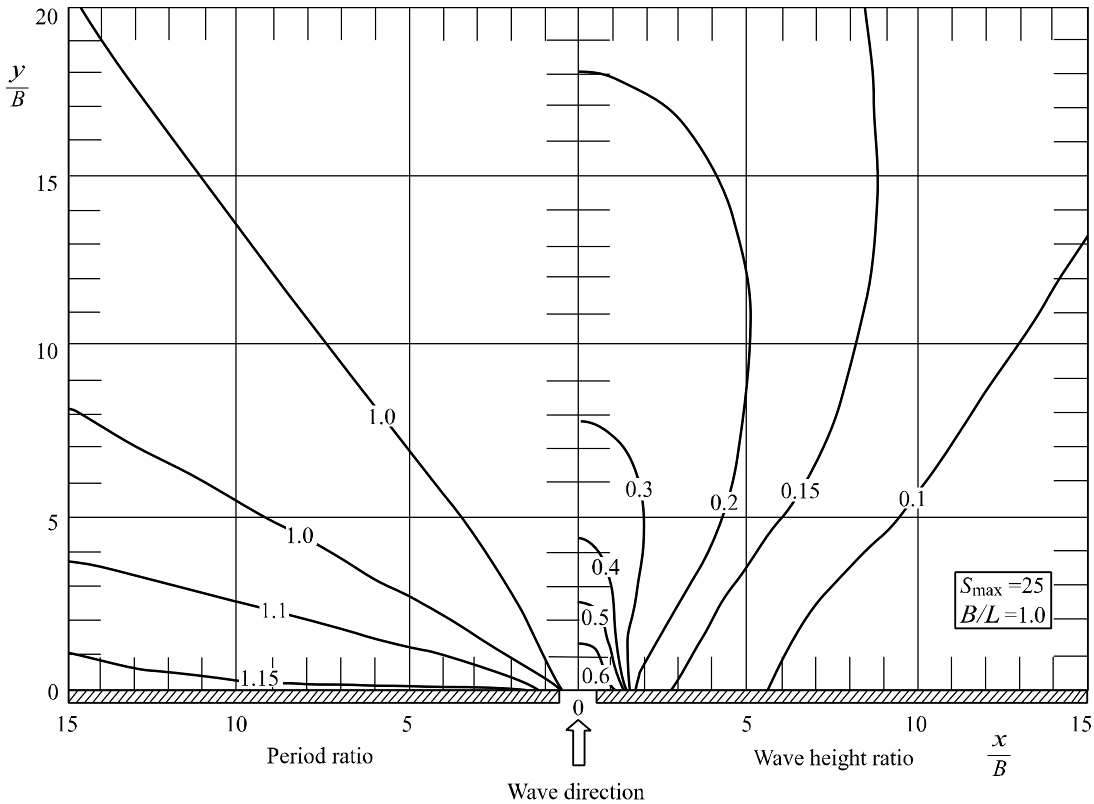

Fig. 1.1.8 (b) Diffraction Diagram for a Breakwater with Opening (*B*/*L* = 1.0)

(c) S_{max}=75

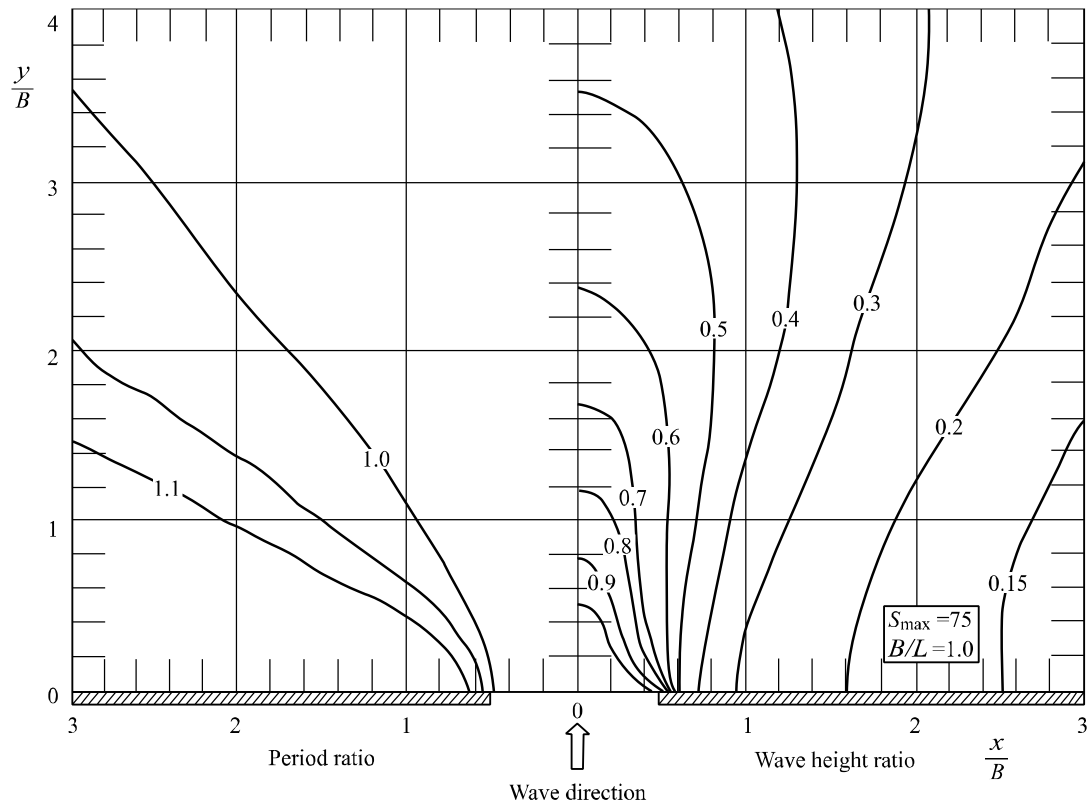

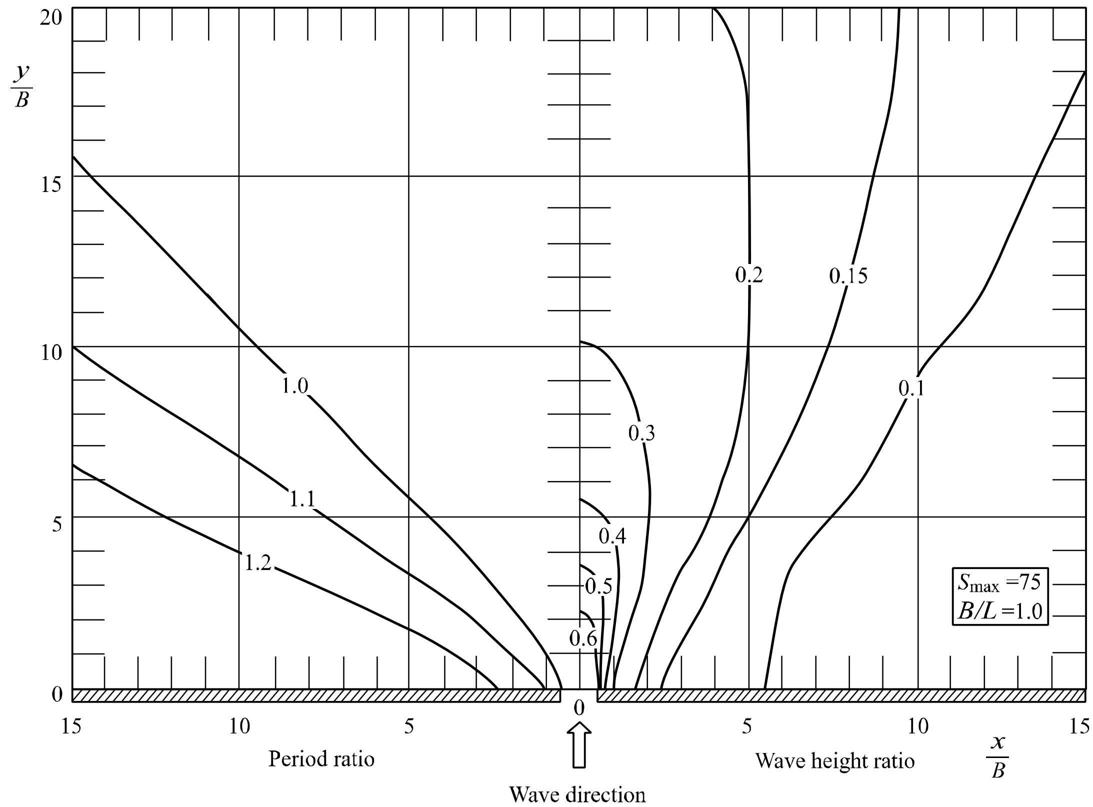

Fig. 1.1.8 (c) Diffraction Diagram for a Breakwater with Opening (*B*/*L* = 1.0)

(a) S_{max}=10

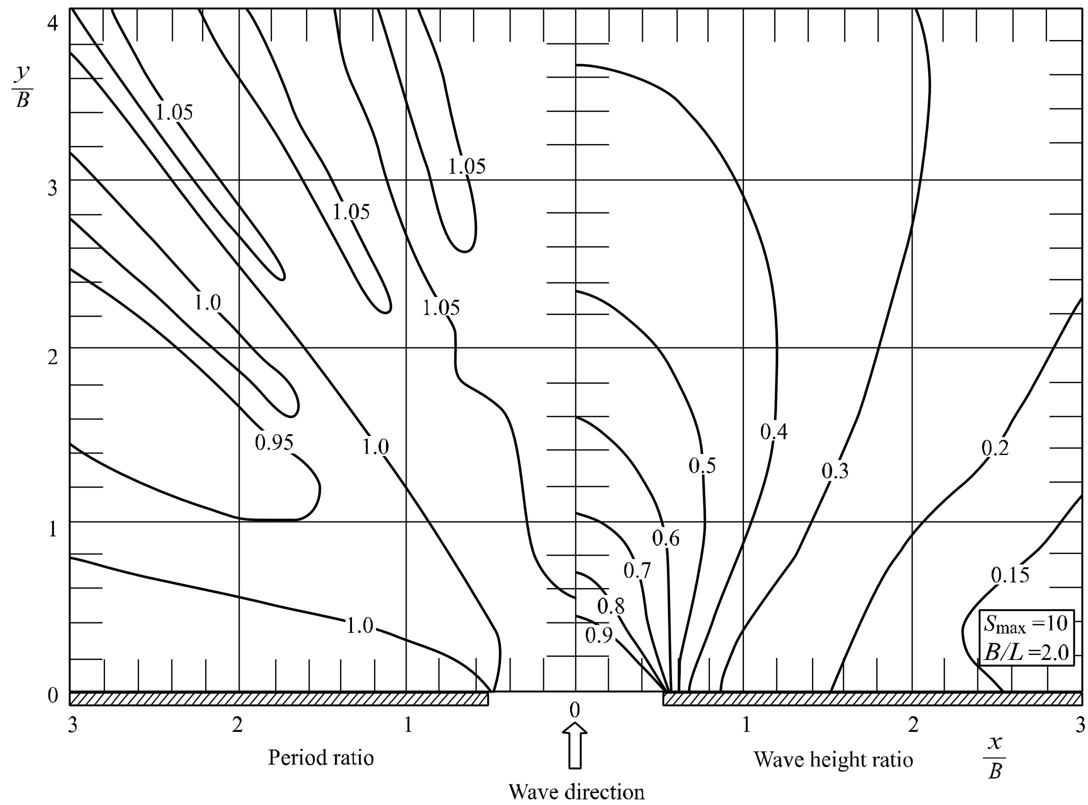

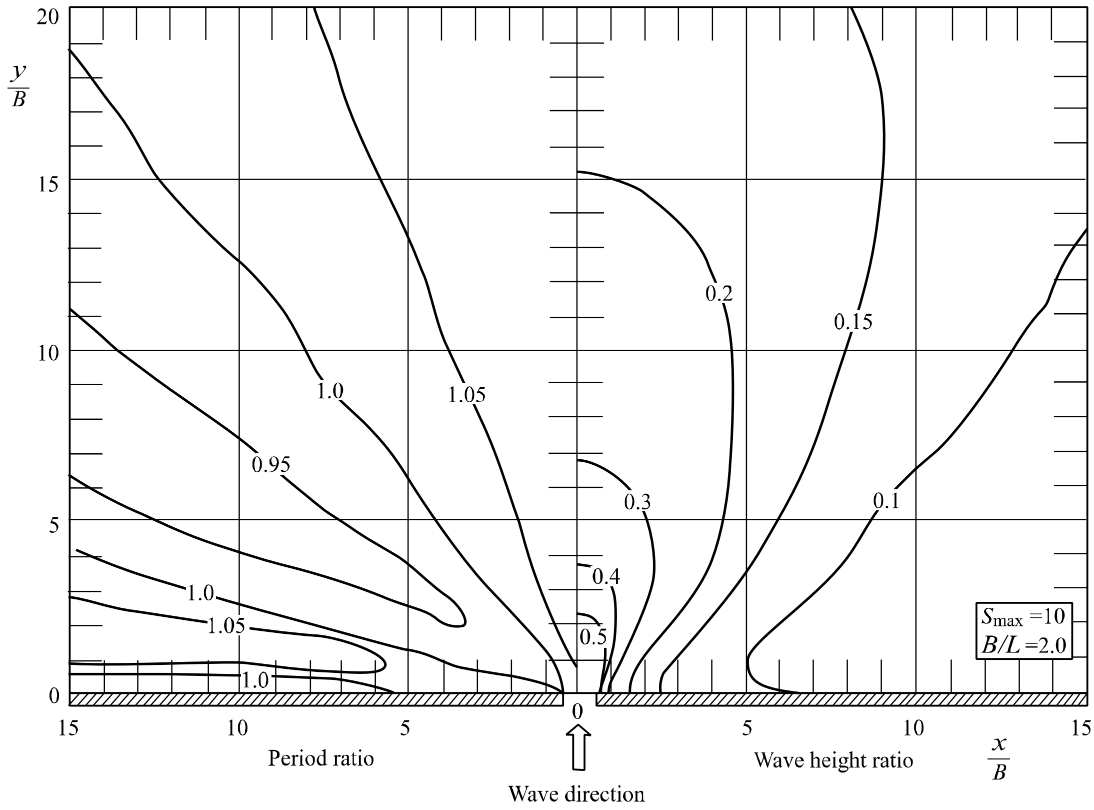

Fig. 1.1.9 (a) Diffraction Diagram for a Breakwater with Opening (*B*/*L* = 2.0)

(b) $S_{\max}$=25

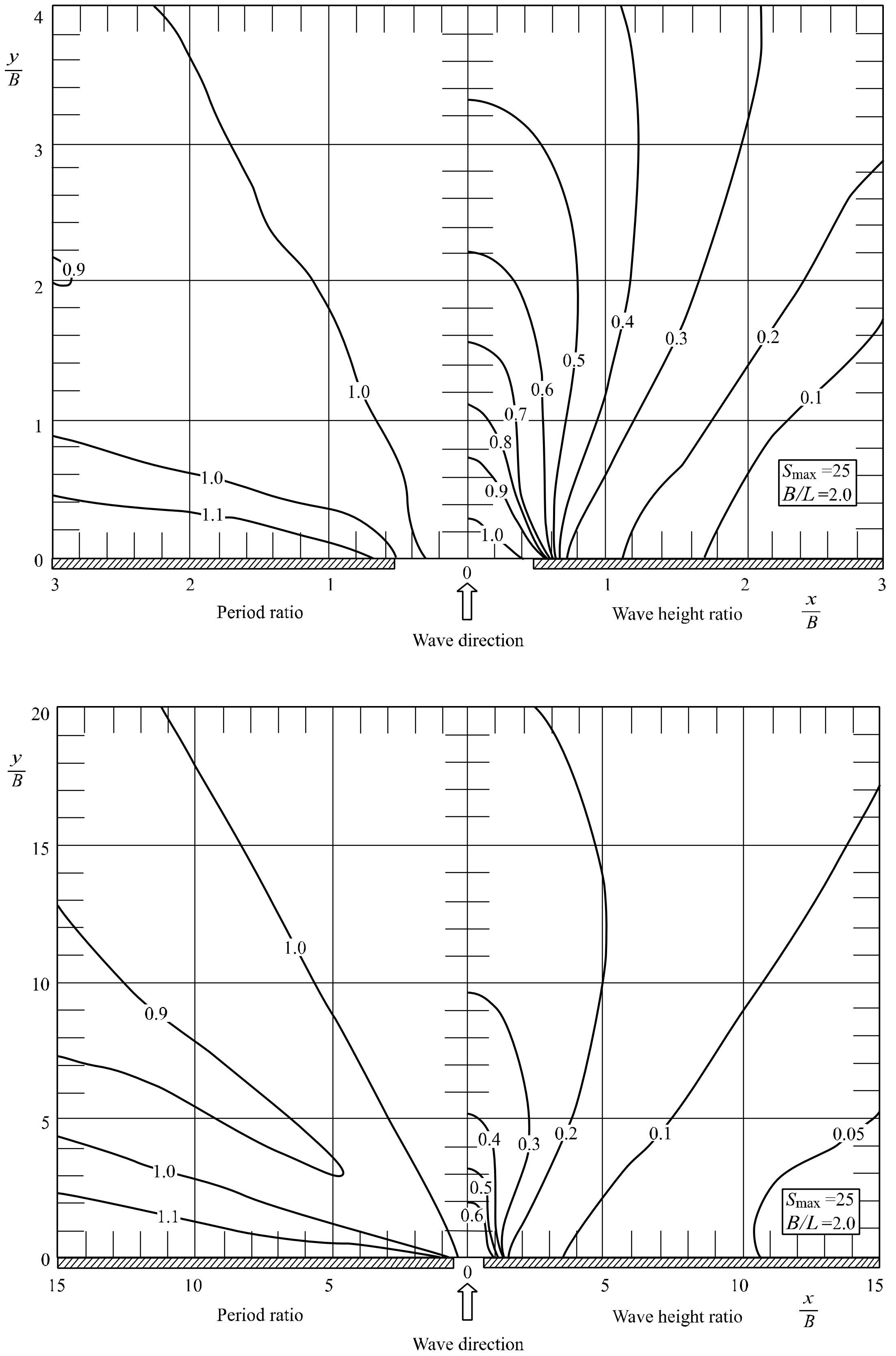

Fig. 1.1.9 (b) Diffraction Diagram for a Breakwater with Opening (*B*/*L* = 2.0)

(c) S_{max}=75

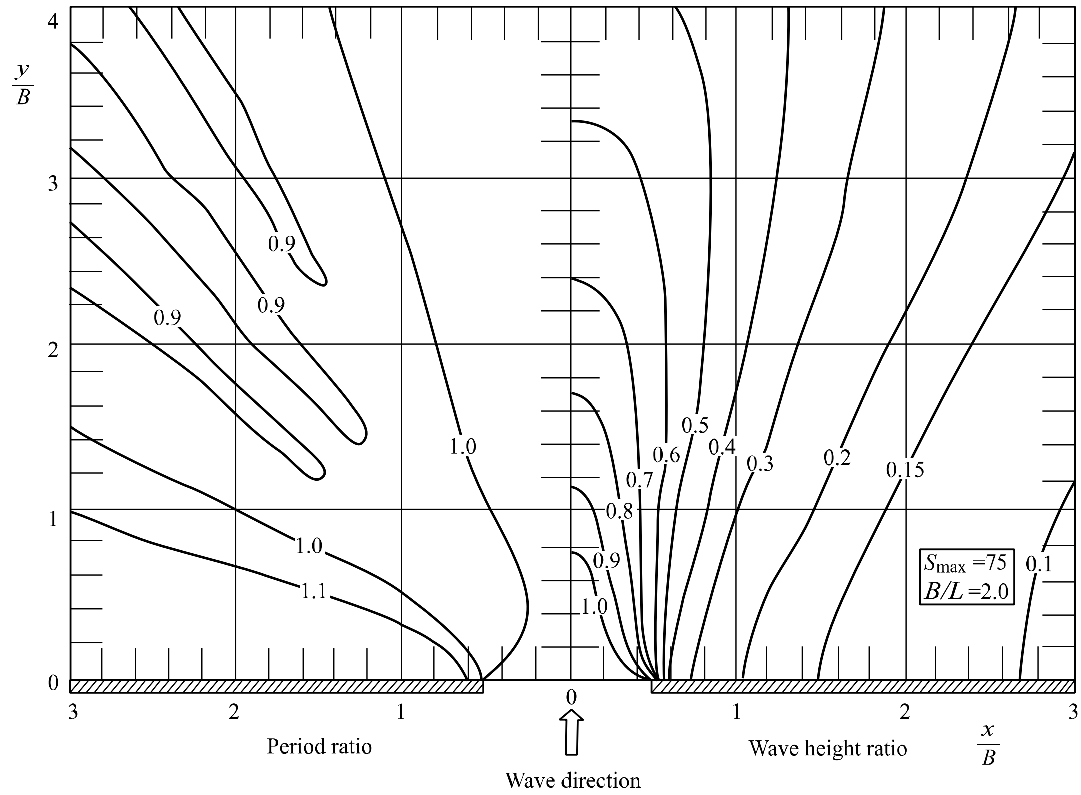

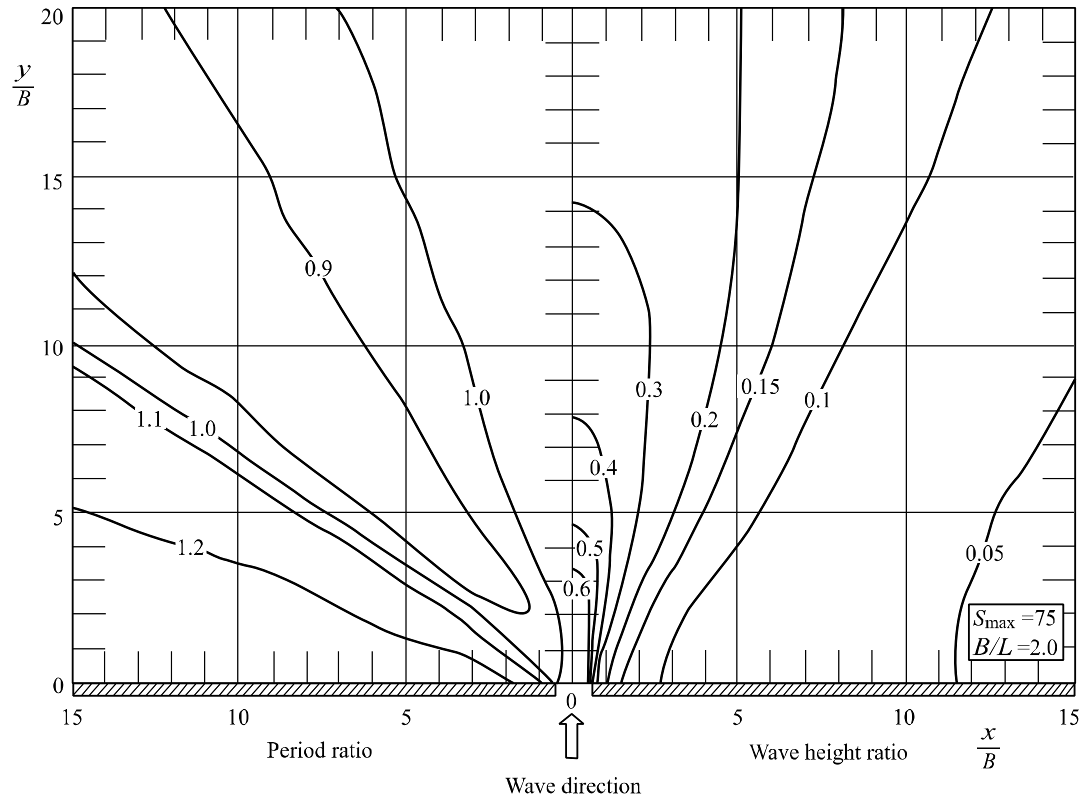

Fig. 1.1.9 (c) Diffraction Diagram for a Breakwater with Opening (*B*/*L* = 2.0)

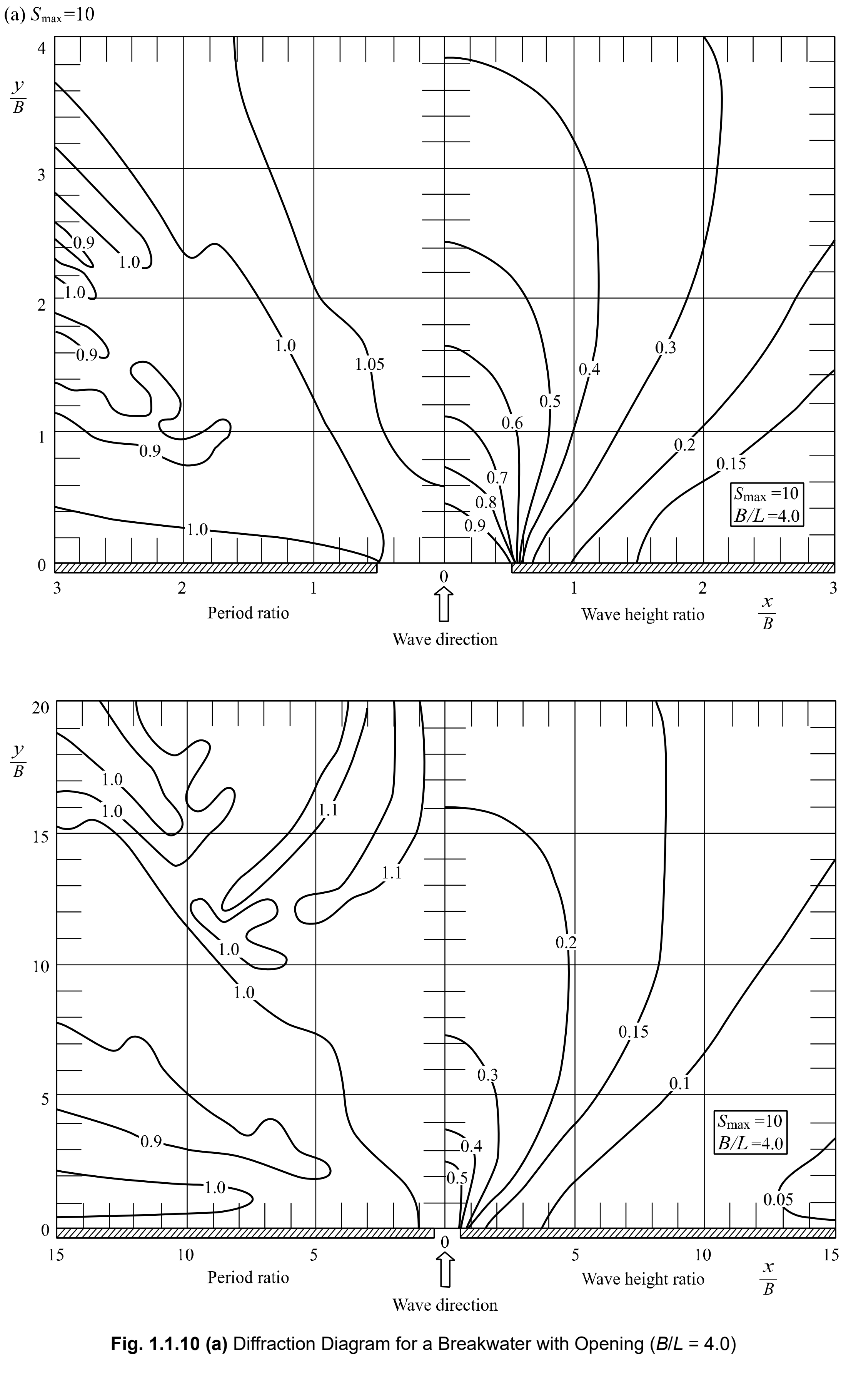

Fig. 1.1.10 (a) Diffraction Diagram for a Breakwater with Opening (B/L = 4.0)

(b) S_{max}=25

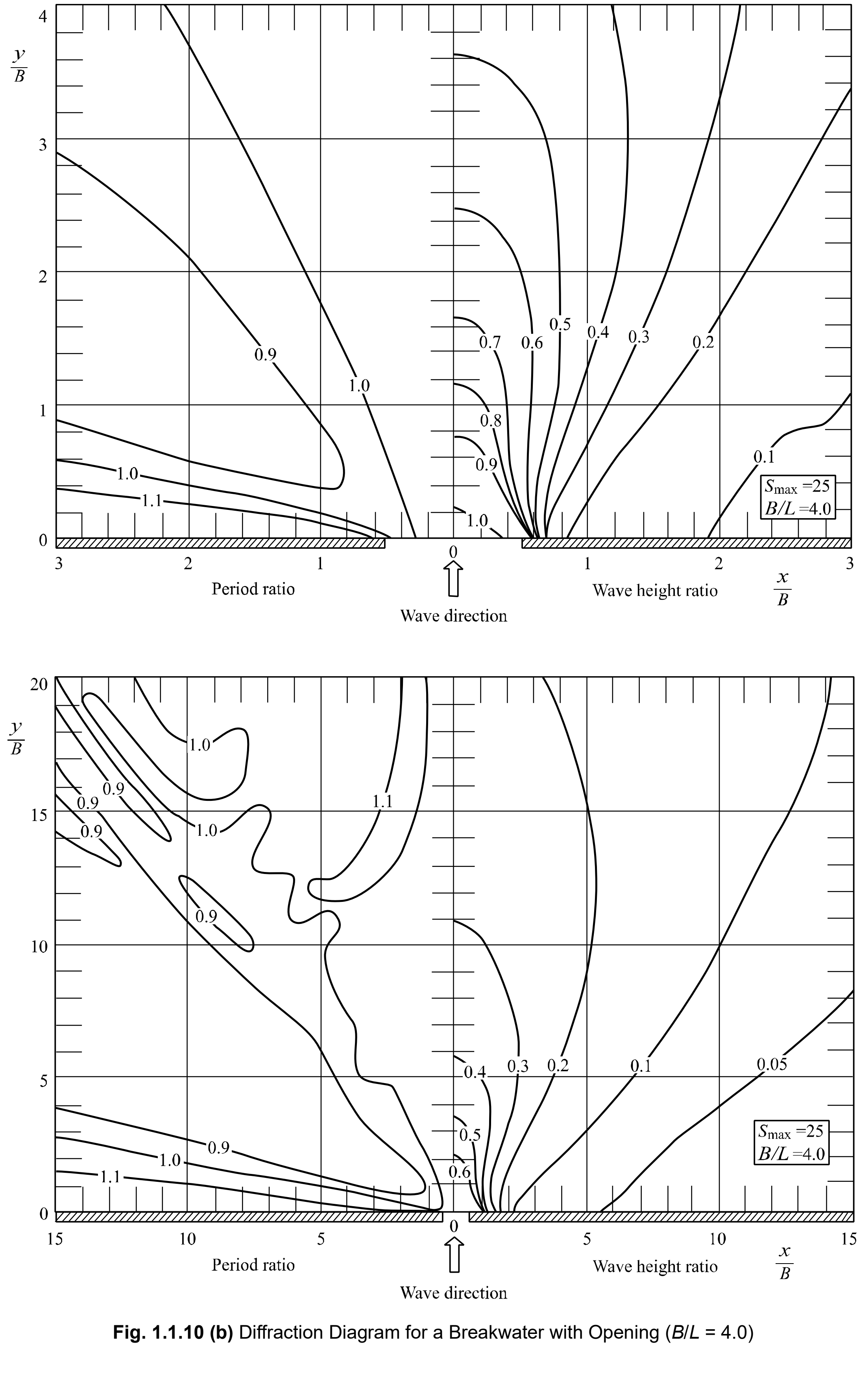

Fig. 1.1.10 (b) Diffraction Diagram for a Breakwater with Opening (B/L = 4.0)

(c) S_{max}=75

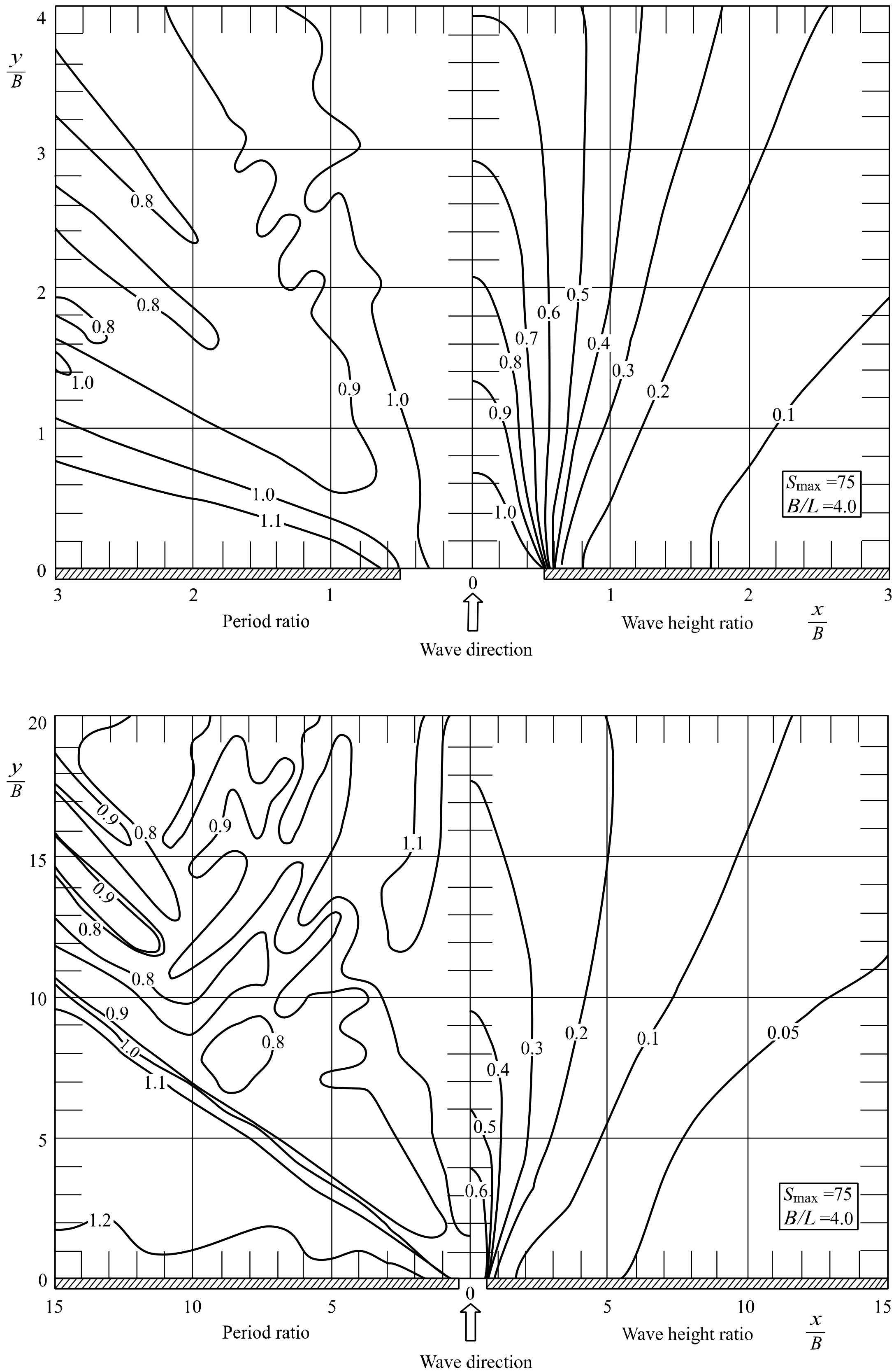

Fig. 1.1.10 (c) Diffraction Diagram for a Breakwater with Opening (*B*/*L* = 4.0)

(a) S_{max}=10

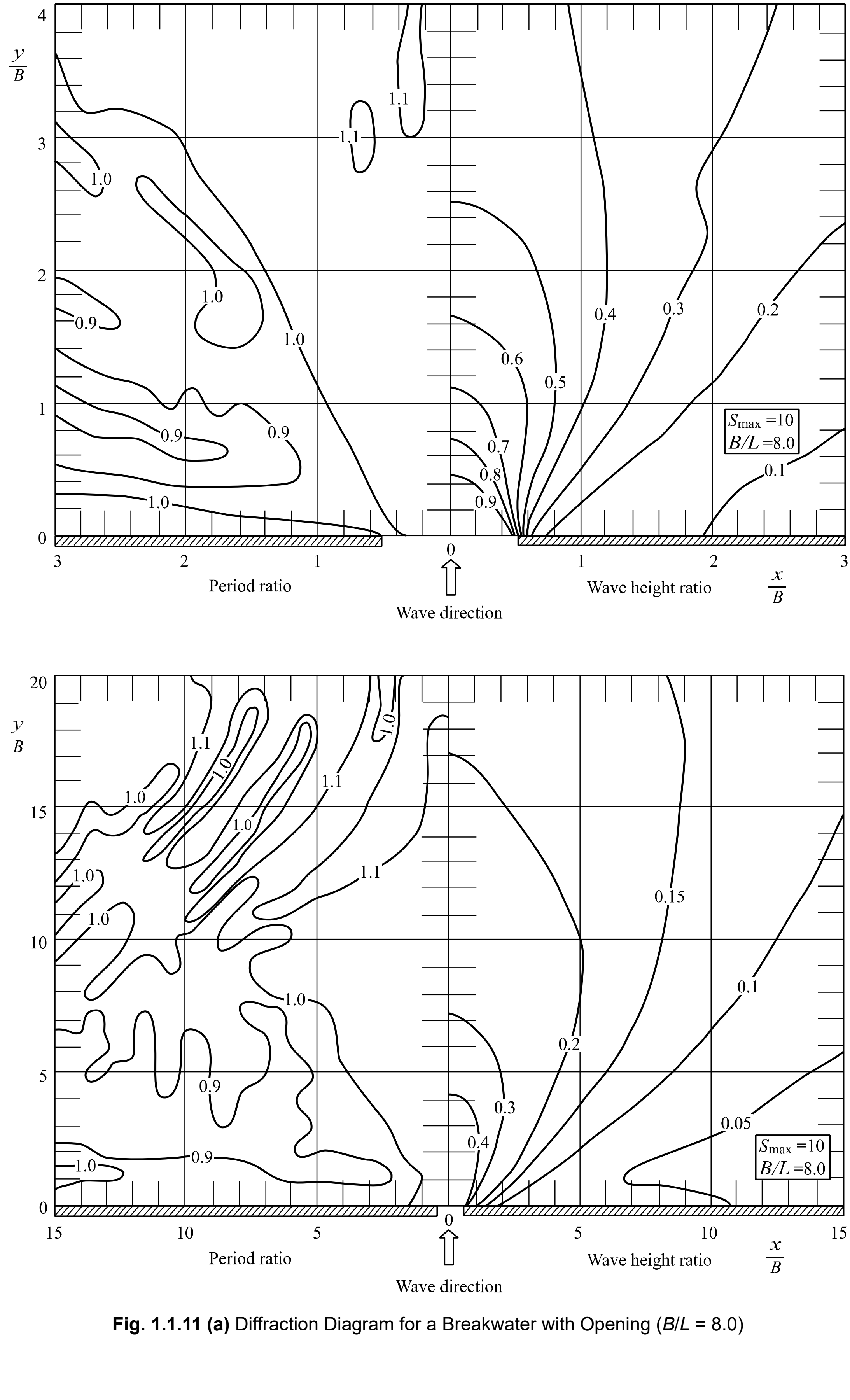

Fig. 1.1.11 (a) Diffraction Diagram for a Breakwater with Opening (B/L = 8.0)

(b) S_{max}=25

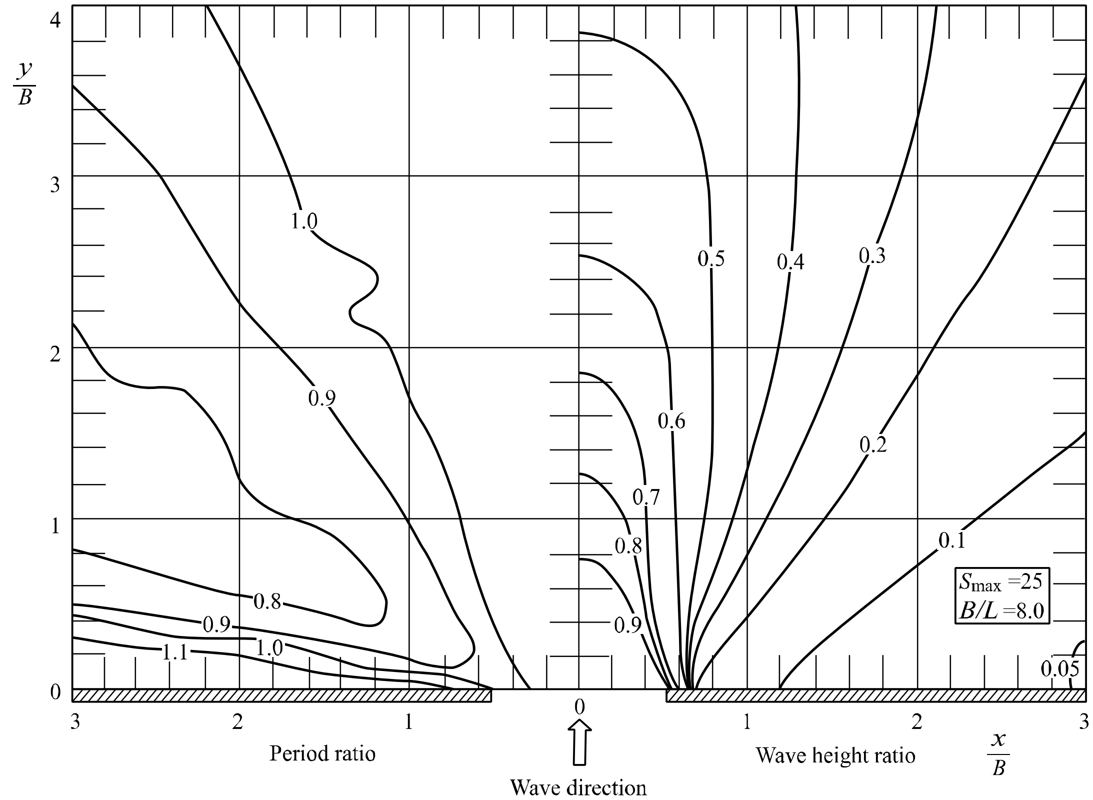

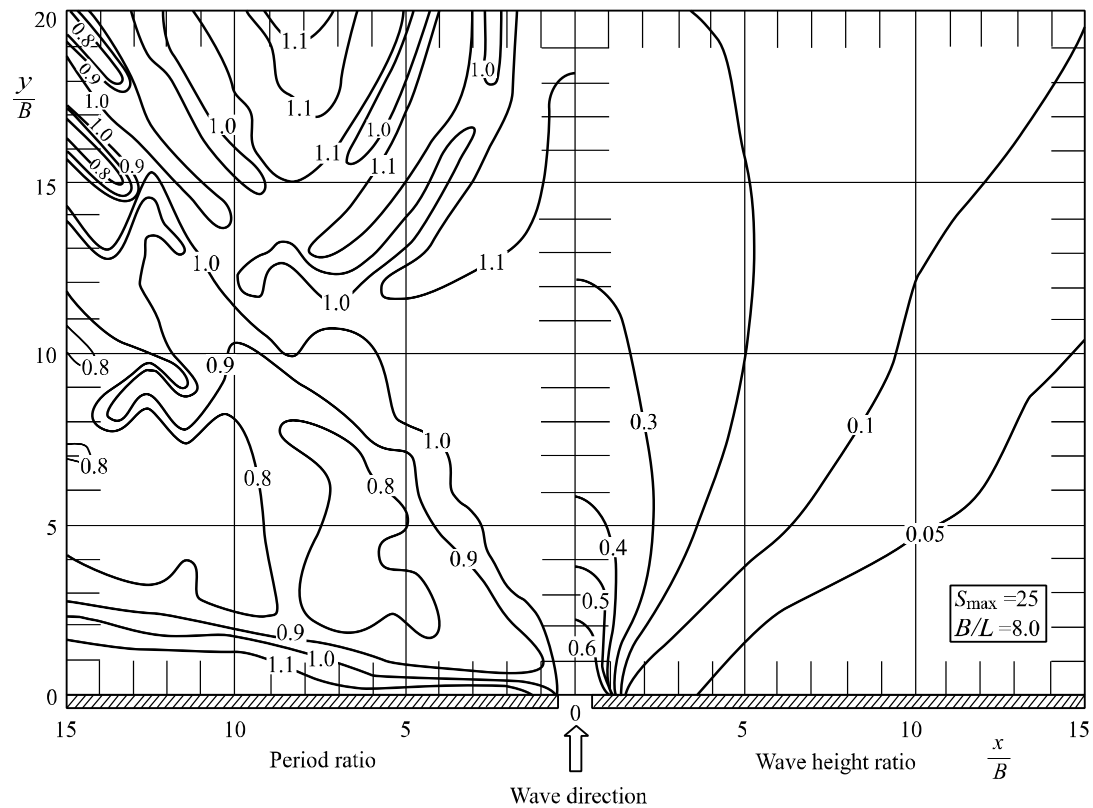

Fig. 1.1.11 (b) Diffraction Diagram for a Breakwater with Opening (B/L = 8.0)

(c) S_{max}=75

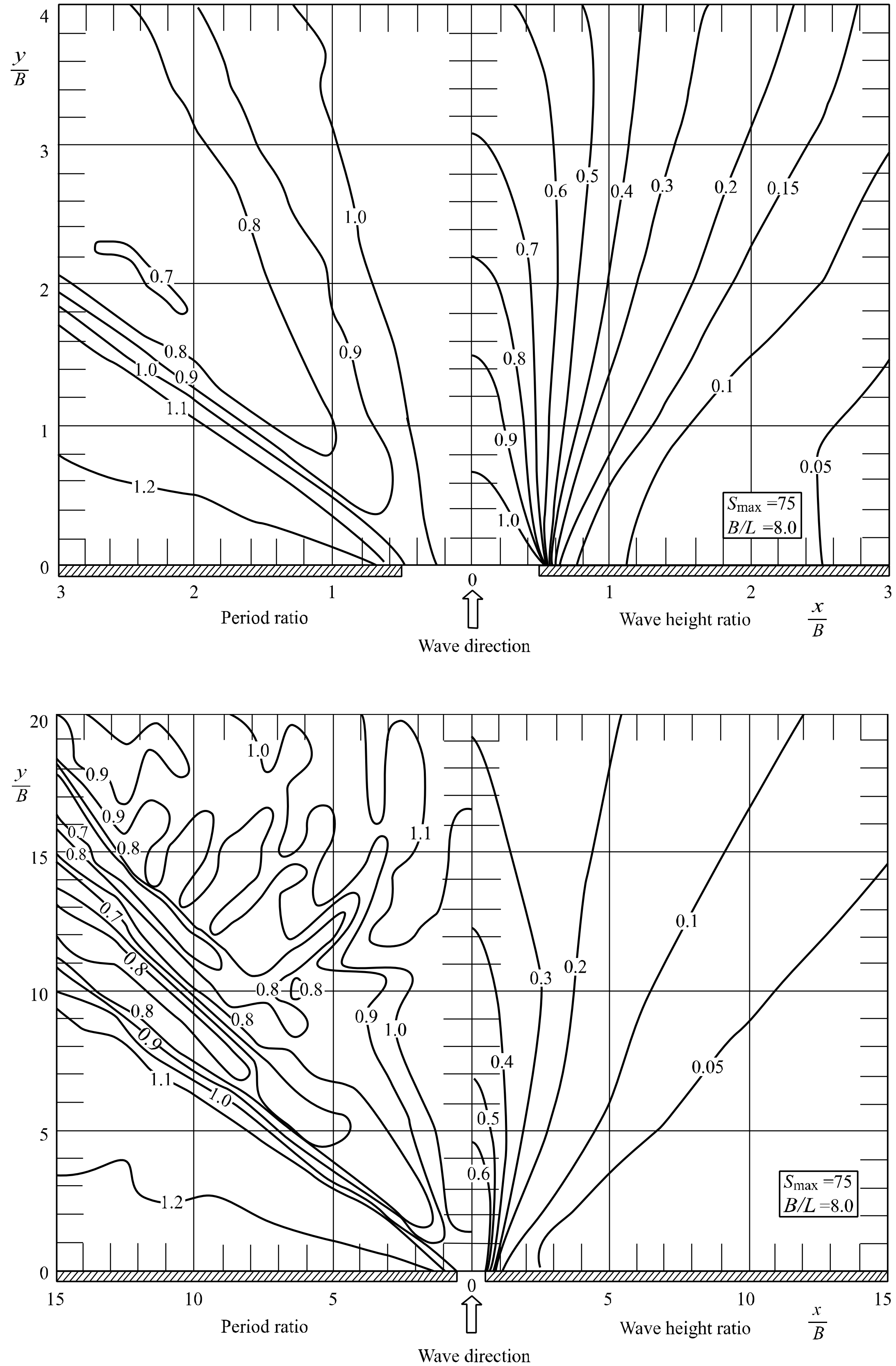

Fig. 1.1.11 (c) Diffraction Diagram for a Breakwater with Opening (B/L = 8.0)

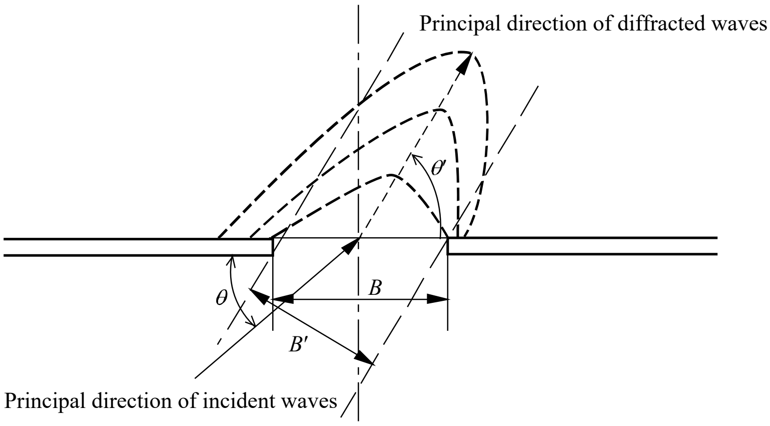

Fig. 1.1.12 Virtual Opening *B*' and Angle of Axis of the Diffracted Wave *θ*'

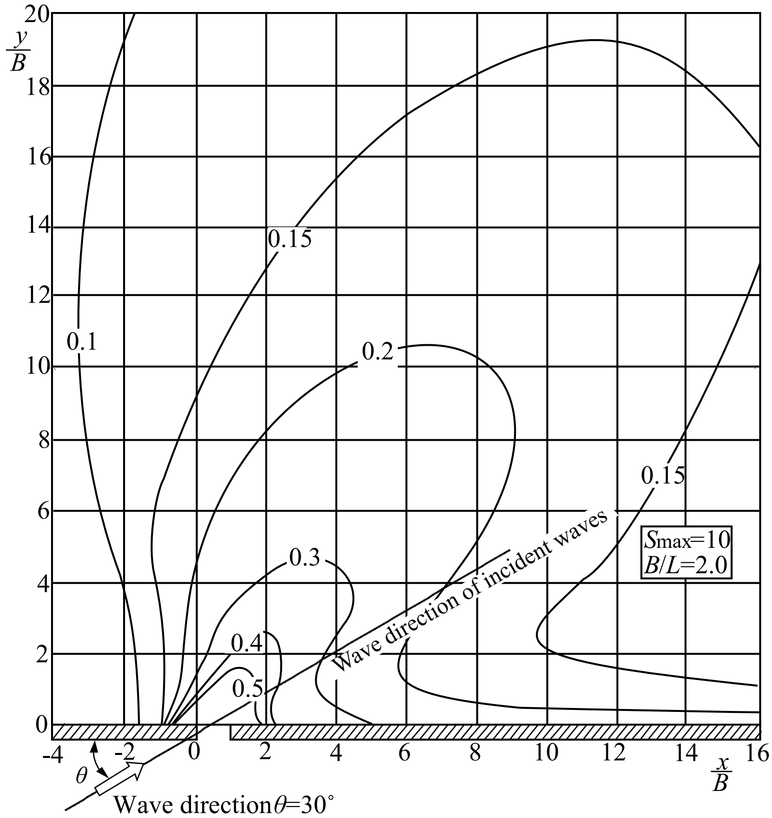

Fig. 1.1.13 (a) Diffraction Diagram for Oblique Incident Waves (*B*/*L* = 2.0, *θ* = 30°, S_{max} = 10)

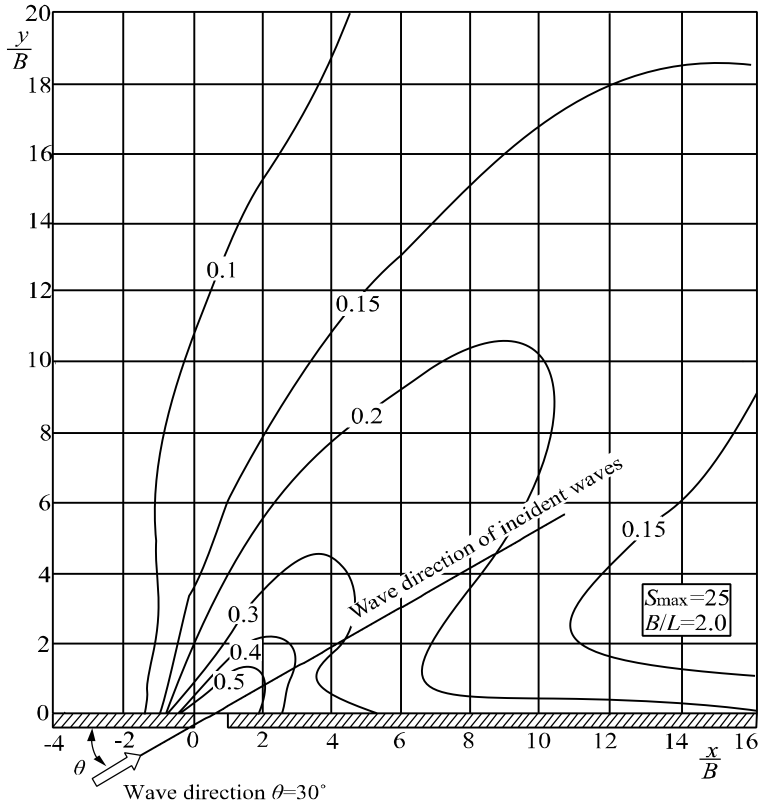

Fig. 1.1.13 (b) Diffraction Diagram for Oblique Incident Waves (B/L = 2.0, θ = 30°, S_{max} = 25)

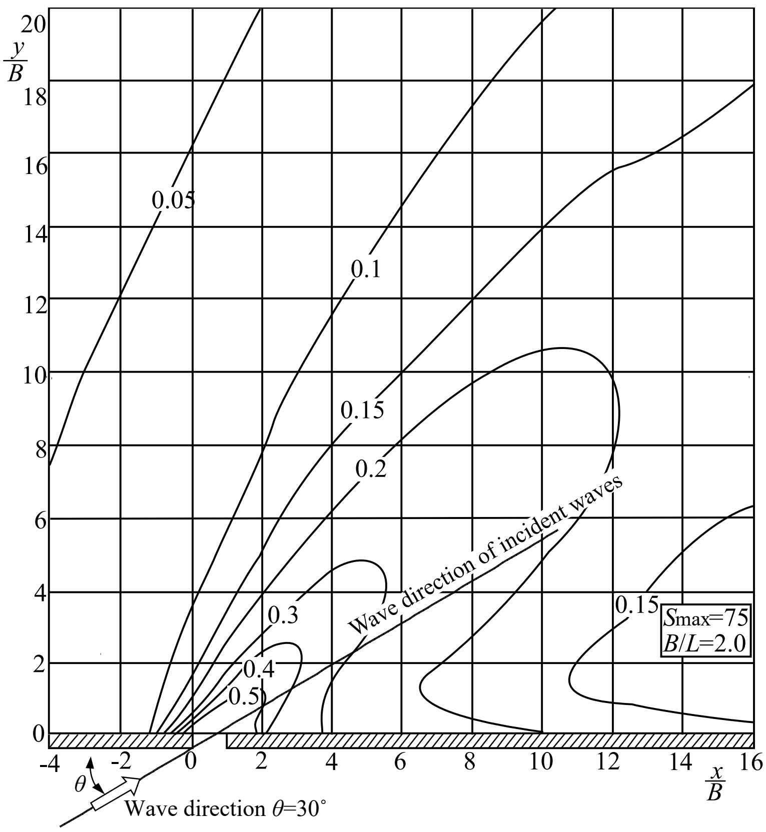

Fig. 1.1.13 (c) Diffraction Diagram for Oblique Incident Waves (B/L = 2.0, θ = 30°, S_{max} = 75)

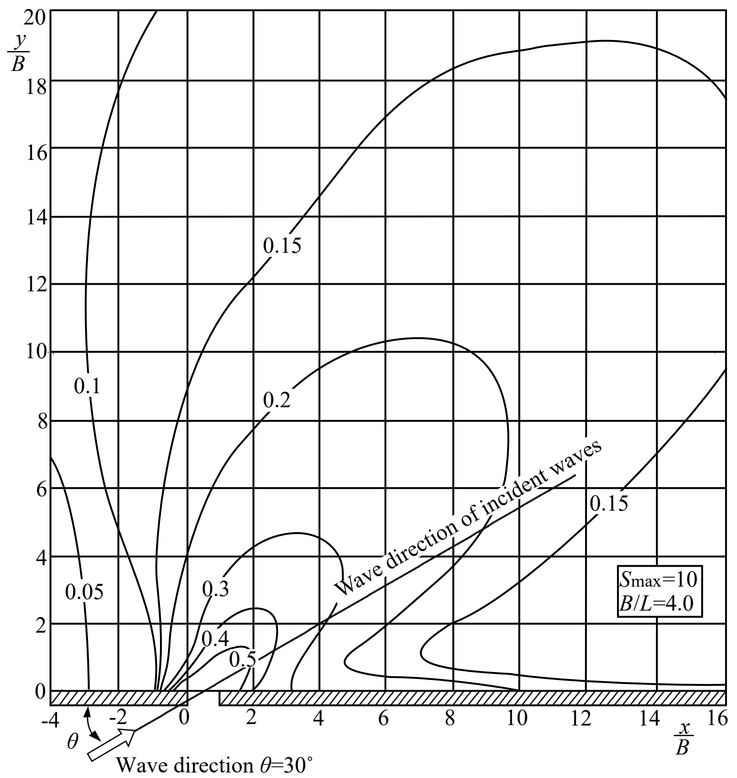

Fig. 1.1.14 (a) Diffraction Diagram for Oblique Incident Waves (B/L = 4.0, θ = 30°, S_{max} = 10)

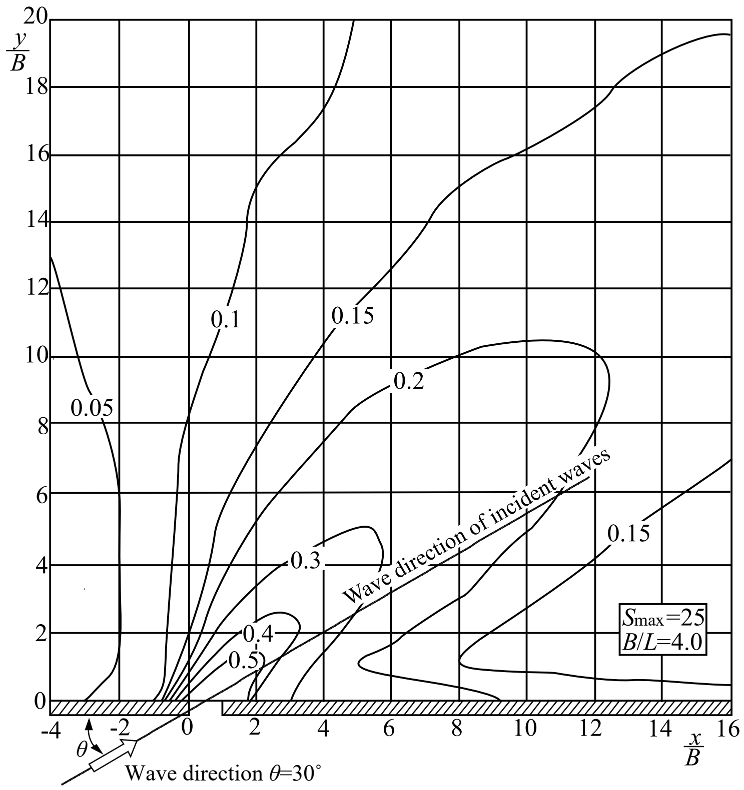

Fig. 1.1.14 (b) Diffraction Diagram for Oblique Incident Waves (B/L = 4.0, θ = 30°, S_{max} = 25)

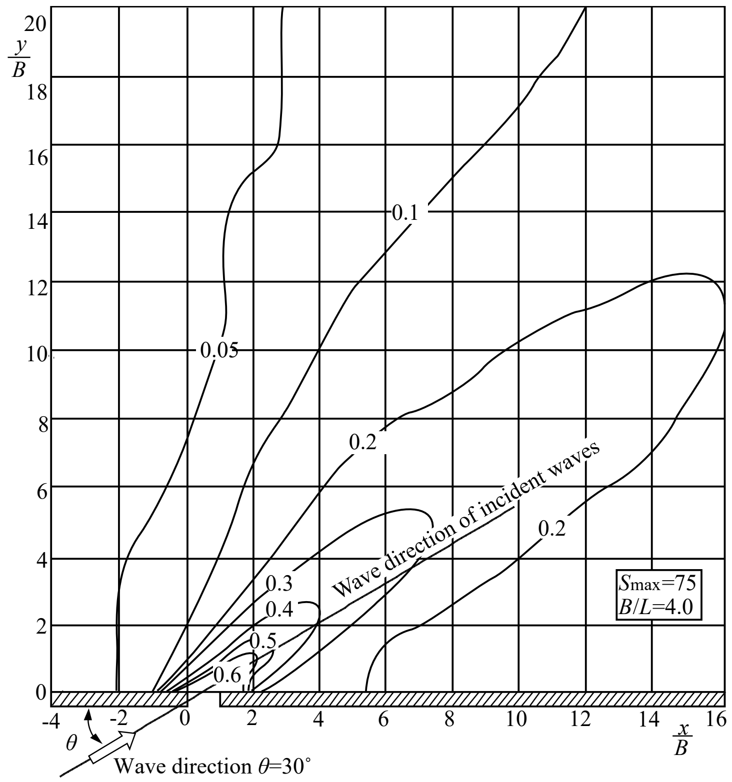

Fig. 1.1.14 (c) Diffraction Diagram for Oblique Incident Waves (B/L = 4.0, θ = 30°, S_{max} = 75)

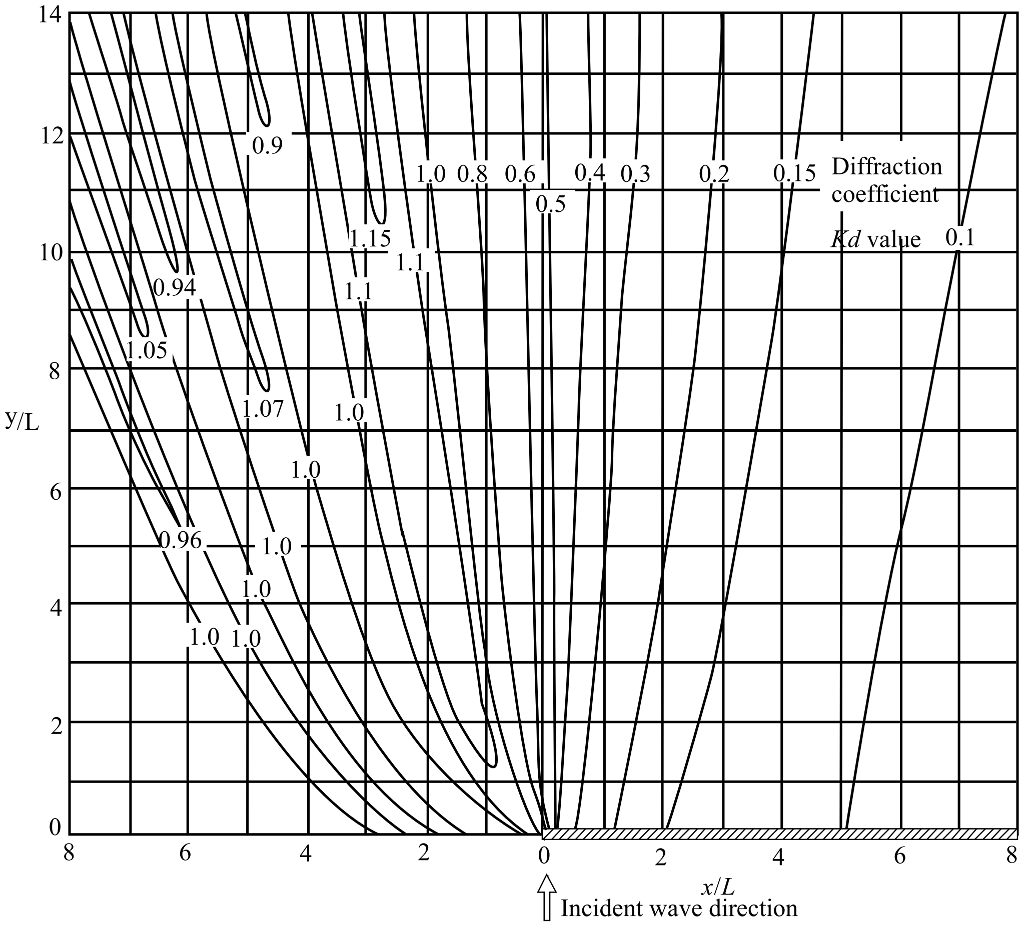

(a) θ_0=90˚

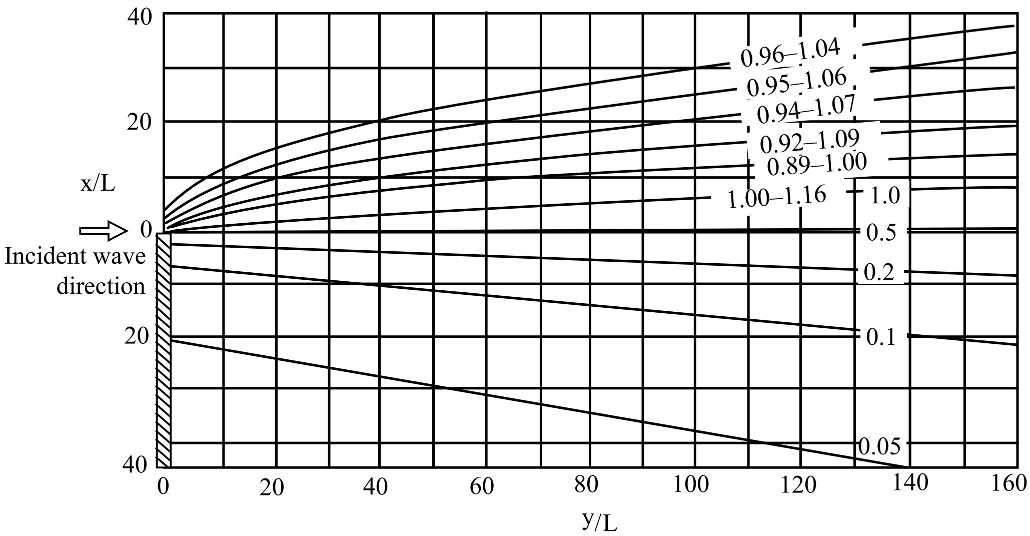

(b) θ_0=90˚

Fig. 1.1.15 (a)(b) Diffraction Diagram for a Semi-Infinite Breakwater and Regular Waves

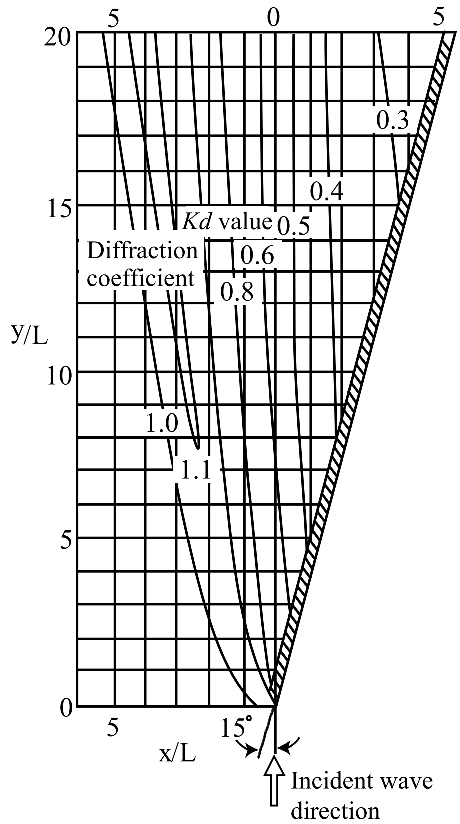

(c) θ_0=15°

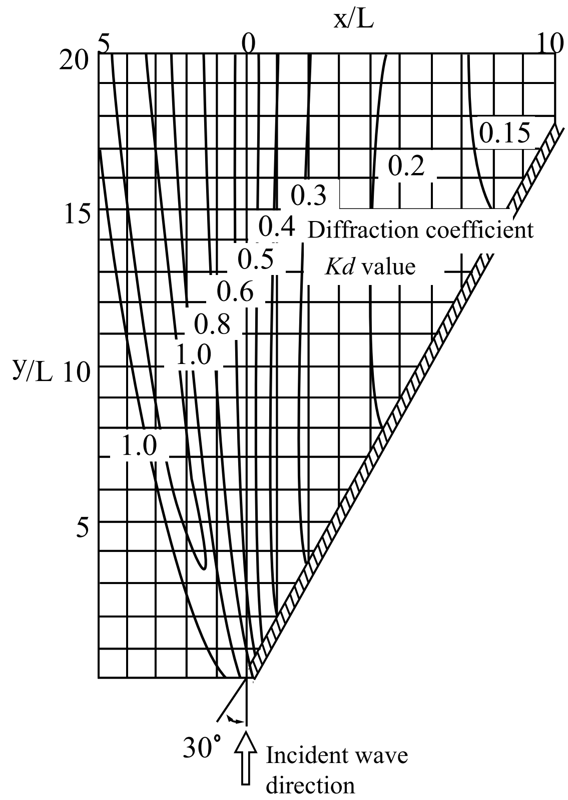

(d) θ_0=30°

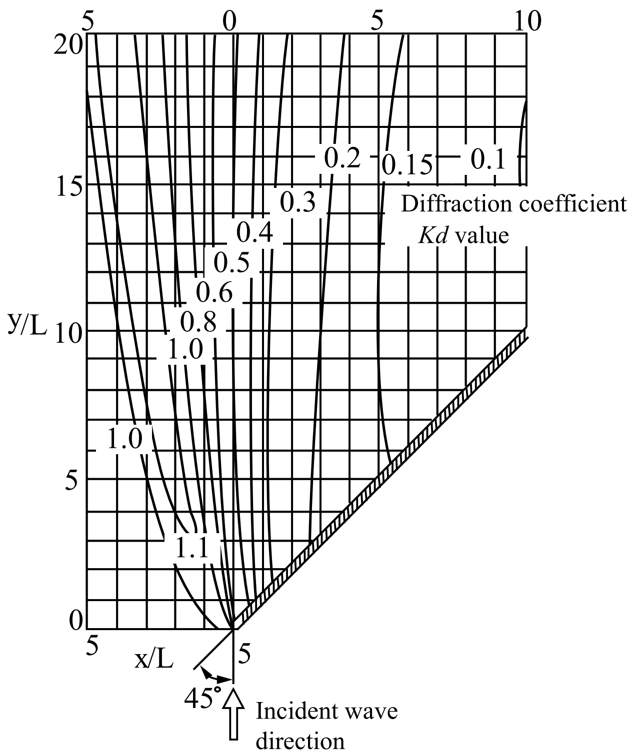

(e) θ_0=45°

Fig. 1.1.15 (c) to (e) Diffraction Diagram for a Semi-Infinite Breakwater and Regular Waves

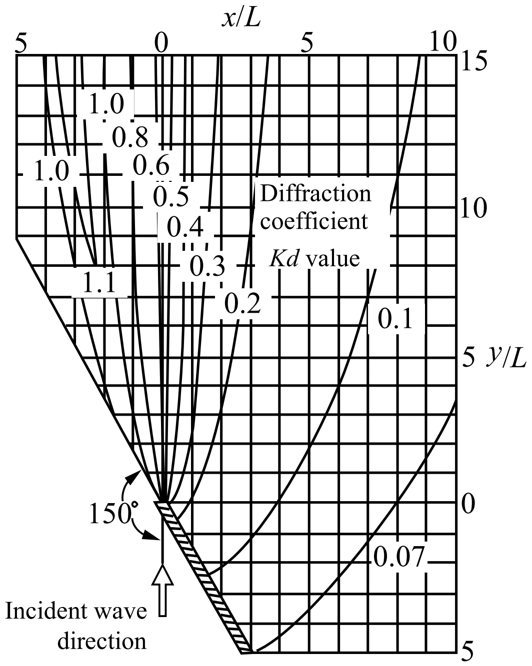

(f) θ_0=150°

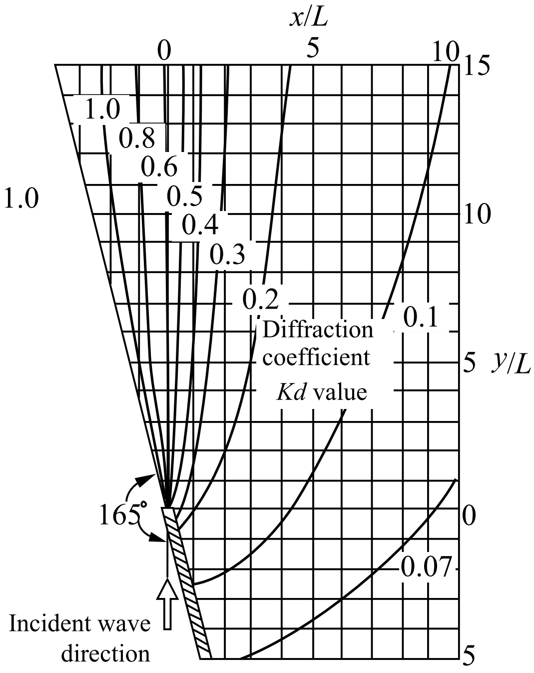

(g) θ_0=165°

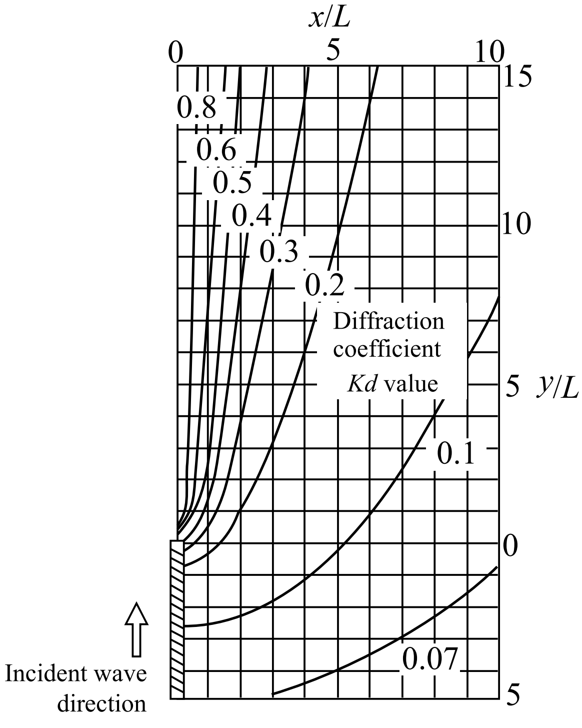

(h) θ_0=180°

Fig. 1.1.15 (f) to (h) Diffraction Diagram for a Semi-Infinite Breakwater and Regular Waves

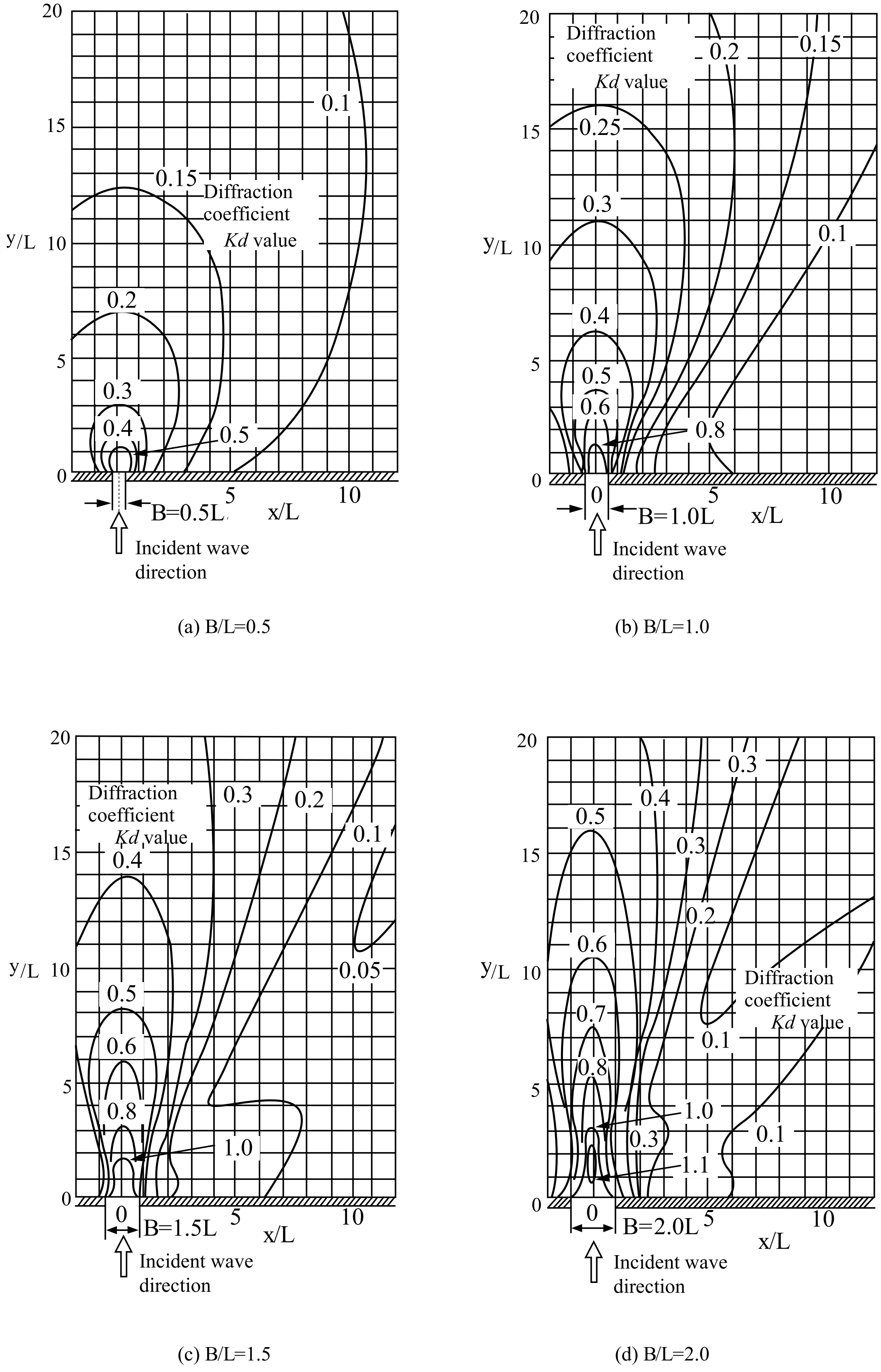

Fig. 1.1.16 (a) to (d) Diffraction Diagram for a Breakwater with Opening and Regular Waves

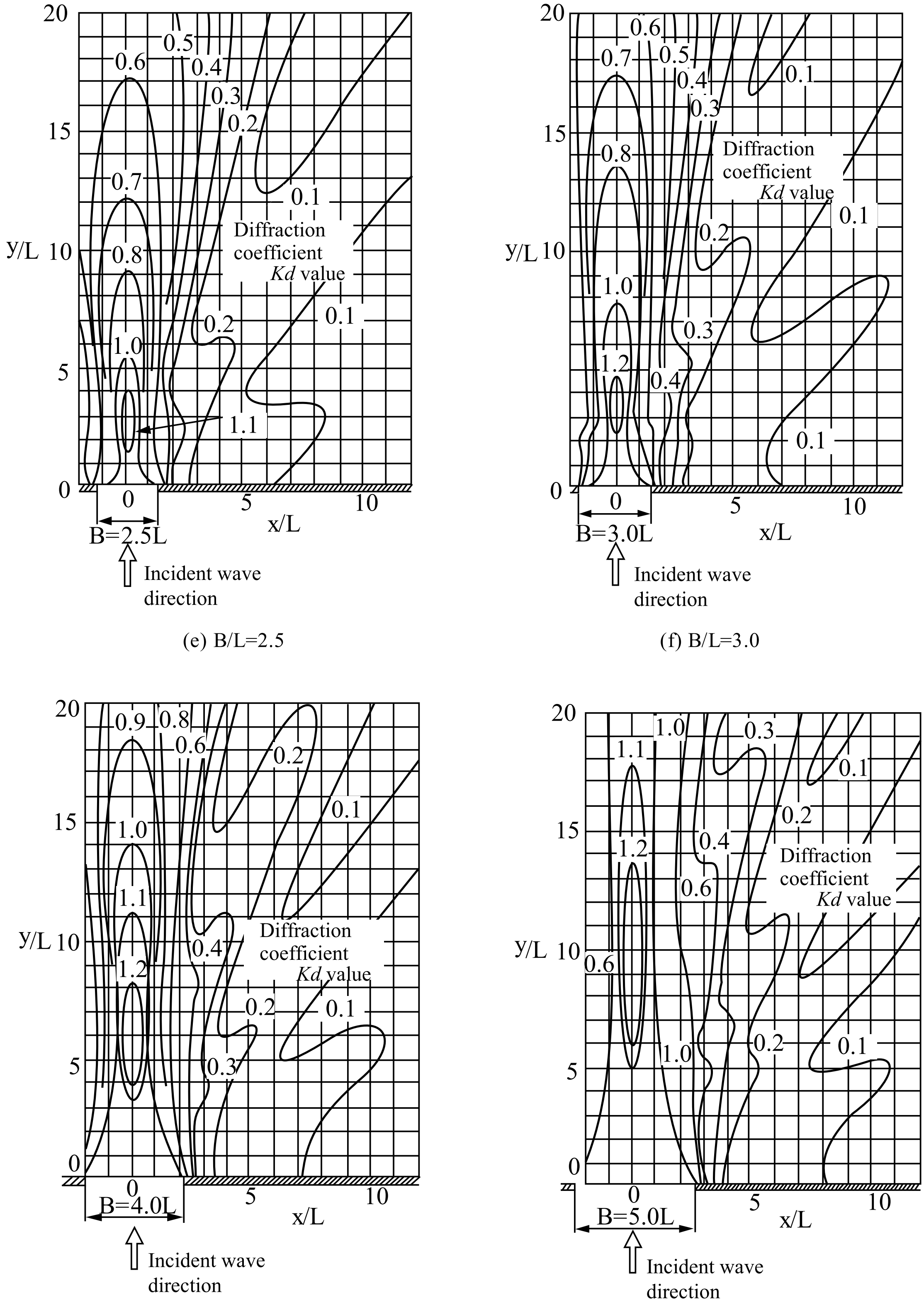

(e) B/L=2.5

(f) B/L=3.0

(g) B/L=4.0

(h) B/L=5.0

Fig. 1.1.16 (e) to (h) Diffraction Diagram for a Breakwater with Opening and Regular Waves

2 Numerical Tables for the Calculation of the Bending Moments of Slabs

(1) General

The numerical tables for the calculation of the bending moments of slabs[1)] are intended to be used in determining the bending moments of slabs supported on three sides and free on one side and slabs supported on four sides when they are subjected to a uniformly distributed load or a triangularly distributed load.

The basic equation for a thin slab (**equation [2.1.1])** was solved by using an analytical method, i.e., by superposing several Levy-type solutions and determining a constant of integration to satisfy the required support condition. The constant of integration was determined by expanding the conditional expression in a Fourier series.

$$\frac{\partial^4 w}{\partial x^4}+2\frac{\partial^4 w}{\partial x^2 \partial y^2}+\frac{\partial^4 w}{\partial y^4}=\frac{P}{D} \tag{2.1.1}$$

where

w : deflection (m)

P : load intensity (kN/m^2)

D : rigidity of the slab (kN･m) $D=\dfrac{Et^3}{12(1-\nu^2)}$

E : Yang's modulus of the slab (kN/m^2)

t : thickness of the slab (m)

ν : Poisson's ratio $\nu=\dfrac{1}{6}$

(2) Numerical tables for slabs supported on three sides and free on one side

Each numerical table is based on a grid of points represented by xy coordinates, in which the y-direction and x-direction correspond to the direction of the free side and the direction perpendicular to the free side, respectively. The side in the y-direction is divided into four equal parts, and the side in the x-direction is divided into six or eight equal parts (**Figs. 2.1.1 [a]** and **[b]**).

The bending moment at each grid point is determined by using **equations (2.1.2)** and **(2.1.3)**.

When $\lambda \le 1$,

$$M_x = Xq{l_x}^2 \qquad M_y = Yq{l_x}^2 \tag{2.1.2}$$

When $\lambda > 1$,

$$M_x = Xq{l_y}^2 \qquad M_y = Yq{l_y}^2 \tag{2.1.3}$$

where

λ : ratio of side lengths $\lambda = l_x / l_y$

M_x, M_y: bending moment in the x- or y-direction at a given point (kN･m/m)

X, Y : bending moment coefficient in the x- or y-direction at a given point

l_x, l_y : length in the x- or y-direction (m)

q : load intensity for a uniformly distributed load or maximum load intensity for a triangularly distributed load (kN/m^2)

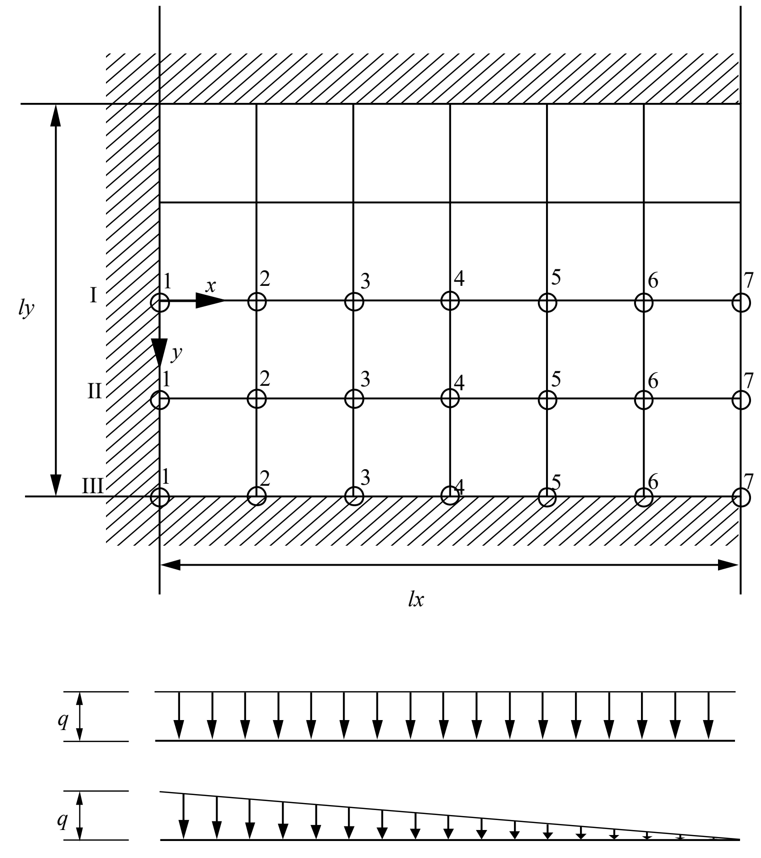

Fig. 2.1.1 (a) Slab Supported on Three Sides and Free on One Side

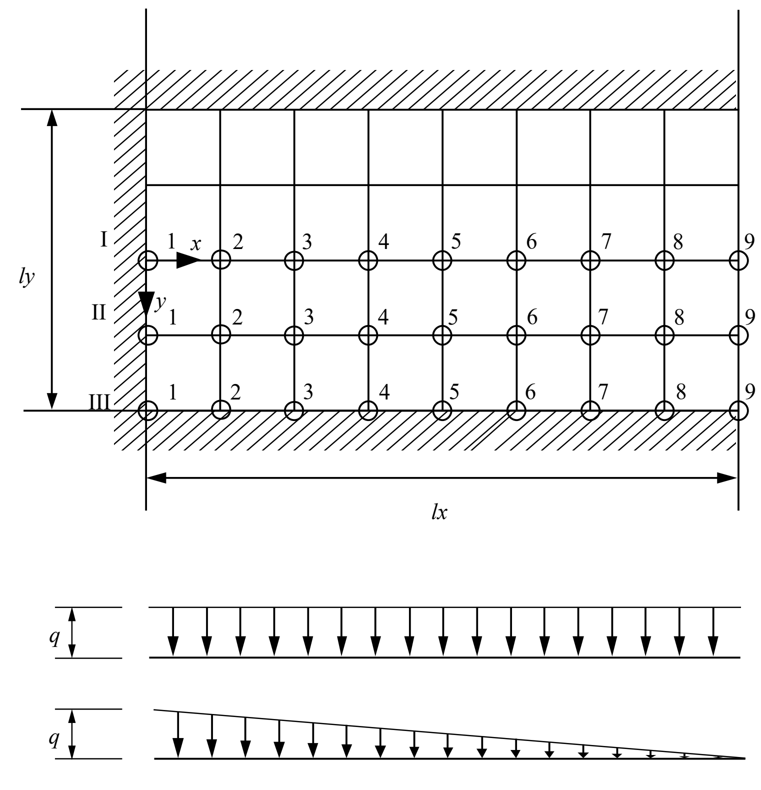

Fig. 2.1.1 (b) Slab Supported on Three Sides and Free on One Side

(3) Numerical tables for slabs supported on four sides

Each numerical table is based on a grid of points represented by *xy* coordinates, in which the *x*- and *y*-directions are determined as shown in **Fig. 2.1.2**, and each side is divided into four equal parts. The bending moment at each grid point is determined by using **equations (2.1.2)** and **(2.1.3)**.

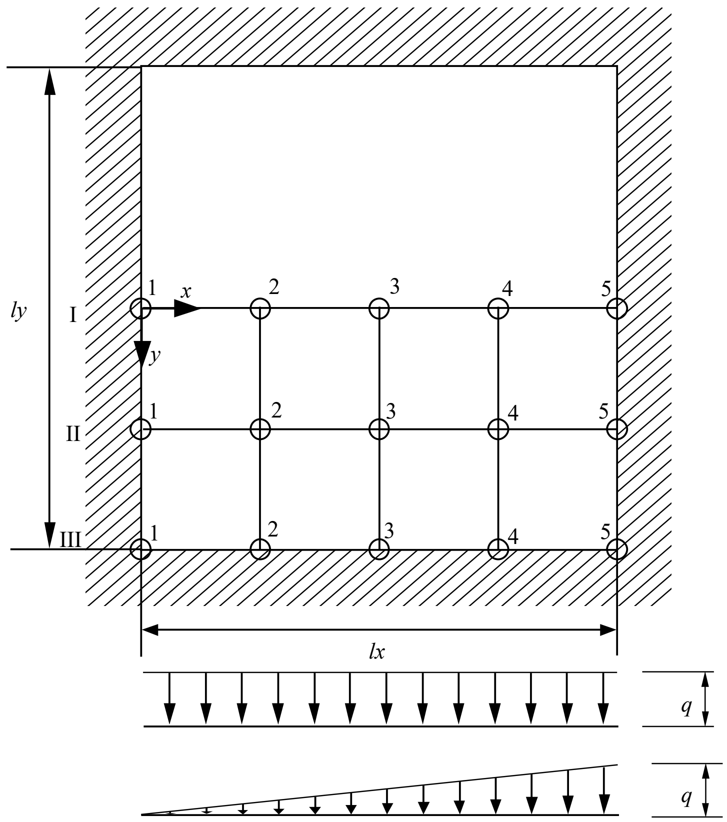

Fig. 2.1.2 Slab Supported on Four Sides

(4) Numerical tables for calculation

For the bending moment coefficient for slabs supported on three sides and free on one side, refer to **Tables 2.1.1 (a)** to **(g)** or **Tables 2.1.2 (a)** to **(g)** when the side in the *x*-direction is divided into six equal parts or eight equal parts, respectively.

For the bending moment coefficient for slabs supported on four sides, refer to **Tables 2.1.3 (a)** to **(e)**.

Table 2.1.1 Numerical Tables for the Calculation of a Slab Supported on Three Sides and Free on One Side (When the Side in the *X*-Direction is Divided into Six Equal Parts and the Side in the *Y*-Direction is Divided into Four Equal Parts)

(a) λ=0.30, 0.40, 0.50

λ	Load	Bending moment coefficient	Coordinate	1	2	3	4	5	6	7
0.30	Uniformly distributed load	*X*	I	−0.3819	−0.2308	−0.1193	−0.0434	0.0002	0.0143	0
			II	−0.2656	−0.1504	−0.0723	−0.0230	0.0035	0.0108	0
			III	0	−0.0031	−0.0128	−0.0249	−0.0379	−0.0533	0
		Y	I	−0.0636	−0.0347	−0.0061	0.0204	0.0436	0.0625	0.0762
			II	−0.0443	−0.0206	0.0024	0.0226	0.0391	0.0519	0.0614
			III	0	−0.0186	−0.0770	−0.1495	−0.2277	−0.3196	−0.4201
	Triangularly distributed load	*X*	I	−0.1353	−0.0654	−0.0219	0.0009	0.0086	0.0067	0
			II	−0.1021	−0.0427	−0.0095	0.0053	0.0082	0.0049	0
			III	0	−0.0023	−0.0061	−0.0092	−0.0116	−0.0141	0
		Y	I	−0.0225	−0.0098	0.0002	0.0078	0.0134	0.0175	0.0207
			II	−0.0170	−0.0056	0.0032	0.0091	0.0127	0.0148	0.0164
			III	0	−0.0137	−0.0366	−0.0554	−0.0697	−0.0845	−0.0981
0.40	Uniformly distributed load	*X*	I	−0.2840	−0.1497	−0.0596	−0.0051	0.0207	0.0220	0
			II	−0.1819	−0.0908	−0.0342	−0.0024	0.0111	0.0113	0
			III	0	−0.0033	−0.0127	−0.0236	−0.0346	−0.0468	0
		Y	I	−0.0473	−0.0188	0.0112	0.0397	0.0645	0.0848	0.1004
			II	−0.0303	−0.0109	0.0074	0.0229	0.0353	0.0448	0.0523
			III	0	−0.0195	−0.0761	−0.1419	−0.2078	−0.2811	−0.3553
	Triangularly distributed load	*X*	I	−0.1084	−0.0431	−0.0058	0.0109	0.0136	0.0084	0
			II	−0.0770	−0.0257	0.0002	0.0094	0.0090	0.0044	0
			III	0	−0.0023	−0.0061	−0.0089	−0.0107	−0.0124	0
		Y	I	−0.0181	−0.0054	0.0052	0.0135	0.0196	0.0239	0.0274
			II	−0.0128	−0.0025	0.0051	0.0096	0.0117	0.0126	0.0133
			III	0	−0.0140	−0.0364	−0.0533	−0.0644	−0.0743	−0.0810
0.50	Uniformly distributed load	*X*	I	−0.2053	−0.0916	−0.0229	0.0136	0.0269	0.0220	0
			II	−0.1269	−0.0538	−0.0124	0.0075	0.0131	0.0098	0
			III	0	−0.0034	−0.0122	−0.0216	−0.0301	−0.0389	0
		Y	I	−0.0342	−0.0079	0.0203	0.0465	0.0688	0.0866	0.1005
			II	−0.0212	−0.0051	0.0093	0.0207	0.0293	0.0356	0.0410
			III	0	−0.0205	−0.0733	−0.1294	−0.1806	−0.2334	−0.2818
	Triangularly distributed load	*X*	I	−0.0858	−0.0267	0.0040	0.0151	0.0144	0.0078	0
			II	−0.0594	−0.0149	0.0051	0.0106	0.0084	0.0035	0
			III	0	−0.0024	−0.0059	−0.0083	−0.0095	−0.0102	0
		Y	I	−0.0143	−0.0021	0.0082	0.0160	0.0212	0.0246	0.0273
			II	−0.0099	−0.0006	0.0059	0.0091	0.0100	0.0097	0.0098
			III	0	−0.0143	−0.0356	−0.0499	−0.0570	−0.0615	−0.0613

Table 2.1.1 Numerical Tables for the Calculation of a Slab Supported on Three Sides and Free on One Side (When the Side in the *X*-direction is Divided into Six Equal Parts and the Side in the *Y*-direction is Divided into Four Equal Parts)

(b) $\lambda = 0.75, 1.00, 1.25$

λ	Load	Bending moment coefficient	Coordinate	1	2	3	4	5	6	7
0.75	Uniformly distributed load	*X*	I	−0.0990	−0.0258	0.0080	0.0197	0.0198	0.0132	0
			II	−0.0602	−0.0145	0.0049	0.0103	0.0088	0.0048	0
			III	0	−0.0035	−0.0101	−0.0156	−0.0195	−0.0227	0
		Y	I	−0.0165	0.0032	0.0236	0.0406	0.0531	0.0619	0.0688
			II	−0.0100	0.0009	0.0093	0.0144	0.0173	0.0189	0.0205
			III	0	−0.0209	−0.0606	−0.0939	−0.1172	−0.1361	−0.1477
	Triangularly distributed load	*X*	I	−0.0519	−0.0067	0.0110	0.0137	0.0095	0.0038	0
			II	−0.0348	−0.0030	0.0075	0.0080	0.0048	0.0013	0
			III	0	−0.0024	−0.0053	−0.0066	−0.0065	−0.0058	0
		Y	I	−0.0087	0.0020	0.0105	0.0155	0.0173	0.0174	0.0175
			II	−0.0058	0.0016	0.0059	0.0070	0.0061	0.0047	0.0037
			III	0	−0.0143	−0.0317	−0.0394	−0.0389	−0.0347	−0.0260
1.00	Uniformly distributed load	*X*	I	−0.0565	−0.0063	0.0106	0.0133	0.0110	0.0069	0
			II	−0.0343	−0.0034	0.0058	0.0064	0.0044	0.0020	0
			III	0	−0.0032	−0.0080	−0.0111	−0.0127	−0.0137	0
		Y	I	−0.0094	0.0059	0.0203	0.0304	0.0364	0.0398	0.0428
			II	−0.0057	0.0023	0.0075	0.0098	0.0105	0.0108	0.0111
			III	0	−0.0195	−0.0478	−0.0665	−0.0763	−0.0822	−0.0838
	Triangularly distributed load	*X*	I	−0.0350	−0.0001	0.0097	0.0089	0.0049	0.0013	0
			II	−0.0229	0.0006	0.0058	0.0047	0.0022	0.0002	0
			III	0	−0.0023	−0.0045	−0.0050	−0.0044	−0.0033	0
		Y	I	−0.0058	0.0035	0.0103	0.0129	0.0124	0.0106	0.0094
			II	−0.0038	0.0021	0.0049	0.0049	0.0038	0.0024	0.0013
			III	0	−0.0137	−0.0270	−0.0300	−0.0261	−0.0196	−0.0108
1.25	Uniformly distributed load	*X*	I	−0.0567	0	0.0133	0.0128	0.0096	0.0061	0
			II	−0.0344	0.0003	0.0069	0.0056	0.0033	0.0014	0
			III	0	−0.0046	−0.0098	−0.0125	−0.0135	−0.0139	0
		Y	I	−0.0095	0.0098	0.0261	0.0354	0.0395	0.0413	0.0435
			II	−0.0057	0.0039	0.0090	0.0106	0.0107	0.0106	0.0107
			III	0	−0.0273	−0.0587	−0.0749	−0.0810	−0.0835	−0.0833
	Triangularly distributed load	*X*	I	−0.0391	0.0035	0.0112	0.0083	0.0038	0.0005	0
			II	−0.0251	0.0026	0.0063	0.0041	0.0014	−0.0002	0
			III	0	−0.0033	−0.0059	−0.0059	−0.0047	−0.0030	0
		Y	I	−0.0065	0.0064	0.0146	0.0162	0.0137	0.0101	0.0079
			II	−0.0042	0.0033	0.0060	0.0054	0.0038	0.0021	0.0008
			III	0	−0.0199	−0.0352	−0.0356	−0.0279	−0.0183	−0.0078

Table 2.1.1 Numerical Tables for the Calculation of a Slab Supported on Three Sides and Free on One Side (When the Side in the *X*-Direction is Divided into Six Equal Parts and the Side in the *Y*-Direction is Divided into Four Equal Parts)

(c) λ = 1.50, 1.75, 2.00

λ	Load	Bending moment coefficient	Coordinate	1	2	3	4	5	6	7
1.50	Uniformly distributed load	*X*	I	−0.0568	0.0048	0.0139	0.0113	0.0083	0.0058	0
			II	−0.0344	0.0029	0.0068	0.0045	0.0025	0.0011	0
			III	0	−0.0058	−0.0112	−0.0133	−0.0138	−0.0139	0
		Y	I	−0.0095	0.0136	0.0307	0.0384	0.0409	0.0416	0.0434
			II	−0.0057	0.0053	0.0100	0.0108	0.0106	0.0104	0.0105
			III	0	−0.0350	−0.0669	−0.0797	−0.0829	−0.0835	−0.0834
	Triangularly distributed load	*X*	I	−0.0420	0.0065	0.0114	0.0071	0.0029	0.0001	0
			II	−0.0266	0.0042	0.0060	0.0031	0.0009	−0.0004	0
			III	0	−0.0044	−0.0070	−0.0065	−0.0047	−0.0028	0
		Y	I	−0.0070	0.0094	0.0183	0.0184	0.0142	0.0094	0.0065
			II	−0.0044	0.0045	0.0067	0.0056	0.0037	0.0019	0.0006
			III	0	−0.0263	−0.0419	−0.0390	−0.0284	−0.0168	−0.0060
1.75	Uniformly distributed load	*X*	I	−0.0568	0.0082	0.0135	0.0099	0.0075	0.0058	0
			II	−0.0344	0.0047	0.0062	0.0035	0.0020	0.0010	0
			III	0	−0.0070	−0.0122	−0.0137	−0.0139	−0.0139	0
		Y	I	−0.0095	0.0172	0.0342	0.0402	0.0414	0.0415	0.0433
			II	−0.0057	0.0065	0.0105	0.0108	0.0105	0.0104	0.0104
			III	0	−0.0421	−0.0730	−0.0823	−0.0836	−0.0833	−0.0840
	Triangularly distributed load	*X*	I	−0.0441	0.0088	0.0108	0.0059	0.0024	0.0001	0
			II	−0.0277	0.0053	0.0053	0.0023	0.0006	−0.0004	0
			III	0	−0.0054	−0.0078	−0.0068	−0.0047	−0.0026	0
		Y	I	−0.0074	0.0124	0.0212	0.0197	0.0142	0.0087	0.0055
			II	−0.0046	0.0054	0.0071	0.0055	0.0036	0.0018	0.0004
			III	0	−0.0324	−0.0470	−0.0410	−0.0283	−0.0155	−0.0049
2.00	Uniformly distributed load	*X*	I	−0.0568	0.0107	0.0125	0.0087	0.0071	0.0060	0
			II	−0.0344	0.0058	0.0054	0.0028	0.0018	0.0011	0
			III	0	−0.0081	−0.0129	−0.0139	−0.0140	−0.0139	0
		Y	I	−0.0095	0.0205	0.0367	0.0411	0.0416	0.0415	0.0432
			II	−0.0057	0.0076	0.0107	0.0107	0.0105	0.0103	0.0104
			III	0	−0.0487	−0.0773	−0.0836	−0.0838	−0.0833	−0.0846
	Triangularly distributed load	*X*	I	−0.0457	0.0105	0.0099	0.0050	0.0022	0.0002	0
			II	−0.0285	0.0060	0.0045	0.0017	0.0004	−0.0003	0
			III	0	−0.0064	−0.0085	−0.0070	−0.0047	−0.0024	0
		Y	I	−0.0076	0.0153	0.0234	0.0204	0.0142	0.0082	0.0047
			II	−0.0048	0.0063	0.0073	0.0055	0.0035	0.0017	0.0004
			III	0	−0.0382	−0.0508	−0.0420	−0.0280	−0.0145	−0.0041

Table 2.1.1 Numerical Tables for the Calculation of a Slab Supported on Three Sides and Free on One Side (When the Side in the *X*-Direction is Divided into Six Equal Parts and the Side in the *Y*-Direction is Divided into Four Equal Parts)

(d) λ=2.25, 2.50, 2.75

λ	Load	Bending moment coefficient	Coordinate	1	2	3	4	5	6	7
2.25	Uniformly distributed load	*X*	I	−0.0567	0.0122	0.0114	0.0080	0.0070	0.0062	0
			II	−0.0343	0.0065	0.0046	0.0023	0.0017	0.0012	0
			III	0	−0.0091	−0.0134	−0.0140	−0.0140	−0.0139	0
		Y	I	−0.0095	0.0235	0.0386	0.0416	0.0416	0.0414	0.0432
			II	−0.0057	0.0084	0.0108	0.0106	0.0104	0.0103	0.0105
			III	0	−0.0546	−0.0802	−0.0842	−0.0839	−0.0834	−0.0852
	Triangularly distributed load	*X*	I	−0.0469	0.0117	0.0089	0.0043	0.0021	0.0003	0
			II	−0.0291	0.0064	0.0038	0.0013	0.0004	−0.0002	0
			III	0	−0.0072	−0.0089	−0.0071	−0.0046	−0.0023	0
		Y	I	−0.0078	0.0179	0.0250	0.0208	0.0141	0.0078	0.0042
			II	−0.0049	0.0070	0.0074	0.0054	0.0035	0.0017	0.0003
			III	0	−0.0434	−0.0534	−0.0424	−0.0277	−0.0137	−0.0034
2.50	Uniformly distributed load	*X*	I	−0.0567	0.0132	0.0104	0.0075	0.0069	0.0063	0
			II	−0.0342	0.0067	0.0039	0.0020	0.0017	0.0013	0
			III	0	−0.0100	−0.0137	−0.0141	−0.0140	−0.0139	0
		Y	I	−0.0094	0.0262	0.0398	0.0417	0.0416	0.0414	0.0432
			II	−0.0057	0.0090	0.0109	0.0106	0.0104	0.0103	0.0105
			III	0	−0.0598	−0.0822	−0.0844	−0.0840	−0.0837	−0.0858
	Triangularly distributed load	*X*	I	−0.0478	0.0123	0.0079	0.0039	0.0021	0.0005	0
			II	−0.0296	0.0065	0.0031	0.0011	0.0004	−0.0001	0
			III	0	−0.0080	−0.0092	−0.0071	−0.0046	−0.0022	0
		Y	I	−0.0080	0.0204	0.0262	0.0209	0.0140	0.0075	0.0038
			II	−0.0049	0.0075	0.0074	0.0053	0.0034	0.0017	0.0003
			III	0	−0.0482	−0.0553	−0.0426	−0.0275	−0.0131	−0.0027
2.75	Uniformly distributed load	*X*	I	−0.0566	0.0136	0.0096	0.0072	0.0069	0.0065	0
			II	−0.0341	0.0067	0.0033	0.0018	0.0016	0.0014	0
			III	0	−0.0107	−0.0139	−0.0141	−0.0140	−0.0140	0
		Y	I	−0.0094	0.0286	0.0407	0.0418	0.0416	0.0414	0.0432
			II	−0.0057	0.0096	0.0108	0.0105	0.0104	0.0103	0.0105
			III	0	−0.0644	−0.0836	−0.0845	−0.0841	−0.0840	−0.0863
	Triangularly distributed load	*X*	I	−0.0486	0.0126	0.0071	0.0037	0.0021	0.0006	0
			II	−0.0299	0.0064	0.0026	0.0009	0.0005	0	0
			III	0	−0.0087	−0.0094	−0.0071	−0.0046	−0.0021	0
		Y	I	−0.0081	0.0226	0.0269	0.0209	0.0139	0.0074	0.0034
			II	−0.0050	0.0080	0.0073	0.0053	0.0034	0.0017	0.0003
			III	0	−0.0524	−0.0566	−0.0427	−0.0273	−0.0126	−0.0021

Table 2.1.1 Numerical Tables for the Calculation of a Slab Supported on Three Sides and Free on One Side (When the Side in the *X*-Direction is Divided into Six Equal Parts and the Side in the *Y*-Direction is Divided into Four Equal Parts)

(e) $\lambda = 3.00, 3.25, 3.50$

λ	Load	Bending moment coefficient	Coordinate	1	2	3	4	5	6	7
3.00	Uniformly distributed load	*X*	I	−0.0565	0.0137	0.0089	0.0070	0.0069	0.0066	0
			II	−0.0339	0.0065	0.0028	0.0017	0.0016	0.0015	0
			III	0	−0.0114	−0.0141	−0.0141	−0.0140	−0.0141	0
		Y	I	−0.0094	0.0308	0.0412	0.0418	0.0416	0.0414	0.0432
			II	−0.0057	0.0100	0.0108	0.0105	0.0104	0.0103	0.0105
			III	0	−0.0685	−0.0845	−0.0845	−0.0843	−0.0843	−0.0868
	Triangularly distributed load	*X*	I	−0.0492	0.0126	0.0064	0.0036	0.0021	0.0007	0
			II	−0.0301	0.0062	0.0021	0.0009	0.0005	0.0001	0
			III	0	−0.0094	−0.0096	−0.0071	−0.0045	−0.0020	0
		Y	I	−0.0082	0.0245	0.0274	0.0209	0.0139	0.0072	0.0031
			II	−0.0050	0.0084	0.0073	0.0053	0.0034	0.0017	0.0003
			III	0	−0.0561	−0.0576	−0.0428	−0.0272	−0.0121	−0.0015
3.25	Uniformly distributed load	*X*	I	−0.0565	0.0136	0.0083	0.0070	0.0068	0.0067	0
			II	−0.0338	0.0062	0.0025	0.0017	0.0015	0.0015	0
			III	0	−0.0120	−0.0142	−0.0141	−0.0141	−0.0141	0
		Y	I	−0.0094	0.0326	0.0415	0.0418	0.0416	0.0414	0.0432
			II	−0.0056	0.0103	0.0107	0.0105	0.0104	0.0104	0.0105
			III	0	−0.0720	−0.0851	−0.0846	−0.0845	−0.0847	−0.0872
	Triangularly distributed load	*X*	I	−0.0496	0.0123	0.0059	0.0035	0.0022	0.0008	0
			II	−0.0302	0.0058	0.0018	0.0008	0.0005	0.0002	0
			III	0	−0.0099	−0.0097	−0.0071	−0.0045	−0.0019	0
		Y	I	−0.0083	0.0263	0.0277	0.0209	0.0139	0.0071	0.0029
			II	−0.0050	0.0086	0.0072	0.0052	0.0034	0.0017	0.0003
			III	0	−0.0594	−0.0583	−0.0428	−0.0271	−0.0116	−0.0008
3.50	Uniformly distributed load	*X*	I	−0.0564	0.0132	0.0079	0.0069	0.0068	0.0067	0
			II	−0.0335	0.0058	0.0022	0.0016	0.0015	0.0015	0
			III	0	−0.0125	−0.0143	−0.0141	−0.0141	−0.0142	0
		Y	I	−0.0094	0.0343	0.0417	0.0417	0.0416	0.0415	0.0432
			II	−0.0056	0.0105	0.0107	0.0104	0.0104	0.0104	0.0105
			III	0	−0.0750	−0.0855	−0.0846	−0.0847	−0.0851	−0.0877
	Triangularly distributed load	*X*	I	−0.0500	0.0119	0.0055	0.0035	0.0022	0.0009	0
			II	−0.0303	0.0054	0.0015	0.0008	0.0005	0.0003	0
			III	0	−0.0104	−0.0098	−0.0072	−0.0045	−0.0019	0
		Y	I	−0.0083	0.0278	0.0279	0.0209	0.0139	0.0071	0.0027
			II	−0.0050	0.0088	0.0072	0.0052	0.0034	0.0017	0.0003
			III	0	−0.0622	−0.0588	−0.0429	−0.0269	−0.0112	−0.0002

Table 2.1.1 Numerical Tables for the Calculation of a Slab Supported on Three Sides and Free on One Side (When the Side in the *X*-Direction is Divided into Six Equal Parts and the Side in the *Y*-Direction is Divided into Four Equal Parts)

(f) $\lambda = 3.75, 4.00, 4.25$

λ	Load	Bending moment coefficient	Coordinate	1	2	3	4	5	6	7
3.75	Uniformly distributed load	*X*	I	−0.0564	0.0127	0.0076	0.0069	0.0068	0.0068	0
			II	−0.0331	0.0053	0.0020	0.0016	0.0014	0.0014	0
			III	0	−0.0129	−0.0143	−0.0141	−0.0141	−0.0143	0
		Y	I	−0.0094	0.0356	0.0418	0.0417	0.0416	0.0415	0.0434
			II	−0.0055	0.0106	0.0106	0.0104	0.0104	0.0104	0.0104
			III	0	−0.0775	−0.0859	−0.0848	−0.0848	−0.0856	−0.0881
	Triangularly distributed load	*X*	I	−0.0505	0.0114	0.0052	0.0034	0.0022	0.0010	0
			II	−0.0302	0.0049	0.0013	0.0008	0.0005	0.0004	0
			III	0	−0.0108	−0.0099	−0.0072	−0.0045	−0.0018	0
		Y	I	−0.0084	0.0291	0.0280	0.0209	0.0138	0.0070	0.0025
			II	−0.0050	0.0089	0.0071	0.0052	0.0034	0.0017	0.0003
			III	0	−0.0647	−0.0593	−0.0431	−0.0268	−0.0107	0.0005
4.00	Uniformly distributed load	*X*	I	−0.0568	0.0121	0.0075	0.0069	0.0067	0.0068	0
			II	−0.0324	0.0048	0.0019	0.0016	0.0014	0.0014	0
			III	0	−0.0133	−0.0144	−0.0142	−0.0142	−0.0143	0
		Y	I	−0.0095	0.0368	0.0419	0.0417	0.0417	0.0415	0.0433
			II	−0.0054	0.0107	0.0106	0.0104	0.0104	0.0104	0.0105
			III	0	−0.0797	−0.0862	−0.0850	−0.0850	−0.0860	−0.0886
	Triangularly distributed load	*X*	I	−0.0505	0.0108	0.0050	0.0034	0.0022	0.0011	0
			II	−0.0302	0.0044	0.0011	0.0007	0.0005	0.0005	0
			III	0	−0.0111	−0.0100	−0.0072	−0.0044	−0.0017	0
		Y	I	−0.0084	0.0302	0.0280	0.0209	0.0138	0.0069	0.0023
			II	−0.0050	0.0090	0.0071	0.0052	0.0034	0.0017	0.0003
			III	0	−0.0668	−0.0598	−0.0432	−0.0266	−0.0103	0.0012
4.25	Uniformly distributed load	*X*	I	−0.0560	0.0115	0.0073	0.0069	0.0067	0.0068	0
			II	−0.0325	0.0044	0.0018	0.0015	0.0013	0.0013	0
			III	0	−0.0136	−0.0144	−0.0142	−0.0142	−0.0144	0
		Y	I	−0.0093	0.0378	0.0419	0.0417	0.0417	0.0416	0.0433
			II	−0.0054	0.0108	0.0106	0.0104	0.0104	0.0104	0.0105
			III	0	−0.0816	−0.0866	−0.0852	−0.0852	−0.0865	−0.0891
	Triangularly distributed load	*X*	I	−0.0507	0.0102	0.0049	0.0034	0.0021	0.0012	0
			II	−0.0301	0.0039	0.0010	0.0007	0.0005	0.0007	0
			III	0	−0.0114	−0.0100	−0.0072	−0.0044	−0.0016	0
		Y	I	−0.0085	0.0311	0.0280	0.0209	0.0138	0.0069	0.0022
			II	−0.0050	0.0090	0.0070	0.0052	0.0034	0.0017	0.0004
			III	0	−0.0687	−0.0603	−0.0434	−0.0265	−0.0098	0.0018

Table 2.1.1 Numerical Tables for the Calculation of a Slab Supported on Three Sides and Free on One Side (When the Side in the *X*-Direction is Divided into Six Equal Parts and the Side in the *Y*-Direction is Divided into Four Equal Parts)

(g) λ=4.50, 4.75, 5.00

λ	Load	Bending moment coefficient	Coordinate	1	2	3	4	5	6	7
4.50	Uniformly distributed load	*X*	I	−0.0560	0.0109	0.0072	0.0068	0.0066	0.0067	0
			II	−0.0322	0.0039	0.0017	0.0015	0.0013	0.0013	0
			III	0	−0.0139	−0.0145	−0.0142	−0.0142	-0.0145	0
		Y	I	−0.0093	0.0387	0.0419	0.0417	0.0417	0.0416	0.0435
			II	−0.0054	0.0108	0.0105	0.0104	0.0103	0.0104	0.0106
			III	0	−0.0832	−0.0869	−0.0854	−0.0854	−0.0869	−0.0896
	Triangularly distributed load	*X*	I	−0.0510	0.0096	0.0048	0.0034	0.0021	0.0012	0
			II	−0.0300	0.0034	0.0009	0.0006	0.0005	0.0008	0
			III	0	−0.0117	−0.0101	−0.0073	−0.0044	−0.0016	0
		Y	I	−0.0085	0.0319	0.0280	0.0209	0.0138	0.0068	0.0021
			II	−0.0050	0.0090	0.0070	0.0052	0.0034	0.0017	0.0005
			III	0	−0.0703	−0.0608	−0.0436	−0.0263	−0.0093	0.0025
4.75	Uniformly distributed load	*X*	I	−0.0555	0.0103	0.0072	0.0068	0.0065	0.0067	0
			II	−0.0315	0.0034	0.0016	0.0014	0.0012	0.0012	0
			III	0	−0.0141	−0.0146	−0.0143	−0.0143	−0.0146	0
		Y	I	−0.0092	0.0394	0.0419	0.0417	0.0417	0.0417	0.0433
			II	−0.0052	0.0107	0.0105	0.0104	0.0103	0.0103	0.0104
			III	0	−0.0846	−0.0873	−0.0856	−0.0856	−0.0874	−0.0901
	Triangularly distributed load	*X*	I	−0.0508	0.0090	0.0047	0.0034	0.0021	0.0014	0
			II	−0.0296	0.0029	0.0007	0.0006	0.0006	0.0009	0
			III	0	−0.0120	−0.0102	−0.0073	−0.0044	−0.0015	0
		Y	I	−0.0085	0.0326	0.0281	0.0209	0.0138	0.0068	0.0020
			II	−0.0049	0.0090	0.0070	0.0052	0.0034	0.0018	0.0006
			III	0	−0.0717	−0.0613	−0.0438	−0.0261	−0.0088	0.0032
5.00	Uniformly distributed load	*X*	I	−0.0552	0.0097	0.0071	0.0068	0.0065	0.0066	0
			II	−0.0309	0.0030	0.0015	0.0014	0.0011	0.0011	0
			III	0	−0.0143	−0.0146	−0.0143	−0.0143	−0.0147	0
		Y	I	−0.0092	0.0399	0.0419	0.0417	0.0417	0.0417	0.0433
			II	−0.0052	0.0107	0.0105	0.0103	0.0103	0.0103	0.0103
			III	0	−0.0858	−0.0877	−0.0858	−0.0858	−0.0879	−0.0906
	Triangularly distributed load	*X*	I	−0.0508	0.0084	0.0046	0.0033	0.0021	0.0015	0
			II	−0.0292	0.0025	0.0006	0.0006	0.0006	0.0010	0
			III	0	−0.0122	−0.0103	−0.0073	−0.0043	−0.0014	0
		Y	I	−0.0085	0.0331	0.0281	0.0209	0.0138	0.0068	0.0019
			II	−0.0049	0.0090	0.0069	0.0052	0.0034	0.0018	0.0007
			III	0	−0.0729	−0.0619	−0.0440	−0.0259	−0.0083	0.0039

Table 2.1.2 Numerical Tables for the Calculation of a Slab Supported on Three Sides and Free on One Side (When the Side in the *X*-Direction is Divided into Eight Equal Parts and the Side in the *Y*-Direction is Divided into Four Equal Parts)

(a) λ=0.30, 0.40, 0.50

λ	Load	Bending moment coefficient	Coordinate	1	2	3	4	5	6	7	8	9
0.30	Uniformly distributed load	*X*	I	−0.3819	−0.2648	−0.1704	−0.0972	−0.0434	−0.0078	0.0109	0.0133	0
			II	−0.2656	−0.1754	−0.1074	−0.0576	−0.0230	−0.0012	0.0094	0.0098	0
			III	0	−0.0014	−0.0075	−0.0157	−0.0249	−0.0346	−0.0451	−0.0582	0
		Y	I	−0.0636	−0.0419	−0.0202	0.0007	0.0204	0.0382	0.0536	0.0665	0.0762
			II	−0.0443	−0.0266	−0.0089	0.0077	0.0226	0.0353	0.0459	0.0545	0.0614
			III	0	−0.0086	−0.0447	−0.0945	−0.1495	−0.2074	−0.2708	−0.3493	−0.4201
	Triangularly distributed load	*X*	I	−0.1353	−0.0802	−0.0407	−0.0145	0.0009	0.0078	0.0086	0.0053	0
			II	−0.1021	−0.0548	−0.0233	−0.0043	0.0053	0.0083	0.0071	0.0037	0
			III	0	−0.0014	−0.0042	−0.0069	−0.0092	-0.0111	−0.0129	−0.0151	0
		Y	I	−0.0225	−0.0128	−0.0045	0.0023	0.0078	0.0122	0.0156	0.0184	0.0207
			II	−0.0170	−0.0082	−0.0009	0.0049	0.0091	0.0120	0.0139	0.0152	0.0164
			III	0	−0.0083	−0.0251	−0.0416	−0.0554	−0.0666	−0.0773	−0.0907	−0.0981
0.40	Uniformly distributed load	*X*	I	−0.2840	−0.1787	−0.0997	−0.0430	−0.0051	0.0167	0.0243	0.0187	0
			II	−0.1819	−0.1099	−0.0589	−0.0242	−0.0024	0.0091	0.0127	0.0096	0
			III	0	−0.0016	−0.0076	−0.0154	−0.0236	−0.0319	−0.0406	−0.0511	0
		Y	I	−0.0473	−0.0262	−0.0037	0.0186	0.0397	0.0587	0.0752	0.0892	0.1004
			II	−0.0303	−0.0157	−0.0014	0.0115	0.0229	0.0325	0.0404	0.0468	0.0523
			III	0	−0.0097	−0.0457	−0.0925	−0.1419	−0.1914	−0.2434	−0.3064	−0.3553
	Triangularly distributed load	*X*	I	−0.1084	−0.0566	−0.0215	0	0.0109	0.0139	0.0117	0.0064	0
			II	−0.0770	−0.0357	−0.0102	0.0037	0.0094	0.0097	0.0070	0.0031	0
			III	0	−0.0014	−0.0042	−0.0068	−0.0089	−0.0104	-0.0117	−0.0132	0
		Y	I	−0.0181	−0.0084	0.0002	0.0075	0.0135	0.0182	0.0219	0.0249	0.0274
			II	−0.0128	−0.0049	0.0017	0.0065	0.0096	0.0114	0.0122	0.0127	0.0133
			III	0	−0.0085	−0.0253	-0.0411	−0.0533	−0.0623	−0.0700	−0.0793	−0.0810
0.50	Uniformly distributed load	*X*	I	−0.2053	-0.1153	−0.0526	-0.0112	0.0136	0.0254	0.0265	0.0181	0
			II	−0.1269	−0.0686	−0.0299	−0.0058	0.0075	0.0127	0.0123	0.0080	0
			III	0	−0.0018	−0.0076	−0.0146	−0.0216	−0.0281	−0.0345	−0.0421	0
		Y	I	−0.0342	−0.0149	0.0062	0.0271	0.0465	0.0637	0.0782	0.0904	0.1005
			II	−0.0212	−0.0090	0.0024	0.0124	0.0207	0.0273	0.0327	0.0370	0.041
			III	0	−0.0108	−0.0457	−0.0878	−0.1294	−0.1684	−0.2072	−0.2527	−0.2818
	Triangularly distributed load	*X*	I	−0.0858	−0.0385	−0.0084	0.0083	0.0151	0.0153	0.0115	0.0058	0
			II	−0.0594	−0.0233	−0.0026	0.0075	0.0106	0.0094	0.0060	0.0024	0
			III	0	−0.0015	−0.0042	−0.0066	−0.0083	−0.0093	−0.0100	−0.0108	0
		Y	I	−0.0143	−0.0050	0.0033	0.0104	0.0160	0.0201	0.0231	0.0253	0.0273
			II	−0.0099	−0.0027	0.0031	0.0070	0.0091	0.0099	0.0099	0.0097	0.0098
			III	0	−0.0088	−0.0253	−0.0398	−0.0499	−0.0561	−0.0602	−0.0648	−0.0613

Table 2.1.2 Numerical Tables for the Calculation of a Slab Supported on Three Sides and Free on One Side (When the Side in the *X*-Direction is Divided into Eight Equal Parts and the Side in the *Y*-Direction is Divided into Four Equal Parts)

(b) λ=0.75, 1.00, 1.25

λ	Load	Bending moment coefficient	Coordinate	1	2	3	4	5	6	7	8	9
0.75	Uniformly distributed load	*X*	I	-0.0990	-0.0395	-0.0053	0.0124	0.0197	0.0205	0.0172	0.0106	0
			II	-0.0602	-0.0229	-0.0025	0.0071	0.0103	0.0096	0.0070	0.0037	0
			III	0	-0.0020	-0.0068	-0.0117	-0.0156	-0.0187	-0.0213	-0.0240	0
		Y	I	-0.0165	-0.0020	0.0137	0.0283	0.0406	0.0504	0.0578	0.0637	0.0688
			II	-0.0100	-0.0017	0.0055	0.0109	0.0144	0.0167	0.0182	0.0192	0.0205
			III	0	-0.0121	-0.0410	-0.0700	-0.0939	-0.1123	-0.1276	-0.1442	-0.1477
	Triangularly distributed load	*X*	I	-0.0519	-0.0149	0.0047	0.0127	0.0137	0.0109	0.0066	0.0025	0
			II	-0.0348	-0.0083	0.0040	0.0082	0.0080	0.0058	0.0030	0.0007	0
			III	0	-0.0015	-0.0040	-0.0057	-0.0066	-0.0066	-0.0063	-0.0059	0
		Y	I	-0.0087	-0.0006	0.0066	0.0121	0.0155	0.0171	0.0175	0.0173	0.0175
			II	-0.0058	0	0.0042	0.0064	0.007	0.0065	0.0054	0.0044	0.0037
			III	0	-0.0091	-0.0238	-0.0344	-0.0394	-0.0399	-0.0378	-0.0351	-0.0260
1.00	Uniformly distributed load	*X*	I	-0.0565	-0.0147	0.0048	0.0121	0.0133	0.0118	0.0092	0.0056	0
			II	-0.0343	-0.0083	0.0029	0.0064	0.0064	0.0050	0.0032	0.0015	0
			III	0	-0.0020	-0.0058	-0.0089	-0.0111	-0.0124	-0.0133	-0.0143	0
		Y	I	-0.0094	0.0018	0.0135	0.0233	0.0304	0.0352	0.0383	0.0405	0.0428
			II	-0.0057	0.0005	0.0053	0.0083	0.0098	0.0104	0.0107	0.0108	0.0111
			III	0	-0.0119	-0.0345	-0.0535	-0.0665	-0.0745	-0.0799	-0.0856	-0.0838
	Triangularly distributed load	*X*	I	-0.0350	-0.0057	0.0068	0.0101	0.0089	0.0060	0.0030	0.0006	0
			II	-0.0229	-0.0029	0.0045	0.0058	0.0047	0.0029	0.0011	0.0001	0
			III	0	-0.0015	-0.0036	-0.0047	-0.0050	-0.0046	-0.0039	-0.0032	0
		Y	I	-0.0058	0.0013	0.0074	0.0113	0.0129	0.0127	0.0115	0.0102	0.0094
			II	-0.0038	0.0009	0.0039	0.0051	0.0049	0.0041	0.0031	0.0020	0.0013
			III	0	-0.0090	-0.0213	-0.0284	-0.0300	-0.0277	-0.0236	-0.0191	-0.0108
1.25	Uniformly distributed load	*X*	I	-0.0567	-0.0083	0.0096	0.0138	0.0128	0.0104	0.0080	0.0051	0
			II	-0.0344	-0.0045	0.0054	0.0069	0.0056	0.0039	0.0023	0.0010	0
			III	0	-0.0029	-0.0075	-0.0107	-0.0125	-0.0133	-0.0138	-0.0143	0
		Y	I	-0.0095	0.0049	0.0188	0.0290	0.0354	0.0388	0.0406	0.0417	0.0435
			II	-0.0057	0.0019	0.0071	0.0096	0.0106	0.0107	0.0106	0.0106	0.0107
			III	0	-0.0174	-0.0447	-0.0641	-0.0749	-0.0799	-0.0826	-0.0859	-0.0833
	Triangularly distributed load	*X*	I	-0.0391	-0.0025	0.0097	0.0109	0.0083	0.0049	0.0020	0	0
			II	-0.0251	-0.0009	0.0058	0.0059	0.0041	0.0021	0.0005	-0.0004	0
			III	0	-0.0022	-0.0048	-0.0060	-0.0059	-0.0051	-0.0040	-0.0029	0
		Y	I	-0.0065	0.0033	0.0114	0.0155	0.0162	0.0145	0.0119	0.0094	0.0079
			II	-0.0042	0.0019	0.0052	0.0060	0.0054	0.0042	0.0029	0.0017	0.0008
			III	0	-0.0135	-0.0291	-0.0361	-0.0356	-0.0305	-0.0239	-0.0172	-0.0078

Table 2.1.2 Numerical Tables for the Calculation of a Slab Supported on Three Sides and Free on One Side (When the Side in the *X*-Direction is Divided into Eight Equal Parts and the Side in the *Y*-Direction is Divided into Four Equal Parts)

(c) λ=1.50, 1.75, 2.00

λ	Load	Bending moment coefficient	Coordinate	1	2	3	4	5	6	7	8	9
1.50	Uniformly distributed load	*X*	I	−0.0568	−0.0030	0.0123	0.0136	0.0113	0.0090	0.0071	0.0050	0
			II	−0.0344	−0.0015	0.0065	0.0063	0.0045	0.0030	0.0018	0.0008	0
			III	0	−0.0038	−0.0089	−0.0119	−0.0133	−0.0137	−0.0139	−0.0142	0
		Y	I	−0.0095	0.0079	0.0235	0.0333	0.0384	0.0406	0.0413	0.0418	0.0434
			II	−0.0057	0.0031	0.0084	0.0104	0.0108	0.0107	0.0105	0.0104	0.0105
			III	0	−0.0231	−0.0534	−0.0716	−0.0797	−0.0823	−0.0831	−0.0852	−0.0834
	Triangularly distributed load	*X*	I	−0.0420	0.0007	0.0114	0.0106	0.0071	0.0039	0.0014	−0.0003	0
			II	−0.0266	0.0009	0.0064	0.0053	0.0031	0.0014	0.0001	−0.0005	0
			III	0	−0.0030	−0.0060	−0.0070	−0.0065	−0.0053	−0.0039	−0.0026	0
		Y	I	−0.007	0.0056	0.0151	0.0189	0.0184	0.0154	0.0117	0.0084	0.0065
			II	−0.0044	0.0029	0.0062	0.0066	0.0056	0.0042	0.0027	0.0015	0.0006
			III	0	−0.0182	−0.0361	−0.0419	−0.0390	−0.0317	−0.0234	−0.0155	−0.0060
1.75	Uniformly distributed load	*X*	I	−0.0568	0.0013	0.0135	0.0126	0.0099	0.0080	0.0068	0.0051	0
			II	−0.0344	0.0009	0.0069	0.0054	0.0035	0.0024	0.0016	0.0008	0
			III	0	−0.0048	−0.0101	−0.0128	−0.0137	−0.0138	−0.0138	−0.0141	0
		Y	I	−0.0095	0.0108	0.0274	0.0364	0.0402	0.0413	0.0415	0.0416	0.0433
			II	−0.0057	0.0043	0.0093	0.0107	0.0108	0.0106	0.0104	0.0104	0.0104
			III	0	−0.0287	−0.0605	−0.0767	−0.0823	−0.0831	−0.0830	−0.0845	−0.0840
	Triangularly distributed load	*X*	I	−0.0441	0.0035	0.0120	0.0096	0.0059	0.0032	0.0012	−0.0003	0
			II	−0.0277	0.0025	0.0064	0.0045	0.0023	0.0010	0	−0.0005	0
			III	0	−0.0039	−0.0070	−0.0077	−0.0068	−0.0054	−0.0038	−0.0024	0
		Y	I	−0.0074	0.0081	0.0185	0.0215	0.0197	0.0157	0.0113	0.0076	0.0055
			II	−0.0046	0.0038	0.0070	0.0068	0.0055	0.0041	0.0026	0.0014	0.0004
			III	0	−0.0231	−0.0420	−0.0459	−0.0410	−0.0321	−0.0227	−0.0141	−0.0049
2.00	Uniformly distributed load	*X*	I	−0.0568	0.0047	0.0138	0.0113	0.0087	0.0075	0.0067	0.0054	0
			II	−0.0344	0.0028	0.0067	0.0045	0.0028	0.0020	0.0016	0.0009	0
			III	0	−0.0057	−0.0110	−0.0133	−0.0139	−0.0139	−0.0138	−0.0140	0
		Y	I	−0.0095	0.0137	0.0307	0.0385	0.0411	0.0416	0.0415	0.0415	0.0432
			II	−0.0057	0.0053	0.0099	0.0108	0.0107	0.0105	0.0104	0.0103	0.0104
			III	0	−0.0340	−0.0662	−0.0800	−0.0836	−0.0832	−0.0827	−0.0841	−0.0846
	Triangularly distributed load	*X*	I	−0.0457	0.0060	0.0120	0.0084	0.0050	0.0028	0.0012	−0.0002	0
			II	−0.0285	0.0038	0.0061	0.0036	0.0017	0.0007	0.0001	−0.0005	0
			III	0	−0.0046	−0.0078	−0.0081	−0.0070	−0.0054	−0.0037	−0.0022	0
		Y	I	−0.0076	0.0105	0.0214	0.0233	0.0204	0.0158	0.0110	0.0070	0.0047
			II	−0.0048	0.0047	0.0075	0.0069	0.0055	0.0040	0.0026	0.0013	0.0004
			III	0	−0.0279	−0.0468	−0.0486	−0.0420	−0.0322	−0.0223	−0.0132	−0.0041

Table 2.1.2 Numerical Tables for the Calculation of a Slab Supported on Three Sides and Free on One Side (When the Side in the *X*-Direction is Divided into Eight Equal Parts and the Side in the *Y*-Direction is Divided into Four Equal Parts)

(d) λ=2.25, 2.50, 2.75

λ	Load	Bending moment coefficient	Coordinate	1	2	3	4	5	6	7	8	9
2.25	Uniformly distributed load	*X*	I	−0.0567	0.0074	0.0135	0.0102	0.0080	0.0072	0.0068	0.0056	0
			II	−0.0343	0.0042	0.0062	0.0037	0.0023	0.0019	0.0017	0.0010	0
			III	0	−0.0065	−0.0118	−0.0137	−0.0140	−0.0138	−0.0137	−0.0140	0
		Y	I	−0.0095	0.0163	0.0334	0.0399	0.0416	0.0417	0.0415	0.0414	0.0432
			II	−0.0057	0.0062	0.0104	0.0108	0.0106	0.0105	0.0104	0.0103	0.0105
			III	0	−0.0390	−0.0706	−0.0820	−0.0842	−0.0831	−0.0824	−0.0838	−0.0852
	Triangularly distributed load	*X*	I	−0.0469	0.0080	0.0116	0.0073	0.0043	0.0026	0.0013	−0.0001	0
			II	−0.0291	0.0048	0.0056	0.0029	0.0013	0.0007	0.0002	−0.0004	0
			III	0	−0.0054	−0.0084	−0.0084	−0.0071	−0.0054	−0.0037	−0.0021	0
		Y	I	−0.0078	0.0128	0.0238	0.0245	0.0208	0.0158	0.0108	0.0065	0.0042
			II	−0.0049	0.0055	0.0078	0.0069	0.0054	0.0039	0.0026	0.0013	0.0003
			III	0	−0.0325	−0.0506	−0.0502	−0.0424	−0.0322	−0.0221	−0.0125	−0.0034
2.50	Uniformly distributed load	*X*	I	−0.0567	0.0094	0.0128	0.0092	0.0075	0.0071	0.0069	0.0059	0
			II	−0.0342	0.0052	0.0056	0.0030	0.0020	0.0018	0.0017	0.0011	0
			III	0	−0.0073	−0.0123	−0.0139	−0.0141	−0.0138	−0.0137	−0.0139	0
		Y	I	−0.0094	0.0189	0.0356	0.0408	0.0417	0.0417	0.0415	0.0414	0.0432
			II	−0.0057	0.0070	0.0106	0.0108	0.0106	0.0104	0.0104	0.0103	0.0105
			III	0	−0.0437	−0.0739	−0.0832	−0.0844	−0.0829	−0.0822	−0.0836	−0.0858
	Triangularly distributed load	*X*	I	−0.0478	0.0096	0.0109	0.0064	0.0039	0.0026	0.0014	0.0001	0
			II	−0.0296	0.0055	0.0051	0.0023	0.0011	0.0006	0.0002	−0.0003	0
			III	0	−0.0061	−0.0089	−0.0085	−0.0071	−0.0054	−0.0037	−0.0020	0
		Y	I	−0.0080	0.0151	0.0257	0.0253	0.0209	0.0157	0.0106	0.0062	0.0038
			II	−0.0049	0.0062	0.0080	0.0068	0.0053	0.0039	0.0026	0.0013	0.0003
			III	0	−0.0368	−0.0534	−0.0511	−0.0426	−0.0322	−0.0220	−0.0120	−0.0027
2.75	Uniformly distributed load	*X*	I	−0.0566	0.0110	0.0121	0.0084	0.0072	0.0070	0.0069	0.0061	0
			II	−0.0341	0.0059	0.0050	0.0025	0.0018	0.0018	0.0018	0.0012	0
			III	0	−0.0080	−0.0127	−0.0140	−0.0141	−0.0138	−0.0137	−0.0139	0
		Y	I	−0.0094	0.0213	0.0373	0.0413	0.0418	0.0417	0.0415	0.0414	0.0432
			II	−0.0057	0.0077	0.0107	0.0107	0.0105	0.0104	0.0104	0.0103	0.0105
			III	0	−0.0480	−0.0763	−0.0839	−0.0845	−0.0827	−0.0820	−0.0836	−0.0863
	Triangularly distributed load	*X*	I	−0.0486	0.0108	0.0101	0.0057	0.0037	0.0026	0.0015	0.0002	0
			II	−0.0299	0.0060	0.0045	0.0019	0.0009	0.0006	0.0003	−0.0002	0
			III	0	−0.0068	−0.0093	−0.0086	−0.0071	−0.0054	−0.0037	−0.0019	0
		Y	I	−0.0081	0.0173	0.0272	0.0257	0.0209	0.0157	0.0105	0.0060	0.0034
			II	−0.0050	0.0068	0.0081	0.0068	0.0053	0.0039	0.0026	0.0013	0.0003
			III	0	−0.0409	−0.0555	−0.0515	−0.0427	−0.0322	−0.0220	−0.0117	−0.0021

Table 2.1.2 Numerical Tables for the Calculation of a Slab Supported on Three Sides and Free on One Side (When the Side in the *X*-Direction is Divided into Eight Equal Parts and the Side in the *Y*-Direction is Divided into Four Equal Parts)

(e) λ=3.00, 3.25, 3.50

λ	Load	Bending moment coefficient	Coordinate	1	2	3	4	5	6	7	8	9
3.00	Uniformly distributed load	*X*	I	−0.0565	0.0121	0.0112	0.0079	0.0070	0.0070	0.0070	0.0063	0
			II	−0.0339	0.0064	0.0044	0.0022	0.0017	0.0018	0.0019	0.0013	0
			III	0	−0.0086	−0.0130	−0.0140	−0.0141	−0.0138	−0.0136	−0.0139	0
		Y	I	−0.0094	0.0235	0.0386	0.0416	0.0418	0.0417	0.0415	0.0414	0.0432
			II	−0.0057	0.0083	0.0108	0.0106	0.0105	0.0104	0.0104	0.0103	0.0105
			III	0	−0.0518	−0.0780	−0.0843	−0.0845	−0.0825	−0.0818	−0.0836	−0.0868
	Triangularly distributed load	*X*	I	−0.0492	0.0116	0.0093	0.0052	0.0036	0.0026	0.0016	0.0003	0
			II	−0.0301	0.0063	0.0039	0.0016	0.0009	0.0006	0.0003	−0.0002	0
			III	0	−0.0074	−0.0095	−0.0086	−0.0071	−0.0054	−0.0037	−0.0019	0
		Y	I	−0.0082	0.0193	0.0284	0.0260	0.0209	0.0157	0.0105	0.0058	0.0031
			II	−0.0050	0.0073	0.0082	0.0067	0.0053	0.0039	0.0026	0.0013	0.0003
			III	0	−0.0446	−0.0569	−0.0516	−0.0428	−0.0323	−0.0222	−0.0114	−0.0015
3.25	Uniformly distributed load	*X*	I	−0.0565	0.0128	0.0104	0.0075	0.0070	0.0070	0.0071	0.0064	0
			II	−0.0338	0.0067	0.0039	0.0019	0.0017	0.0019	0.0019	0.0014	0
			III	0	−0.0092	−0.0132	−0.0141	−0.0141	−0.0137	−0.0136	−0.0140	0
		Y	I	−0.0094	0.0256	0.0395	0.0417	0.0418	0.0417	0.0416	0.0414	0.0432
			II	−0.0056	0.0088	0.0108	0.0106	0.0105	0.0104	0.0104	0.0103	0.0105
			III	0	−0.0553	−0.0791	−0.0845	−0.0846	−0.0823	−0.0816	−0.0837	−0.0872
	Triangularly distributed load	*X*	I	−0.0496	0.0122	0.0085	0.0048	0.0035	0.0026	0.0017	0.0004	0
			II	−0.0302	0.0064	0.0034	0.0014	0.0008	0.0006	0.0004	−0.0001	0
			III	0	−0.0080	−0.0096	−0.0086	−0.0071	−0.0054	−0.0037	−0.0019	0
		Y	I	−0.0083	0.0212	0.0293	0.0261	0.0209	0.0156	0.0105	0.0057	0.0029
			II	−0.0050	0.0077	0.0082	0.0066	0.0052	0.0039	0.0026	0.0013	0.0003
			III	0	−0.0479	−0.0578	−0.0516	−0.0428	−0.0325	−0.0224	−0.0112	−0.0008
3.50	Uniformly distributed load	*X*	I	−0.0564	0.0133	0.0097	0.0072	0.0069	0.0070	0.0071	0.0065	0
			II	−0.0335	0.0068	0.0035	0.0018	0.0016	0.0019	0.0020	0.0015	0
			III	0	−0.0097	−0.0133	−0.0141	−0.0141	−0.0137	−0.0136	−0.0140	0
		Y	I	−0.0094	0.0275	0.0402	0.0418	0.0417	0.0417	0.0416	0.0414	0.0432
			II	−0.0056	0.0092	0.0107	0.0105	0.0104	0.0104	0.0104	0.0104	0.0105
			III	0	−0.0583	−0.0798	−0.0846	−0.0847	−0.0821	−0.0814	−0.0838	−0.0877
	Triangularly distributed load	*X*	I	−0.0500	0.0125	0.0079	0.0046	0.0035	0.0026	0.0017	0.0004	0
			II	−0.0303	0.0064	0.0030	0.0012	0.0008	0.0006	0.0004	−0.0001	0
			III	0	−0.0085	−0.0097	−0.0086	−0.0072	−0.0054	−0.0038	−0.0018	0
		Y	I	−0.0083	0.0230	0.0299	0.0261	0.0209	0.0156	0.0104	0.0056	0.0027
			II	−0.0050	0.0081	0.0081	0.0066	0.0052	0.0039	0.0026	0.0013	0.0003
			III	0	−0.0509	−0.0583	−0.0514	−0.0429	−0.0327	−0.0226	−0.0111	−0.0002

Table 2.1.2 Numerical Tables for the Calculation of a Slab Supported on Three Sides and Free on One Side (When the Side in the *X*-Direction is Divided into Eight Equal Parts and the Side in the *Y*-Direction is Divided into Four Equal Parts)

(f) λ=3.75, 4.00, 4.25

λ	Load	Bending moment coefficient	Coordinate	1	2	3	4	5	6	7	8	9
3.75	Uniformly distributed load	*X*	I	−0.0564	0.0135	0.0091	0.0070	0.0069	0.0071	0.0071	0.0066	0
			II	−0.0331	0.0068	0.0031	0.0016	0.0016	0.0019	0.0021	0.0015	0
			III	0	−0.0102	−0.0134	−0.0141	−0.0141	−0.0137	−0.0135	−0.0140	0
		Y	I	−0.0094	0.0292	0.0407	0.0418	0.0417	0.0417	0.0416	0.0414	0.0434
			II	−0.0055	0.0096	0.0107	0.0105	0.0104	0.0104	0.0104	0.0104	0.0104
			III	0	−0.0609	−0.0802	−0.0847	−0.0848	−0.0820	−0.0812	−0.0840	−0.0881
	Triangularly distributed load	*X*	I	−0.0505	0.0126	0.0073	0.0045	0.0034	0.0027	0.0018	0.0005	0
			II	−0.0302	0.0063	0.0027	0.0012	0.0008	0.0006	0.0004	0	0
			III	0	−0.0089	−0.0097	−0.0085	−0.0072	−0.0055	−0.0038	−0.0018	0
		Y	I	−0.0084	0.0246	0.0304	0.0261	0.0209	0.0156	0.0104	0.0055	0.0025
			II	−0.0050	0.0084	0.0081	0.0065	0.0052	0.0039	0.0027	0.0012	0.0003
			III	0	−0.0536	−0.0584	−0.0512	−0.0431	−0.0329	−0.0228	−0.0110	0.0005
4.00	Uniformly distributed load	*X*	I	−0.0568	0.0135	0.0086	0.0069	0.0069	0.0071	0.0072	0.0067	0
			II	−0.0324	0.0067	0.0028	0.0015	0.0016	0.0020	0.0021	0.0016	0
			III	0	−0.0105	−0.0134	−0.0141	−0.0142	−0.0136	−0.0136	−0.0140	0
		Y	I	−0.0095	0.0307	0.0411	0.0418	0.0417	0.0417	0.0416	0.0415	0.0433
			II	−0.0054	0.0099	0.0106	0.0104	0.0104	0.0104	0.0104	0.0104	0.0105
			III	0	−0.0632	−0.0802	−0.0847	−0.0850	−0.0818	−0.0810	−0.0842	−0.0886
	Triangularly distributed load	*X*	I	−0.0505	0.0125	0.0068	0.0044	0.0034	0.0027	0.0018	0.0005	0
			II	−0.0302	0.0061	0.0025	0.0011	0.0007	0.0006	0.0003	0	0
			III	0	−0.0093	−0.0097	−0.0085	−0.0072	−0.0055	−0.0039	−0.0018	0
		Y	I	−0.0084	0.0261	0.0307	0.0261	0.0209	0.0156	0.0105	0.0054	0.0023
			II	−0.0050	0.0086	0.0080	0.0065	0.0052	0.0039	0.0027	0.0012	0.0003
			III	0	−0.0560	−0.0583	−0.0510	−0.0432	−0.0331	−0.0231	−0.0109	0.0012
4.25	Uniformly distributed load	*X*	I	−0.0560	0.0134	0.0081	0.0068	0.0069	0.0071	0.0072	0.0068	0
			II	−0.0325	0.0065	0.0026	0.0015	0.0015	0.0020	0.0022	0.0016	0
			III	0	−0.0108	−0.0133	−0.0141	−0.0142	−0.0136	−0.0135	−0.0141	0
		Y	I	−0.0093	0.0321	0.0413	0.0418	0.0417	0.0417	0.0416	0.0415	0.0433
			II	−0.0054	0.0101	0.0106	0.0104	0.0104	0.0104	0.0105	0.0104	0.0105
			III	0	−0.0651	−0.0801	−0.0848	−0.0852	−0.0816	−0.0807	−0.0844	−0.0891
	Triangularly distributed load	*X*	I	−0.0507	0.0123	0.0064	0.0043	0.0034	0.0027	0.0018	0.0006	0
			II	−0.0301	0.0059	0.0023	0.0011	0.0007	0.0005	0.0003	0	0
			III	0	−0.0097	−0.0097	−0.0085	−0.0072	−0.0056	−0.0039	−0.0018	0
		Y	I	−0.0085	0.0274	0.0309	0.0261	0.0209	0.0157	0.0105	0.0054	0.0022
			II	−0.0050	0.0088	0.0080	0.0065	0.0052	0.0039	0.0027	0.0012	0.0004
			III	0	−0.0580	−0.0580	−0.0507	−0.0434	−0.0334	−0.0234	−0.0108	0.0018

Table 2.1.2 Numerical Tables for the Calculation of a Slab Supported on Three Sides and Free on One Side (When the Side in the *X*-Direction is Divided into Eight Equal Parts and the Side in the *Y*-Direction is Divided into Four Equal Parts)

(g) λ=4.50, 4.75, 5.00

λ	Load	Bending moment coefficient	Coordinate	1	2	3	4	5	6	7	8	9
4.50	Uniformly distributed load	X	I	−0.0560	0.0132	0.0078	0.0067	0.0068	0.0071	0.0073	0.0069	0
			II	−0.0322	0.0063	0.0025	0.0014	0.0015	0.0021	0.0023	0.0016	0
			III	0	−0.0111	−0.0133	−0.0141	−0.0142	−0.0136	−0.0134	−0.0141	0
		Y	I	−0.0093	0.0334	0.0415	0.0418	0.0417	0.0416	0.0416	0.0415	0.0435
			II	−0.0054	0.0103	0.0106	0.0104	0.0104	0.0105	0.0105	0.0104	0.0106
			III	0	−0.0667	−0.0798	−0.0849	−0.0854	−0.0814	−0.0804	−0.0847	−0.0896
	Triangularly distributed load	X	I	−0.0510	0.0120	0.0061	0.0043	0.0034	0.0026	0.0018	0.0006	0
			II	−0.0300	0.0056	0.0022	0.0012	0.0006	0.0005	0.0002	0.0001	0
			III	0	−0.0100	−0.0096	−0.0084	−0.0073	−0.0056	−0.0040	−0.0018	0
		Y	I	−0.0085	0.0286	0.0311	0.0261	0.0209	0.0157	0.0105	0.0053	0.0021
			II	−0.0050	0.0090	0.0080	0.0065	0.0052	0.0039	0.0027	0.0012	0.0005
			III	0	−0.0598	−0.0576	−0.0505	−0.0436	−0.0336	−0.0238	−0.0108	0.0025
4.75	Uniformly distributed load	X	I	−0.0555	0.0129	0.0076	0.0067	0.0068	0.0072	0.0073	0.0069	0
			II	−0.0315	0.0061	0.0024	0.0014	0.0014	0.0021	0.0023	0.0016	0
			III	0	−0.0113	−0.0132	−0.0142	−0.0143	−0.0135	−0.0134	−0.0142	0
		Y	I	−0.0092	0.0345	0.0416	0.0417	0.0417	0.0416	0.0416	0.0415	0.0433
			II	−0.0052	0.0105	0.0105	0.0103	0.0104	0.0105	0.0105	0.0104	0.0104
			III	0	−0.0679	−0.0794	−0.0850	−0.0856	-0.0811	−0.0801	−0.0849	−0.0901
	Triangularly distributed load	X	I	−0.0508	0.0117	0.0059	0.0043	0.0034	0.0026	0.0018	0.0007	0
			II	−0.0296	0.0053	0.0022	0.0012	0.0006	0.0005	0.0002	0.0001	0
			III	0	−0.0102	−0.0095	−0.0084	−0.0073	−0.0056	−0.0040	−0.0018	0
		Y	I	−0.0085	0.0297	0.0311	0.0260	0.0209	0.0157	0.0105	0.0053	0.0020
			II	−0.0049	0.0091	0.0080	0.0065	0.0052	0.0039	0.0027	0.0012	0.0006
			III	0	−0.0612	−0.0571	−0.0502	−0.0438	−0.0339	−0.0241	−0.0108	0.0032
5.00	Uniformly distributed load	X	I	−0.0552	0.0126	0.0074	0.0066	0.0068	0.0072	0.0074	0.0069	0
			II	−0.0309	0.0059	0.0023	0.0013	0.0014	0.0022	0.0024	0.0016	0
			III	0	−0.0115	−0.0132	−0.0142	−0.0143	−0.0135	−0.0133	−0.0142	0
		Y	I	−0.0092	0.0355	0.0416	0.0417	0.0417	0.0416	0.0416	0.0416	0.0433
			II	−0.0052	0.0106	0.0105	0.0103	0.0103	0.0105	0.0106	0.0104	0.0103
			III	0	−0.0689	−0.0790	−0.0851	−0.0858	−0.0809	−0.0798	−0.0852	−0.0906
	Triangularly distributed load	X	I	−0.0508	0.0113	0.0058	0.0043	0.0033	0.0026	0.0017	0.0007	0
			II	−0.0292	0.0050	0.0022	0.0012	0.0006	0.0004	0.0001	0.0001	0
			III	0	−0.0104	−0.0094	−0.0083	−0.0073	−0.0057	−0.0041	−0.0018	0
		Y	I	−0.0085	0.0306	0.0311	0.0260	0.0209	0.0157	0.0105	0.0053	0.0019
			II	−0.0049	0.0092	0.0080	0.0065	0.0052	0.0039	0.0026	0.0012	0.0007
			III	0	−0.0625	−0.0565	−0.0500	−0.0440	−0.0342	−0.0245	−0.0107	0.0039

Table 2.1.3 Numerical Tables for the Calculation of a Slab Supported on Four Sides (When the Side in the *X*-Direction is Divided into Four Equal Parts and the Side in the *Y*-Direction is Divided into Four Equal Parts)

(a) λ=0.30, 0.40, 0.50

λ	Load	Bending moment coefficient	Coordinate	1	2	3	4	5
0.30	Uniformly distributed load	*X*	I	−0.0835	0.0104	0.0418	0.0104	−0.0835
			II	−0.0813	0.0108	0.0398	0.0108	−0.0813
			III	0	−0.0058	−0.0095	−0.0058	0
		Y	I	−0.0139	0.0017	0.0070	0.0017	−0.0139
			II	−0.0136	0.0038	0.0103	0.0038	−0.0136
			III	0	−0.0345	−0.0569	−0.0345	0
	Triangularly distributed load	*X*	I	−0.0334	0.0016	0.0209	0.0089	−0.0501
			II	−0.0323	0.0018	0.0199	0.0091	−0.0490
			III	0	−0.0021	−0.0047	−0.0036	0
		Y	I	−0.0059	0.0003	0.0035	0.0015	−0.0084
			II	−0.0054	0.0013	0.0052	0.0025	−0.0082
			III	0	−0.0126	−0.0284	−0.0218	0
0.40	Uniformly distributed load	*X*	I	−0.0839	0.0107	0.0418	0.0107	−0.0839
			II	−0.0749	0.0106	0.0356	0.0106	−0.0749
			III	0	−0.0058	−0.0095	−0.0058	0
		Y	I	−0.0140	0.0023	0.0080	0.0023	−0.0140
			II	−0.0125	0.0057	0.0129	0.0057	−0.0125
			III	0	−0.0345	−0.0569	−0.0345	0
	Triangularly distributed load	*X*	I	−0.0336	0.0017	0.0209	0.0090	−0.0503
			II	−0.0292	0.0017	0.0178	0.0089	−0.0457
			III	0	−0.0021	−0.0048	−0.0036	0
		Y	I	−0.0056	0.0005	0.0040	0.0017	−0.0084
			II	−0.0049	0.0021	0.0065	0.0036	−0.0076
			III	0	−0.0127	−0.0284	−0.0218	0
0.50	Uniformly distributed load	*X*	I	−0.0828	0.0110	0.0407	0.0110	−0.0828
			II	−0.0669	0.0100	0.0308	0.0100	−0.0669
			III	0	−0.0058	−0.0095	−0.0058	0
		Y	I	−0.0138	0.0038	0.0105	0.0038	−0.0138
			II	−0.0112	0.0068	0.0139	0.0068	−0.0112
			III	0	−0.0345	−0.0570	−0.0345	0
	Triangularly distributed load	*X*	I	−0.0331	0.0019	0.0203	0.0092	−0.0497
			II	−0.0254	0.0015	0.0154	0.0084	−0.0415
			III	0	−0.0021	−0.0048	−0.0037	0
		Y	I	−0.0055	0.0013	0.0052	0.0025	−0.0083
			II	−0.0042	0.0025	0.0070	0.0042	−0.0069
			III	0	−0.0127	−0.0285	−0.0219	0

Table 2.1.3 Numerical Tables for the Calculation of a Slab Supported on Four Sides (When the Side in the *X*-Direction is Divided into Four Equal Parts and the Side in the *Y*-Direction is Divided into Four Equal Parts)

(b) λ=0.75, 1.00, 1.25

λ	Load	Bending moment coefficient	Coordinate	1	2	3	4	5
0.75	Uniformly distributed load	*X*	I	−0.0701	0.0110	0.0318	0.0110	−0.0701
			II	−0.0477	0.0078	0.0200	0.0078	−0.0477
			III	0	−0.0058	−0.0094	−0.0058	0
		Y	I	−0.0117	0.0089	0.0179	0.0089	−0.0117
			II	−0.0080	0.0069	0.0125	0.0069	−0.0080
			III	0	−0.0345	−0.0565	−0.0345	0
	Triangularly distributed load	*X*	I	−0.0268	0.0020	0.0159	0.0091	−0.0433
			II	−0.0167	0.0010	0.0100	0.0068	−0.0310
			III	0	−0.0021	−0.0047	−0.0036	0
		Y	I	−0.0045	0.0037	0.0090	0.0052	−0.0072
			II	−0.0026	0.0024	0.0062	0.0045	−0.0052
			III	0	−0.0126	−0.0283	−0.0218	0
1.00	Uniformly distributed load	*X*	I	−0.0513	0.0096	0.0206	0.0096	−0.0513
			II	−0.0324	0.0059	0.0116	0.0059	−0.0324
			III	0	−0.0054	−0.0086	−0.0054	0
		Y	I	−0.0086	0.0116	0.0206	0.0116	−0.0086
			II	−0.0054	0.0059	0.0096	0.0059	−0.0054
			III	0	−0.0324	−0.0513	−0.0324	0
	Triangularly distributed load	*X*	I	−0.0179	0.0015	0.0103	0.0080	−0.0334
			II	−0.0101	0.0006	0.0058	0.0052	−0.0223
			III	0	−0.0019	−0.0043	−0.0036	0
		Y	I	−0.0030	0.0047	0.0103	0.0069	−0.0056
			II	−0.0017	0.0018	0.0048	0.0040	−0.0037
			III	0	−0.0116	−0.0257	−0.0208	0
1.25	Uniformly distributed load	*X*	I	−0.0559	0.0119	0.0189	0.0119	−0.0559
			II	−0.0343	0.0067	0.0097	0.0067	−0.0343
			III	0	−0.0074	−0.0111	−0.0074	0
		Y	I	−0.0093	0.0181	0.0295	0.0181	−0.0093
			II	−0.0057	0.0074	0.0108	0.0074	−0.0057
			III	0	−0.0442	−0.0664	−0.0442	0
	Triangularly distributed load	*X*	I	−0.0171	0.0017	0.0095	0.0102	−0.0389
			II	−0.0092	0.0006	0.0048	0.0061	−0.0251
			III	0	−0.0025	−0.0055	−0.0049	0
		Y	I	−0.0029	0.0069	0.0147	0.0111	−0.0065
			II	−0.0015	0.0021	0.0054	0.0053	−0.0042
			III	0	−0.0151	−0.0332	−0.0291	0

Table 2.1.3 Numerical Tables for the Calculation of a Slab Supported on Four Sides (When the Side in the *X*-Direction is Divided into Four Equal Parts and the Side in the *Y*-Direction is Divided into Four Equal Parts)

(c) λ=1.50, 1.75, 2.00

λ	Load	Bending moment coefficient	Coordinate	1	2	3	4	5
1.50	Uniformly distributed load	*X*	I	−0.0570	0.0133	0.0158	0.0133	−0.0570
			II	−0.0346	0.0071	0.0073	0.0071	−0.0346
			III	0	−0.0090	−0.0126	−0.0090	0
		Y	I	−0.0095	0.0234	0.0354	0.0234	−0.0095
			II	−0.0058	0.0086	0.0112	0.0086	−0.0058
			III	0	−0.0538	−0.0756	−0.0538	0
	Triangularly distributed load	*X*	I	−0.0149	0.0017	0.0079	0.0116	−0.0421
			II	−0.0079	0.0006	0.0036	0.0065	−0.0267
			III	0	−0.0029	−0.0063	−0.0061	0
		Y	I	−0.0025	0.0083	0.0177	0.0151	−0.0079
			II	−0.0013	0.0023	0.0056	0.0063	−0.0045
			III	0	−0.0172	−0.0378	−0.0365	0
1.75	Uniformly distributed load	*X*	I	−0.0571	0.0139	0.0128	0.0139	−0.0571
			II	−0.0346	0.0071	0.0052	0.0071	−0.0346
			III	0	−0.0102	−0.0135	−0.0102	0
		Y	I	−0.0095	0.0275	0.0389	0.0275	−0.0095
			II	−0.0058	0.0094	0.0112	0.0094	−0.0058
			III	0	−0.0611	−0.0805	−0.0611	0
	Triangularly distributed load	*X*	I	−0.0128	0.0018	0.0064	0.0121	−0.0442
			II	−0.0068	0.0006	0.0026	0.0065	−0.0278
			III	0	−0.0031	−0.0067	−0.0071	0
		Y	I	−0.0021	0.0090	0.0194	0.0185	−0.0074
			II	−0.0011	0.0024	0.0056	0.0070	−0.0046
			III	0	−0.0184	−0.0403	−0.0427	0
2.00	Uniformly distributed load	*X*	I	−0.0570	0.0139	0.0105	0.0139	−0.0570
			II	−0.0345	0.0068	0.0038	0.0068	−0.0345
			III	0	−0.0112	−0.0138	−0.0112	0
		Y	I	−0.0095	0.0308	0.0407	0.0308	−0.0095
			II	−0.0058	0.0100	0.0110	0.0100	−0.0058
			III	0	−0.0669	−0.0828	−0.0669	0
	Triangularly distributed load	*X*	I	−0.0112	0.0018	0.0052	0.0121	−0.0458
			II	−0.0059	0.0006	0.0019	0.0062	−0.0287
			III	0	−0.0032	−0.0069	−0.0080	0
		Y	I	−0.0019	0.0094	0.0203	0.0214	−0.0077
			II	−0.0010	0.0025	0.0055	0.0075	−0.0048
			III	0	−0.0192	−0.0414	−0.0477	0

Table 2.1.3 Numerical Tables for the Calculation of a Slab Supported on Four Sides (When the Side in the *X*-Direction is Divided into Four Equal Parts and the Side in the *Y*-Direction is Divided into Four Equal Parts)

(d) λ=2.25, 2.50, 2.75

λ	Load	Bending moment coefficient	Coordinate	1	2	3	4	5
2.25	Uniformly distributed load	*X*	I	−0.0569	0.0136	0.0089	0.0136	−0.0569
			II	−0.0345	0.0063	0.0028	0.0063	−0.0345
			III	0	−0.0119	−0.0140	−0.0119	0
		Y	I	−0.0095	0.0335	0.0415	0.0335	−0.0095
			II	−0.0058	0.0104	0.0108	0.0104	−0.0058
			III	0	−0.0714	−0.0837	−0.0714	0
	Triangularly distributed load	*X*	I	−0.0099	0.0019	0.0045	0.0117	−0.0470
			II	−0.0052	0.0006	0.0014	0.0057	−0.0293
			III	0	−0.0033	−0.0070	−0.0086	0
		Y	I	−0.0016	0.0097	0.0207	0.0238	−0.0079
			II	−0.0009	0.0025	0.0054	0.0079	−0.0049
			III	0	−0.0196	−0.0419	−0.0518	0
2.50	Uniformly distributed load	*X*	I	−0.0569	0.0129	0.0080	0.0129	−0.0569
			II	−0.0345	0.0057	0.0023	0.0057	−0.0345
			III	0	−0.0125	−0.0140	−0.0125	0
		Y	I	−0.0095	0.0356	0.0418	0.0356	−0.0095
			II	−0.0058	0.0106	0.0107	0.0106	−0.0058
			III	0	−0.0749	−0.0839	−0.0749	0
	Triangularly distributed load	*X*	I	−0.0089	0.0019	0.0040	0.0110	−0.0480
			II	−0.0047	0.0006	0.0011	0.0051	−0.0298
			III	0	−0.0033	−0.0070	−0.0092	0
		Y	I	−0.0015	0.0099	0.0209	0.0257	−0.0080
			II	−0.0008	0.0026	0.0053	0.0081	−0.0050
			III	0	−0.0200	−0.0420	−0.0549	0
2.75	Uniformly distributed load	*X*	I	−0.0568	0.0122	0.0074	0.0122	−0.0568
			II	−0.0344	0.0051	0.0020	0.0051	−0.0344
			III	0	−0.0130	−0.0140	−0.0130	0
		Y	I	−0.0095	0.0373	0.0419	0.0373	−0.0095
			II	−0.0058	0.0108	0.0106	0.0108	−0.0058
			III	0	−0.0775	−0.0839	−0.0775	0
	Triangularly distributed load	*X*	I	−0.0080	0.0019	0.0037	0.0102	−0.0488
			II	−0.0042	0.0006	0.0010	0.0045	−0.0302
			III	0	−0.0034	−0.0070	−0.0096	0
		Y	I	−0.0013	0.0100	0.0210	0.0272	−0.0081
			II	−0.0007	0.0026	0.0053	0.0082	−0.0050
			III	0	−0.0202	−0.0419	−0.0573	0

Table 2.1.3 Numerical Tables for the Calculation of a Slab Supported on Four Sides (When the Side in the *X*-Direction is Divided into Four Equal Parts and the Side in the *Y*-Direction is Divided into Four Equal Parts)

(e) $\lambda = 3.00$

λ	Load	Bending moment coefficient	Coordinate	1	2	3	4	5
3.00	Uniformly distributed load	*X*	I	−0.0568	0.0113	0.0071	−0.0113	−0.0568
			II	−0.0344	0.0045	0.0018	−0.0045	−0.0344
			III	0	−0.0133	−0.0140	−0.0133	0
		Y	I	−0.0095	0.0386	0.0419	0.0386	−0.0095
			II	−0.0058	0.0108	0.0105	0.0108	−0.0058
			III	0	−0.0795	−0.0837	−0.0795	0
	Triangularly distributed load	*X*	I	−0.0074	0.0019	0.0036	0.0094	−0.0495
			II	−0.0039	0.0006	0.0009	0.0039	−0.0306
			III	0	−0.0034	−0.0070	−0.0099	0
		Y	I	−0.0012	0.0102	0.0209	0.0284	−0.0083
			II	−0.0006	0.0026	0.0052	0.0082	−0.0051
			III	0	−0.0204	−0.0419	−0.0591	0

[Reference]

1) Osami HORII, Koji MOTO, New charts of bending stresses in the rectangular flat plates, TECHNICAL NOTE OF PORT AND HARBOUR RESEARCH INSTITUTE MINISTRY OF TRANSPORT, JAPAN NO.43, pp.1-20, 1968 (in Japanese)

3 Required Rudder Angles and Drift Angles of Each Type of Ship with Different Wind Angles When the K-Value is One to Seven

Table 3.1.1 Required Rudder Angles and Drift Angles of Each Type of Ship with Different Wind Angles When the *K*-Value is 1 to 7 (D_0/d_0 = 1.2)

① Cargo ship

	K-value (wind speed/ ship speed)	Wind angle (°)												
		0	15	30	45	60	75	90	105	120	135	150	165	180
Required rudder angle (°)	1	0.00	0.02	0.05	0.10	0.17	0.23	0.28	0.28	0.26	0.20	0.14	0.07	0.00
	2	0.00	0.07	0.20	0.41	0.68	0.93	1.10	1.14	1.03	0.82	0.55	0.27	0.00
	3	0.00	0.16	0.44	0.92	1.52	2.10	2.48	2.56	2.31	1.84	1.24	0.62	0.01
	4	0.00	0.28	0.79	1.63	2.70	3.73	4.41	4.55	4.11	3.26	2.20	1.10	0.01
	5	0.00	0.43	1.23	2.55	4.22	5.83	6.89	7.10	6.43	5.10	3.44	1.71	0.02
	6	0.00	0.62	1.77	3.67	6.08	8.40	9.93	10.23	9.26	7.34	4.95	2.46	0.02
	7	0.00	0.84	2.41	5.00	8.28	11.43	13.51	13.92	12.60	9.99	6.74	3.35	0.03
Drift angle (°)	1	0.00	0.00	0.01	0.01	0.01	0.02	0.02	0.01	0.01	0.01	0.00	0.00	0.00
	2	0.00	0.01	0.03	0.04	0.06	0.07	0.07	0.06	0.04	0.03	0.01	0.01	0.00
	3	0.00	0.03	0.06	0.10	0.13	0.15	0.15	0.13	0.10	0.06	0.03	0.01	0.00
	4	0.00	0.05	0.11	0.17	0.23	0.27	0.27	0.23	0.18	0.11	0.05	0.02	0.00
	5	0.00	0.08	0.17	0.27	0.36	0.42	0.42	0.37	0.27	0.17	0.09	0.03	0.00
	6	0.00	0.12	0.25	0.39	0.52	0.60	0.60	0.53	0.39	0.25	0.12	0.05	0.00
	7	0.00	0.16	0.34	0.53	0.71	0.82	0.82	0.72	0.54	0.33	0.17	0.06	0.00

② Small cargo ship

	K-value (wind speed/ ship speed)	Wind angle (°)												
		0	15	30	45	60	75	90	105	120	135	150	165	180
Required rudder angle (°)	1	0.00	0.03	0.07	0.13	0.20	0.27	0.31	0.32	0.30	0.24	0.17	0.09	0.00
	2	0.00	0.11	0.27	0.51	0.80	1.07	1.25	1.30	1.20	0.98	0.68	0.35	0.00
	3	0.00	0.25	0.62	1.15	1.79	2.40	2.82	2.92	2.70	2.20	1.53	0.78	0.01
	4	0.00	0.44	1.10	2.04	3.18	4.26	5.01	5.20	4.80	3.91	2.72	1.39	0.01
	5	0.00	0.69	1.71	3.19	4.97	6.66	7.82	8.12	7.50	6.12	4.25	2.17	0.02
	6	0.00	1.00	2.47	4.59	7.16	9.59	11.26	11.70	10.80	8.81	6.12	3.12	0.03
	7	0.00	1.36	3.36	6.25	9.74	13.06	15.33	15.92	14.70	11.99	8.33	4.25	0.04
Drift angle (°)	1	0.00	0.01	0.01	0.02	0.02	0.02	0.02	0.02	0.02	0.01	0.01	0.00	0.00
	2	0.00	0.02	0.04	0.07	0.09	0.10	0.10	0.08	0.06	0.04	0.02	0.01	0.00
	3	0.00	0.05	0.10	0.15	0.19	0.22	0.21	0.19	0.14	0.10	0.05	0.02	0.00
	4	0.00	0.09	0.18	0.27	0.34	0.38	0.38	0.33	0.26	0.17	0.10	0.04	0.00
	5	0.00	0.14	0.28	0.42	0.53	0.60	0.60	0.52	0.40	0.27	0.15	0.06	0.00
	6	0.00	0.20	0.40	0.60	0.77	0.86	0.86	0.75	0.58	0.38	0.21	0.09	0.00
	7	0.00	0.27	0.55	0.82	1.05	1.17	1.17	1.03	0.79	0.52	0.29	0.12	0.00

③Container ship (14,000 TEU)

	K-value (wind speed/ ship speed)	Wind angle (°)												
		0	15	30	45	60	75	90	105	120	135	150	165	180
Required rudder angle (°)	1	0.00	0.19	0.41	0.66	0.95	1.26	1.53	1.71	1.74	1.57	1.19	0.64	0.00
	2	0.00	0.76	1.62	2.64	3.81	5.03	6.12	6.84	6.95	6.27	4.77	2.58	0.00
	3	0.00	1.72	3.65	5.94	8.57	11.32	13.78	15.40	15.64	14.11	10.72	5.80	0.00
	4	0.00	3.05	6.49	10.56	15.23	20.12	24.49	27.38	27.80	25.08	19.06	10.31	0.00
	5	0.00	4.77	10.15	16.50	23.80	****	****	****	****	****	29.79	16.11	0.00
	6	0.00	6.87	14.61	23.77	****	****	****	****	****	****	****	23.20	0.00
	7	0.00	9.35	19.88	****	****	****	****	****	****	****	****	****	0.00
Drift angle (°)	1	0.00	0.04	0.07	0.10	0.11	0.12	0.11	0.09	0.08	0.06	0.04	0.02	0.00
	2	0.00	0.16	0.30	0.40	0.45	0.46	0.43	0.38	0.31	0.23	0.15	0.08	0.00
	3	0.00	0.36	0.67	0.89	1.02	1.04	0.98	0.85	0.70	0.52	0.35	0.17	0.00
	4	0.00	0.64	1.19	1.59	1.81	1.85	1.74	1.52	1.24	0.93	0.62	0.31	0.00
	5	0.00	0.99	1.85	2.48	2.83	****	****	****	****	****	0.96	0.48	0.00
	6	0.00	1.43	2.67	3.57	****	****	****	****	****	****	****	0.69	0.00
	7	0.00	1.95	3.63	****	****	****	****	****	****	****	****	****	0.00

Table 3.1.1 Required Rudder Angles and Drift Angles of Each Type of Ship with Different Wind Angles When the K-Value is One to Seven (D_0/d_0 = 1.2)

④ Container ship (10,000 TEU)

	K-value (wind speed/ ship speed)	Wind angle (°)												
		0	15	30	45	60	75	90	105	120	135	150	165	180
Required rudder angle (°)	1	0.00	0.11	0.25	0.41	0.59	0.79	0.96	1.06	1.07	0.96	0.72	0.39	0.00
	2	0.00	0.45	0.98	1.62	2.37	3.15	3.83	4.25	4.28	3.83	2.89	1.56	0.00
	3	0.00	1.02	2.21	3.66	5.34	7.08	8.61	9.56	9.63	8.62	6.51	3.50	0.00
	4	0.00	1.82	3.93	6.50	9.49	12.59	15.30	17.00	17.13	15.32	11.57	6.23	0.00
	5	0.00	2.84	6.13	10.15	14.82	19.67	23.91	26.57	26.76	23.94	18.07	9.73	0.00
	6	0.00	4.09	8.83	14.62	21.34	28.33	****	****	****	****	26.02	14.01	0.00
	7	0.00	5.56	12.02	19.90	29.05	****	****	****	****	****	****	19.07	0.00
Drift angle (°)	1	0.00	0.03	0.06	0.08	0.09	0.09	0.09	0.08	0.06	0.04	0.03	0.01	0.00
	2	0.00	0.12	0.23	0.31	0.35	0.36	0.34	0.30	0.24	0.18	0.12	0.06	0.00
	3	0.00	0.27	0.51	0.69	0.80	0.82	0.78	0.68	0.55	0.40	0.26	0.13	0.00
	4	0.00	0.48	0.91	1.23	1.41	1.46	1.38	1.20	0.97	0.72	0.47	0.23	0.00
	5	0.00	0.76	1.42	1.92	2.21	2.28	2.15	1.88	1.52	1.12	0.73	0.36	0.00
	6	0.00	1.09	2.05	2.77	3.18	3.28	****	****	****	****	1.05	0.51	0.00
	7	0.00	1.48	2.79	3.77	4.33	****	****	****	****	****	****	0.70	0.00

⑤ Container ship (6,000 TEU Over-Panamax)

	K-value (wind speed/ ship speed)	Wind angle (°)												
		0	15	30	45	60	75	90	105	120	135	150	165	180
Required rudder angle (°)	1	0.00	0.08	0.18	0.29	0.43	0.56	0.67	0.74	0.73	0.65	0.49	0.26	0.00
	2	0.00	0.33	0.71	1.17	1.70	2.24	2.68	2.94	2.93	2.59	1.94	1.04	0.01
	3	0.00	0.74	1.60	2.64	3.83	5.03	6.04	6.62	6.59	5.83	4.37	2.35	0.02
	4	0.00	1.32	2.84	4.69	6.81	8.95	10.74	11.78	11.71	10.36	7.76	4.18	0.04
	5	0.00	2.05	4.44	7.33	10.63	13.98	16.78	18.40	18.30	16.19	12.13	6.52	0.06
	6	0.00	2.96	6.39	10.56	15.31	20.13	24.16	26.50	26.35	23.32	17.47	9.40	0.09
	7	0.00	4.03	8.70	14.37	20.84	27.40	****	****	****	****	23.78	12.79	0.12
Drift angle (°)	1	0.00	0.02	0.04	0.05	0.06	0.06	0.06	0.05	0.04	0.03	0.02	0.01	0.00
	2	0.00	0.08	0.14	0.19	0.23	0.23	0.22	0.20	0.16	0.12	0.08	0.04	0.00
	3	0.00	0.17	0.32	0.44	0.51	0.53	0.50	0.44	0.36	0.26	0.17	0.08	0.00
	4	0.00	0.30	0.57	0.78	0.90	0.94	0.89	0.78	0.63	0.47	0.30	0.15	0.00
	5	0.00	0.47	0.89	1.21	1.41	1.47	1.39	1.22	0.99	0.73	0.47	0.23	0.00
	6	0.00	0.68	1.28	1.75	2.03	2.11	2.01	1.76	1.42	1.05	0.68	0.33	0.00
	7	0.00	0.92	1.75	2.38	2.76	2.87	****	****	****	****	0.92	0.45	0.00

⑥ Container ship (4,000 TEU Panamax)

	K-value (wind speed/ ship speed)	Wind angle (°)												
		0	15	30	45	60	75	90	105	120	135	150	165	180
Required rudder angle (°)	1	0.00	0.07	0.14	0.22	0.30	0.39	0.46	0.51	0.52	0.47	0.36	0.19	0.00
	2	0.00	0.28	0.57	0.88	1.21	1.55	1.84	2.04	2.07	1.87	1.43	0.78	0.01
	3	0.00	0.63	1.28	1.98	2.73	3.48	4.15	4.59	4.65	4.21	3.21	1.75	0.02
	4	0.00	1.12	2.28	3.53	4.85	6.19	7.38	8.16	8.27	7.48	5.71	3.11	0.03
	5	0.00	1.75	3.56	5.51	7.58	9.67	11.52	12.75	12.93	11.69	8.93	4.86	0.05
	6	0.00	2.51	5.13	7.94	10.92	13.93	16.59	18.37	18.61	16.83	12.86	7.01	0.07
	7	0.00	3.42	6.99	10.80	14.86	18.96	22.59	25.00	25.34	22.91	17.50	9.53	0.09
Drift angle (°)	1	0.00	0.02	0.03	0.04	0.04	0.04	0.04	0.04	0.03	0.02	0.02	0.01	0.00
	2	0.00	0.06	0.11	0.15	0.17	0.17	0.16	0.14	0.12	0.09	0.06	0.03	0.00
	3	0.00	0.14	0.26	0.34	0.38	0.39	0.36	0.32	0.27	0.21	0.14	0.07	0.00
	4	0.00	0.25	0.46	0.60	0.68	0.69	0.65	0.57	0.48	0.37	0.26	0.13	0.00
	5	0.00	0.39	0.71	0.94	1.06	1.07	1.01	0.89	0.75	0.58	0.40	0.21	0.00
	6	0.00	0.55	1.03	1.36	1.53	1.55	1.45	1.28	1.08	0.84	0.58	0.30	0.00
	7	0.00	0.76	1.40	1.85	2.08	2.10	1.98	1.75	1.46	1.14	0.79	0.40	0.00

Table 3.1.1 Required Rudder Angles and Drift Angles of Each Type of Ship with Different Wind Angles When the *K*-Value is One to Seven (D_0/d_0 = 1.2)

⑦ Bulk carrier (very large ore carrier)

	K-value (wind speed/ ship speed)	Wind angle (°)												
		0	15	30	45	60	75	90	105	120	135	150	165	180
Required rudder angle (°)	1	0.00	0.01	0.03	0.07	0.12	0.16	0.20	0.20	0.18	0.15	0.10	0.05	0.00
	2	0.00	0.05	0.14	0.29	0.48	0.66	0.78	0.81	0.74	0.59	0.40	0.20	0.00
	3	0.00	0.11	0.31	0.65	1.07	1.48	1.76	1.82	1.66	1.32	0.90	0.45	0.00
	4	0.00	0.20	0.56	1.15	1.90	2.63	3.12	3.23	2.95	2.35	1.60	0.80	0.00
	5	0.00	0.31	0.87	1.80	2.97	4.11	4.88	5.05	4.60	3.68	2.50	1.25	0.00
	6	0.00	0.44	1.25	2.59	4.28	5.92	7.02	7.27	6.63	5.30	3.60	1.80	0.00
	7	0.00	0.60	1.71	3.52	5.83	8.05	9.56	9.90	9.02	7.21	4.90	2.45	0.00
Drift angle (°)	1	0.00	0.00	0.00	0.01	0.01	0.01	0.01	0.01	0.01	0.00	0.00	0.00	0.00
	2	0.00	0.01	0.02	0.03	0.04	0.05	0.05	0.04	0.03	0.02	0.01	0.00	0.00
	3	0.00	0.02	0.04	0.07	0.09	0.10	0.10	0.09	0.07	0.04	0.02	0.01	0.00
	4	0.00	0.04	0.08	0.12	0.16	0.18	0.19	0.16	0.12	0.08	0.04	0.01	0.00
	5	0.00	0.06	0.12	0.19	0.25	0.29	0.29	0.25	0.19	0.12	0.06	0.02	0.00
	6	0.00	0.08	0.18	0.27	0.36	0.42	0.42	0.36	0.27	0.17	0.09	0.03	0.00
	7	0.00	0.11	0.24	0.37	0.49	0.57	0.57	0.50	0.37	0.23	0.12	0.04	0.00

⑧ Bulk carrier (capesize)

	K-value (wind speed/ ship speed)	Wind angle (°)												
		0	15	30	45	60	75	90	105	120	135	150	165	180
Required rudder angle (°)	1	0.00	0.01	0.04	0.08	0.12	0.17	0.20	0.21	0.19	0.15	0.11	0.05	0.00
	2	0.00	0.06	0.16	0.31	0.50	0.67	0.80	0.83	0.76	0.61	0.42	0.21	0.00
	3	0.00	0.13	0.35	0.69	1.11	1.52	1.79	1.86	1.70	1.38	0.95	0.48	0.00
	4	0.00	0.24	0.63	1.23	1.98	2.70	3.18	3.30	3.03	2.45	1.68	0.85	0.01
	5	0.00	0.37	0.99	1.93	3.10	4.22	4.98	5.16	4.73	3.82	2.63	1.33	0.01
	6	0.00	0.54	1.42	2.78	4.46	6.07	7.17	7.43	6.82	5.50	3.78	1.91	0.02
	7	0.00	0.73	1.93	3.78	6.07	8.26	9.75	10.12	9.28	7.49	5.15	2.60	0.02
Drift angle (°)	1	0.00	0.00	0.01	0.01	0.01	0.01	0.01	0.01	0.01	0.01	0.00	0.00	0.00
	2	0.00	0.01	0.02	0.03	0.04	0.05	0.05	0.04	0.03	0.02	0.01	0.00	0.00
	3	0.00	0.02	0.05	0.07	0.09	0.11	0.11	0.09	0.07	0.05	0.02	0.01	0.00
	4	0.00	0.04	0.08	0.13	0.16	0.19	0.19	0.16	0.12	0.08	0.04	0.02	0.00
	5	0.00	0.06	0.13	0.20	0.26	0.29	0.29	0.26	0.19	0.13	0.07	0.03	0.00
	6	0.00	0.09	0.19	0.28	0.37	0.42	0.42	0.37	0.28	0.18	0.10	0.04	0.00
	7	0.00	0.12	0.25	0.39	0.50	0.57	0.57	0.50	0.38	0.25	0.13	0.05	0.00

⑨ Bulk carrier (New Panamax)

	K-value (wind speed/ ship speed)	Wind angle (°)												
		0	15	30	45	60	75	90	105	120	135	150	165	180
Required rudder angle (°)	1	0.00	0.01	0.04	0.07	0.11	0.15	0.18	0.19	0.17	0.14	0.09	0.05	0.00
	2	0.00	0.06	0.14	0.28	0.45	0.61	0.72	0.74	0.68	0.55	0.38	0.19	0.00
	3	0.00	0.12	0.32	0.63	1.01	1.37	1.62	1.68	1.53	1.24	0.85	0.43	0.00
	4	0.00	0.22	0.58	1.12	1.80	2.44	2.88	2.98	2.73	2.20	1.51	0.76	0.00
	5	0.00	0.35	0.90	1.76	2.81	3.82	4.49	4.65	4.26	3.43	2.36	1.18	0.00
	6	0.00	0.50	1.30	2.53	4.04	5.49	6.47	6.70	6.14	4.95	3.39	1.71	0.00
	7	0.00	0.68	1.77	3.44	5.51	7.48	8.81	9.12	8.35	6.73	4.62	2.32	0.00
Drift angle (°)	1	0.00	0.00	0.01	0.01	0.01	0.01	0.01	0.01	0.01	0.01	0.00	0.00	0.00
	2	0.00	0.01	0.02	0.03	0.04	0.05	0.05	0.04	0.03	0.02	0.01	0.00	0.00
	3	0.00	0.02	0.05	0.07	0.10	0.11	0.11	0.10	0.07	0.05	0.03	0.01	0.00
	4	0.00	0.04	0.09	0.13	0.17	0.20	0.20	0.17	0.13	0.09	0.05	0.02	0.00
	5	0.00	0.07	0.14	0.21	0.27	0.31	0.31	0.27	0.21	0.13	0.07	0.03	0.00
	6	0.00	0.09	0.20	0.30	0.39	0.45	0.45	0.39	0.30	0.19	0.10	0.04	0.00
	7	0.00	0.13	0.27	0.41	0.53	0.61	0.61	0.53	0.41	0.26	0.14	0.06	0.00

Table 3.1.1 Required Rudder Angles and Drift Angles of Each Type of Ship with Different Wind Angles When the K-Value is One to Seven (D_0/d_0 = 1.2)

⑩ Bulk carrier

	K-value (wind speed/ship speed)	Wind angle (°)												
		0	15	30	45	60	75	90	105	120	135	150	165	180
Required rudder angle (°)	1	0.00	0.01	0.04	0.07	0.10	0.14	0.16	0.17	0.15	0.12	0.09	0.04	0.00
	2	0.00	0.06	0.15	0.27	0.42	0.56	0.65	0.67	0.61	0.50	0.34	0.17	0.00
	3	0.00	0.13	0.33	0.61	0.94	1.25	1.46	1.51	1.38	1.11	0.77	0.39	0.00
	4	0.00	0.24	0.58	1.08	1.67	2.23	2.60	2.68	2.45	1.98	1.36	0.69	0.01
	5	0.00	0.37	0.91	1.68	2.61	3.48	4.06	4.18	3.83	3.09	2.13	1.08	0.01
	6	0.00	0.53	1.31	2.42	3.76	5.01	5.84	6.02	5.51	4.46	3.07	1.56	0.01
	7	0.00	0.72	1.78	3.30	5.11	6.82	7.95	8.20	7.51	6.06	4.18	2.12	0.02
Drift angle (°)	1	0.00	0.00	0.00	0.01	0.01	0.01	0.01	0.01	0.01	0.00	0.00	0.00	0.00
	2	0.00	0.01	0.02	0.03	0.03	0.04	0.04	0.03	0.03	0.02	0.01	0.00	0.00
	3	0.00	0.02	0.04	0.06	0.07	0.08	0.08	0.07	0.06	0.04	0.02	0.01	0.00
	4	0.00	0.03	0.07	0.10	0.13	0.15	0.15	0.13	0.10	0.07	0.04	0.02	0.00
	5	0.00	0.05	0.10	0.16	0.21	0.23	0.24	0.21	0.16	0.11	0.06	0.03	0.00
	6	0.00	0.07	0.15	0.23	0.30	0.34	0.34	0.30	0.23	0.16	0.09	0.04	0.00
	7	0.00	0.10	0.20	0.31	0.40	0.46	0.46	0.41	0.32	0.21	0.12	0.05	0.00

⑪ Small bulk carrier

	K-value (wind speed/ship speed)	Wind angle (°)												
		0	15	30	45	60	75	90	105	120	135	150	165	180
Required rudder angle (°)	1	0.00	0.03	0.07	0.14	0.22	0.30	0.35	0.37	0.34	0.28	0.19	0.10	0.00
	2	0.00	0.11	0.28	0.54	0.87	1.18	1.40	1.47	1.36	1.11	0.77	0.40	0.00
	3	0.00	0.24	0.63	1.22	1.95	2.66	3.16	3.30	3.06	2.50	1.74	0.89	0.01
	4	0.00	0.43	1.11	2.16	3.46	4.73	5.61	5.87	5.45	4.45	3.10	1.58	0.01
	5	0.00	0.67	1.74	3.38	5.41	7.39	8.77	9.17	8.51	6.95	4.84	2.47	0.02
	6	0.00	0.96	2.51	4.87	7.80	10.64	12.63	13.21	12.25	10.01	6.97	3.56	0.03
	7	0.00	1.31	3.41	6.62	10.61	14.48	17.19	17.98	16.68	13.63	9.49	4.84	0.04
Drift angle (°)	1	0.00	0.01	0.01	0.02	0.02	0.03	0.03	0.02	0.02	0.01	0.01	0.00	0.00
	2	0.00	0.02	0.05	0.07	0.09	0.11	0.11	0.09	0.07	0.05	0.03	0.01	0.00
	3	0.00	0.05	0.11	0.17	0.21	0.24	0.24	0.21	0.16	0.10	0.06	0.02	0.00
	4	0.00	0.10	0.20	0.29	0.38	0.42	0.42	0.37	0.28	0.19	0.10	0.04	0.00
	5	0.00	0.15	0.31	0.46	0.59	0.66	0.66	0.58	0.44	0.29	0.16	0.07	0.00
	6	0.00	0.22	0.44	0.66	0.85	0.96	0.95	0.83	0.64	0.42	0.23	0.09	0.00
	7	0.00	0.29	0.60	0.90	1.15	1.30	1.30	1.14	0.87	0.57	0.31	0.13	0.00

⑫ Very large crude carrier

	K-value (wind speed/ship speed)	Wind angle (°)												
		0	15	30	45	60	75	90	105	120	135	150	165	180
Required rudder angle (°)	1	0.00	0.01	0.03	0.06	0.10	0.14	0.17	0.17	0.16	0.12	0.08	0.04	0.00
	2	0.00	0.03	0.11	0.24	0.41	0.57	0.68	0.70	0.63	0.49	0.33	0.16	0.00
	3	0.00	0.08	0.24	0.54	0.92	1.28	1.53	1.57	1.41	1.11	0.74	0.36	0.00
	4	0.00	0.13	0.43	0.95	1.63	2.28	2.71	2.79	2.51	1.97	1.31	0.65	0.01
	5	0.00	0.21	0.67	1.49	2.55	3.57	4.24	4.36	3.92	3.07	2.05	1.01	0.01
	6	0.00	0.30	0.97	2.14	3.67	5.14	6.11	6.28	5.64	4.43	2.95	1.45	0.01
	7	0.00	0.41	1.32	2.91	4.99	6.99	8.31	8.55	7.68	6.02	4.01	1.98	0.02
Drift angle (°)	1	0.00	0.00	0.00	0.01	0.01	0.01	0.01	0.01	0.01	0.00	0.00	0.00	0.00
	2	0.00	0.01	0.02	0.03	0.04	0.05	0.05	0.04	0.03	0.02	0.01	0.00	0.00
	3	0.00	0.02	0.04	0.07	0.10	0.11	0.11	0.10	0.07	0.04	0.02	0.01	0.00
	4	0.00	0.04	0.08	0.13	0.17	0.20	0.20	0.18	0.13	0.08	0.04	0.01	0.00
	5	0.00	0.06	0.12	0.20	0.27	0.31	0.32	0.28	0.20	0.12	0.06	0.02	0.00
	6	0.00	0.08	0.17	0.28	0.38	0.45	0.46	0.40	0.29	0.18	0.08	0.03	0.00
	7	0.00	0.11	0.24	0.38	0.52	0.61	0.62	0.54	0.40	0.24	0.11	0.04	0.00

Table 3.1.1 Required Rudder Angles and Drift Angles of Each Type of Ship with Different Wind Angles When the *K*-Value is One to Seven (D_0/d_0 = 1.2)

⑬ Small tanker

	K-value (wind speed/ ship speed)	Wind angle (°)												
		0	15	30	45	60	75	90	105	120	135	150	165	180
Required rudder angle (°)	1	0.00	0.01	0.04	0.10	0.16	0.22	0.26	0.27	0.24	0.19	0.13	0.06	0.00
	2	0.00	0.06	0.18	0.38	0.64	0.89	1.06	1.09	0.98	0.77	0.52	0.25	0.00
	3	0.00	0.13	0.40	0.86	1.44	2.01	2.38	2.44	2.20	1.73	1.16	0.57	0.01
	4	0.00	0.24	0.71	1.52	2.56	3.57	4.23	4.35	3.91	3.08	2.06	1.02	0.01
	5	0.00	0.37	1.11	2.38	4.01	5.57	6.60	6.79	6.12	4.82	3.22	1.59	0.01
	6	0.00	0.53	1.60	3.43	5.77	8.03	9.51	9.78	8.81	6.93	4.64	2.29	0.02
	7	0.00	0.72	2.18	4.66	7.86	10.92	12.94	13.31	11.99	9.44	6.32	3.12	0.03
Drift angle (°)	1	0.00	0.00	0.01	0.01	0.01	0.02	0.02	0.01	0.01	0.01	0.00	0.00	0.00
	2	0.00	0.01	0.03	0.04	0.06	0.07	0.07	0.06	0.04	0.03	0.01	0.00	0.00
	3	0.00	0.03	0.06	0.10	0.13	0.15	0.15	0.13	0.10	0.06	0.03	0.01	0.00
	4	0.00	0.05	0.11	0.17	0.23	0.27	0.27	0.24	0.18	0.11	0.05	0.02	0.00
	5	0.00	0.08	0.17	0.27	0.36	0.42	0.43	0.37	0.27	0.17	0.08	0.03	0.00
	6	0.00	0.11	0.24	0.39	0.52	0.61	0.61	0.53	0.39	0.24	0.12	0.04	0.00
	7	0.00	0.16	0.33	0.53	0.71	0.83	0.83	0.73	0.54	0.33	0.16	0.06	0.00

⑭ Very large pure car carrier (PCC)

	K-value (Wind speed/ ship speed)	Wind angle (°)												
		0	15	30	45	60	75	90	105	120	135	150	165	180
Required rudder angle (°)	1	0.00	0.26	0.55	0.87	1.23	1.61	1.95	2.19	2.23	2.03	1.55	0.84	0.00
	2	0.00	1.06	2.20	3.49	4.94	6.44	7.82	8.76	8.94	8.11	6.20	3.37	0.00
	3	0.00	2.38	4.95	7.86	11.11	14.50	17.59	19.70	20.11	18.26	13.96	7.58	0.00
	4	0.00	4.23	8.81	13.97	19.75	25.78	****	****	****	****	24.81	13.47	0.00
	5	0.00	6.61	13.76	21.84	****	****	****	****	****	****	****	21.05	0.00
	6	0.00	9.52	19.81	****	****	****	****	****	****	****	****	****	0.00
	7	0.00	12.95	26.97	****	****	****	****	****	****	****	****	****	0.00
Drift angle (°)	1	0.00	0.06	0.11	0.15	0.17	0.17	0.16	0.14	0.11	0.09	0.06	0.03	0.00
	2	0.00	0.24	0.44	0.59	0.67	0.69	0.64	0.56	0.46	0.34	0.23	0.11	0.00
	3	0.00	0.53	0.99	1.33	1.51	1.54	1.45	1.27	1.03	0.77	0.51	0.25	0.00
	4	0.00	0.94	1.76	2.36	2.69	2.75	****	****	****	****	0.90	0.45	0.00
	5	0.00	1.47	2.75	3.68	****	****	****	****	****	****	****	0.70	0.00
	6	0.00	2.12	3.96	****	****	****	****	****	****	****	****	****	0.00
	7	0.00	2.88	5.39	****	****	****	****	****	****	****	****	****	0.00

⑮ Large PCC

	K-value (wind speed/ ship speed)	Wind angle (°)												
		0	15	30	45	60	75	90	105	120	135	150	165	180
Required rudder angle (°)	1	0.00	0.16	0.34	0.56	0.81	1.07	1.30	1.45	1.47	1.32	1.01	0.55	0.01
	2	0.00	0.64	1.36	2.22	3.22	4.27	5.19	5.80	5.88	5.29	4.02	2.18	0.02
	3	0.00	1.43	3.06	5.01	7.25	9.60	11.69	13.05	13.23	11.91	9.05	4.91	0.05
	4	0.00	2.54	5.44	8.90	12.89	17.07	20.78	23.20	23.52	21.18	16.10	8.74	0.08
	5	0.00	3.97	8.50	13.90	20.14	26.66	****	****	****	****	25.15	13.65	0.13
	6	0.00	5.72	12.23	20.02	29.01	****	****	****	****	****	****	19.66	0.18
	7	0.00	7.79	16.65	27.25	****	****	****	****	****	****	****	26.75	0.25
Drift angle (°)	1	0.00	0.04	0.08	0.10	0.12	0.12	0.11	0.10	0.08	0.06	0.04	0.02	0.00
	2	0.00	0.16	0.31	0.41	0.47	0.49	0.46	0.40	0.32	0.24	0.15	0.08	0.00
	3	0.00	0.37	0.69	0.93	1.07	1.10	1.03	0.90	0.72	0.53	0.35	0.17	0.00
	4	0.00	0.65	1.22	1.65	1.89	1.95	1.83	1.60	1.29	0.95	0.62	0.30	0.00
	5	0.00	1.02	1.91	2.58	2.96	3.04	****	****	****	****	0.96	0.47	0.00
	6	0.00	1.47	2.75	3.71	4.26	****	****	****	****	****	****	0.68	0.01
	7	0.00	1.99	3.74	5.05	****	****	****	****	****	****	****	0.92	0.01

Table 3.1.1 Required Rudder Angles and Drift Angles of Each Type of Ship with Different Wind Angles When the *K*-Value is One to Seven (D_0/d_0 = 1.2)

⑯ PCC

	K-value (wind speed/ ship speed)	Wind angle (°)												
		0	15	30	45	60	75	90	105	120	135	150	165	180
Required rudder angle (°)	1	0.00	0.16	0.35	0.59	0.88	1.18	1.44	1.61	1.63	1.46	1.10	0.60	0.01
	2	0.00	0.64	1.41	2.37	3.51	4.71	5.76	6.43	6.50	5.83	4.42	2.39	0.02
	3	0.00	1.45	3.18	5.34	7.90	10.59	12.96	14.48	14.63	13.13	9.94	5.38	0.05
	4	0.00	2.58	5.65	9.49	14.04	18.82	23.04	25.74	26.02	23.33	17.66	9.56	0.09
	5	0.00	4.03	8.82	14.83	21.93	29.41	****	****	****	****	27.60	14.94	0.14
	6	0.00	5.80	12.71	21.35	****	****	****	****	****	****	****	21.51	0.20
	7	0.00	7.90	17.30	29.06	****	****	****	****	****	****	****	29.28	0.27
Drift angle (°)	1	0.00	0.05	0.10	0.13	0.15	0.16	0.15	0.13	0.10	0.08	0.05	0.02	0.00
	2	0.00	0.21	0.39	0.53	0.61	0.63	0.60	0.52	0.42	0.30	0.19	0.09	0.00
	3	0.00	0.46	0.87	1.19	1.37	1.42	1.34	1.17	0.93	0.68	0.44	0.21	0.00
	4	0.00	0.82	1.55	2.11	2.44	2.52	2.39	2.08	1.66	1.21	0.78	0.38	0.00
	5	0.00	1.29	2.43	3.29	3.81	3.94	****	****	****	****	1.21	0.59	0.01
	6	0.00	1.85	3.49	4.74	****	****	****	****	****	****	****	0.85	0.01
	7	0.00	2.52	4.75	6.46	****	****	****	****	****	****	****	1.15	0.01

⑰ Liquefied natural gas carrier

	K-value (wind speed/ ship speed)	Wind angle (°)												
		0	15	30	45	60	75	90	105	120	135	150	165	180
Required rudder angle (°)	1	0.00	0.09	0.21	0.37	0.57	0.78	0.95	1.05	1.04	0.91	0.68	0.36	0.00
	2	0.00	0.37	0.85	1.50	2.29	3.12	3.81	4.20	4.16	3.66	2.72	1.45	0.01
	3	0.00	0.82	1.90	3.37	5.16	7.02	8.57	9.44	9.36	8.23	6.12	3.27	0.03
	4	0.00	1.46	3.38	5.99	9.17	12.48	15.24	16.79	16.65	14.63	10.88	5.82	0.05
	5	0.00	2.29	5.29	9.36	14.33	19.50	23.81	26.23	26.01	22.85	16.99	9.09	0.08
	6	0.00	3.30	7.61	13.48	20.64	28.07	****	****	****	****	24.47	13.09	0.12
	7	0.00	4.49	10.36	18.35	28.10	****	****	****	****	****	****	17.81	0.16
Drift angle (°)	1	0.00	0.03	0.06	0.09	0.10	0.11	0.10	0.09	0.07	0.05	0.03	0.02	0.00
	2	0.00	0.13	0.25	0.35	0.41	0.44	0.42	0.37	0.29	0.21	0.13	0.06	0.00
	3	0.00	0.30	0.57	0.78	0.93	0.98	0.94	0.82	0.65	0.47	0.29	0.14	0.00
	4	0.00	0.53	1.01	1.39	1.65	1.75	1.67	1.46	1.16	0.83	0.51	0.24	0.00
	5	0.00	0.82	1.57	2.18	2.58	2.73	2.62	2.28	1.81	1.29	0.80	0.38	0.00
	6	0.00	1.18	2.26	3.14	3.71	3.93	****	****	****	****	1.16	0.55	0.00
	7	0.00	1.61	3.08	4.27	5.06	****	****	****	****	****	****	0.74	0.01

⑱ Liquefied petroleum gas carrier

	K-value (wind speed/ ship speed)	Wind angle (°)												
		0	15	30	45	60	75	90	105	120	135	150	165	180
Required rudder angle (°)	1	0.00	0.05	0.12	0.22	0.34	0.46	0.55	0.59	0.57	0.49	0.35	0.19	0.00
	2	0.00	0.21	0.50	0.89	1.36	1.84	2.20	2.36	2.28	1.95	1.41	0.74	0.00
	3	0.00	0.48	1.12	2.01	3.07	4.13	4.95	5.32	5.13	4.38	3.18	1.67	0.00
	4	0.00	0.85	1.99	3.57	5.46	7.34	8.80	9.46	9.12	7.79	5.66	2.96	0.00
	5	0.00	1.33	3.11	5.57	8.53	11.48	13.75	14.78	14.25	12.18	8.84	4.63	0.00
	6	0.00	1.91	4.49	8.02	12.28	16.53	19.80	21.28	20.52	17.54	12.72	6.67	0.00
	7	0.00	2.60	6.11	10.92	16.72	22.49	26.95	28.97	27.93	23.87	17.32	9.08	0.00
Drift angle (°)	1	0.00	0.01	0.02	0.03	0.04	0.04	0.04	0.04	0.03	0.02	0.01	0.01	0.00
	2	0.00	0.05	0.09	0.13	0.16	0.18	0.17	0.15	0.12	0.08	0.05	0.02	0.00
	3	0.00	0.11	0.21	0.30	0.37	0.40	0.38	0.34	0.26	0.18	0.11	0.05	0.00
	4	0.00	0.19	0.38	0.54	0.65	0.70	0.68	0.60	0.47	0.32	0.19	0.09	0.00
	5	0.00	0.30	0.59	0.84	1.02	1.10	1.07	0.93	0.73	0.50	0.30	0.13	0.00
	6	0.00	0.44	0.85	1.21	1.47	1.59	1.54	1.34	1.05	0.72	0.43	0.19	0.00
	7	0.00	0.59	1.16	1.64	2.00	2.16	2.09	1.83	1.43	0.98	0.58	0.26	0.00

Table 3.1.1 Required Rudder Angles and Drift Angles of Each Type of Ship with Different Wind Angles When the *K*-Value is One to Seven (D_0/d_0 = 1.2)

⑲ Refrigerated cargo carrier

	K-value (wind speed/ ship speed)	Wind angle (°)												
		0	15	30	45	60	75	90	105	120	135	150	165	180
Required rudder angle (°)	1	0.00	0.04	0.09	0.16	0.25	0.34	0.40	0.42	0.40	0.33	0.23	0.12	0.00
	2	0.00	0.15	0.36	0.66	1.02	1.37	1.62	1.70	1.59	1.31	0.93	0.48	0.00
	3	0.00	0.33	0.80	1.48	2.29	3.08	3.64	3.82	3.57	2.95	2.08	1.07	0.01
	4	0.00	0.58	1.42	2.62	4.08	5.48	6.47	6.79	6.35	5.25	3.70	1.91	0.02
	5	0.00	0.91	2.22	4.10	6.37	8.56	10.11	10.61	9.92	8.21	5.78	2.98	0.03
	6	0.00	1.31	3.20	5.91	9.17	12.33	14.57	15.28	14.29	11.82	8.33	4.29	0.04
	7	0.00	1.78	4.35	8.04	12.49	16.78	19.83	20.80	19.45	16.09	11.33	5.84	0.05
Drift angle (°)	1	0.00	0.01	0.02	0.02	0.03	0.03	0.03	0.03	0.02	0.01	0.01	0.00	0.00
	2	0.00	0.03	0.06	0.09	0.11	0.13	0.13	0.11	0.09	0.06	0.03	0.01	0.00
	3	0.00	0.07	0.14	0.20	0.26	0.29	0.28	0.25	0.19	0.13	0.08	0.03	0.00
	4	0.00	0.12	0.24	0.36	0.45	0.51	0.50	0.44	0.35	0.23	0.13	0.06	0.00
	5	0.00	0.19	0.38	0.56	0.71	0.79	0.79	0.69	0.54	0.37	0.21	0.09	0.00
	6	0.00	0.27	0.55	0.81	1.02	1.14	1.13	1.00	0.78	0.53	0.30	0.13	0.00
	7	0.00	0.37	0.75	1.10	1.39	1.55	1.54	1.36	1.06	0.72	0.41	0.18	0.00

⑳ Large passenger ship (twin-propeller, twin-rudder ship)

	K-value (wind speed/ ship speed)	Wind angle (°)												
		0	15	30	45	60	75	90	105	120	135	150	165	180
Required rudder angle (°)	1	0.00	0.30	0.60	0.92	1.28	1.71	2.15	2.54	2.73	2.59	2.04	1.13	0.00
	2	0.00	1.19	2.40	3.68	5.14	6.82	8.62	10.16	10.92	10.35	8.18	4.53	0.00
	3	0.00	2.69	5.40	8.28	11.56	15.36	19.39	22.86	24.56	23.29	18.40	10.19	0.00
	4	0.00	4.77	9.60	14.73	20.56	27.30	****	****	****	****	****	18.11	0.00
	5	0.00	7.46	15.00	23.01	****	****	****	****	****	****	****	28.30	0.00
	6	0.00	10.74	21.60	****	****	****	****	****	****	****	****	****	0.00
	7	0.00	14.62	29.40	****	****	****	****	****	****	****	****	****	0.00
Drift angle (°)	1	0.00	0.15	0.28	0.36	0.39	0.39	0.35	0.31	0.26	0.20	0.14	0.07	0.00
	2	0.00	0.60	1.10	1.43	1.57	1.55	1.42	1.23	1.03	0.81	0.56	0.29	0.00
	3	0.00	1.36	2.48	3.22	3.53	3.48	3.19	2.78	2.31	1.82	1.27	0.65	0.00
	4	0.00	2.41	4.41	5.72	6.28	6.18	****	****	****	****	****	1.16	0.00
	5	0.00	3.77	6.89	8.94	****	****	****	****	****	****	****	1.82	0.00
	6	0.00	5.43	9.93	****	****	****	****	****	****	****	****	****	0.00
	7	0.00	7.38	13.51	****	****	****	****	****	****	****	****	****	0.00

㉑ Passenger ship (twin-propeller, twin-rudder ship)

	K-value (wind speed/ ship speed)	Wind angle (°)												
		0	15	30	45	60	75	90	105	120	135	150	165	180
Required rudder angle (°)	1	0.00	0.17	0.36	0.58	0.83	1.10	1.36	1.56	1.63	1.51	1.17	0.64	0.01
	2	0.00	0.70	1.45	2.31	3.30	4.39	5.44	6.24	6.52	6.03	4.68	2.57	0.02
	3	0.00	1.57	3.27	5.20	7.43	9.87	12.25	14.05	14.66	13.56	10.52	5.79	0.05
	4	0.00	2.79	5.81	9.25	13.21	17.55	21.77	24.97	26.07	24.11	18.71	10.29	0.10
	5	0.00	4.36	9.07	14.45	20.64	27.43	****	****	****	****	29.23	16.08	0.15
	6	0.00	6.28	13.07	20.80	29.72	****	****	****	****	****	****	23.15	0.22
	7	0.00	8.55	17.78	28.32	****	****	****	****	****	****	****	****	0.29
Drift angle (°)	1	0.00	0.08	0.15	0.20	0.23	0.23	0.21	0.18	0.15	0.12	0.08	0.04	0.00
	2	0.00	0.33	0.61	0.80	0.90	0.91	0.85	0.74	0.61	0.46	0.31	0.16	0.00
	3	0.00	0.74	1.37	1.81	2.03	2.05	1.90	1.66	1.36	1.04	0.70	0.35	0.00
	4	0.00	1.31	2.43	3.22	3.61	3.64	3.39	2.95	2.42	1.84	1.24	0.63	0.01
	5	0.00	2.05	3.80	5.03	5.64	5.69	****	****	****	****	1.94	0.98	0.01
	6	0.00	2.95	5.47	7.24	8.12	****	****	****	****	****	****	1.42	0.01
	7	0.00	4.02	7.45	9.85	****	****	****	****	****	****	****	****	0.02

Table 3.1.1 Required Rudder Angles and Drift Angles of Each Type of Ship with Different Wind Angles When the K-Value is One to Seven (D_0/d_0 = 1.2)

㉒ Ferry (twin-propeller, single-rudder ferry)

	K-value (wind speed/ ship speed)	Wind angle (°)												
		0	15	30	45	60	75	90	105	120	135	150	165	180
Required rudder angle (°)	1	0.00	0.11	0.25	0.44	0.66	0.90	1.11	1.24	1.26	1.13	0.85	0.46	0.00
	2	0.00	0.45	1.01	1.75	2.65	3.60	4.44	4.98	5.03	4.50	3.40	1.84	0.02
	3	0.00	1.02	2.28	3.94	5.96	8.10	10.00	11.20	11.32	10.13	7.66	4.14	0.04
	4	0.00	1.81	4.05	7.00	10.59	14.41	17.77	19.91	20.12	18.02	13.61	7.36	0.07
	5	0.00	2.82	6.34	10.94	16.55	22.51	27.77	****	****	28.15	21.27	11.49	0.11
	6	0.00	4.06	9.12	15.76	23.83	****	****	****	****	****	****	16.55	0.15
	7	0.00	5.53	12.42	21.45	****	****	****	****	****	****	****	22.53	0.21
Drift angle (°)	1	0.00	0.05	0.10	0.14	0.16	0.16	0.16	0.13	0.11	0.08	0.05	0.02	0.00
	2	0.00	0.21	0.40	0.54	0.63	0.65	0.62	0.54	0.43	0.31	0.20	0.10	0.00
	3	0.00	0.47	0.90	1.22	1.42	1.47	1.40	1.21	0.97	0.71	0.45	0.22	0.00
	4	0.00	0.84	1.60	2.17	2.52	2.62	2.48	2.16	1.73	1.26	0.80	0.39	0.00
	5	0.00	1.32	2.49	3.39	3.94	4.09	3.88	****	****	1.96	1.25	0.61	0.01
	6	0.00	1.90	3.59	4.89	5.67	****	****	****	****	****	****	0.87	0.01
	7	0.00	2.58	4.88	6.65	****	****	****	****	****	****	****	1.19	0.01

4 Linear Dispersion Relations of Waves

Table 4.1.1(a) Table of Water Depth, Period, Wave Length, and Wave Velocity

Period (S) / Water depth (m)	3.0		4.0		5.0		6.0		7.0		8.0		9.0		10.0	
	Wave length (m)	Wave velocity (m/s)	Wave length (m)	Wave velocity (m/s)	Wave length (m)	Wave velocity (m/s)	Wave length (m)	Wave velocity (m/s)	Wave length (m)	Wave velocity (m/s)	Wave length (m)	Wave velocity (m/s)	Wave length (m)	Wave velocity (m/s)	Wave length (m)	Wave velocity (m/s)
0.5	6.39	2.13	8.67	2.17	10.92	2.18	13.16	2.19	15.39	2.20	17.62	2.20	19.84	2.20	22.06	2.21
1.0	8.69	2.90	11.99	3.00	15.23	3.05	18.43	3.07	21.61	3.09	24.78	3.10	27.94	3.10	31.09	3.11
1.5	10.21	3.40	14.37	3.59	18.40	3.68	22.36	3.73	26.29	3.76	30.19	3.77	34.08	3.79	37.95	3.80
2.0	11.30	3.77	16.22	4.05	20.94	4.19	25.57	4.26	30.14	4.31	34.67	4.33	39.18	4.35	43.68	4.37
2.5	12.09	4.03	17.71	4.43	23.08	4.62	28.31	4.72	33.46	4.78	38.56	4.82	43.62	4.85	48.67	4.87
3.0	12.67	4.22	18.95	4.74	24.92	4.98	30.71	5.12	36.39	5.20	42.01	5.25	47.58	5.29	53.13	5.31
3.5	13.09	4.36	19.98	5.00	26.52	5.30	32.84	5.47	39.02	5.57	45.13	5.64	51.18	5.69	57.19	5.72
4.0	13.36	4.46	20.85	5.21	27.93	5.59	34.75	5.79	41.42	5.92	47.98	6.00	54.48	6.05	60.92	6.09
4.5	13.60	4.53	21.57	5.39	29.18	5.84	36.49	6.08	43.61	6.23	50.61	6.33	57.53	6.39	64.40	6.44
5.0	13.75	4.58	22.18	5.55	30.29	6.06	38.07	6.34	45.63	6.52	53.05	6.63	60.38	6.71	67.64	6.76
6.0	13.91	4.64	23.11	5.78	32.17	6.43	40.84	6.81	49.24	7.03	57.47	7.18	65.57	7.29	73.58	7.36
7.0	13.99	4.66	23.75	5.94	33.67	6.73	43.19	7.20	52.39	7.48	61.37	7.67	70.20	7.80	78.92	7.89
8.0	14.02	4.67	24.19	6.05	34.86	6.97	45.19	7.53	55.16	7.88	64.86	8.11	74.38	8.26	83.77	8.38
9.0	14.03	4.68	24.47	6.12	35.81	7.16	46.91	7.82	57.61	8.23	68.01	8.50	78.19	8.69	88.22	8.82
10.0	14.03	4.68	24.65	6.16	36.56	7.31	48.37	8.06	59.78	8.54	70.85	8.86	81.68	9.08	92.32	9.23
11.0	14.04	4.68	24.77	6.19	37.15	7.43	49.62	8.27	61.72	8.82	73.44	9.18	84.89	9.43	96.12	9.61
12.0	14.04	4.68	24.84	6.21	37.60	7.52	50.69	8.45	63.44	9.06	75.80	9.48	87.85	9.76	99.67	9.97
13.0	14.04	4.68	24.89	6.22	37.95	7.59	51.60	8.60	64.98	9.28	77.96	9.74	90.59	10.07	102.98	10.30
14.0	14.04	4.68	24.91	6.23	38.22	7.64	52.38	8.73	66.35	9.48	79.93	9.99	93.14	10.35	106.07	10.61
15.0	14.04	4.68	24.93	6.23	38.42	7.68	53.03	8.84	67.58	9.65	81.73	10.22	95.51	10.61	108.98	10.90
16.0	14.04	4.68	24.94	6.23	38.57	7.71	53.58	8.93	68.66	9.81	83.39	10.42	97.71	10.86	111.71	11.17
17.0	14.04	4.68	24.95	6.24	38.68	7.74	54.04	9.01	69.63	9.95	84.90	10.61	99.77	11.09	114.29	11.43
18.0	14.04	4.68	24.95	6.24	38.77	7.75	54.42	9.07	70.49	10.07	86.29	10.79	101.68	11.30	116.71	11.67
19.0	14.04	4.68	24.95	6.24	38.83	7.77	54.74	9.12	71.25	10.18	87.56	10.95	103.47	11.50	119.00	11.90
20.0	14.04	4.68	24.95	6.24	38.87	7.77	55.00	9.17	71.92	10.27	88.72	11.09	105.14	11.68	121.16	12.12
22.0	14.04	4.68	24.95	6.24	38.93	7.79	55.39	9.23	73.03	10.43	90.76	11.35	108.14	12.02	125.12	12.51
24.0	14.04	4.68	24.96	6.24	38.96	7.79	55.65	9.28	73.89	10.56	92.46	11.56	110.76	12.31	128.66	12.87
26.0	14.04	4.68	24.96	6.24	38.98	7.80	55.83	9.30	74.54	10.65	93.86	11.73	113.04	12.56	131.83	13.18
28.0	14.04	4.68	24.96	6.24	38.98	7.80	55.94	9.32	75.03	10.72	95.02	11.88	115.01	12.78	134.66	13.47
30.0	14.04	4.68	24.96	6.24	38.99	7.80	56.02	9.34	75.40	10.77	95.97	12.00	116.72	12.97	137.19	13.72
35.0	14.04	4.68	24.96	6.24	38.99	7.80	56.11	9.35	75.96	10.85	97.64	12.20	120.03	13.34	142.38	14.24
40.0	14.04	4.68	24.96	6.24	38.99	7.80	56.14	9.36	76.22	10.89	98.61	12.33	122.26	13.58	146.25	14.63
50.0	14.04	4.68	24.96	6.24	38.99	7.80	56.15	9.36	76.39	10.91	99.46	12.43	124.71	13.86	151.16	15.12
60.0	14.04	4.68	24.96	6.24	38.99	7.80	56.15	9.36	76.42	10.92	99.72	12.46	125.71	13.97	153.68	15.37
70.0	14.04	4.68	24.96	6.24	38.99	7.80	56.15	9.36	76.42	10.92	99.79	12.47	126.10	14.01	154.91	15.49
Deepwater wave	14.04	4.68	24.96	6.24	38.99	7.80	56.15	9.36	76.43	10.92	99.82	12.48	126.34	14.04	155.97	15.60

Table 4.1.1(b) Table of Water Depth, Period, Wave Length, and Wave Velocity

Period (S) / Water depth (m)	11.0		12.0		13.0		14.0		15.0		16.0		18.0		20.0	
	Wave length (m)	Wave velocity (m/s)	Wave length (m)	Wave velocity (m/s)	Wave length (m)	Wave velocity (m/s)	Wave length (m)	Wave velocity (m/s)	Wave length (m)	Wave velocity (m/s)	Wave length (m)	Wave velocity (m/s)	Wave length (m)	Wave velocity (m/s)	Wave length (m)	Wave velocity (m/s)
1.0	34.2	3.11	37.4	3.12	40.5	3.12	43.7	3.12	46.8	3.12	50.0	3.12	56.2	3.12	62.5	3.13
2.0	48.2	4.38	52.6	4.39	57.1	4.39	61.6	4.40	66.0	4.40	70.5	4.40	79.4	4.41	88.2	4.41
3.0	58.6	5.33	64.2	5.35	69.6	5.36	75.1	5.37	80.6	5.37	86.1	5.38	97.0	5.39	107.9	5.39
4.0	67.3	6.12	73.7	6.14	80.1	6.16	86.5	6.18	92.8	6.19	99.1	6.20	111.8	6.21	124.4	6.22
5.0	74.9	6.81	82.0	6.84	89.2	6.86	96.3	6.88	103.4	6.90	110.5	6.91	124.7	6.93	138.8	6.94
6.0	81.5	7.41	89.4	7.45	97.3	7.78	105.1	7.51	113.0	7.53	120.8	7.55	136.3	7.57	151.8	7.59
7.0	87.6	7.96	96.1	8.01	104.7	8.05	113.2	8.08	121.6	8.11	130.1	8.13	146.9	8.16	163.7	8.19
8.0	93.1	8.46	102.3	8.52	111.4	8.57	120.6	8.61	129.6	8.64	138.7	8.67	156.7	8.71	174.7	8.74
9.0	98.1	8.92	108.0	9.00	117.7	9.05	127.4	9.10	137.1	9.14	146.7	9.17	165.9	9.22	185.0	9.25
10.0	102.8	9.35	113.2	9.44	123.6	9.50	133.8	9.56	144.1	9.60	154.2	9.64	174.5	9.69	194.7	9.73
12.0	111.3	10.12	122.8	10.24	134.2	10.33	145.6	10.40	156.8	10.45	168.0	10.50	190.3	10.57	212.5	10.63
14.0	118.8	10.80	131.3	10.95	143.8	11.06	156.1	11.15	168.3	11.22	180.5	11.28	204.7	11.37	228.7	11.44
16.0	125.5	11.41	139.0	11.58	152.4	11.72	165.7	11.83	178.8	11.92	191.9	11.99	217.9	12.11	243.7	12.18
18.0	131.4	11.95	145.9	12.16	160.3	12.33	174.4	12.46	188.5	12.57	202.4	12.65	230.1	12.78	257.6	12.88
20.0	136.8	12.44	152.3	12.69	167.5	12.88	182.5	13.04	197.4	13.16	212.2	13.26	241.5	13.42	270.6	13.53
22.0	141.7	12.89	158.1	13.17	174.1	13.39	190.0	13.57	205.7	13.72	221.3	13.83	252.2	14.01	282.8	14.14
24.0	146.2	13.29	163.4	13.61	180.3	13.87	197.0	14.07	213.5	14.23	229.9	14.37	262.3	14.57	294.3	14.72
26.0	150.2	13.66	168.3	14.02	186.0	14.31	203.5	14.53	220.8	14.72	237.9	14.87	271.8	15.10	305.3	15.26
28.0	153.9	13.99	172.8	14.40	191.3	14.72	209.6	14.97	227.6	15.17	245.5	15.34	280.8	15.60	315.7	15.78
30.0	157.3	14.30	176.9	14.74	196.2	15.10	215.3	15.38	234.1	15.60	252.7	15.79	289.4	16.08	325.6	16.28
35.0	164.4	14.95	186.0	15.50	207.2	15.94	228.1	16.29	248.7	16.58	269.0	16.81	309.1	17.17	348.6	17.43
40.0	170.1	15.46	193.5	16.12	216.5	16.65	239.1	17.08	261.4	17.43	283.4	17.71	326.7	18.15	369.3	18.46
45.0	174.5	15.86	199.6	16.64	224.4	17.26	248.7	17.76	272.6	18.17	296.2	18.51	342.6	19.03	388.1	19.41
50.0	178.0	16.18	204.7	17.06	231.0	17.77	256.9	18.35	282.5	18.83	307.6	19.23	357.0	19.83	405.4	20.27
55.0	180.7	16.42	208.8	17.40	236.6	18.20	264.0	18.86	291.1	19.41	317.8	19.86	370.1	20.56	421.3	21.06
60.0	182.7	16.61	212.1	17.68	241.4	18.57	270.3	19.31	298.8	19.92	326.9	20.43	382.0	21.22	435.9	21.80
70.0	185.5	16.86	216.9	18.08	248.7	19.13	280.3	20.02	311.6	20.77	342.4	21.40	403.0	22.39	462.1	23.10
80.0	187.0	17.00	220.0	18.33	253.7	19.52	287.7	20.55	321.5	21.43	354.9	22.18	420.5	23.36	484.6	24.23
90.0	187.8	17.07	221.9	18.49	257.2	19.78	293.0	20.93	329.1	21.94	364.9	22.80	435.3	24.19	504.2	25.21
100.0	188.3	17.11	223.0	18.58	259.5	19.96	297.0	21.21	334.9	22.32	372.8	23.30	447.8	24.88	521.2	26.06
120.0	188.6	17.15	224.1	18.67	261.9	20.15	301.6	21.54	342.5	22.83	383.9	23.99	466.9	25.94	548.8	27.44
140.0	188.7	17.15	224.4	18.70	262.9	20.23	303.8	21.70	346.6	23.11	390.6	24.41	480.1	26.67	569.5	28.48
160.0	188.7	17.16	224.5	18.71	263.3	20.26	304.9	21.78	348.7	23.25	394.4	24.65	489.1	27.17	585.0	29.25
180.0	188.7	17.16	224.6	18.72	263.5	20.27	305.3	21.81	349.8	23.32	396.6	24.79	495.0	27.50	596.4	29.82
200.0	188.7	17.16	224.6	18.72	263.6	20.27	305.5	21.82	350.4	23.36	397.8	24.87	498.8	27.71	604.6	30.23
Deepwater wave	188.7	17.16	224.6	18.72	263.6	20.28	305.7	21.84	350.9	23.40	399.3	24.96	505.3	28.07	623.7	31.19

Table 4.1.1(c) Table of Water Depth, Period, Wave Length, and Wave Velocity

Period (S) / Water depth (m)	2.2		2.4		2.6		2.8		3.0		3.2		3.5		4.0	
	Wave length (m)	Wave velocity (m/s)	Wave length (m)	Wave velocity (m/s)	Wave length (m)	Wave velocity (m/s)	Wave length (m)	Wave velocity (m/s)	Wave length (m)	Wave velocity (m/s)	Wave length (m)	Wave velocity (m/s)	Wave length (m)	Wave velocity (m/s)	Wave length (m)	Wave velocity (m/s)
0.1	2.15	0.976	2.35	0.978	2.55	0.980	2.75	0.981	2.95	0.983	3.15	0.983	3.45	0.985	3.94	0.986
0.2	2.99	1.361	3.28	1.363	3.57	1.372	3.85	1.376	4.14	1.379	4.42	1.382	4.85	1.385	5.55	1.388
0.3	3.61	1.643	3.97	1.655	4.32	1.663	4.68	1.670	5.03	1.676	5.38	1.681	5.90	1.686	6.77	1.693
0.4	4.11	1.870	4.53	1.887	4.94	1.901	5.35	1.912	5.76	1.921	6.17	1.928	6.78	1.936	7.79	1.947
0.5	4.53	2.059	5.00	2.084	5.47	2.103	5.93	2.118	6.39	2.131	6.85	2.141	7.53	2.153	8.69	2.167
0.6	4.89	2.222	5.41	2.255	5.93	2.280	6.44	2.300	6.95	2.316	7.45	2.329	8.21	2.345	9.45	2.364
0.7	5.20	2.364	5.77	2.404	6.33	2.436	6.89	2.462	7.45	2.482	8.00	2.499	8.81	2.518	10.17	2.542
0.8	5.47	2.388	6.09	2.538	6.70	2.577	7.30	2.607	7.90	2.632	8.49	2.653	9.37	2.677	10.82	2.706
0.9	5.72	2.598	6.38	2.657	7.03	2.703	7.67	2.740	8.31	2.770	8.94	2.794	9.88	2.823	11.43	2.857
1.0	5.93	2.695	6.63	2.764	7.33	2.818	8.01	2.861	8.69	2.896	9.36	2.924	10.35	2.958	11.99	2.999
1.1	6.12	2.782	6.87	2.861	7.60	2.923	8.32	2.973	9.04	3.013	9.75	3.045	10.80	3.085	12.52	3.131
1.2	6.29	2.859	7.08	2.949	7.85	3.019	8.61	3.075	9.36	3.121	10.11	3.158	11.21	3.203	13.02	3.256
1.3	6.44	2.928	7.27	3.028	8.08	3.107	8.88	3.170	9.66	3.222	10.44	3.264	11.60	3.314	13.50	3.374
1.4	6.58	2.989	7.44	3.100	8.29	3.188	9.12	3.258	9.95	3.316	10.76	3.363	11.97	3.419	13.94	3.486
1.5	6.70	3.044	7.60	3.165	8.48	3.262	9.35	3.340	10.21	3.403	11.06	3.455	12.31	3.517	14.37	3.592
1.6	6.80	3.092	7.74	3.225	8.66	3.331	9.56	3.416	10.46	3.486	11.34	3.543	12.64	3.611	14.77	3.693
1.7	6.90	3.135	7.87	3.278	8.82	3.394	9.76	3.487	10.69	3.562	11.60	3.625	12.95	3.700	15.16	3.789
1.8	6.98	3.173	7.99	3.327	8.97	3.452	9.95	3.552	10.90	3.635	11.85	3.703	13.24	3.784	15.53	3.881
1.9	7.05	3.206	8.09	3.371	9.11	3.505	10.12	3.614	11.11	3.702	12.08	3.776	13.52	3.864	15.88	3.970
2.0	7.12	3.236	8.19	3.411	9.24	3.554	10.28	.3.670	11.30	3.766	12.30	3.845	13.79	3.940	16.22	4.054
Deepwater wave	7.55	3.431	8.98	3.743	10.54	4.055	12.23	4.367	14.04	4.679	15.97	4.991	19.11	5.459	24.96	6.239

Note: For a period of 2.0 seconds or less, multiply the water depth and wave length values shown in Tables 4.1.1(a) and 4.1.1(b) by 0.01, and multiply the period and wave velocity values by 0.1.